Toxicological effects of nanoparticle deposition in the liver

Modrzynska, Justyna

Publication date:
2018

Document Version
Publisher's PDF, also known as Version of record

Toxicological effects of nanoparticle deposition in the liver

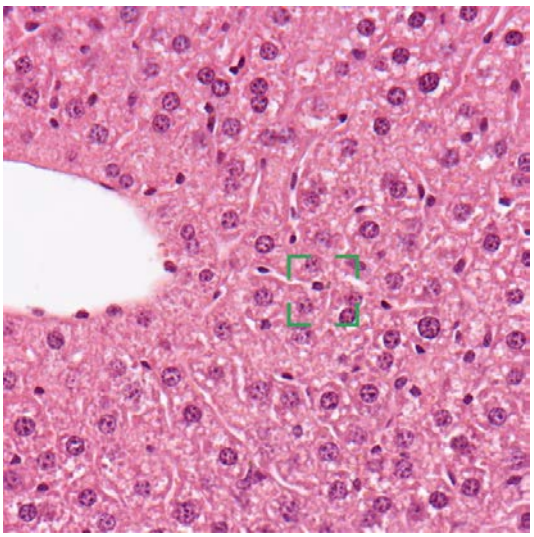

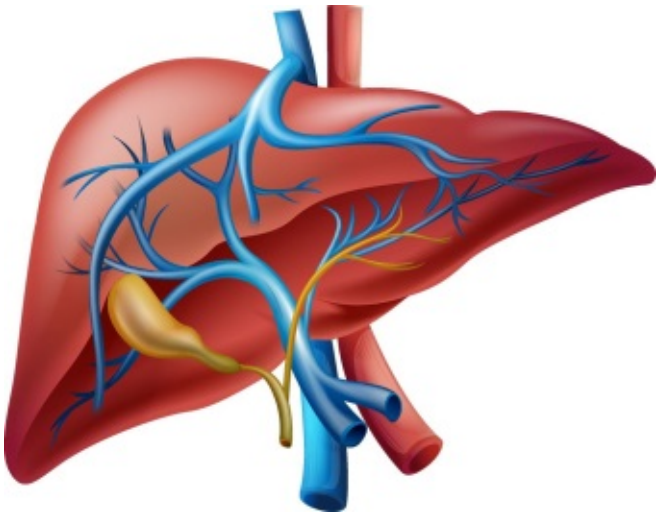

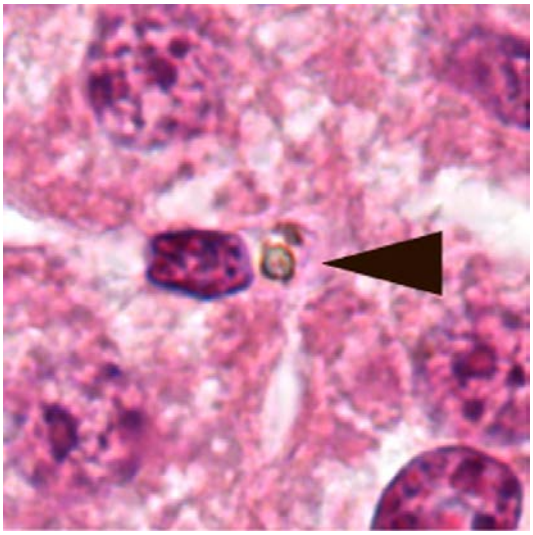

Justyna Modrzyńska
PhD Thesis
October 2017

DTU Food
National Food Institute

PhD thesis by Justyna Modrzyńska

October 2017

Toxicological effects of nanoparticle deposition in the liver

Research Group for Risk-Benefit, National Food Institute, Technical University of Denmark

National Research Centre for the Working Environment, Denmark

***Per aspera ad astra* –**

Przez trudy do gwiazd

SUPERVISORS

Principal supervisor

Senior Researcher **Gitte Ravn-Haren**

National Food Institute, Technical University of Denmark

Research Group for Risk-Benefit

Co-supervisors:

Professor **Ulla Birgitte Vogel**

National Research Centre for the Working Environment, Denmark

Senior Researcher **Anne Thoustrup Saber**

National Research Centre for the Working Environment, Denmark

Senior Researcher **Katrin Löschner**

National Food Institute, Technical University of Denmark

Research Group for Nano-Bio Science

Former supervisors:

Alicja Mortensen, PhD

National Research Centre for the Working Environment, Denmark

Erik Huusfeldt Larsen, PhD

National Food Institute, Technical University of Denmark

PREFACE AND ACKNOWLEDGEMENTS

It's been a long and challenging journey and here, I would like to express my sincere gratitude to many people that have contributed to this PhD work – I would have never accomplished the aims if it wasn't for you!

Great thanks to my main supervisor - Gitte Ravn-Haren - who made the last few months of the PhD work much easier. Thank you for your invaluable support, friendship and, most importantly, for your incessant faith in my ability to finish this task. You were always there for me, even when I thought I didn't need your assistance and I am not sure if I could ever pay you back!

Ulla Vogel – thank you that you believed in me and gave me the opportunity to become a part of the scientific world. Things were not always as we wanted and expected, but you always had time and never-ending enthusiasm, and you left your door open for both the trivial and clever questions. You have challenged me and it resulted in the development of a new, matured scientist.

Anne Thoustrup Saber – you were my anchor at NFA and my "role model" of a wise researcher and dedicated mother. Thank you for both professional and everyday-life advices, fruitful discussions and positive atmosphere coming along with a warm smile whenever I needed.

Katrin Löschner – thank you for the trip to the world of tricky analytical chemistry analysis. For your countless great ideas of how to solve the next insolvable problem, sharing your knowledge and for your patience although it was not always so easy.

I would like to express my special thanks to Erik Huusfeldt Larsen who was my co-supervisor and who is now enjoying non-academia life. You mesmerized me with the analytical chemistry and its power in the world of nano as well as provided me with the tools I needed to complete my PhD. It has been fantastic to be part of your research group and I really missed our collaboration.

Alicja Mortensen – thank you for your valuable input and constructive comments that improved this thesis, all the efforts and good laughs that we had during the whole period.

This work would never be possible without the excellent laboratory and technical support. Therefore, I would like to thank Annette Landin, Sarah Grundt Simonsen, Anne-Marie Ørngreen, Maja Danielsen and other technicians from DTU for your priceless help in conducting animal experiments. Many thanks to Birgitte Koch Herbst, Marianne Hansen and Rie Romme Rasmussen, also from DTU, that have introduced the ICP-MS enigma to me. Last but not least, I would like to send warm acknowledgements to Anne-Karin Asp, Anne Abildtrup, Michael Guldbrandsen, Zdenka Orabi Kyjovska, Lourdes Pedersen and Elzbieta Christiansen from NFA for their assistance and help that have been worth a lot. I have learnt so much from you all and I will definitely use this knowledge in my future career.

I would also wish to thank all my colleagues from both DTU and NFA, for the inspiring conversations and for the opportunity to share ups and downs of the young scientist life.

Finally, I want to send my deep gratitude to my family. To my little daughter Hanna, for being my sunshine in the cloudy days and the best achievement in my life. You are an inexhaustible source of pure joy and happiness that makes my life better and complete. To my son Antoni, for being the biggest motivation to finalize this thesis. And, eventually, to my beloved husband Kuba, for being my best friend, always with me whenever I needed. You are constantly one step ahead, serving with help and support. Thank you for all you did and all you will do.

The work presented in this thesis was conducted at the Technical University of Denmark, National Food Institute, in the Research Group for Risk-Benefit and in the Research Group for Nano-Bio Science and at the National Research Centre for the Working Environment. The project started on the 1st of September 2012, was prolonged by the sick and maternity leaves, and the final thesis was handed in October 2017. The work was financially supported by The Danish Centre for Nanosafety (grant no. 20110092173-3) from the Danish Working Environment Research Foundation.

Justyna Modrzyńska

October 2017

TABLE OF CONTENT

SUMMARY

A number of studies have demonstrated that pulmonary exposure to nanoparticles (NPs) by inhalation or intratracheal instillation leads to size-dependent accumulation of particles and causes adverse pulmonary effects including, among others, inflammation, induction of acute phase response and histopathological alterations of the lung tissue. Upon deposition in the respiratory tract particles appear to translocate readily across the alveolar epithelium, through interstitium and further into systemic circulation getting access to the extrapulmonary sites and reaching various distant organs. The degree of translocation strongly depends on particles size, chemical composition, solubility, shape, surface properties etc. A portion of lung-deposited particles could also be transported up into the pharynx by the mucociliary escalator and when swallowed, cause secondary exposure via gastrointestinal tract (GIT). Liver, among other secondary organs, seems to be the major tissue for sequestration of extrapulmonary-translocated NPs. When particles reach the liver, they accumulate in the Kupffer cells, residence liver macrophages, from where their clearance is protracted. It has been shown that particles were still present in the liver 6 months after exposure. Prolonged hepatic accumulation of NPs raises questions about the possible acute and long-term toxicological consequences.

Deposition of NPs in the liver makes it very susceptible to many diseases and causes disturbances in its normal functioning. Our research group has previously demonstrated that inhalation and intratracheal instillation of CB Printex 90 and TiO_2 NPs induced genotoxicity in terms of increased DNA strand break levels and increased levels of oxidative DNA damage in the liver tissue. Moreover, recent epidemiological studies indicated association between exposure to particulate air pollutions and development of liver cancer.

This PhD aimed at investigating toxicological effects of NP accumulation in the liver. We have decided to focus primarily on NP-elicited genotoxicity, inflammation, acute phase response as well as evaluating several other systemic endpoints including histopathology of lung and liver tissue, general liver biochemistry and haematology. Extrapulmonary translocation and liver deposition were also assessed in the study. Close attention was given to the nature of NP-induced genotoxicity observed in the liver tissue – whether it is caused by the presence of translocated

particles or by indirect effects of inflammation and acute phase response in the lungs that could trigger production of secondary messengers and, in turn, induce secondary genotoxicity in the liver tissue. Moreover, potential contribution from the secondary oral exposure could also result in the observed genotoxic effect.

To achieve the aims 324 young adult C57BL/6 female mice were exposed by single intratracheal instillation (IT), intravenous injection (IV) and oral gavage (PO) to 162 μg/mouse of titanium dioxide (TiO_2), cerium oxide (CeO_2) or carbon black (CB) NPs and terminated 1, 28 and 180 days post-exposure.

In **Manuscript 1** we investigated liver deposition of TiO_2 and CeO_2 NPs following IT, IV and PO exposure. Our results indicated similar extrapulmonary translocation of both particles to the liver following IT exposure. Despite different chemical composition, shape and potential differences in solubility that could affect hepatic accumulation calculated translocation rates for TiO_2 and CeO_2 NPs were comparable and stood at 1.24 ± 1.98 % and 2.87 ± 3.37 %, respectively of the initial pulmonary dose. No NPs were detected in the liver following oral gavage which indicates that the main translocation route for pulmonary-deposited NPs is the translocation via systemic circulation and that secondary oral exposure did not contribute to the observed liver deposition. Moreover, analysis of size distribution of CeO_2 NPs revealed that they underwent *in vivo*-induced size transformation over time both in lung and liver tissue.

In order to extend the knowledge in understanding the mechanism responsible for the hepatic genotoxicity (i.e. primary or secondary NP-driven genotoxicity) in **Manuscript 2** we evaluated induction of pulmonary inflammation, pulmonary and hepatic acute phase response and genotoxicity following exposure to TiO_2, CeO_2 and CB NPs. Indications of presence of all three NPs in the liver following IT and IV exposure were found. We observed increased number of DNA strand breaks in the liver after IT and IV exposure to CB NPs but not after exposure to TiO_2 or CeO_2. Pulmonary inflammation was observed for all three NPs on day 1 and day 28 following IT exposure. Pulmonary acute phase response was also detected for all nanomaterials and lasted up to day 180. Induction of hepatic acute phase response was transient and measurable only on day 1 in IT and IV exposed groups to TiO_2 and CeO_2 NPs. In contrast to TiO_2 and CeO_2 NPs, only CB

NPs generated reactive oxygen species (ROS) in an acellular assay. In a holistic view our data indicate that DNA damages in the liver tissue are likely caused by the direct effects of translocated CB NPs and further production of ROS rather than by systemic inflammation and acute phase response.

In **Manuscript 3** we assessed various blood markers, liver biochemical parameters, analyzed changes in body as well as in liver weight, and performed histopathological evaluation of liver and lung tissue in order to determine potential consequences of (prolonged) accumulation of NPs in the liver. We did not observe any significant alterations in mice body weights at any of the analyzed time points. Moreover, exposure to CeO_2 and CB NPs did not induce changes in the liver weight. Oral exposure to TiO_2 decreased absolute and relative liver weight but it was regarded as a chance finding. Haematological analysis of blood revealed occasional and negligible alterations of a few markers. No changes in the selected biochemical parameters were measured. Histopathological examination of the liver tissue revealed high inflammatory background in all vehicle and NP-exposed groups regardless the administration route and it was impossible to determine whether these changes were treatment-related. Similarly, necrotic changes could not be uniquely associated with the treatment. In general, we concluded that neither IT, IV nor PO exposure to TiO_2, CeO_2 or CB NPs induced any significant systemic or hepatotoxic effects.

Overall, collected data suggest that liver is an important endpoint in the assessment of NP safety and more studies will enable broadening the knowledge and clarify whether NPs pose a liver-threat.

DANSK RESUMÉ

En række undersøgelser har vist, at eksponering af lunger for nanopartikler (NP'er) fører til størrelsesafhængig partikelakkumulering og forårsager skadelige effekter i lungerne, herunder inflammation, opregulering af akutfaseresponset og histopatologiske forandringer. Efter deponering i luftvejene translokerer NP'erne over i kredsløbet, hvorfra de kan nå andre organer. Graden af translokation afhænger af partikelstørrelse, kemisk sammensætning, opløselighed, form, overfladeegenskaber mv. Leveren synes at være det primære organ, hvor sekvestrering af translokerede NP'er finder sted. De akkumulerer i Kupffer-celler, leverens specialiserede makrofager, hvorfra deres clearance er langsommelig. Langvarig ophobning af NP'er i leveren rejser spørgsmål om mulige akutte og langsigtede toksikologiske effekter af NP'er.

Formålet med denne ph.d. var at undersøge mulige toksikologiske effekter af NP'ers akkumulering i lever med primært fokus på genotoksicitet, inflammation, akutfaserespons, samt andre systemiske end-points, histopatologi af lunge- og levervæv, leverenzymaktiviteter og hæmatologi. Ekstrapulmonær translokation og leverdeponering blev ligeledes vurderet. Særlig opmærksomhed blev givet til typen af NP-induceret genotoksicitet observeret i leveren - om den skyldes tilstedeværelsen af translokerede partikler eller indirekte virkninger af inflammation og akutfasespons i lunger, der kunne udløse produktion af sekundære messengers og dermed fremkalde sekundær genotoksicitet i levervæv.

Ialt 324 yngre voksne C57BL/6 hunmus blev eksponeret for en enkelt dosis vehikel eller 162 µg/mus af titandioxid (TiO_2), ceriumoxid (CeO_2) eller carbon black (CB) NP'er ved enten intratracheal instillation (IT), intravenøs injektion (IV) eller oral gavage (PO). Aflivninger fandt sted 1, 28 eller 180 dage efter eksponering.

I **Manuskript 1** undersøgte vi leverdeponering af TiO_2 og CeO_2 NP'er efter IT og PO eksponering. Vores resultater indikerede sammenligneligt niveau of translokation af begge typer partikler til leveren efter IT-eksponering på trods af forskellig kemisk sammensætning, form og mulige forskelle i opløselighed. Beregnede lever mængder af NP'er var for TiO_2 og CeO_2 NP'er var henholdsvis 1.24 ± 1.98 % og 2.87 ± 3.37 %. Der blev ikke påvist nogen NP'er i leveren efter oral

dosering, hvilket indikerer, at NP'er deponeret i lunger primært translokerer via det systemiske kredsløb, og at sekundær oral eksponering ikke bidrager til den observerede leverdeponering. Desuden viste analysen af størrelsesfordeling af CeO_2 NP'er, at de gennemgik in vivo-induceret størrelsestransformation og blev mindre over tid både i lunge- og levervæv.

For at undersøge mekanismen bag levergenotoksiciteten (dvs. om der er tale om primær eller sekundær NP-drevet genotoksicitet) evaluerede vi i **Manuskript 2** om eksponering for TiO_2, CeO_2 eller CB NP'er forårsagede pulmonær inflammation, inducerede akutfaserespons eller genotoksicitet i lunge og lever. Vi fandt indikationer på tilstedeværelse af alle tre NP'er i leveren efter IT- og IV-eksponering. Vi observerede øget antal DNA-strengsbrud i leveren efter IT- og IV-eksponering for CB-NP'er, men ikke efter eksponering for TiO_2 eller CeO_2. Pulmonær inflammation blev observeret for alle tre NP'er på dag 1 og dag 28 efter IT-eksponering. Pulmonær akutfasespons blev også påvist for alle nanomaterialer og varede op til dag 180. TiO_2 og CeO_2 NP'er inducerede et forbigående og målbart hepatisk akutfasespons på dag 1 i IT- og IV-eksponerede grupper. Kun CB NP'er genererede reaktive oxygen forbindelser (ROS) i et acellulært assay. Dette indikerer, at DNA-skader i leveren sandsynligvis skyldes direkte påvirkninger af translokerede CB-NP'er og dannelsen af ROS, og ikke systemisk inflammation og akutfaserespons.

I **Manuskript 3** undersøgte vi forskellige blodmarkører og leverenzymaktiviteter, analyserede ændringer i krops- og levervægte og udførte histopatologisk evaluering af lever- og lungevæv for at bestemme mulige virkninger af (langvarig) ophobning af NP'er i leveren. Vi observerede ikke nogen signifikante ændringer i kropsvægt. Endvidere påvirkede eksponering for CeO_2 og CB NP'er ikke levervægt. Oral indgift af TiO_2 reducerede absolut og relativ levervægt, men dette fund betragtet som et chancefund. Hæmatologisk analyse af blod afslørede lejlighedsvise og ubetydelige ændringer af nogle få markører. Ingen ændringer i leverenzymaktiviteter blev målt. Histopatologisk undersøgelse af levervæv afslørede høj baggrundsinflammation hos alle vehikel- og NP-eksponerede grupper uanset administrationsvej, og derfor var det umuligt at afgøre, om observerede forandringer hos NP-doserede dyr kan relateres til behandlingen. På samme måde kunne nekrotiske forandringer ikke entydigt tilskrives behandlingen. Vi konkluderer, at hverken

IT, IV eller PO eksponering for TiO_2, CeO_2 eller CB NP'er inducerer signifikante systemiske eller hepatotoksiske effekter.

Samlet set tyder de indsamlede data på, at leveren er et vigtigt målorgan i vurderingen af NP'er, og flere undersøgelser vil gøre det muligt at udvide kendskabet til NP'er og afklare, om de udgør en reel trussel mod leveren.

LIST OF ABBREVIATIONS

ALP – alkaline phosphatase

ALT – alanine aminotransferase

AM – alveolar macrophages

ApoA-1 – apolipoprotein A1

AST – aspartate aminotransferase

BALF – bronchoalveolar lavage fluid

CB – carbon black

CeO_2 – cerium oxide

CRP – c-reactive protein

DCFH – 2',7' – dichlorodihydrofluorescein

DLS – dynamic light scattering

DNA SB – DNA strand breaks

EDFM – enhanced darkfield microscopy

EDTA – ethylenediaminetetraacetic acis

EM – electron microscopy

GAPDH – glyceraldehyde-3-phosphate dehydrogenase

GIT – gastrointestinal tract

HCT – hematocrit

HDL – high-density lipoprotein

H&E – hematoxylin and eosin staining

HGB – hemoglobin

HPRT – hypoxanthine-guanine phosphoribosyl transferase

ICP-MS – inductively coupled plasma mass spectrometry

IL-1 – interleukin 1

IL-6 – interleukin 6

IL-8 – interleukin 8

IFN-γ – interferon-γ

IT – intratracheal instillation

IV – intravenous injection

KCs – Kupffer cells

LAP – leucocyte alkaline phosphatase

LCAT – lecithin-cholesterol acyltransferase

LDL – low-density lipoprotein

LMP agarose – low-melting point agarose

MCH – mean cell hemoglobin

MCHC – mean corpuscular hemoglobin concentration

MCV – mean corpuscular volume

mRNA – messenger RNA

NPs – nanoparticles

PChE – plasma cholinesterase

PDGF – platelet-derived growth factor

PLT – platelets

PM – particulate matter

PMNL – polymorphonuclear neutrophilic leukocytes

PO – oral gavage

real-time RT-PCR – real-time reverse transcription polymerase chain reaction

RBC – red blood cells

RES – reticuloendothelial system

RNS – reactive nitrogen species

ROS – reactive oxygen species

SAA – serum amyloid A

spICP-MS – single particle inductively coupled mass spectrometry

TGF-β – transforming growth factor β

TiO_2 – titanium dioxide

TNF-α – tumor necrosis factor α

UFPs – ultrafine particles

WBC – white blood cells

1. INTRODUCTION

1.1 Nanoparticles – two-faced materials

The sub micrometer scale, better known as a nanometer scale, offers new and unique properties to everyday consumer and industrial products. Manmade NPs are widely used in virtually every sector including manufacturing of sporting goods, tires, stain-resistant clothing, sunscreens, cosmetics, electronics and more and more often in the food sector (as food additives, dietary supplements or in food packaging) and in medicine (as drug-delivery agents or for diagnostic and imaging purposes) [1,2].

The Royal Society of London defined the term 'nanoscience' as follow:

> *"Nanoscience is the study of phenomena and manipulation of materials at atomic, molecular and macromolecular scales, where the properties differ significantly from those at larger scale"* [3].

Indeed, unique properties exhibited by NPs are attributed to their small size and relatively large surface area. Other physicochemical features of NPs that allow seemingly infinite applications and that distinguish them from their bulk counterparts are unusual surface structure, solubility, shape, aggregation and chemical composition [1]. Although, mankind has been exposed to airborne nanosized particles for centuries due to volcanic activities, forest fires, fine sand, disintegration of meteorites entering the atmosphere or cosmic dust, recent development of nanotechnology has led to augmented human exposure [4].

On the one hand, the exceptional properties possessed by engineered nanomaterials offer novel potential and beneficial applications unavailable up to now. On the other hand, widespread use in the consumer products and lack or limited knowledge of toxicological effects of nano-scale products continuously rising concern about general safety of nanomaterials and unpredictable health consequences.

As a matter of fact, several studies demonstrated association between particle exposure and increased incidence of different adverse effects on biological systems at the organismal, cellular, subcellular and, eventually, genomic and protein level. Moreover, particle ability to readily

translocate from the site of exposure to various distant organs exacerbates potential deleterious effects [1].

Numerous epidemiological investigations showed positive correlation between exposure to ambient particulate matter and increased morbidity and mortality attributed to cardiovascular diseases [5]. Furthermore, constant exposure to air pollution results in respiratory tract disorders such as asthma or lung cancer [6,7]. Recently, animal studies demonstrated that air pollutants are able to induce liver toxicity and cause liver inflammation and steatosis [8].

In the present work, the main focus will be on particle biodistribution and subsequent biological effects induced by exposure and further deposition of NPs with a special consideration of the liver outcomes.

1.2 Biodistribution of administered particles

Increased production of NP-containing products will inevitably result in augmented human exposure. Since NPs due to their unique properties are widely used in different fields many possible routes of accessing human body exist. NPs could either enter the body by inhalation (NPs present in the ambient air and/or in the workplace), ingestion (dietary supplements, food or water containing NPs) or injection (medical usage of nanomaterials for drug delivery or diagnostic).

Dermal exposure is also one of the most frequent routes of NP administration, but since it was not included in this study, it will not be further discussed.

1.2.1 Biodistribution of inhaled NPs

2300 km of airways, 500 million alveoli and 75-140 m^2 of surface area. These magnificent numbers characterize human lungs (as reviewed in: [9]). Lungs are in a continuous contact with the ambient environment and therefore pulmonary exposure is considered as the most relevant administration route for particles present both at the home address as well as in the occupational environment. Deposition pattern of inhaled particles strongly depends on particle size: large particles are mainly deposited in the upper airways (nasal, pharyngeal and laryngeal regions) while smaller particles penetrate deeper pulmonary regions with a subsequent deposition in tracheobronchial and alveolar regions [4,10]. In order to keep mucosal surface free of particles they are cleared from the respiratory tract via two clearance pathways: physical translocation and chemical clearance mechanisms. Chemical clearance refers only to biosoluble particles or soluble particle constituents whereas physical translocation involves several diverse processes that are particle-size-dependent and characteristic only for specific regions of the respiratory tract (Fig. 1).

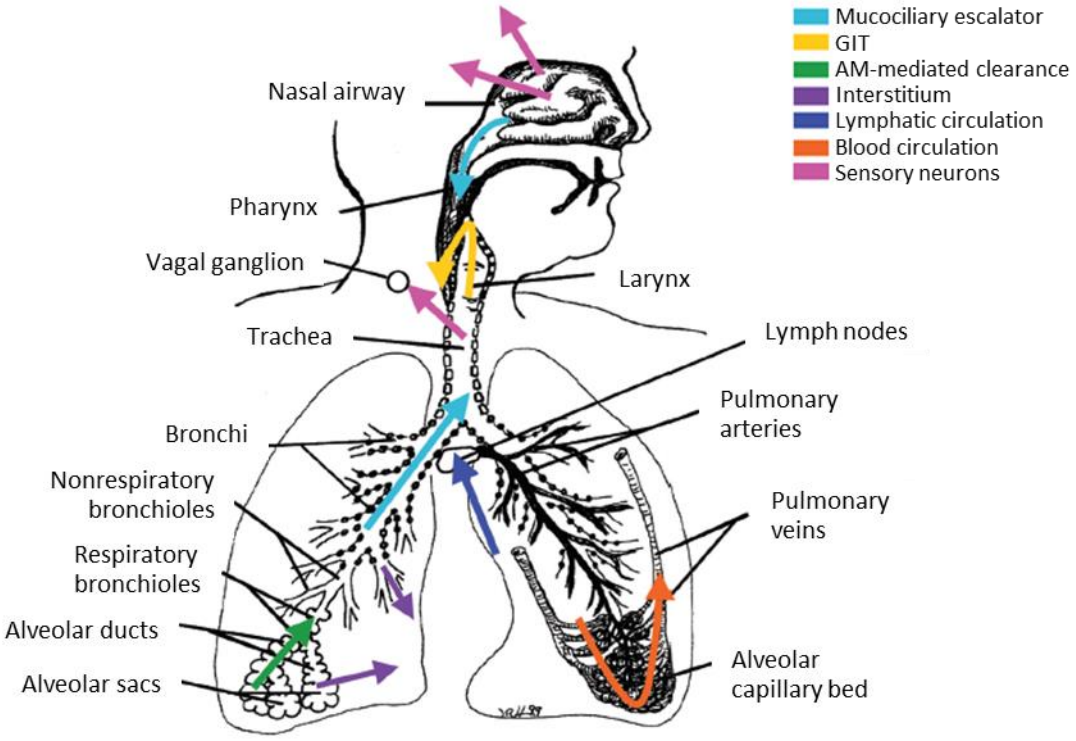

Figure 1. Different clearance pathways of deposited particles from the respiratory tract. AM – alveolar macrophages, GIT – gastrointestinal tract (modified from [4]).

Physical clearance mediated by alveolar macrophages is the most prominent way of removing particles deposited in the alveolar region. Chemotactically attracted macrophages phagocyte the foreign material and gradually move it towards the mucociliary escalator, prevalent clearance mechanism in the upper airways, that transports particles away from the lungs [4,9]. Mucus, with the internalized particles, is moved by the action of the ciliated cells to the pharynx and, if swallowed, could induce secondary exposure via GIT [2,9]. Particles could also be excreted through the mouth [11] and removed by coughing [12]. Several studies conducted over the last few decades [13–16] indicated that larger particles could be retrieved with the macrophages by the lavage procedure, while the vast majority of small particles (ultrafine particles, UFPs) retained in the lungs. This indicates that UFPs are able to translocate through the epithelial cell layer to the interstitium and further to the extrapulmonary sites by blood circulation [4]. Large surface area of the alveoli together with less than 400 nm distance between alveolar lumen and the blood capillaries establish favorable conditions for accessing systemic circulation [9]. Several

secondary tissues are the target sites of extrapulmonary translocated NPs, however, liver seems to be one of the major organs that sequestrates circulating particles [13,17–21]. Neuronal uptake of inhaled particles was also demonstrated [22,23].

1.2.2 Biodistribution of ingested NPs

Gastrointestinal tract (GIT), next to lung and skin, is an important portal of entry for particles present in water, food (as food additives), drugs or cosmetics (e.g. toothpaste). Moreover, inhaled particles cleared from the lungs by the action of ciliated cells could be swallowed and thereby induce GIT exposure. Most of the studies that investigated the uptake of particles demonstrated negligible or lack of absorption of the tested materials from the GIT [24–28]. In a quantitative biokinetic study of TiO_2 after oral application most of the gavaged [^{48}V]TiO_2 NPs were excreted via feces while only a small fraction of the material (0.6 % after 1 h and about 0.05 % after 7 days) bestrode intestinal barrier and was absorbed by the liver, lungs, kidney, brain, spleen, uterus and skeleton [29]. On the other hand, a significant increase in Ti concentration was reported in the liver and kidney of female CD-1 (ICR) mice exposed to 80 nm TiO_2 NPs by single oral gavage and in kidney of mice exposed to 25 nm TiO_2 NPs 14 days post exposure [25]. Conflicting results are very likely due to the differences in the used doses as well as type, size and phase of studied NPs. The mechanism of NP absorption from the GIT is poorly understood but the role of Peyer's patches (PP, aggregations of intestinal lymphatic tissue) containing M-cells (specialized phagocytic enterocytes) as well as contribution of normal enterocytes in particle uptake was suggested [2,30–32].

1.2.3 Biodistribution of injected NPs

Nowadays, NPs are commonly used in so called 'nanomedicine' as contrast agents, carriers for drugs and gene delivery agents [33]. Many of these applications require direct administration of NPs into systemic circulation. Biodistribution of NPs following intravenous injection is influenced by myriad factors including size and shape of particles, surface properties or morphology of the blood vessel endothelium. Moreover, upon accessing the systemic circulation NPs are surrounded by different blood proteins (in a process called 'opsonization') that could determine cellular uptake of particles by specific types of cells only [34,35]. Selected opsonins (e.g. the

complement proteins, IgG and laminin) can be absorbed on the surface of NPs. This allows for quicker recognition of the foreign material by immune cells of the mononuclear phagocytic system, like macrophages, and results in faster phagocytosis of particles from the blood stream [34,36]. Liver, spleen, lymph nodes and bone marrow, collectively make up the reticuloendothelial system (RES, also known as the monocyte–macrophage cell system) thus particles recognized and removed by macrophages are primary deposited in the organs of RES [34]. Essential role of Kupffer cells, resident macrophages localized in the liver, in NP clearance was previously reported [37]. The width of splenic inter-endothelial cell slits that aims at filtering old or damaged red blood cells is approximately 200 nm therefore larger particles are most likely taken up by the spleen [34]. In addition to the hepatic and splenic clearance, NPs can be excreted in kidneys by glomerular filtration however, the specific size-dependent mechanism of renal clearance prevents urinary excretion of particles larger than 8 nm [38].

1.3 Adverse health effects upon exposure to NPs

As shown in numerous studies, NPs can pass through various defence mechanisms of the human body and be distributed to the secondary organs, distant from the exposure site. However, many details concerning interactions between NPs and biological systems remain unknown. Presence of NPs in the body may cause adverse health effects such as inflammation, acute phase response, genotoxicity as well as severely alter physiological structure and function of the affected tissues.

1.3.1 Pulmonary inflammation

Lungs are constantly exposed to air that contains a wide range of pollutants including respirable particles and therefore, efficient mechanisms that protect the host from the invading foreign materials must exist. Epithelial cells and alveolar macrophages (AM) play a pivotal role in a surveillance of the respiratory tract. Epithelial cells are capable of synthesizing of various inflammatory mediators, e.g. interleukin-8 (IL-8), that chemotactically attract phagocytic cells to the site of particles invasion (hence suggesting an important role of epithelial cells in particle-induced inflammation) [39]. AM are resident lung macrophages which major job is phagocytosis of opsonised and non-opsonised particles. Toll-like receptors (TLRs) on the surface of macrophages are responsible for the recognition of invading pathogens. Upon activation, AM play a crucial pro-inflammatory role by secreting different cytokines and other mediators that orchestrate a cascade of immune response [40]. Among all secreted cytokines that initiate the inflammatory process, tumor necrosis factor α (TNF-α) seems to be the most prominent agent. Bioactivity of TNF-α includes inducement of adhesion molecule expression, stimulation of reactive oxygen species (ROS) and reactive nitrogen species (RNS) production by leukocytes and, most importantly, stimulation of the production of other pro-inflammatory cytokines, i.e. interleukin-1 (IL-1), interleukin-6 (IL-6), platelet-derived growth factor (PDGF) and transforming growth factor α (TGF-α) that further propagate the immune response [41].

Augmented release of cytotoxic mediators such as ROS and RNS by activated macrophages can lead to oxidative stress and result in oxidative DNA damage and subsequent genotoxicity [39,42]. Moreover, sustained inflammation is associated with the induction of fibrosis and carcinogenesis [39].

1.3.2 Acute phase response

Many previous studies demonstrated that pulmonary inflammation caused by exposure to NPs is associated with the induction of acute phase response [43–46].

The acute phase response is an orchestrated, systemic response (part of the innate immune system) that is triggered by different stimuli: trauma, tissue injury, inflammation, infection, stress or neoplasia [47]. Several different proteins, collectively known as acute phase proteins, are secreted into plasma in order to restore the body homeostasis. We can distinguish both positive acute phase proteins whose concentrations increase (like serum amyloid A – SAA, c-reactive protein – CRP, haptoglobin, ceruloplasmin, fibrinogen, and constituents of the complement system), as well as negative acute phase proteins (albumin, transferrin, factor XII, insulin-like growth factor and others) whose concentrations decrease during the acute phase response [48]. Acute phase proteins are predominantly produced by the liver hepatocytes [47].

The acute phase response is individually moderated and different plasma concentrations of acute phase proteins in patients with similar disorders could exist. It is believed, that those disparities are caused by differences in the production of specific cytokines, intercellular signaling polypeptides, that govern the response [48]. Cytokines are important mediators produced by different types of activated cells (monocytes, macrophages, fibroblasts, endothelium, platelets, keratinocytes, T cells) and their major role is to modulate and regulate the immune response in order to restore and maintain internal stability by the recruitment of inflammatory cells from systemic circulation and by inducing production of other cytokines [47,49,50]. The key-cytokines, that play an essential role in the production of acute phase proteins are: interleukin-6 (IL-6), interleukin-1β (IL-1β), tumor necrosis factor α (TNF-α), interferon-γ (IFN-γ), transforming growth factor β (TGF-β) and interleukin-8 (IL-8). Stimulation of the production of acute phase proteins such as SAA, CRP, complement C3, haptoglobin (in rats) is induced by IL-1-like cytokines, which include IL-1α, IL-1β, TNF-α and TNF-β. Whereas fibrinogen, human haptoglobin, α1-antichymotrypsin, α1-antitrypsin, and α2- macroglobulin (rat) are induced by IL-6-like cytokines which comprise IL-6 and its family members [51]. In the production of acute phase

proteins cytokines could act in a cascade or in a network, stimulating (inhibiting or enhancing,) other cytokines to forward the biological message [48].

Serum amyloid A (SAA), a multifunctional apolipoprotein, is one of the major acute phase proteins. Plasma SAA concentration could be increased up to 1000-fold during the acute phase response. In humans, there are four isoforms of the *SAA* gene: *SAA1* and *SAA2* that are acute phase response-hyperinducible, *SAA3* that is a pseudogene and *SAA4* that is expressed constitutively [49]. In mice five members of the *SAA* family exist (*Saa1, Saa2, Saa3, Saa4* now referred to as *Saa-ps1* a pseudogene and *Saa5* now referred to as *Saa4*). Genome mapping and transcriptional orientation indicate that human *SAA1* and *SAA2* and murine *Saa1* and *Saa2* are homologs. *SAA* genes are highly conserved, which indicates their important biological function in vertebrates [52]. Mouse *Saa1* and *Saa2* mRNA has a hepatic origin while *Saa3* mRNA was found to be a product of macrophage secretion [52]. Previous studies confirmed that *Saa3* was the most upregulated acute phase gene and/or the most differentially expressed gene. Therefore, it can serve as a biomarker to monitor the development of pulmonary acute phase response [45,46,53–57]. Similarly, *Saa1* was the most differentially expressed acute phase response gene in the liver (as demonstrated by [58]) and it can be used in the detection of hepatic acute phase response. During inflammation and acute phase response, SAA is replacing apolipoprotein A-1 (ApoA-1) in the third fraction of high-density lipoprotein (HDL3) causing partial depletion of ApoA-1 from HDL [52,59,60]. ApoA-1 is a cofactor of lecithin-cholesterol acyltransferase (LCAT), enzyme which major role is to esterify cholesterol allocated for extracellular transport. Moreover, it has been reported that SAA inhibits LCAT activity [61]. Taken together, these findings indicate that SAA, when incorporated into HDL, can impair cholesterol efflux [43].

1.3.3 Particle-induced genotoxicity

There are a number of studies demonstrating that exposure to particles leads to irreversible alterations in the DNA structure and is associated with the increased risk of lung cancer development [62–66]. Particles themselves as well as systemic effects induced by NPs (inflammation, augmented cell proliferation and ROS generation) play a crucial role in triggering genotoxicity followed by mutagenesis and, eventually, onset of cancer [62].

Oxidative stress, known as an impairment in the production of ROS and the ability of the antioxidant system to scavenge the free radicals, is presently considered as a main mechanism underlying particle-induced genotoxicity. Particle characteristics like shape, size, solubility, surface activity, carrier function and surface chemistry can contribute to the acellular ability of particles to elicit genotoxic effects. In example, free radicals or oxidative groups as well as transition metals or organic compounds could be directly bounded to the surface of particles and therefore stimulate increased oxidant formation [62,67]. The cellular pathways involve particle-induced production of ROS/RNS by target cells (vascular endothelial cells and lung epithelial cells) in absence of inflammation, or by activated phagocytic cells during inflammation [62].

We can distinguish two separate mechanisms of NP-induced genotoxicity: primary and secondary genotoxicity. Primary genotoxicity refers to the genetic alterations evoked by NPs in the absence of inflammation. Particles can induce DNA lesions directly by a physical interaction with genetic material in the nucleus or essential components that ensure its integrity (e.g. mitotic spindle) or indirectly, by formation of ROS by NP-activated cells (i.e. arising from mitochondria-produced ROS or by membrane bound NADPH oxidases) or by depletion of antioxidants [68,69]. Inhibition of DNA repair mechanism, demonstrated for many ions, could also be responsible for the primary indirect particles genotoxicity [68]. Secondary genotoxicity is characterized by the presence of inflammation driven by activated phagocytes: macrophages and polymorphonuclear neutrophilic leukocytes (PMNL), attracted to the site of particle deposition. ROS, RNS and possibly other mediators produced by activated cells strike on DNA and lead to genetic damages [68,69].

Since only a sufficient dose of particles is able to induce lung inflammation there is a threshold in the occurrence of secondary genotoxicity [70]. ROS are capable of inducing oxidation of DNA bases, DNA strand breaks or formation of lipid peroxidation-mediated DNA adducts [70]. Sustained ROS production occurs in particle-induced inflammation. It is well documented that persistent inflammation [62,71] and increased ROS production by activated phagocytes [72,73] are associated with carcinogenesis.

1.3.4 Histopathological alterations of liver and lung tissues

Once NPs are administered to the body their deposition in the tissue due to the slow clearance and low particle solubility could be prolonged. Constant presence of NPs could lead to grievous histopathological changes. Several studies have shown that regardless of the administration route, chemical composition and size of NPs a wide range of severe tissue alterations in liver and lungs occurred upon particle exposure.

Repeated intraperitoneal injection of Ag NPs (2000 mg/kg bw, particle size <100 nm) caused swollen hepatic cells, narrowing of the sinusoidal lumen and appearance of hypertrophied Kupffer cells [74]. Liver histopathological evaluation following intragastric exposure to TiO_2 NPs (10 mg/kg bw, particle size 5 nm) for 90 consecutive days demonstrated focal inflammatory cell infiltration, nucleus vacancy, vein congestion and edema in the liver tissue [75]. Intratracheal exposure to CeO_2 NPs (1.0/3.5/7.0 mg/kg bw, particle size 10.14 ± 0.76 nm) exhibited evidence of liver pathology expressed as dose-dependent hydropic degeneration and enlargement of hepatocytes, binucleation of some hepatocytes, sinusoidal dilatation, occasionally focal inflammation and accumulation of granular material [76].

A variety of changes in lung tissue including pulmonary fibrosis [77], multifocal microgranuloma [78], chronic alveolar inflammation including alveolaritis, granulomatous lesions, alveolar wall thickening and alveolar macrophage accumulation [79], pulmonary emphysema, macrophages accumulation, extensive disruption of alveolar septa, type II pneumocyte hyperplasia, and epithelial cell apoptosis [80] were reported following exposure to different NPs.

1.4 Liver as an important endpoint in particle toxicity

Liver, followed by spleen, sequestrates a vast majority of the NPs that entered the human body. Deposited foreign material is retained in the liver and could elicit adverse, toxic effects. Therefore, assessment of liver toxicity is a crucial step in the evaluation of NP-induced noxious effects.

1.4.1 Liver structure and functions

Liver structure is organized around the main branches of the portal vein with polyhedron units called hepatic lobules merged together with a connective tissue. The classical liver lobule is made up of a central vein and areas of connective tissue, a portal area, that contains interlobular branches of a hepatic artery and a portal vein, biliary ductules, a lymphatic vessel and nerves (Fig. 2) [81].

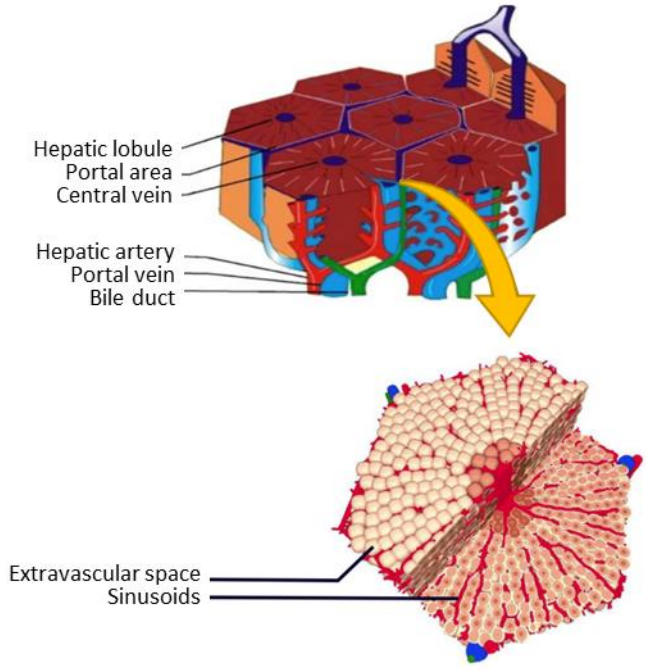

Figure 2. Structure of mammalian liver tissue (modified from [82]).

Both parenchymal cells (i.e. hepatocytes) and nonparenchymal cells (i.e. Kupffer cells, sinusoidal cells, stellate cells and intrahepatic lymphocytes) build up liver lobules. Hepatocytes make up ca.

80 % of the total liver volume and are responsible for performing the majority of the liver functions. Nonparenchymal cells, located in the sinusoidal compartment of the liver tissue, constitute 40 % of the total number of liver cells and are involved in filtration, secretion of cytokines, antigen presenting cell function (sinusoidal endothelial cells), phagocytosis, secretion of mediators of the inflammatory response (Kupffer cells) and vitamin A storage (stellate cells)[81].

Generally speaking, liver is a metabolic center of the body that supplies the energy, regulates glucose level and, among others, synthesizes and degrades plasma proteins. Moreover, as a defence center is responsible for the metabolism of xenobiotics, scavenging ROS, phagocytosis, uptake and neutralization of bacteria, viruses and foreign materials (including particulate matter) and is involved in the induction of acute phase response. Liver serves as a blood reservoir, regulates blood pH as well as controls the hormonal system and acts as a immunoregulator [81].

1.4.2 Kupffer cells – essential role in NP clearance

Kupffer cells (KCs), resident liver macrophages, are essential components of the mononuclear phagocytic system and constitute up to 80-90 % of the total body macrophages [83]. Hepatic localization within the sinusoidal lumen leads to the constant exposition of KCs to gut-derived bacteria, bacterial endotoxins and microbial debris from the GIT and other intruders that reached the liver via the portal vein [83]. They are also highly specialized in the clearance of foreign materials including particles [84]. Upon activation, macrophages secrete a broad range of different mediators (i.e. ROS, eicosanoids, nitric oxide, carbon monoxide, TNF-α and other cytokines) and therefore, take part in the modulation of hepatic inflammatory response [81]. However, dysregulation of this process can lead to chronic inflammation and, eventually, to the liver injury [84].

A study of the role of KCs following intravenous administration of Ag NPs demonstrated the crucial role of KCs in the hepatic anti-inflammatory response to Ag NPs [85]. Vascular infusion of CeO_2 NPs resulted in the avid uptake of nanoceria by KCs as early as 1 h post-exposure [86]. KC-mediated hepatic injury was also studied *in vitro* and *in vivo* with silica NPs. *In vitro* study using

Buffalo rat liver cells revealed that KCs upon stimulation by SiO_2 NPs secreted large amounts of ROS, TNF-α and nitric oxide. *In vivo* exposure to SiO_2 NPs caused KCs hyperplasia, hepatic inflammation and oxidative stress. Overall, these data suggest KC-mediated liver injury with the primary mechanism involving the production of reactive mediators by KCs [87].

1.4.3 NP-induced hepatotoxicity

NPs, regardless of the exposure route, when getting access to the systemic circulation are primarily taken up by the liver. Deposited particles can interfere with normal liver functions and cause liver toxicity followed by liver injury.

Intratracheal instillation of rats with CeO_2 NPs (7.0 mg/kg bw, particle size 10.14 ± 0.76 nm) resulted in increased liver ceria concentration followed by a significant reduction of the liver weight. NP exposure was also associated with elevated serum alanine transaminase (ALT) activity, reduced albumin (ALB) and decreased serum triglyceride (TG) levels which could be related to the histopathological alterations of the liver tissue. Gene expression analysis of serum proteins revealed statistically significant changes in the level of biomarkers correlating with the acute hepatic injury [76]. Several previous studies showed that exposure to TiO_2 caused significant elevation of serum biochemical parameters (ALT, alkaline phosphatase – ALP, aspartate aminotransferase – AST, lactate dehydrogenase – LDH, plasma cholinesterase – PChE, and leucocyte alkaline phosphatase – LAP) [88], liver oxidative stress [89], imbalance in blood sugars and lipid metabolism [90], liver inflammation and significant alterations of several inflammatory cytokines [91]. Oral exposure to carbon black in lean Zucker rats was associated with oxidative stress and hepatocyte steatosis. This was in a good agreement with a concomitant *in vitro* study using cultured human hepatocyte (HepG2) cell line that showed increased intracellular lipid content after CB NPs treatment [92]. It was also demonstrated that inhalation [57] and intratracheal instillation [54] of CB NPs (particle size 14 nm) induced genotoxicity in the liver tissue. Furthermore, there is a growing concern that exposure to air pollutants, including CB NPs, could be associated with increased risk of hepatic cancer [93–96].

2. HYPOTHESES AND AIMS

This PhD work was primarily focused on the assessment of toxicological effects caused by NPs accumulation in the liver.

It is hypothesized that:

- upon pulmonary exposure, deposited particles are cleared from the respiratory tract mainly by macrophage-mediated phagocytosis however, a small fraction of particles can get access to the systemic circulation and undergo extrapulmonary translocation to various secondary organs, including liver;
- translocation rate depends on size, shape, surface properties and chemical composition of NPs;
- a fraction of deposited particles that was transported up in the respiratory tract by the mucociliary escalator could be swallowed and therefore cause secondary exposure via GIT;
- deposited particles cause inflammation, induction of acute phase response, genotoxicity and tissue lesions;
- particle-mediated genotoxicity could be induced via two potential mechanisms: primary or secondary genotoxicity; primary genotoxicity refers to DNA damages caused by direct physical interaction between particles and genomic DNA or ROS formation by NP-activated cells in the absence of inflammation; secondary genotoxicity refers to DNA damages caused by ROS and other mediators released during particle-induced inflammation.

The specific aims of this PhD work were:

- to investigate possible toxicological effects of NP accumulation in the liver;
- to investigate what is the direct cause of previously observed hepatic genotoxicity following intratracheal instillation: a physical presence of translocated particles or a systemic effect caused by inflammation and acute phase response that trigger the production of secondary messengers and, in turn, induce secondary genotoxicity in the liver tissue.

In order to achieve these aims a group of 324 mice were divided into 36 experimental groups and exposed by single intratracheal instillation (IT), intravenous injection (IV) and oral gavage (PO) to titanium dioxide (TiO_2), cerium oxide (CeO_2) and carbon black (CB) NPs. Animals were euthanized 1, 28 and 180 days following exposure and several endpoints were evaluated: detection of NPs in the liver and lung tissue by enhanced darkfield microscopy (EDFM), determination of Ti and Ce NP mass concentrations in the liver and lungs by inductively coupled plasma mass spectrometry (ICP-MS), determination of size distribution profile of CeO_2 NPs in the liver by single-particle inductively coupled plasma mass spectrometry (spICP-MS), assessment of particle-induced acute phase response in the liver and lungs by real-time reverse transcription polymerase chain reaction (real-time RT-PCR), evaluation of particle-induced genotoxicity in the liver, lungs and bronchoalveolar lavage (BAL) cells by comet assay, assessment of pulmonary inflammation by analyzing cellular composition of BAL fluid (BALF), determination of ROS-generating ability of NPs by 2',7'–dichlorodihydrofluorescein (DCFH) assay, histopathological examination of particle-induced tissue lesions in the liver and lung tissue by light microscopy, evaluation of acute toxicity elicited by NPs exposure based on the assessment of general biochemical and haematological biomarkers.

Results of the present study are reported in the following manuscripts:

1. *In vivo*-induced size transformation of CeO_2 NPs in both lung and liver does not affect long-term accumulation of Ce in liver following pulmonary exposure

2. Primary genotoxicity in the liver following pulmonary exposure to carbon black nanoparticles in mice

3. Histopathological changes in the liver following pulmonary, oral and intravenous exposure to three different nanoparticles in mice

3. MATERIALS AND METHODS

3.1 Characterization of particles used in the present study

In the present study we investigated liver toxicity following intratracheal, intravenous and oral exposure to three NPs: titanium dioxide (TiO_2), cerium oxide (CeO_2) and carbon black (CB). The test materials used in this work were selected due to the similarity in the primary particle size (Table 1). Moreover, CB was included as a reference material that has been extensively studied in our laboratory and due to the elicited genotoxicity in the liver tissue previously observed after inhalation and intratracheal instillation. Similarly to CB NPs both TiO_2 and CeO_2 were also used in the previous studies conducted by our research group (NANOSUSTAIN and HINAMOX projects, respectively) but in contrast to CB NPs, TiO_2 as well as CeO_2 NPs are easily detectable by inductively coupled plasma mass spectrometry (ICP-MS), the major analytical technique used in this work to qualitatively determine deposition of particles in the selected tissues.

Table 1. Key physicochemical parameters of the tested nanomaterials

	TiO_2	**CeO_2**	**CB**
Source	NanoAmor[b]	Degussa/Quimidroga[a]	Evonik-Degussa
Product form	Powder	powder	Powder
Primary particle size	10.5 nm[b]	13.0 ± 12.1 nm[a]	14 nm[d]
Specific surface area	139.1 m^2/g [b]	56.7 m^2/g[a]	295 m^2/g[e]
Particle density	4,23 g/cm^3 [f]	7.29 g/cm^3 [a]	2.1 g/cm^3 [e]

[a] [97]; [b] [98]; [c] [99]; [d] [100]; [e] [101]; [f] [102]

3.1.1 Titanium dioxide (TiO_2)

TiO_2 is produced in large quantities and extensively used as a whitening agent due to its brightness and high refractive index [24]. It is an important component of paints, coatings, cosmetics (sunscreen, toothpaste) and pharmaceuticals [103]. Moreover, it has been approved as a food additive in Europe (also known as E171) used in candies and chewing gum [104] or as a pigment to whiten skim milk [103]. TiO_2 NPs have been classified by The International Agency for Research on Cancer (IARC) as possibly carcinogenic to humans (Group 2B) [105]. Several *in vitro* and *in vivo* studies reported TiO_2 NP-induced genotoxicity [106–109] and oxidative stress

[110–113]. Exposure to TiO_2 NPs was also linked to neutrophil infiltration [114,115] and pulmonary toxicity [80,114] as reviewed by Johnston [116].

3.1.2 Cerium oxide (CeO_2)

CeO_2 NPs are extensively used in several consumer products as polishing agents for glass mirrors, television tubes and ophthalmic lenses [117], oxygen sensors [118], diesel fuel catalysts to improve combustion and reduce consumption of fuels [117] and in solid oxide fuel cells [119]. The Organization for Economic Co-operation and Development (OECD) has recently included CeO_2 NPs among other particles as a high-priority nanomaterial that requires comprehensive toxicological evaluation [120]. It has been previously demonstrated that administration of CeO_2 particles caused inflammation [121–124], pulmonary damage and fibrosis [122,125], and *in vivo* and *in vitro* genotoxicity [126,127]. It was also reported by Nalabotu and co-workers [76] that intratracheal instillation of CeO_2 NPs resulted in decreased liver weight, histopathological alterations of the liver tissue and elevated level of ALT. Contradictory information has been published regarding anti-/pro-inflammatory properties exhibited by CeO_2 NPs. On the one hand several researchers reported CeO_2 NP-induced oxidative stress [124,128] however, other studies claimed therapeutic properties – cardioprotective, neuroprotective and retinoprotective – exhibited by CeO_2 NPs [129–131].

3.1.3 Carbon black (CB)

Carbon black NPs (CB NPs, including Printex 90 used in the present work) are carbonaceous core-particles that are formed by the controlled combustion. CB NPs are used principally as reinforcing agents in tires and other rubber goods. They are also often used as a black pigment in printing inks, paints, and plastics [132]. IARC recently classified CB NPs as potentially carcinogenic to humans [133]. It can serve as a benchmark material in the study of ultrafine air pollution [134] since the toxicity of CB NPs has been well described and evaluated by several *in vivo* and *in vitro* studies. It has also been documented that intratracheal instillation and inhalation of CB NPs was associated with increased recruitment of neutrophils to the site of exposure [46,135,136], genotoxicity [56,57,99] and induction of acute phase response [54]. Recent studies have shown that exposure to CB NPs caused substantial alterations in global

expression of pulmonary and hepatic genes such as changes in genes responsible for lipid homeostasis in lung and liver tissue or changes in expression of genes involved in the inflammatory processes [44,137].

3.2 Animal model and exposure routes

3.2.1 C57BL/6 mice

C57BL/6 (B6JBOM-F) female mice were used as an animal model since this strain is commonly used in our laboratory and therefore, it is easy to handle and maintain by our animal technicians. Moreover, direct comparison of the data obtained in this study with the previous findings was possible.

3.2.2 Exposure routes for NP administration

NP suspensions were administered via three different routes of exposure: intratracheal instillation, intravenous injection and oral gavage. Regardless the administration route all mice from the treated groups received a single dose of 162 μg of TiO_2, CeO_2, or CB NP suspension in a volume of 50 μl. Control groups received 50 μl of 2 % serum that was used as a vehicle for the preparation of NP suspensions. The dose used in the experiment is equal to the pulmonary deposition after nine 8-h working days at the Danish occupational exposure limit of 3.5 mg/m^3 for CB or after thirteen 8-h working days at the Danish occupational exposure limit of 10 mg/m^3 for TiO_2. Animals were euthanized after 1, 28 or 180 days following the exposure. A graphical presentation of the experimental set-up is shown in Fig. 3.

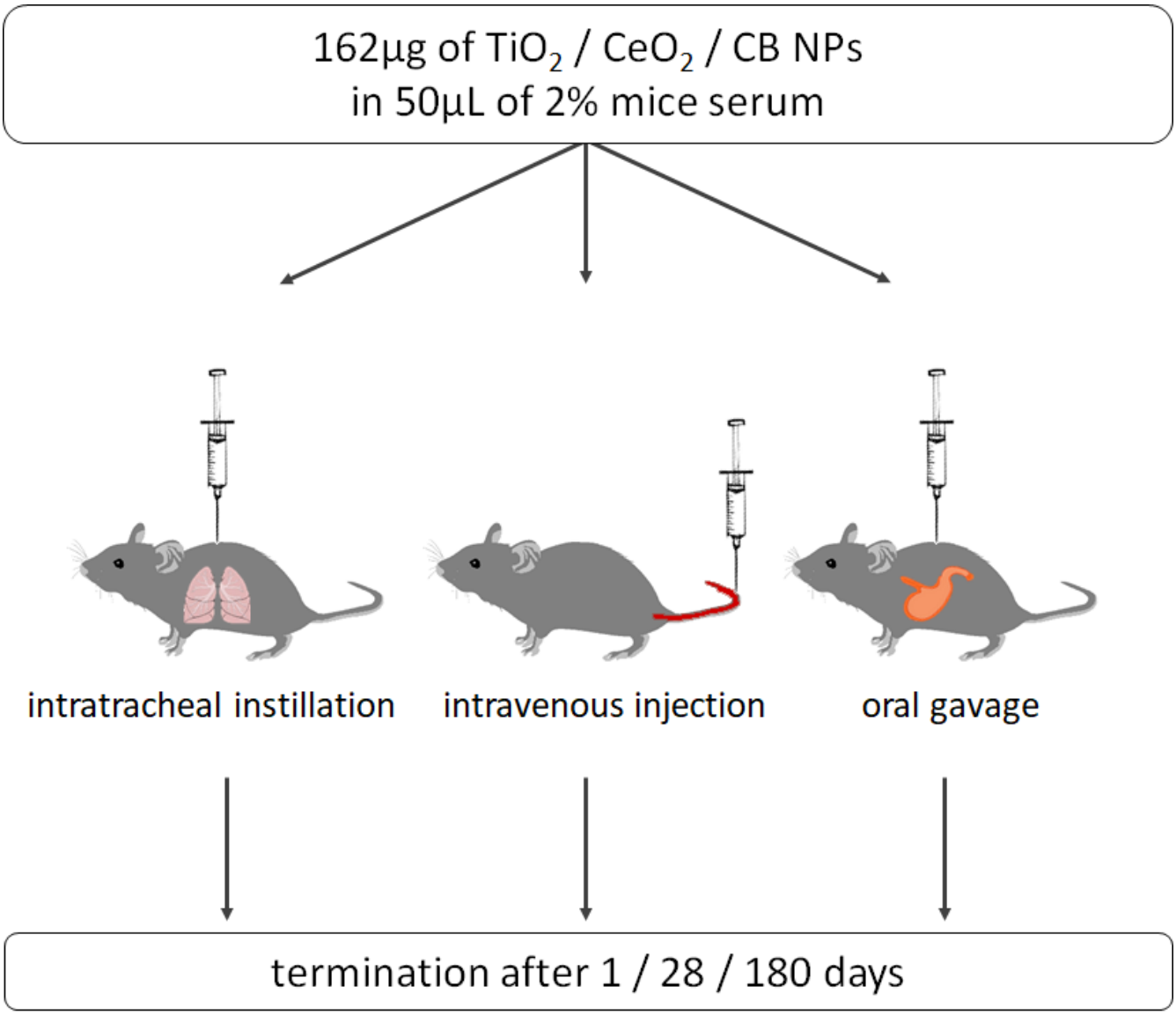

Figure 3. Overview of the experimental set-up used in the study.

3.3 Methods and techniques used in the present study

Table 2 presents an overview of the different methods used to determine the effects of NP administration in the liver and lung tissue as well as in blood and plasma collected from the exposed mice.

Table 2. Overview of the techniques and tissues used in the study

Tissue / Method	Liver	Lung	Blood	Plasma
ICP-MS	X	X		
spICP-MS	X	X		
EDFM	X	X		
Comet assay	X	X		
RT-PCR	X	X		
BFM	X	X		
Haematology			X	
Biochemistry				X

ICP-MS – inductively coupled plasma mass spectrometry, spICP-MS – single particle inductively coupled plasma mass spectrometry, EDFM – enhanced darkfield microscopy, RT-PCR – reverse transcriptase polymerase chain reaction, BFM – brightfield microscopy

3.3.1 Particle size determination by dynamic light scattering

Dynamic light scattering (DLS) was used to determine the hydrodynamic diameter (hydrodynamic since it refers to the movements of particles within a fluid) of NPs in the dosed suspensions. DLS relates the speed of particle diffusion due to the Brownian motions – random movements of particles due to the collision with surrounding solvent molecules, to the size of particles. Big particles are characterized by slow Brownian motions while small particles move much further and more rapidly. When the laser beam hits the particle the intensity of the scattered light fluctuations is measured followed by the determination of the geometrical structure and particle state of motion. In order to measure the hydrodynamic diameter the Stokes-Einstein equation is applied. The obtained hydrodynamic diameter is in fact a diameter of a sphere that has the exact same diffusion coefficient (velocity of the Brownian motions) as the measured particle [138,139].

3.3.2 Determination of NP presence in biological tissues

3.3.2.1 CytoViva® Enhanced Darkfield Hyperspectral Microscopy

Enhanced darkfield microscopy (EDFM) is a relatively new technique that enables optical detection of nanoparticles in biological tissues. EDFM compared to electron microscopy (EM) offers more rapid and less costly possibility to visualize and identify nanomaterials in different tissues. Even though EM could operate at higher magnification and resolution than EDFM, the cost of ownership and time needed for the training are in favor of EDFM [140]. Moreover, no additional sample preparation (e.g. labelling) is required since sample preparation for EDFM is the same as for the regular light microscopy. It also gives an opportunity to visualize particles that are difficult to detect by other methods (e.g. ICP-MS) such as CB NPs. In the present study we used a relatively new tool called CytoViva® Hyperspectral Microscopy (Auburn, Alabama, USA) that combined hyperspectral imaging technology with patented enhanced darkfield microscopy that in contrast to the conventional darkfield instruments provides images with better contrast and higher signal-to-noise ratio [141,142].

3.3.2.2 Inductively coupled plasma mass spectrometry

Inductively Coupled Plasma Mass Spectrometry (ICP-MS) is a powerful analytical technique that allows accurate quantitative and semi-quantitative determination of presence and content of most elements from the periodic table in virtually any material. The greatest advantages of this technique are: a very low detection limit (down to part per trillion = 1 ng/L), simultaneous measurement of different isotopes of the same element and high productivity. Liquid sample is introduced with a peristaltic pump and breaks into fine droplets by a nebulizer before entering the argon plasma. Plasma, that operates at 6000 °C, dries the sample, dissociates the molecules, removes an electron from the components and forms singly charged ions. Once ions are produced in plasma they are directed to the mass spectrometer via the interference region that ensures efficient transport of ions. Before entering the final chamber where the mass spectrometer and detector are placed, an ion deflection device separates ions from neutrals and photons to achieve the highest performance of the instrument and to decrease the background noise. The mass spectrometer is a filtering device that allows only analyte ions of a specific mass-

to-charge ratio (m/z) to reach the detector separating all the non-analyte, interfering and matrix ions away. Emerging from the mass spectrometer ions strike the active surface of the detector and electronic signal is generated. Thereafter, data handling software translates the electronic signal into the analyte concentration using ICP-MS calibration standards with the known contents of the analyte [143–145].

3.3.2.3 Single particle inductively coupled plasma mass spectrometry

ICP-MS can also operate at, so called, single particle mode (spICP-MS, single particle inductively coupled plasma mass spectrometry) that allows not only detection and quantification of NPs but also their physicochemical characterization [146]. It measures the size of NPs (if shape is known or assumed), assesses agglomeration and/or size distribution and allows differentiation between signal generated by soluble ions (background) and single particle [147]. In the conventional ICP-MS multiple intensity readings are integrated over long time intervals (i.e. dwell time of 0.3 – 1 s) and an averaged continuous signal is generated for the analyte (Fig. 4a). In contrast, when operating at the single particle mode each intensity reading is integrated over short dwell times (i.e. 10 ms or less) resulting in a separate peak for each detected particle (Fig. 4b) [148,149].

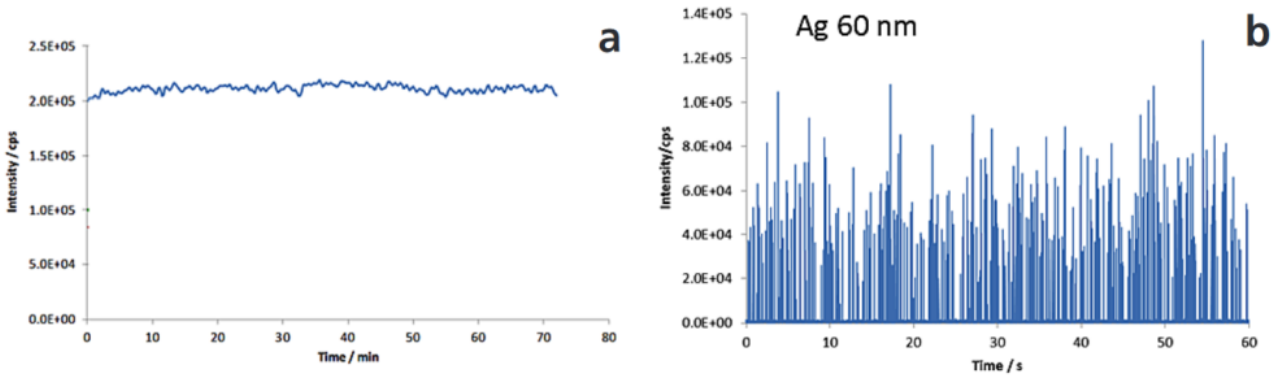

Figure 4. ICP-MS signal from measuring a dissolved analyte (a), a signal from measuring 60 nm Ag NPs (b) (reproduced from: [149]).

The fundamental assumption behind spICP-MS analysis tells that if the dwell time is short enough, constant flow rate is assured and particle suspension is sufficiently diluted each pulse represents a single particle event. If the assumption is correct then pulse frequency can be

directly translated into particle/aggregate number concentration and height (i.e. intensity) of each pulse can be directly referred to particle size (mass) [148].

3.3.3 Assessment of particle-induced toxicity

Several toxic endpoints (i.e. inflammation, acute phase response, genotoxicity, alterations of blood parameters, changes in liver biochemistry and histopathological evaluation of exposed tissue) were determined in order to evaluate systemic deleterious effects elicited by exposure to NPs.

3.3.3.1 BAL fluid cellular composition – assessment of pulmonary inflammation

Lung inflammation is characterized by the recruitment of inflammatory cells, primarily polymorphonuclear neutrophils and alveolar macrophages, and is a common response to pulmonary exposure to NPs [53,100,150].

Assessment of pulmonary inflammation was accomplished by the determination of bronchoalveolar lavage (BAL) fluid cellular composition. Lungs from control and NP exposed mice were flushed twice with sterile saline (0.8 ml of 0.9 % of NaCl) and BAL cells were separated on microscope slides by centrifugation, fixed in ethanol and stained with May-Grünwald-Giemsa dye. Cellular composition (i.e. number of macrophages, neutrophils, lymphocytes and eosinophils) was determined on 100 cells under light microscope using the differential counting method.

3.3.3.2 Comet assay – assessment of genotoxicity

Comet assay (also known as a single cell gel electrophoresis) was used to analyze DNA strand breaks (DNA SB) and alkali-labile sites in the liver, lungs and BAL cells collected from mice exposed to NPs. It has been demonstrated that exposure to NPs is associated with the induction of genotoxic effects [54,57,62,151] and presence of DNA lesions is a crucial step in cancer development [152,153].

In a standard comet assay procedure selected tissue is homogenized to yield single cells that are subsequently encapsulated in a low-melting point (LMP) agarose and embedded on a microscope

slide. When the agarose is solidified, the slide is submerged in a lysis solution that contains a high salt and detergent concentrations in order to lyse cell membranes. Prior to electrophoresis, the slide is incubated in an alkaline solution (pH > 13) to unwind the DNA. Alkaline environment is also maintained during electrophoresis where negatively charged DNA migrates towards the positively charged anode. Following electrophoresis, the slide is neutralized, fixed and stained with a fluorescent dye to allow visualization and scoring by a fluorescent microscopy. The obtained image resembles a "comet" where the "head" represents intact DNA and the "tail" represents DNA SB. The amount of DNA liberated from the nuclei during electrophoresis is proportional to the amount of damaged DNA [154–156].

3.3.3.3 Real time RT-PCR – assessment of pulmonary and hepatic acute phase response induction

Particle-induced pulmonary acute phase response is a common organismal response to the lung-administered NPs [46]. It has also been hypothesized that lung inflammation followed by induction of pulmonary acute phase response arising after exposure to NPs could evoke production of cytokines, that in turn, induce acute phase response in the liver [4,157].

Serum amyloid A (SAA) is one of the major acute phase response proteins [48] and therefore, in the present study, we investigated alterations of pulmonary *Saa3* and hepatic *Saa1* mRNA expression levels by the real time reverse transcription polymerase chain reaction (real time RT-PCR).

RT-PCR is a standard method used for detection and quantification of target mRNA in order to determine gene expression level. The biggest advantages of this technique are: high sensitivity, accurate quantification and possibility to scale-up the analysis (high-throughput method). In principle, the major aim of the analysis is to follow formation of PCR-products that are amplified in each PCR cycle. It is a two-steps method. First step is a reverse transcription of isolated mRNA into complementary DNA (cDNA). Thereafter, cDNA is used as a template in a PCR reaction. In the present study, 18S rRNA was used as a reference gene to normalize the quantity of the template loaded to each reaction and to reduce variation of reverse transcription efficiency. 18S rRNA,

together with β-actin, glyceraldehyde-3-phosphate dehydrogenase (GAPDH), hypoxanthine-guanine phosphoribosyl transferase (HPRT), belongs to, so called, housekeeping genes group, that is characterized by a constitutive expression level unaffected by the treatment. In order to monitor progress of PCR reaction and to be able to quantify the expression level of reference (18S rRNA) and target (Saa) genes specific TaqMan® probes (Applied Biosystem) were used. Each probe consists of a fluorescent reporter dye attached to the 5' end and a quencher dye attached to the 3' end. As long as the reporter dye and quencher stay in a close proximity, fluorescent signal is repressed. However, during the PCR cycle complementary to the cDNA strand is amplified by a *Taq* DNA polymerase with endonuclease activity that cleaves the reported dye away from the quencher and thereby fluorescence can be emitted. Two major parameters characterize RT-PCR reaction: baseline and threshold cycle (C_t). Baseline refers to the number of cycles where the fluorescence is not detectable (is below detection limit of the instrument). C_t refers to the number of cycles where the fluorescent signal is above background fluorescence and is detected for the first time (threshold level of detection) [158–161]. In order to evaluate results of the PCR analysis, the target gene was first normalized to the 18S rRNA using the following equation: $\Delta C_t = C_{t\ target} - C_{t\ reference}$. Thereafter, relative gene expression was determined using the comparative Ct method ($2^{-\Delta Ct}$) [162].

3.3.3.4 Brightfield microscopy – assessment of particle-induced histopathological changes

Several previous studies demonstrated NP-induced histopathological changes in the liver and lung tissue that occurred upon exposure [76,88,163]. In order to evaluate particle-related changes in the liver and lung tissue, microscopic evaluation using brightfield microscopy was performed.

Briefly, on the termination day small chunks of the liver tissue were sampled and fixed by submerging in 4 % neutral formalin buffer for 24h. Thereafter, samples were dehydrated and embedded in paraffin blocks. Lungs were removed intact, filled with formalin and submerged in 4 % neutral buffered formalin. Liver and lung tissue sections of 4–6 µm thickness were cut and stained with hematoxylin and eosin.

3.3.3.5 DCFH-assay – assessment of ROS generation ability exhibited by NPs

NP-induced oxidative stress (imbalance between generation of ROS induced by NPs and ability of biological systems to detoxify the reactive mediators) is presently considered as a main mechanism of genotoxicity caused by exposure to NPs [164]. Therefore, we measured the ability of NPs to generate ROS in a cell-free environment by the 2',7'-dichlorofluorescein (DCFH) assay.

2',7'-dichlorofluorescein diacetate (DCFH-DA) is a non-polar, non-fluorescent compound that easily crosses cell membranes and is chemically hydrolysed (by NaOH) to polar, non-fluorescent 2′,7′-dichlorodihydrofluorescein ($DCFH_2$) that is trapped within the cells. In the presence of particle-generated ROS, $DCFH_2$ is rapidly oxidized to highly fluorescent 2',7'-dichlorofluorescein (DCF). The emitted fluorescence is spectrofluorimetrically measured. Excitation and emission wavelengths are λ_{ex} = 490 nm and λ_{em} = 520 nm, respectively [165].

3.3.3.6 Haematology and biochemistry – assessment of general biomarkers for particle-induced toxicity

Previous studies reported minute alterations of general blood parameters following exposure to NPs [74,166–169]. In the present study levels of basic haematological parameters including white blood cells (WBC), red blood cells (RBC), hemoglobin (HGB), hematocrit (HCT), mean corpuscular volume (MCV), mean cell hemoglobin (MCH), mean corpuscular hemoglobin concentration (MCHC) and platelets (PLT) were determined in order to evaluate welfare of animals exposed to NPs.

In order to measure the core blood parameters, blood from the facial vein (~ 100 µl) was sampled and collected in EDTA tubes to prevent clot formation. Prior to the analysis blood was rotated for 20 min to equally distribute the EDTA powder. Subsequently, the abc™ Animal Blood Counter instrument (Horiba Abx, Scil Abc Vet Animal Blood Counter) was used to measure the selected blood biomarkers.

Changes in the basic clinical biochemistry parameters after exposure to NPs were formerly described [76,170]. Levels of the three major liver enzymes, i.e. alanine aminotransferase (ALT), alkaline phosphatase (ALP) and aspartate aminotransferase (AST), were determined in the

present study. Liver enzyme activities were measured in plasma from mice exposed by intratracheal instillation, intravenous injection and oral gavage, and terminated 28 days after exposure using Pentra 400 (Horiba ABX, Montpellier, France) with commercially available kits (Horiba ABX Medical, Montpellier, France; catalogue no. A11A01627, A11A01626 and A11A01629, respectively). Samples from each exposure group were run in the same batch in random order to decrease variation and a control sample was included for every 15th sample.

4. SUMMARY OF RESULTS

The main findings accomplished in this PhD project are listed below. More detailed description of the performed experiments and collected results can be found in the attached manuscripts.

4.1 Manuscript 1

In vivo-induced size transformation of CeO_2 NPs in both lung and liver does not affect long-term accumulation of Ce in liver following pulmonary exposure

The main purpose of this study was to investigate liver deposition of cerium oxide (CeO_2) and titanium dioxide (TiO_2) NPs following intratracheal instillation. CeO_2 and TiO_2 NPs exhibit similar primary particle size (13 and 10.5 nm, respectively) but different chemical composition, shape and potential differences in their solubility might affect hepatic accumulation. In addition, we wanted to assess possible changes in size distribution of liver- and lung-deposited CeO_2 NPs.

Orally exposed groups were included in the study to evaluate if the presence of particles in the liver could be explained by the swallowing of a portion of lung-deposited particles as a result of mucociliary escalator-mediated clearance that would lead to the secondary exposure via GIT. Intravenously administered groups were included as reference groups to assess the amount of particles that reach the liver bypassing the extrapulmonary translocation.

Presence of particles translocated from lung to the liver was confirmed by enhanced darkfield microscopy (EDFM) whereas inductively coupled plasma mass spectrometry (ICP-MS) determined mass concentration of Ce and Ti sequestrated in the liver tissue. EDFM analysis revealed that the foreign material was predominantly found in the liver sinusoids and often in close proximity to small nuclei, probably phagocytized by Kupffer cells (Fig. 5). ICP-MS analysis showed elevated concentration of Ce detected in the liver tissue 28 and 180 days post-exposure and elevated concentration of Ti detected in the liver tissue 180 days post-exposure (Fig. 6A and B). Calculated translocation rates were comparable and stood at 2.87 ± 3.37 % and 1.24 ± 1.98 % of the initial pulmonary dose for CeO_2 and TiO_2 NPs, respectively. No NPs were detected in the liver following oral gavage. Analysis of CeO_2 NP size distribution revealed that the size of

particles had decreased over time in both liver and lung tissue resulting in the onset of smaller particles (Fig. 7A and B).

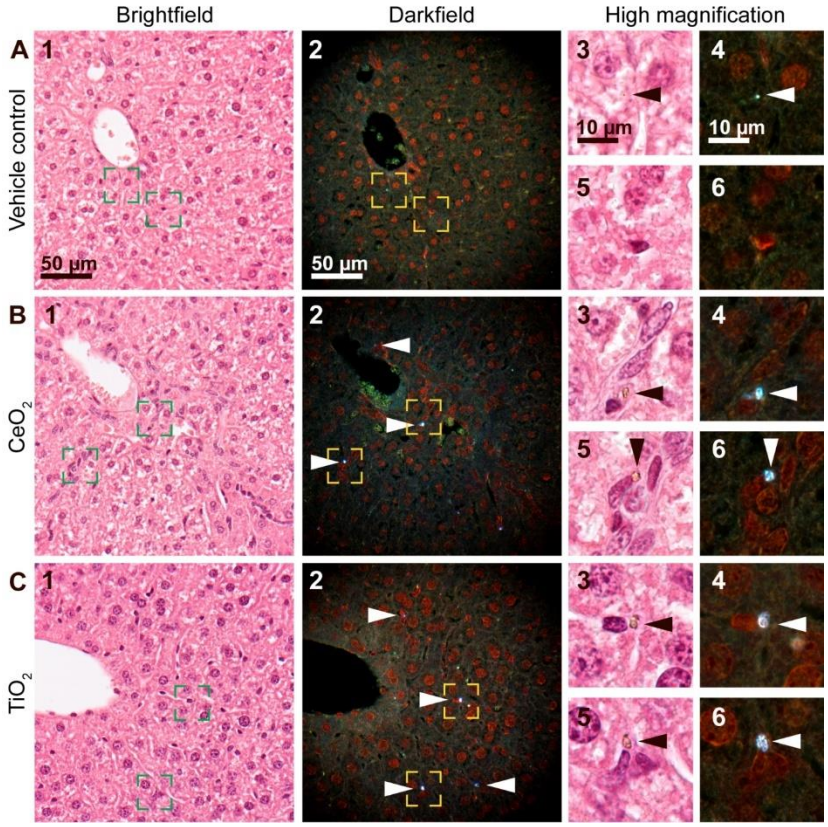

Figure 5. Brightfield (1) and enhanced darkfield (2) microscopy images of H&E stained liver tissue from intratracheally instilled mice that received a control vehicle (A) or 162 µg/animal of CeO_2 (B) or TiO_2 (C) NPs at 180 days post-exposure. In the liver sections from mice exposed to CeO2 and TiO2 foreign material aggregates were observed using enhanced darkfield microscopy, mainly in sinusoids and often close to small nuclei (B and C, respectively, 2, 4 and 6, white arrowheads). The aggregates were not detectable in brightfield at 40x magnification (B1, C1) but exhibited a brownish appearance at 100x magnification (B and C, 3 and 5, black arrowheads). Appearance of a typical artefact is shown (A, 3-4, arrowheads). Panels 3-6 correspond to the rectangular zones in panel 1-2 captured at higher magnification.

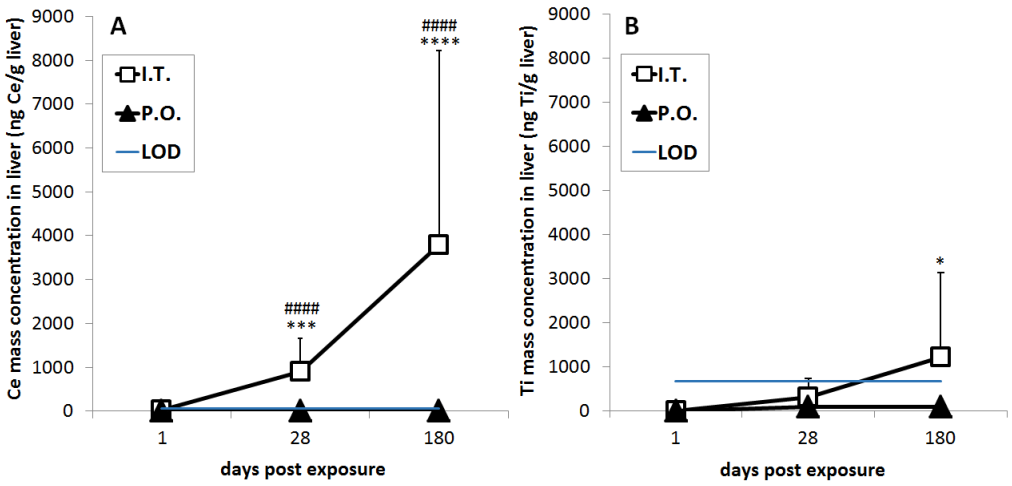

Figure 6. Mass concentration of Ce (A) and Ti (B) in the liver tissue measured by ICP-MS following intratracheal instillation and oral gavage of CeO2 and TiO2 NPs, respectively. Data are presented as mean + SD. An asterisk (*) denotes P ≤ 0.05, (***) P ≤ 0.001, (****) P < 0.0001 of Ce or Ti mass concentration in exposed groups compared to vehicle controls. Hashtags (###) denote P < 0.001 and (####) P < 0.0001 of Ce mass concentration in intratracheally exposed group (IT) compared to orally exposed groups (PO). LOD – Limit of detection.

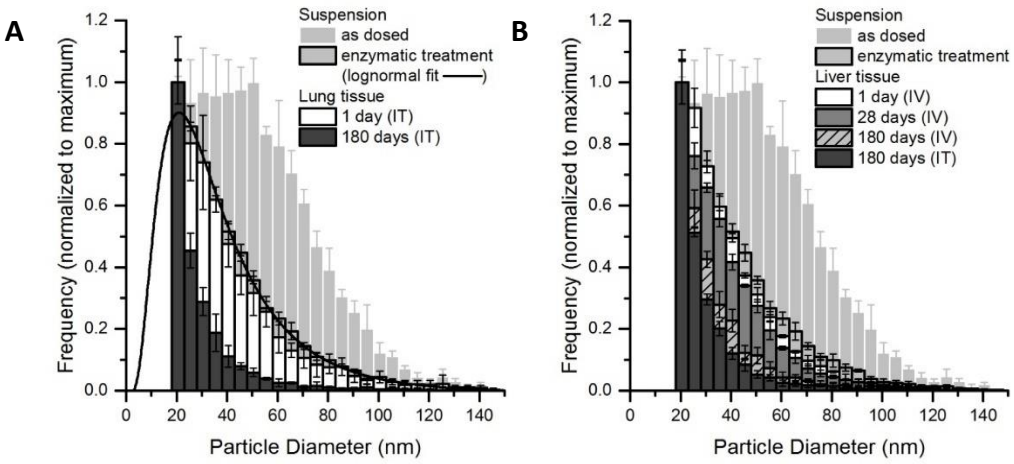

Figure 7. Particle size distribution of CeO_2 NPs in lung tissue (A) 1 day (N=6) and 180 days (N=4) after intratracheal instillation and in liver tissue (B) 1 day (N=3), 28 days (N=2), 180 days (n=3) after intravenous injection and 180 days (N=5) after intratracheal instillation measured by spICP-MS and normalized to the maximum of the distribution. The particle size distribution of CeO_2 NPs in the dosed suspension with and without enzymatic treatment is shown for comparative reasons.

4.2 Manuscript 2

Primary genotoxicity in the liver following pulmonary exposure to carbon black nanoparticles in mice

The major objective of this study was to determine the exact mechanism responsible for the genotoxic effect previously observed in the liver following pulmonary exposure to NPs. Two distinct mechanisms have been proposed:

- primary genotoxicity mechanism due to physical interaction between particles and genomic DNA and by ROS-mediated DNA damage in the absence of inflammation;
- secondary genotoxicity mechanism due to particle-induced systemic inflammation and acute phase response with subsequent release of various secondary mediators (ROS/RNS, cytokines, chemokines) that are capable of inducing downstream toxic effects resulting in DNA damages in the liver.

Therefore, we investigated induction of pulmonary inflammation, pulmonary and hepatic acute phase response and genotoxicity following intratracheal (IT), intravenous (IV) and oral (PO) exposure to TiO_2, CeO_2 and CB NPs.

All three NPs elicited similar level of pulmonary inflammation in terms of increased neutrophil influx that lasted up to day 28 and had decreased in a time-dependent manner. Sustained pulmonary acute phase response was measured for all NPs and was observed up to day 180 (Fig. 8A). An interim induction of hepatic acute phase response was measured on day 1 in IT and IV exposed groups to TiO_2 and CeO_2 NPs (Fig. 8B). Furthermore, an increased number of DNA strand breaks was found only in the CB groups exposed by IV and IT (Fig. 9A and B). Unlike the TiO_2 and CeO_2 NPs, only CB NPs were capable to induce production of ROS in the cell-free assay.

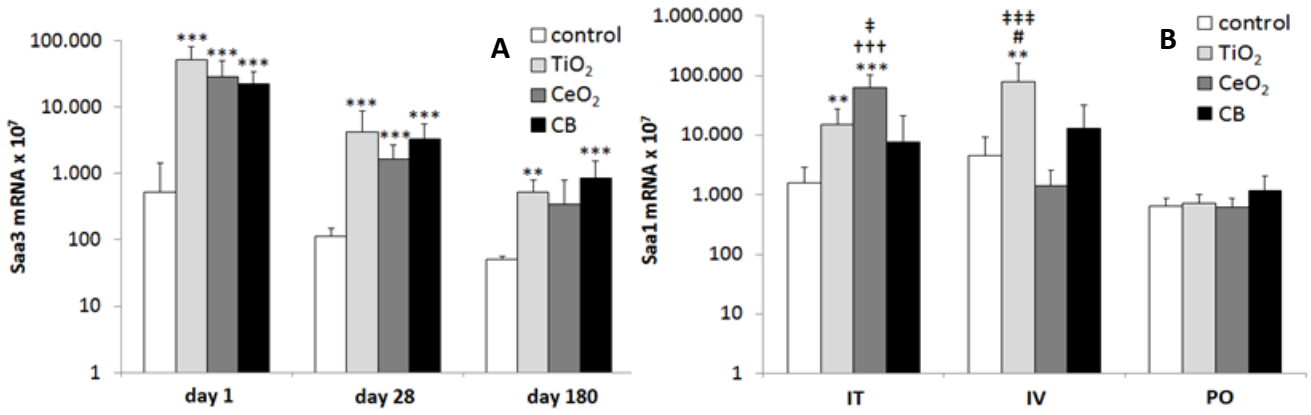

Figure 8A. Pulmonary *Saa3* mRNA expression levels in mice following IT administration of 162 µg of TiO_2, CeO_2 or CB NPs 1, 28 and 180 days after the exposure and **B** Hepatic *Saa1* mRNA expression levels in mice following IT, IV and PO of 162 µg of TiO_2, CeO_2 or CB 1 day after exposure. All values are presented as mean + SD. Asterisks (**) denote P ≤ 0.01 and (***) P ≤ 0.001 of *Saa1*/*Saa3* mRNA level in exposed groups versus vehicle control. Hashtag (#) denotes P ≤ 0.05 of *Saa1* mRNA level in TiO_2 vs CB groups. Crosses (†††) denote P ≤ 0.001 of *Saa1* mRNA level in CeO_2 vs CB groups. Double cross (‡) denotes P ≤ 0.05 and (‡‡‡) denote P ≤ 0.001 of *Saa1* mRNA level in TiO_2 vs CeO_2 groups.

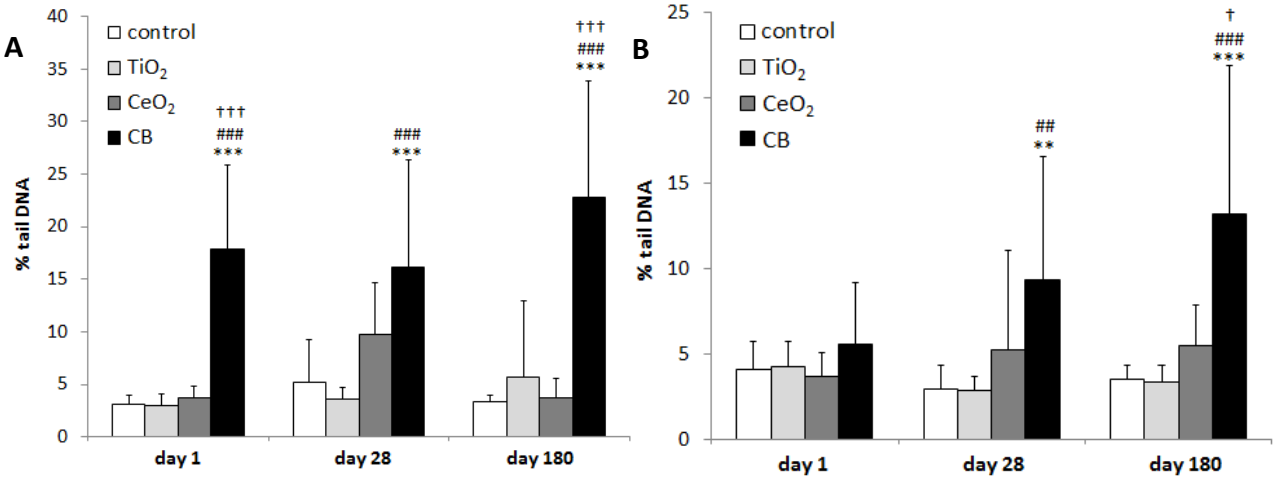

Figure 9. DNA strand break levels (% tail DNA) in the liver tissue detected by comet assay following **A** intravenous injection and **B** intratracheal instillation of 162 µg of TiO_2, CeO_2 or CB NPs measured 1, 28 and 180 days after exposure. Particle exposed groups n=9, vehicle control n=9. All values are presented as mean + SD. Asterisks (**) denote P ≤ 0.01, (***) denote P ≤ 0.001 of DNA SB level in exposed groups versus vehicle control. Hashtags (##) denote P ≤ 0.01, (###) denote P ≤ 0.001 of DNA SB level in TiO2 vs CB groups. Cross (†) denotes P ≤ 0.05, (†††) denote P ≤ 0.001 of DNA SB level in CeO_2 vs CB groups.

4.3 Manuscript 3

Histopathological changes in the liver following pulmonary, oral and intravenous exposure to three different nanoparticles in mice

In this study we investigated potential toxicological consequences of short- and long-term deposition of NPs in the liver. Therefore, several systemic and liver-related endpoints were evaluated including: assessment of body and liver weight (absolute and relative liver weight), analysis of selected haematological and biochemical parameters and histopathological examination of lung and liver tissue.

We found no significant changes in body weight of mice exposed by IT, IV and PO at any of the analyzed time points. Only oral administration of TiO_2 NPs decreased absolute and relative liver weight, 28 and 180 days post-exposure, respectively, whereas exposure to CeO_2 and CB NPs had no significant effects on the organ mass. Occasional and minor alterations in a few blood markers were measured. In addition, there were no significant changes in any of the analyzed biochemical parameters measured 28 days post-exposure.

Histopathological examination of the lung tissue revealed presence of inflammatory changes. Liver tissue examination (Fig. 10) showed high incidence of inflammation in both control and NPs exposed groups regardless of the exposure route and the origin of inflammation remained unclear. Similarly, necrotic changes could not be unambiguously related with the treatment since increased numbers of necrotic changes were also noted in the control groups. An increased number of binucleate hepatocytes, a common finding in aging mice, was seen on day 1 and it might indicate hepatocytic regeneration typically seen after a toxic insult. Hypertrophy of Kupffer cells observed 1 day following IV exposure to TiO_2 and CB NPs could be related to the phagocytosis of NPs.

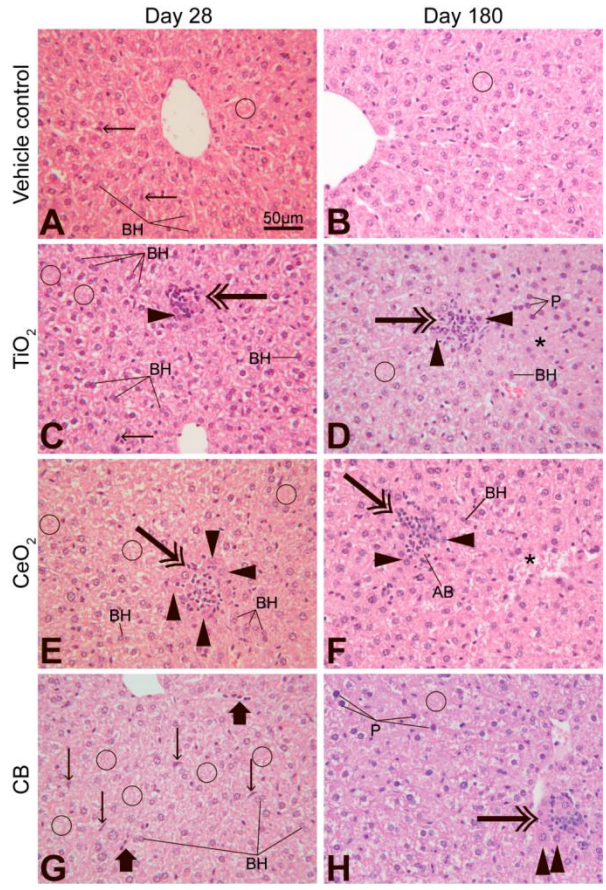

Figure 10. Microscopic changes in the liver of mice 28 or 180 days after single intratracheal instillation (IT) of a vehicle (A-B), TiO2 (C-D), CeO2 (E-F) or CB (G-H) NPs. A-B: microfoci of necrosis (circles), hypertrophy of Kupffer cells (tiny arrows), binucleate hepatocytes (BH). C-D: PNCF (double arrows), eosinophilic necrosis (arrowheads), microfoci of necrosis (circles), pyknosis of nuclei (P), hyperplasia of Kupffer cells (thick arrow), binucleate hepatocytes (BH), vacuolar degeneration (white spaces in hepatocytes). E-F: PNCF (double arrows), eosinophilic necrosis (arrowheads), microfoci of necrosis (circles), area of necrosis (asterisk), binucleate hepatocytes (BH), apoptotic body (AB). G-H: PNCF (double arrow), eosinophilic necrosis (arrowheads), microfoci of necrosis (circles), hypertrophy of Kupffer cells (tiny arrows), hyperplasia of Kupffer cells (thick arrows), pyknosis of nuclei (P), vacuolar degeneration (white spaces in hepatocytes). HE staining, scale bar in A applies to all images.

5. DISCUSSION

The main objectives of my PhD study were to evaluate potential toxicological effects of NP deposition in the liver following pulmonary exposure as well as to determine the specific mechanism for particle-induced genotoxicity in the liver that has been previously observed following pulmonary exposure to TiO_2 and CB NPs [54,57,150].

5.1. Experimental set-up

Inhalation is a physiological route of exposure to NPs present in the ambient air. Therefore, most studies on pulmonary exposure to different NPs frequently use inhalation as a major administration route. The biggest advantage of the inhalation is the fact that it provides a natural way for the delivery of foreign materials thus deposition, distribution and clearance pattern resemble real-life scenario. However, this exposure method is often more time consuming, considered to be more expensive since larger quantities of the test materials are required and it also carries risk of unintended exposure for workers. The major limitation of the inhalation technique is the difficulty to precisely determine the deposited dose. Possibly dermal and/or fur contamination may occur during the procedure which could increase the delivery dose and subsequent fur grooming could lead to the GIT exposure [171].

Intratracheal instillation, in contrast to inhalation, allows precise control of the delivery dose. Because in our study we exposed mice via three different routes it was of utmost importance to accurately determine the administered dose in order to directly compare results from different exposure groups. In addition, intratracheal instillation allows administration of different materials within a short window-time, requires small quantities of test substance and is safe for staff performing the procedure [171]. It has also been demonstrated that intratracheal instillation resulted in even distribution in all lung lobes [172,173]. The obvious disadvantage of intratracheal instillation is the unnatural distribution of instilled material compared to the inhalation exposure – all particle, regardless size, are deposited deeper in the lungs. It bypasses upper respiratory tract regions: nasal and pharynx, that are naturally exposed to particles upon inhalation [171].

Despite existing differences in pulmonary exposure by inhalation and intratracheal instillation [174] the latter is an accepted and commonly used method for pulmonary exposure to toxicants, including NPs.

Oral administration was included to evaluate the role of secondary oral exposure since it has been hypothesized that upon pulmonary administration a fraction of the deposited particles could be transported up from the respiratory tract via mucociliary escalator and, when swallowed, induce GIT exposure and lead to NP sequestration in the liver [4]. Moreover, the oral route is relevant for NPs contained in food and water [175,176] or used as a drug component [177].

Exposure via intravenous injection was included in the present study to evaluate toxicological effects and to determine clearance rate of particles accumulated in the liver. Several studies documented that NPs could reach the blood circulation after pulmonary exposure [13,178]. Intratracheal instillation of 30 nm gold particles in rats resulted in the presence of a vast amount of administered NPs in the platelets of pulmonary capillaries [179]. When NPs reach the systemic circulation they are distributed throughout the body with liver followed by spleen being the major organs for particle deposition [4]. Intravenous injection is also the quickest method to deliver chemicals and is relevant for diagnostic and biomedical applications of NPs [4,180,181].

Three types of NPs, i.e. titanium dioxide (TiO_2), cerium oxide (CeO_2) and carbon black (CB), were used in the study. The chosen particles exhibit similar primary size (10.5 - 14 nm), are produced in large quantities and widely used in versatile industrial and consumer products. Moreover, our research group used TiO_2 and CeO_2 in the previous studies (NANOSUSTAIN and HINAMOX projects, respectively), where a detailed physicochemical characterization was performed. CB is a benchmark nanomaterial extensively used by our group in many toxicological evaluations [100,134]. Therefore, historical data to compare results from this study exist. Moreover, CB NPs were chosen because they consistently induced DNA SB in the liver [54,57,136]. TiO_2 and CeO_2 are easily detected by the applied analytical technique - ICP-MS - that allows accurate quantitative analysis of particles in biological tissues. Detection of CB NPs by ICP-MS due to the high abundance of carbon in the ambient air was not possible. We did not decide to label CB NPs

due to the risk of leakage or dissociation of the label from NPs that might skew the data interpretation [182,183]. Instead, we included CytoViva Enhanced Hyperspectral Microscopy to confirm the presence of all three NPs in the selected tissues.

C57BL/6 (B6JBOM-F) female mice were chosen as an animal model for the present study since this strain is commonly used in our laboratory. Therefore, direct comparison with the previous findings was possible. Mice share many common genetic as well as physiologic, anatomic and metabolic features with the humankind that make the extrapolation of the results from animal to human studies easier than from e.g. *in vitro* studies. Moreover, rats have a tendency for particles overload thus mice are a more suitable model to study effects of particle exposure [184]. 324 mice were used in the study and one could think of the future reduction of number of mice used in the experimental work by using methods that enable obtainment of comparable levels of knowledge from fewer animals and replacement by using well established cell lines or computer models that allow prediction of toxic effects of chemicals (The 3R method).

Regardless the exposure route all mice received a single dose of 162 μg of TiO_2, CeO_2 or CB NP suspension in a volume of 50 μl. Control mice received 50 μl of 2 % serum that served as a vehicle for the preparation of the NP suspensions. The chosen dose used in this work is equal to the pulmonary deposition during thirteen 8-h working days at the Danish occupational exposure limit of 10 mg/m^3 for TiO_2 or during nine 8-h working days at the Danish occupational exposure limit of 3.5 mg/m^3 for CB. These dose calculations assume that 33.8 % of the inhaled particulate matter is deposited in the pulmonary region [151], that the inhalation of particulate air during 8-h work shift is 1.8 L/h [185] and that comparable deposition patterns exist in man and mouse. The dose is realistic for the occupational exposure and does not elicit acute toxic effects as we demonstrated in our study by the lack of adverse effects on basic haematological and biochemical parameters. The exposure concentration was carefully selected based on the previous studies from our research group that aimed in detection of inflammatory response, acute phase response and genotoxicity following exposure to NPs without evoking acute toxicity.

Previous studies [54,57,150] have shown that pulmonary exposure to CB and TiO_2 NPs caused oxidative stress and hepatic genotoxicity. However, they did not present any evidences for the

physical presence of translocated particles in the tissue where the toxic effects were observed. Therefore, it remained unclear whether the genotoxicity and observed toxic systemic effects were due to the direct interaction between particles and the distant tissue or rather by infiltration of circulating inflammatory cells and activation of signaling cascade as a result of pulmonary inflammation followed by acute phase response in the lungs. Hence, in the present study, we confirmed the presence of extrapulmonary translocated NPs in the liver after intratracheal instillation by ICP-MS and EDFM techniques.

Analytical methods play a pivotal role in filling gaps in toxicological knowledge regarding safety usage of nanomaterials before they are incorporated into consumer products. They are widely used to determine tissue concentration and composition of NPs (ex. ICP-MS, Electron-Dispersive X-ray Spectroscopy EDS), allow their visualization and localization within cells and tissues as well as provide crucial information about NP uptake (ex. Transmission Electron Microscopy TEM, EDFM) and last but not least, enable physicochemical characterization of nanomaterials (ex. spICP-MS, DLS, High Resolution Transmission Electron Microscopy HRTEM). Moreover, a combination of different techniques opens the door to the cognition of a "nanoworld" even widely [186]. Constant development of analytical methodology provide nanotoxicologists with new tools that enable deeper insight into the dynamic interface between particles and biological systems [187].

The robustness of the ICP-MS method in determination of particles concentration and chemical composition has been demonstrated by numerous research groups [188,189]. Therefore, in the present work we decided to use the ICP-MS technique to detect and to quantify concentrations of CeO_2 and TiO_2 NPs in the liver tissue.

Husain and co-workers [19] suggested that previously observed lack of evidence for the translocation of nano-TiO_2 to the liver [190] might be due to the high limit of detection caused by polyatomic interferences from other molecules of similar molecular weight. In my work Ce concentrations were measured by the regular ICP-MS instrument whereas Triple Quadrupole ICP-MS instrument was used to determine concentration of Ti in the liver and lung tissue. The selected tool is able to overcome polyatomic interferences that imperil accurate determination of

trace elements, as Ti. The use of ammonia as a reactive gas, removes the polyatomic interferences by the formation of Ti-ammonia clusters with higher, but unique, mass-to-charge ratio.

Darkfield microscopy combined with hyperspectral imaging (as applied in the CytoViva Enhanced Darkfield Hyperspectral Microscopy system, EDFM) is a novel yet powerful tool suitable for visualization and characterization of different nanomaterials in various complex matrices. Usefulness of the CytoViva method in the detection and characterization of Ti, Ce and Ag NPs has been previously demonstrated [191]. By using EDFM we proved that we are able to confirm the presence of all 3 NPs in the liver tissue after intratracheal instillation. This denotes the translocation of instilled particles from lungs to the liver. It was possible to track down particles even when presented in a low quantity due to the minor degree of translocation and therefore limited liver burden. We decided to use EDFM not electron microscopy (EM) because it offers more rapid and less costly possibility to visualize and identify nanomaterials in the tissue. Even though EM could operate at higher magnification and resolution than EDFM, the cost of ownership and time needed for the training are in favor of EDFM [140]. Moreover, no additional sample preparation is required since sample preparation for EDFM is the same as for the regular light microscopy. Light microscopy would not be suitable to accomplish the aim since it is inapplicable in characterization of nanomaterial dispersion due to its much lower spatial resolution [187]. So far, we were unable to create a reference spectral library, that consists of unique spectral signatures for each sample element and would allow us to precisely map all the foreign material in the analyzed tissues. Additional work is required to build the library in order to identify and localize NPs of the same chemical composition.

5.2 Biological implications following exposure to NPs

Pulmonary exposure to NPs is associated with the production of pro-inflammatory cytokines (i.e. tumor necrosis factor α - TNF-α, interleukin 1 β - IL-1β and interleukin 6 - IL-6) most likely by alveolar macrophages (AM) that engulfed inhaled or instilled particles [192]. However, a recently conducted study revealed that AM were not involved in the induction of the inflammatory response in lungs after intratracheal exposure to carbon NPs. Instead, type II (ATII) alveolar epithelial cells, that exhibited the highest induction of pro-inflammatory gene expression, could

be the initiators of acute neutrophilic pulmonary inflammation [193]. Upon secretion of pro-inflammatory mediators, the inflammatory reaction is further propagated by migration and egression of inflammatory cells (i.e. neutrophils and eosinophils) into alveolar space, to the sites of inflammation [194,195]. Ongoing lung inflammation leads to induction of pulmonary acute phase response [136]. It is characterized by the increased release of several cytokines and other mediators, collectively known as acute phase proteins, from the inflamed areas [48]. Many scientists suggested that pulmonary inflammation followed by systemic exposure to circulating cytokines induces, in turn, acute phase response in the liver [4,43,157]. However, several studies conducted in our research group have determined that pulmonary exposure to NPs is indeed associated with a strong and sustained acute phase response in lungs whereas no or negligible induction of hepatic acute phase response was observed [43]. On the contrary, strong induction of hepatic acute phase response was observed after exposure to multi-walled carbon nanotubes [58,196]. The possible reason for the divergent response between liver and lung tissue could be due to the different impact of particles on residing macrophages. Particles in the lungs are retrieved by the AM that in turn, impairs their phagocytic function [197,198], whereas phagocytic activity of Kupffer cells, resident liver macrophages, was not affected by the ultrafine CB NP accumulation [199].

Serum Amyloid A, SAA (murine Saa), is one of the major acute phase proteins. Saa is considered a murine homologue of C-reactive protein (CRP), the major marker used to assess acute phase response in human [200], that is only moderately affected by the various inflammatory factors in mice [43,201]. Previous research [43,45,46,56,202] demonstrated that *Saa3* mRNA was the most upregulated acute phase gene during pulmonary acute phase response and, frequently, the most differentially expressed gene. *Saa1* was the most differentially expressed acute phase response gene in the liver [58]. Therefore, we decided to use the expression level of *Saa3* mRNA as a biomarker to monitor development of pulmonary acute phase response and *Saa1* mRNA as a biomarker to monitor development of hepatic acute phase response [135,163].

Chronic particle-elicited inflammation in lungs leads to augmented systemic release of reactive oxygen species (ROS) and reactive nitrogen species (RNS) (and possibly other mediators) from

activated phagocytes (macrophages and/or neutrophils) and results in oxidative attack on genetic material evoking DNA damage (according to the mechanism of secondary genotoxicity). Nonetheless, in the absence of inflammation, genetic damage induced by NPs is also possible (according to the mechanism of primary genotoxicity). This may occur via direct pathways (i.e. physical interaction between particles and genomic DNA) or via indirect pathways (i.e. ROS production by metals or organic constituents) [203].

Pulmonary exposure is the most relevant route of exposure for particles present in the ambient air. This applies for both occupational exposure in the workplace and incidental exposure at the home address. Inhaled particles deposit in the pulmonary region and the deposition pattern strongly depends on particle size. Upon deposition particles are cleared from the respiratory tract by several defense mechanisms in order to keep the mucosal surfaces free from the foreign material. A fraction of lung-deposited particles is removed from the upper airways as a result of mucociliary escalator-mediated clearance. When the fraction is swallowed it results in secondary exposure through the GIT. Additionally, particles deposited in the alveolar region can cross the air-blood barrier and by getting access to the systemic circulation and to the regional lymph nodes are translocated to various secondary organs of the body. Most of the previous studies reported low rate of translocation of pulmonary-deposited particles. Particle translocation to the distant tissues strongly depends on size, shape, solubility and surface properties of administered nanomaterials.

It has been previously demonstrated by several scientists that liver is one of the major organs for sequestration of NPs translocated from lungs after pulmonary exposure as well as for NPs that reached the liver after intended administration (e.g. as a contrast or drug delivery agent). Several epidemiological studies showed that pulmonary exposure to NPs is strongly associated with the increased risk of respiratory and cardiovascular disorders [63,204] but there are many gaps in the knowledge regarding possible consequences of (long-term) hepatic accumulation of NPs and the exact molecular mechanism responsible for particle-induced liver toxicity has to be elucidated. Therefore, in the present study, we decided to focus our attention on the assessment of crucial endpoints related to the liver structure and function. Selected liver and systemic

endpoints, i.e. inflammation, acute phase response, genotoxicity, alteration of blood parameters, changes in liver biochemistry and histopathological evaluation of the exposed tissues, are common toxic effects elicited by NPs and numerous previous studies have shown their usefulness in the assessment of health risk posed by NP administration [46,54,76,100,205,206].

Liver, as a prominent metabolic center of the body, is involved in several crucial metabolic processes that maintain body well-being. Moreover, as a defense center is aligned in detoxification of xenobiotic and other foreign materials like NPs. Hepatic sequestration of a vast amount of NPs that entered the body makes the liver very prone to many diseases and cause disturbances in its normal functioning. A detailed mechanism by which NPs evoke liver diseases remains unclear due to the significant diversity of NPs and NP components.

Adverse hepatotoxic effects of ambient particulate matter (PM) air pollutants, including CB, have been demonstrated. Several studies using animal models showed that exposure to PM or CB is associated with the increased generation of ROS, oxidative DNA damage, production of pro-inflammatory cytokines, lipid peroxidation and alterations in lipid homeostasis, perturbations in glucose metabolism as well as with mutagenic and carcinogenic activity (as reviewed in [8]). Moreover, it has been demonstrated that ultrafine CB NPs exert prothrombotic changes on the endothelial surface of hepatic microvessels by inducing platelet accumulation in the hepatic microcirculation in mice in the absence of inflammatory response in the liver [199]. Such noxious effects of NPs could lead to the progression of manifold, both acute and chronic, liver diseases like hepatotoxicity, non-alcoholic fatty liver disease (NAFLD), type II diabetes, liver fibrosis and, eventually, liver cancer [8].

Air pollution, a complex mixture of thousands of chemical compounds including particles, has been classified by the International Agency for Research on Cancer (IARC) as a potent carcinogen [207]. While it is well documented that exposure to particulate matter air pollution is associated with lung cancer [63] occurrence of other cancers, like liver cancer, in relation to air pollution have been poorly studied. Even though the burden of translocated particles in the liver is several orders of magnitude lower than in the lungs, it might be sufficient to induce development of liver cancer. Previous epidemiological studies investigated the association between urban air

pollution and the onset of liver cancer [93–96,208]. Most of the studies concluded that the ambient air pollution was associated with a higher risk of liver cancer development. Moreover, meta-analysis of epidemiological studies with cigarette smokers showed that tobacco smoking is also associated with the increased risk of this cancer [209]. The possible explanation of how pulmonary exposure to NPs is associated with the carcinogenic process in the liver is extrapulmonary translocation of inhaled particles via systemic circulation and protracted elimination of NPs once deposited in the liver followed by induction of oxidative stress [210].

The three following tables (i.e. Table 3, Table 4, Table 5) summarize results from the relevant previous studies where NP-induced hepatotoxicity and other systemic toxic endpoints after exposure to TiO_2, CeO_2 and CB NPs were assessed. In general, all three NPs were able to induce a wide range of deleterious effects: inflammation, oxidative stress, genotoxicity, acute phase response, alterations of the liver tissue structure and changes in expression of various genes or biochemical parameters in the liver tissue. In the present study, we found that all three NPs elicited similar pulmonary inflammation that lasted up to day 28 after intratracheal exposure. Pulmonary acute phase response was observed also for the three NPs at all assessed time points. Negligible and transient induction of hepatic acute phase response was seen only on day 1 following intratracheal instillation and intravenous injection of TiO_2 and CeO_2 NPs. An increased number of DNA SB in the liver tissue was observed exclusively in CB exposed groups 28 and 180 days following intratracheal exposure and 1, 28 and 180 days following intravenous injection. Increased production of ROS was observed only for CB NPs. There were no alterations in any of the selected liver enzymes. Occasional and minor alterations in a few blood markers were measured. Histopathological changes in the liver tissue could not be explicitly related to NP exposure due to the high background of pathological changes in the control groups. Indications of NP presence in the liver tissue were found for all materials. Based on our results we concluded that pulmonary response (inflammation and acute phase response) was similar for all tested NPs whereas only CB NPs induced genotoxicity in the liver and increased the production of ROS. Apart from that, no overt liver or systemic toxicity was observed after exposure to TiO_2, CeO_2 or CB NPs.

Nemmar and Nalabotu [76,211] demonstrated that intratracheal instillation of CeO_2 NPs was associated with oxidative stress, inflammation, histopathological changes and genotoxicity in the liver tissue. However, in my study exposure to CeO_2 caused induction of pulmonary inflammation and acute phase response but negligible induction of hepatic acute phase response. No other hepatotoxic effects of CeO_2 administration were seen. The discrepancy between my study and their study could be due to the different physicochemical characteristics of CeO_2 NPs (e.g. surface area or shape) or animal model used in the mentioned studies (BALB/C mice and Sprague Dawley rats, respectively). Moreover, many researchers [212,213] have demonstrated antioxidant activity exhibited by CeO_2 NPs in scavenging of both ROS and RNS that could explain the lack of CeO_2 NP-induced ROS production observed in my study. Kumari, in the two selected experiments [126,214], found severe hepatotoxic effects after oral exposure of CeO_2 NPs. In contrast, in my study there were no noxious effects of CeO_2 NPs administration after oral exposure. However, the dose used in the Kumari study was extremely high, i.e. up to 2000 or 600 mg/kg bw, respectively, compared to 9 mg/kg bw administered in my study which could explain the observed differences. In the selected studies presented in Table 3 intravenous injection of CeO_2 NPs was associated with hepatic injury, oxidative stress and pathological lesions in the liver (granuloma formation, apoptosis) but as for the oral route, a relatively high dose of cerium, i.e. 85 or 100 mg/kg bw was used [128,215]. In the study performed by Hirst and colleagues [216] no overt toxicity was observed after intravenous or intraperitoneal administration of 0.5 mg/kg bw of CeO_2 NPs, a dose that is much more similar to the dose used in my study.

In the selected experiments presented in Table 4 pulmonary exposure to TiO_2 NPs resulted in oxidative stress and inflammatory response in the liver, changes in expression of genes involved in hepatic acute phase response and hepatic genotoxicity [19,150,217]. In contrast, Liang [218] and Yin [219] have shown that exposure to TiO_2 NPs had only little influence on the liver function. This is in a good agreement with my study where pulmonary administration of TiO_2 NPs was only related to the transient induction of hepatic acute phase response observed in the liver after day 1 but not after day 28 or day 180. Despite very low bioavailability reported for TiO_2 NPs after oral exposure [220], Cui [75,221], Wang [24,25], Sycheva [109] and Shrivastava [222] found several hepatotoxic effects of TiO_2 NPs following oral administration: liver inflammation, tissue

damage, oxidative stress, disturbances in the normal liver function and genotoxicity. In my study oral exposure to TiO_2 NPs resulted in decreased absolute and relative liver weight 28 days post-exposure. However, both Wang and Sycheva used a relatively high dose of TiO_2, i.e. 200 and 1000 mg/kg bw, respectively, that could elucidate the discrepancy. It is well known that size and surface area are closely related to the extent of toxic effects induced by NPs - the smaller the size/the larger the surface area is the greater toxicity could be evoked [25,223]. In the study conducted by Cui [75] the size of TiO_2 NPs was 5 nm and the surface area was 174.8 m^2/g (compared to 10.5 nm and 139.1 m^2/g for TiO_2 NPs used in my study) and exposure to these NPs resulted in severe damage of mice liver tissue. Moreover, the 10 mg/kg bw dose was administered intragastrically for 90 consecutive days thus the total exposure dose was much higher than I used. Discrepant results were also reported for the intravenously administered TiO_2 NPs. In the study conducted by Suzuki [224], Umbreit [225] and Elgrabli [226] no hepatotoxic effects of TiO_2 NPs were observed despite the fact that presence of Ti particles in the liver tissue was confirmed. On the other hand, both Xu [227] and Ma [88] reported acute liver toxicity followed by histopathological changes in the liver tissue, inflammatory response and alterations in basic haematological and biochemical parameters. However, also in this case, a high dose of TiO_2 was used, i.e. 1387 or 150 mg/kg bw, respectively. Umbreit and colleagues also injected high amount of TiO_2 NPs, i.e. 560 mg/kg bw, but apart from monitoring changes in body weight gain and histological evaluation of the liver tissue, they did not look for any other hepatic or systemic toxic endpoints. Liu and colleagues in the two selected studies [89,90] concluded that injection of TiO_2 NPs caused severe damage to the liver demonstrated by increased liver weight, changes in several biochemical parameters and induction of oxidative stress. These alterations were however observed in the high exposure groups (i.e 50, 100 and 150 mg/kg bw) and, in addition 5 nm NPs were used which could be a reason for the more pronounced toxicity.

Even though neither TiO_2 nor CeO_2 NPs induced genotoxicity in the liver tissue and no other severe signs of hepatotoxicity assessed in the present study were observed we cannot unambiguously classify them as safe. Numerous studies demonstrated gross toxicity of TiO_2 and CeO_2 NPs towards liver and other organs and contradictions in the obtained results could be due to the physical and chemical features that result in different biological responses even when

administered NPs are of the same chemical composition. Immensity of the physicochemical properties exhibited by NPs such as size, surface area, shape, structure and elemental composition makes the investigation and prediction of their noxious effects very complex and challenging.

Table 3. Summary of studies assessing CeO_2 NPs-induced toxicity

Ref.	Animal model	Route of exposure	Dose	Exposure time	NPs size (nm)	Assessed liver and other relevant systemic end-points
[211]	Balb/c mice	IT	0.5 mg/kg	24 h	20	* significant reduction of antioxidant SOD activity * significant increase of TNF-α and IL-6 levels * significant increase of DNA SB level in the liver tissue measured by comet-assay **Conclusion: intratracheal exposure to CeO_2 NPs induced oxidative stress, inflammation and genotoxicity in the liver tissue**
[76]	SD rats	IT	1.0/3.5/7.0 mg/kg	28 d	10 ± 1	* the highest dose significantly reduced liver weight * significant increase of liver ceria levels in the highest exposure group * significant elevation of serum ALT level, reduced ALB level, reduced TG level in the group exposed to 7.0 mg/kg CeO_2 and diminished Na:K ratio in all exposed groups * evidence of (dose-dependent) liver pathology: hydropic degeneration of hepatocytes around the central vein region with sparing of the immediate periportal region, enlargement of hepatocytes, enlargement of the nucleus in the hepatocytes, binucleation of some hepatocytes, dilatation of the sinusoids, occasional focal inflammation areas in a few of the exposed rats **Conclusion: intratracheal exposure to CeO_2 NPs may be associated with (dose-dependent) hepatotoxicity**
[126]	Wistar rats	PO	5 - 2000 mg/kg	14 d	23 ± 2	* rats exposed to the highest dose showed dullness, irritation, moribund symptoms and insignificant reductions in feed intake, bw gain and relative organ weight * tissue damage and focal areas of necrosis in the liver of rats exposed to the highest dose * significant increase of DNA damage at the dose of 1000 mg/kg in the liver cells and peripheral blood leukocytes (measured by comet assay), micronucleus formation in bone marrow and blood cells and total cytogenic changes in bone marrow * significant alterations of ALP and LDH activity in serum and GSH content in the liver at the highest dose * elevated CeO_2 concentration in the liver **Conclusion: oral exposure to CeO_2 NPs elicited genotoxicity, biochemical alterations and hepatic damage at the high dose level**
[214]	Wistar rats	PO	30/300/ 600 mg/kg	28 d	24 ± 2	* rats exposed to high doses of CeO_2 NPs exhibited dullness, irritation, moribund symptoms and insignificant loss in feed intake, bw gain and relative organ weight * significant increase of % tail DNA in the liver and peripheral blood leukocytes of rats exposed to 300 and 600 mg/kg bw/day (as assessed by comet assay) * significant increase of ALP and LDH activity in animals exposed to 300 and 600 mg/kg bw/day * significant reduction of GSH content in the liver, kidneys and brain of animals exposed to 300 and 600 mg/kg bw/day * histopathological alterations in the liver, spleen and brain tissue

						Conclusion: prolonged oral exposure to CeO_2 NPs caused genetic damage, biochemical alterations and histological changes after retention in vital organs of rats at high concentrations
[128]	SD rats	IV	85 mg/kg	1h/ 20h /30 d	5	* sequestration of CeO_2 NPs by Kupffer cells with subsequent bioretention in parenchymal cells, in hepatocytes; the agglomerated nanoceria were localized to the plasma membrane facing bile canaliculi; hepatic stellate also sequestrated nanoceria * within the sinusoids deposited nanoceria was associated with granuloma formation comprised of Kupffer cells and intermingling CD3+T cells * significant elevation of serum AST level at 1 and 20 h, but subsided by the day 30 after exposure * nanoceria infusion affected hepatocellular programmed cell death in the liver as revealed by TUNEL assay; significant elevation of apoptotic cell counts * increased hepatic protein carbonyl level, significant decrease in the liver CAT and GPx activity seen 30 days following ceria infusion **Conclusion: CeO_2 NPs induced hepatic injury and oxidative stress**
[215]	SD rats	IV	~100 mg/kg	1/7/30/90 d	30	* retention of CeO_2 NPs by organs of the mononuclear phagocyte system (spleen, liver, bone marrow) and associated with adverse changes * no appreciable clearance of CeO_2 NPs over the 90 days post-exposure period * short-term reduction in body weight * granulomas in the liver * splenomegaly * time-dependent oxidative stress observed in the liver and spleen **Conclusion: despite abnormal changes detected in the liver and spleen IV exposure to CeO_2 NPs did not elicit profound toxicity**
[216]	CD-1 mice	PO/IV/IP	0.5 mg/kg	weekly exposure for 2 or 5 w	3 - 5	* following IV and IP administration the greatest deposition of CeO_2 NPs was observed in the spleen followed by the liver, lungs, and kidneys; PO administration showed that mice excreted greater than 95% of CeO_2 NPs via feces within 24 h after exposure * increased WBC counts in IV and IP exposed groups * potential of CeO_2 NPs to reduce oxidative stress in vivo **Conclusion: lack of overt toxicity induced by CeO_2 NPs; the obtained results suggested that CeO_2 NPs may be a useful antioxidant to diminish oxidative stress**
[86]	SD rats	VI	85 mg/kg	30 or 90 d	30	* reduced body weight gain during the first week after administration of CeO_2 NPs * histopathological changes observed in the liver tissue (granuloma formation, hepatic apoptosis) * mild (not statistically significant) increase of ALT level **Conclusion: retention of CeO_2 NPs in the liver over 90 days post-exposure period increased hepatic apoptosis and led to granuloma formation**

ALB – albumin, ALT – alanine transaminase, AST – aspartate transaminase, bw – body weight, CAT – catalase, DNA SB – DNA strand breaks, GPx – glutathione peroxidase, GSH – glutathione, IL-6 – interleukin 6, IP – intraperitoneal injection, IV – intravenous injection, IT – intratracheal instillation, LDH – lactate dehydrogenase, PO – oral exposure, SOD – superoxide dismutase, TG – triglycerides, TNF-α – tumor necrosis factor α, VI – vascular infusion, WBC – white blood cells;

Table 4. Summary of studies assessing TiO_2 NPs-induced toxicity

Ref.	Animal model	Route of exposure	Dose	Exposure time	NPs size (nm)	Assessed liver and other relevant systemic end-points
[217]	Wistar rats	IT	3.5 or 17.5 mg/kg	5 w	23 ± 5	* significant increase of MDA and NO level for both doses and significant decrease of GSH level for both doses measured in peripheral blood * significant increase of MDA level and significant decrease of SOD and GSH level for both doses measured in the liver homogenate * significant increase of IL-1 and significant decrease of IFN-γ and TNF-α in the high dose group * significant increase of WBC level for both doses * histopathological changes in the liver tissue (persistent and progressive liver inflammatory response) **Conclusion: intratracheal instillation of TiO_2 induced oxidative stress, inflammatory response and led to pathological alterations of the liver tissue**
[218]	SD rats	IT	0.5/5/50 mg/kg	7 d	5 /21	* significant decrease of SOD activity in plasma and liver tissue in a group exposed to 0.5 mg/kg of TiO_2-S210 * significant increase of MDA level in the liver tissue in 5 mg/kg and 50 mg/kg exposed groups * no significant histopathologic changes observed in the liver tissue **Conclusions: intratracheal exposure to TiO_2 did not significantly altered function of the liver tissue**
[19]	C57BL/6 mice	IT	18 or 162 μg/mouse	24h or 28d	21	* hyperspectral imaging of the liver tissue confirmed presence of TiO_2 NPs in the liver of mice exposed to both doses at both post-exposure time points * 63 genes in the liver (involved in the acute phase response - 49 genes at 24 h and 14 genes at 28 d) were differentially expressed **Conclusion: extrapulmonary translocated TiO_2 NPs induced significant changes in expression of genes involved in hepatic acute phase response**
[150]	C57BL/6 mice	IT	18/54/162 μg/mouse	1/3/28 d	10	* significant increase of DNA SB level in the liver tissue for both TiO_2 NPs * significant increase in *Saa1* mRNA levels in the highest dose for both TiO_2 NPs **Conclusion: intratracheal exposure of unmodified and positively charged TiO_2 NPs induced genotoxicity and acute phase response in the liver tissue**
[219]	Kunming mice	IH	6.34 ± 0.22 mg/m3	8 h/d, for 3 w	20	* significant increase of Ti content in the liver tissue * significant decrease of WBC and LYMPH level and significant increase of RETIC, NEUT and PLT level * significant increase of ALT and AST level * no obvious pathological changes in the liver **Conclusion: function of the liver tissue was slightly influenced by the administration of TiO_2 NPs**

[75]	ICR mice	PO	10 mg/kg	90 d	5	* increased Ti content in the liver * histopathological alterations of the liver tissue (indications of inflammation and hepatocyte damage) * significant reduction of WBC, LYMPH, NEUT * increased level of ALT, AST, ALP, and of LDH, Tchol and TG * significant changes in gene expression profile (up- or down-regulation of genes involved in immune/inflammatory response, apoptosis, oxidative stress, metabolic process, response to stress, cell cycle, ion transport, signal transduction, cell proliferation, cytoskeleton, and cell differentiation) **Conclusion: oral exposure to TiO_2 induced inflammatory response, liver tissue damage and hepatic dysfunction**
[24]	SD rats	PO	10/50/200 mg/kg	30 d	75 ± 15	* histopathological changes in the liver tissue of young rats observed for the two highest doses (liver edema, hydropic degeneration, perilobular cell swelling); infiltration of inflammatory cells observed in the liver of adult rats in the 10 and 50 mg/kg TiO_2 NPs-treated groups * changes in several biochemical parameters measured in young rats serum for the two highest doses (GLU, LDL-C, AST, ALT/AST, TBIL, HBDH, CK); changes in TBIL and BUN measured in the serum of adult rats * increased plasma GSH/GSSG ratio in both young and adult rats **Conclusion: hepatotoxic effects induced by exposure to TiO_2 NPs were more sever in young than in adult SD rats**
[109]	CBAB6F1 mice	PO	40/200/ 1000 mg/kg	7 d	33	* increased number of DNA SB in the liver tissue **Conclusion: orally administered TiO_2 NPs induced genotoxicity in the liver tissue**
[221]	ICR mice	PO	5/10/50 mg/kg	60 d	7	* changes in normal hepatocytes ultrastructure: mitochondria swelling (5 mg/kg), apoptotic cells (10 mg/kg), apoptotic cells and apoptotic body (50 mg/kg) * ROS accumulation and lipid peroxidation in 10 and 50 mg/kg exposed groups * significant changes in expression of selected genes (decrease of the stress-related gene expression levels of SOD, CAT, GPx, MT, HSP 70, GSTs, P53, and transferrin); significant enhancement of cytochrome p4501A expression level in 10 and 50 mg/kg exposed groups **Conclusion: intragastric administration of 10 and 50 mg/kg TiO_2 NPs caused oxidative stress and resulted in alterations of normal hepatocytes structure**
[222]	Swiss albino rats	PO	500 mg/kg	21 d	50-75	* indications of oxidative stress in erythrocytes: lipid peroxidation, increased free radical generation, alterations in GSH, GPx and GST activities, reduction in SOD and CAT activities * significant increase of ROS production in the liver, significant elevation in TBARS level, significant reduction in SOD and CAT activities in the liver **Conclusion: oxidative stress in erythrocytes and liver tissue occurred after oral administration of TiO_2 NPs**

Table 4. – continued

Ref.	Animal model	Route of exposure	Dose	Exposure time	NPs size (nm)	Assessed liver and other relevant systemic end-points
[25]	ICR mice	PO	5 g/kg	14 d	28 /80	* changes of serum biochemical parameters (ALT/AST, LDH) * indications of hepatic injury (hydropic degeneration around the central vein and spotty necrosis of hepatocytes) * significantly elevated hepatic Ti content in mice exposed to 80 nm TiO_2 NPs **Conclusion: orally administered TiO_2 NPs translocated to the liver and caused hepatic injury and changes of biochemical parameters**
[88]	ICR mice	IV	5/10/50/ 100/150 mg/kg	14 d	5	* increased relative liver weight of animals treated with 50, 100, 150 mg/kg of TiO_2 NPs * significantly elevated content of TiO_2 NPs in the liver of all exposed animals * alterations in gene expression of several inflammatory cytokines: NF-κB, MMIF, TNF-α, IL-6, IL-1β, cross-reaction protein, IL-4, and IL-10 in all exposed groups * alterations of several biochemical parameters: ALT, AST, ALP, LDH, PChE, LAP, ALB, GLB in the high exposure groups * histopathological changes of the liver tissue in 100 and 150 mg/kg exposed groups **Conclusion: intravenous administration of TiO_2 NPs induced inflammatory response and injury of the liver tissue**
[226]	SD rats	IV	1.7 mg/rat	10 min, 1h, 1/7/ 28/56d	< 25	* increased Ti content in the liver for all assessed time points * no significant histopathological alterations of the liver tissue * no significant changes in any of the assessed liver biochemical and blood parameters **Conclusion: lack of toxic effects of intravenously administered TiO_2 NPs**
[224]	C57BL/6J mice	IV	2/10/50 mg/kg	4 w	~146 (DLS)	* majority of the injected TiO_2 NPs in the liver were found in the sinuses and inside Kupffer cells whereas some were occasionally observed in the liver parenchymal cells * level of DNA damage (assessed by comet assay) as well as frequency of gpt and spi- mutations in the liver tissue were not affected by the TiO_2 administration **Conclusion: exposure to TiO_2 did not induce genotoxic effects in the mouse liver**
[227]	ICR mice	IV	140/300/ 645/1387 mg/kg	14 d	40 ± 5	* decreased food and water intake and decreased physical activity in the 1387 mg/kg dose group observed 7 days after treatment * significant decrease in relative liver weight in the 300 and 645 mg/kg dose groups * significant decrease of direct bilirubin and indirect bilirubin in the 300 and 645 mg/kg dose groups * significant increase of WBC counts in the 645 mg/kg dose group * histopathological lesions (inflammatory cells infiltration, granulomas lesions, necrosis of hepatocytes, multifocal lesions) were observed in the liver **Conclusion: intravenous injection of different doses of TiO_2 NPs could lead to acute liver toxicity**

[225]	Balb/c mice	IV/SI	IV: 56 or 560 mg/kg; SI: 560 or 5600 mg/kg	1/2 d 2/4/12/ 26 w	12 - 30	* mice in the high s.i. dose group exhibited greater body weight gain at weeks 2 and 4 * presence of TiO_2 agglomerates in the liver tissue confirmed by light microscopy * no liver tissue damaged was observed at any assessed time point **Conclusion: despite the presence of administered TiO_2 NPs in the liver tissue no overt histopathological changes were observed**
[113]	B6C3F1 mice	IP	50 mg/kg	3 d	10	* increased Ti content in the liver * DNA damage in the liver tissue (as assessed by Comet assay) and increased oxidative DNA damage in the liver tissue (as assessed by enzyme-modified Comet assay) * significant changes in gene expression profile (up- or down-regulation of genes involved in metabolic processes) **Conclusion: intraperitoneal exposure to TiO_2 induced genotoxicity and interrupted metabolic homeostasis in the liver**
[228]	Wistar rats	IP	63/126/ 252 mg/rat	24 or 48 h	50 ± 6	* significant increase of serum GOT and ALP activity * histopathological changes of hepatocytes (hydropic degeneration, cloudy swelling, fatty degeneration, portal and lobular infiltration by chronic inflammatory cells) **Conclusion: TiO_2 NPs induced histologic changes in hepatocytes and compromised normal liver function**
[229]	ICR mice	IP/IH	138 mg/kg of IP + 1mg of TiO2 NPs via nasal exposure for the next 7 days	7 d	< 25	* 15 out of 1400 selected proteins exhibited greater than 2-fold expressional changes in response to TiO_2 administration (the proteins were involved in inflammation, apoptosis and antioxidative response) * significant increase of ALT, AST and ALP level in serum * decrease of CAT and SOD activity (assessed by the measurement of band intensity on the activity staining gel) **Conclusion: differentially expressed proteins may be involved in TiO_2 NPs-induced hepatotoxicity**
[230]	Swiss mice	IP	50/250/ 500 mg/kg	7/14/45 d	21	* significant decrease in hepatic total protein, glutathione and total antioxidant capacity; significant increase in AST, ALT, CAT, NO and MDA levels measured for all doses and time points * increased number of aberrant cells in the mice bone marrow 45 days post-injection of 500 mg of TiO_2 NPs/kg body weight * histopathological changes of the liver tissue **Conclusion: function of liver enzymes, markers of oxidative stress and liver histological structure were greatly influenced in a dose and time-dependent manner by IP injection of TiO_2 NPs resulting in profound hepatotoxicity**

Table 4. – continued

Ref.	Animal model	Route of exposure	Dose	Exposure time	NPs size (nm)	Assessed liver and other relevant systemic end-points
[231]	Wistar rats	IP	1.6 g/100 g	3 or 12 months	5/10/150	* histological evaluation confirmed presence of TiO_2 NPs in the liver parenchyma, either outside the cells or phagocytosed by Kupffer cells at both time points * histopathological changes in the liver tissue (foci of necrosis, inflammatory cells infiltration) at 3 and 12 months post-exposure * significant time-dependent decrease in TiO_2 NPs (10nm) concentration was observed in liver * significant increase of CAT (all treatment groups) and TRAP (5 nm exposed group) activity in the liver tissue **Conclusion: exposure to different size TiO_2 was associated with pathological lesions and oxidative stress in the liver tissue**
[89]	ICR mice	ACI	5/10/50/100/150 mg/kg	14 d	5	* increased relative liver weight of mice exposed to 50, 100 and 150 mg/kg bw of TiO_2 NPs * significant increase of hepatic Ti level in all experimental groups * significant increase of production of superoxide radical anion, H_2O_2 and MDA levels in the liver of mice exposed to 50, 100, and 150 mg/kg bw of TiO_2 NPs * significant reduction in activities of hepatic antioxidative enzymes i.e. SOD, CAT, GPx and APx in the liver of mice exposed to 50, 100 and 150 mg/kg bw of TiO_2 NPs **Conclusion: antioxidative responses of liver were reduced in mice treated with TiO_2 NPs**
[90]	ICR mice	ACI	5/10/50/100/150 mg/kg	14 d	5	* significant accumulation of Ti in the liver of mice from all experimental groups * increased relative liver weight of mice exposed to 50, 100 and 150 mg/kg bw of TiO_2 NPs * significant changes in biochemical liver parameters (i.e. elevation of ALT, ALP, LAP, ChE, TP, ALB and reduction of TBIL level) of mice exposed to 50, 100 and 150 mg/kg bw of TiO_2 NPs * significantly elevated contents of TG, GLU and HDL cholesterol **Conclusion: high doses of TiO_2 NPs caused severe damage to the liver**

ACI – abdominal cavity injection, ALB – albumin, ALP – alkaline phosphatase, ALT – alanine transaminase, APx – ascorbate peroxidase, AST – aspartate transaminase, BUN – blood urea nitrogen, CAT – catalase, ChE – cholinesterase, CK – creatine kinase, DNA SB – DNA strand breaks, GLB – globulin, GLU – glucose, GOT – glutamate oxaloacetate transaminase, GPx – glutathione peroxidase, GSH – glutathione, GSSG – glutathione disulfide, GSTs – glutathione S transferase, HBDH – hydroxybutyrate dehydrogenase, HDL – high-density lipoprotein, HSP70 – heat shock protein 70, IFN-γ – interferon γ, IH – inhalation, IL-1 – interleukin 1, IL-4 – interleukin 4, IL-6 – interleukin 6, IL-10 – interleukin 10, IP – intraperitoneal injection, IT – intratracheal administration, IV – intravenous injection, LAP – leukocyte alkaline phosphatase, LDH – lactate dehydrogenase, LDL-c – low-density lipoprotein c, LYMPH – lymphocytes, MDA – malondialdehyde, MMIF – macrophage migration inhibitory factor, MT – metallothionein, NEUT – neutrophils, NF-κB – nucleic factor-kappa B, NO – nitrogen oxide, PChE – cholinesterase, PLT – platelets, PO – oral gavage, RETIC – reticulocytes, ROS – reactive oxygen species, SAA1 – serum amyloid A (1^{st} isoform), SI – subcutaneous injection, SOD – superoxide dismutase, TBARS – thiobarbituric acid reactive substances, TBIL – total bilirubin, Tchol – total cholesterol, TG – triglycerides, TNF-α – tumor necrosis factor α, TRAP – total reactive antioxidant potential, WBC – white blood cells;

Table 5. Summary of studies assessing CB NPs-induced toxicity

Ref.	Animal model	Route of exposure	Dose	Exposure time	NPs size (nm)	Assessed liver and other relevant systemic end-points
[54]	C57BL/6 mice	IT	18/54/162 μg/mouse	1/3/28 d	14	* lack of hepatic acute phase response (based on *Saa3* mRNA expression level) * significantly increased number of DNA SB in the liver tissue on day 1 and 28 for all doses **Conclusion: pulmonary deposition of CB NPs induced genotoxicity in the liver, the secondary tissue**
[44]	C57BL/6 mice	IT	18/54/162 μg/mouse	1/3/28 d	14	* changes in global hepatic gene expression (significant upregulation of HMG-CoA reductase pathway) * significant upregulation of Saa3 gene in the liver tissue on day 1 following the exposure * elevated SAA protein level in plasma of mice exposed to 162 μg of CB NPs * alterations in cholesterol homeostasis (decreased HDL and increased LDL level) **Conclusion: pulmonary exposure to CB NPs triggered molecular signaling cascades and affected liver metabolism**
[57]	C57BL/6 mice	IH/IT	42 mg/m^3 11/54/ 268 μg/mouse	Dams were monitored until weaning and some offspring until adolescence	14	* significantly increased number of DNA SB in the liver of time-mated mice and their offspring after inhalation exposure * no changes in the number of DNA SB in the liver following intratracheal instillation **Conclusion: maternal exposure to CB NPs by inhalation induced DNA liver damage in mothers and in *in utero* exposed offspring**
[232]	C57BL/6 mice	IT	11/54/268 μg/mouse	Newborns were monitored until postnatal day 2 (4 d after the last maternal exposure) and dams were monitored until 26 to 27 d post-exposure	14	* altered expression of genes associated with oxidative stress in dams (inflammatory chemokines, cytokine receptors, glycoproteins) * significant changes in hepatic gene expression in both male and female newborn offspring **Conclusion: significant hepatic response observed in male and female offspring exposed in utero to the highest dose of CB NPs**

DNA SB – DNA strand breaks, HDL – high density lipoprotein, HMG-CoA reductase – 3-hydroxy-3-methyl-glutaryl-coenzyme A reductase, IH – inhalation, IT – intratracheal instillation, LDL – low-density lipoprotein, Saa3 – serum amyloid A (3rd isoform);

The main objective of my PhD study was to elucidate what mechanism underlays the genotoxicity that has been previously found in the liver tissue after pulmonary exposure to TiO_2 and CB NPs [54,57,150]. Two separate mechanisms contributing to the observed genotoxicity have been proposed: primary genotoxicity that refers to the occurrence of DNA damages as a result of direct effects of (translocated) particles and their ability to induce increased production of ROS or secondary genotoxicity that refers to the DNA lesions that are formed as a result of lung-mediated inflammation and acute phase response followed by infiltration and circulation of various secondary molecular mediators (cytokines, chemokines, ROS, RNS) that could initiate downstream toxic effects in secondary organs.

It was previously speculated [54] that CB NPs as an active generators of ROS (in both cellular [233] and acellular systems [99]) and inflammatory response in lungs after pulmonary exposure would mediate secondary genotoxicity by means of inflammation and oxidative stress. However, none of the mentioned studies where the genotoxic effect of CB NPs (or of TiO_2 NPs) was observed confirmed the physical presence of particles in the liver tissue. In this study, we corroborated extrapulmonary translocation of TiO_2 and CeO_2 NPs to the liver tissue by means of ICP-MS and demonstrated presence of CB NPs in the liver after intratracheal instillation by using enhanced darkfield and standard brightfield microscopy. Moreover, we have shown that hepatic genotoxicity induced by CB NPs occurred at the later time points (e.g. 28 and 180 days) after intratracheal exposure. This is in a good agreement with belated detection of TiO_2 and CeO_2 NPs that were detected in the liver tissue 180 days (in case of TiO_2 NPs) or 28 and 180 days (in case of CeO_2 NPs) post-exposure. This delay in the detection could reflect the time that is needed for the extrapulmonary translocation of NPs.

Among the studied particles only CB NPs induced increased formation of ROS as we determined in the cell-free assay. Increased generation of ROS and consequent oxidative stress are one of the most frequently reported effects associated with NP exposure [234]. The exact cellular mechanism for particle-induced ROS production remains unclear and more studies are needed to better understand this phenomenon. However, this mechanism seems to be different for different NPs. That could be due to the fact that many acellular properties such as particle surface area, size, chemical composition, and presence of metals or other foreign components could modify the

toxicity of NPs. Therefore, thorough physicochemical characterization of NPs is required since some of the intrinsic properties exhibited by NPs, even by particles of the same chemical composition, could lead to increased or decreased catalysation of ROS [234]. In my study, low level of endotoxin detected on the surface of CB NPs (0.142 EU/mg CB NPs) [54] excluded the hypothesis that organic impurities (e.g. polycyclic aromatic hydrocarbons) contributed to the observed genotoxic effect.

Intratracheal instillation of TiO_2, CeO_2 and CB NPs resulted in similar lung inflammation and long-lasting pulmonary acute phase response. We found no significant differences between particles in terms of generated response in the lung tissue. Moreover, in the present study hepatic acute phase response was observed only on day 1 following intratracheal instillation and intravenous injection of TiO_2 and CeO_2 NPs but not after exposure to CB NPs. Potential explanations that could elucidate transient and negligible hepatic acute phase response are: 1) dosing-related stress is responsible for the temporary induction of systemic acute phase response, 2) very short duration of hepatic acute phase response makes the detection hindered, 3) liver as the major organ responsible for detoxification of foreign materials has defense mechanisms against translocated particles (as suggested by [19]), 4) particles used in the present study involve other molecular pathways and induce different, than *Saa*, acute phase proteins (as suggested by [135]). In addition, lack or negligible induction of inflammatory and acute phase response in the liver was previously reported by our research group after exposure to CB (Printex 90) and diesel exhaust (NIST) NPs or multi-walled carbon nanotubes [43,54,135]. Therefore, it is very unlikely that the observed DNA SB in the liver tissue are caused by the liver inflammation as a result of pulmonary exposure and release of circulating cytokines. If that was the case, then all three NPs would induce genotoxicity in the liver whereas in my study it was only observed in the CB-exposed groups.

Moreover, Risom and colleagues [235] demonstrated that the DNA SB were rapidly repaired within a few hours following the induction. However, in our study DNA SB were observed in the liver 28 and 180 days following intravenous injection and intratracheal instillation suggesting that they were most likely generated continuously throughout the post exposure period. NPs are deposited in the liver primary in the Kupffer cells [37] and hepatic retention is protracted [210].

Therefore, we think that the potential reason for the continuous induction of newly formed DNA SB is the physical presence of NPs in the liver.

In the experiment conducted by Jackson and colleagues [57] an increased number of DNA SB was found in the liver of dams exposed to CB NPs by inhalation but not after intratracheal instillation. They concluded that the whole-body inhalation exposure led to the secondary uptake of NPs by the GIT due to the fur grooming. To address that issue, we included the oral route in our study. Based on the obtained results, i.e. lack of particles detected in the liver and no hepatotoxic or systemic effects following oral exposure, we think that the secondary oral exposure does not contribute to the observed genotoxicity. Our results are in a good agreement with other studies where the translocation of insoluble NPs via GIT in rodents was shown to be very limited [13,27,236].

Taken together, all three NPs induced similar long-lasting pulmonary inflammation and acute phase response, and all three NPs were observed in the liver following pulmonary exposure. However, only CB NPs induced hepatic genotoxicity and led to the increased production of ROS. Therefore, we concluded that the primary genotoxicity associated with the physical presence of CB NPs and further generation of ROS may be responsible for the observed DNA SB in the liver.

In addition, results from studies conducted by Bourdon [44] and Jackson [232] revealed that intratracheal instillation of CB NPs induced significant changes in hepatic gene expression and caused perturbations in cholesterol homeostasis (decreased HDL and increased LDL levels). It has been previously reported that pulmonary deposition of NPs impairs cholesterol homeostasis and altered levels of lipids circulating in the blood [43,237]. Therefore, it is reasonable to simultaneously study different endpoints due to the variability in responses and toxic effects induced by NPs. Different assays have different advantages and limitations thus by using a set of different tests, complementary to each other, we reduce the risk that the actual toxicity might be overlooked.

Particle-induced lung inflammation followed by sustained acute phase response could contribute to increased risk of cardiovascular disease and atherosclerosis [63,204]. Moreover, genotoxic effect of CB NPs observed after intravenous injection and intratracheal instillation suggests that

the exposure could be, in a long-term perspective, one of the crucial factors that leads to the development of liver cancer.

6. CONCLUSIONS AND PERSPECTIVES

In this thesis, I have assessed hepatotoxic effects of NP deposition in the liver following intratracheal instillation (IT), intravenous injection (IV) and oral gavage (PO).

It has been demonstrated that all three NPs used in the present study, i.e. TiO_2, CeO_2 and CB, underwent extrapulmonary translocation following lung exposure and were sequestrated in the liver as assessed by ICP-MS and EDFM. No particles were detected in the liver following oral gavage suggesting that the main translocation route for pulmonary-administered NPs is translocation via systemic circulation rather than secondary uptake by the GIT due to the action of mucociliary escalator as a part of the lung clearance process.

Both TiO_2 and CeO_2 exhibited similar primary size (i.e. 10.5 and 13.0, respectively) and despite of differences in shape, chemical composition and potential differences in solubility, the calculated translocation rates for TiO_2 and CeO_2 NPs were comparable. This suggests that the main feature that governs extrapulmonary translocation to the secondary organs is the primary size of particles.

The observed particle size distributions of CeO_2 NPs changed over the 180 days post exposure period with a noticeable shift towards smaller particle size which indicates that CeO_2 NPs undergo *in vivo*-induced size transformation over time both in lung and liver tissue. However, the observed changes did not affect long-term accumulation of CeO_2 NPs in the liver.

Based on the obtained results, all the tested NPs were capable of inducing similar level of pulmonary inflammation followed by sustained induction of acute phase response in the lungs that lasted up to day 180. Increased DNA SB levels were observed only in the CB NPs groups exposed by intratracheal instillation and intravenous injection. This suggests that the observed hepatic genotoxicity following exposure to CB NPs was likely caused by the physical presence of translocated particles rather than by the effects of circulating secondary mediators released during pulmonary inflammation and acute phase response in the lungs. In addition, hepatic acute phase response was observed only in CeO_2 and TiO_2 exposed groups while DNA lesions were found only in the liver of mice exposed to CB NPs. This suggests that hepatic acute phase

response did not contribute to the observed genotoxic effects. Moreover, occurrence of genotoxicity at the later time points, i.e. 28 and 180 days, but not after day 1 following intratracheal exposure indicates the time that is needed for particles being translocated from lungs to the liver.

Among the particles used in the study, CB NPs were the most potent ROS generators. This suggests that increased ROS production followed by oxidative stress could be responsible for the observed primary genotoxicity.

No significant alterations in body weight, relative and absolute liver weight as well as in selected haematological and biochemical markers were observed. A few parameters were occasionally and negligibly altered but since no consistent patterns were found we regarded them as chance findings. Overall, collected data suggests that exposure to TiO_2, CeO_2 and CB NPs, regardless the administration route, did not induce prominent systemic (apart from pulmonary inflammation and acute phase response) and hepatic (apart from DNA SB generated by CB NPs) toxicity.

High inflammatory background in the liver of control and exposed groups hindered histopathological examination and we were not able to determine whether the observed changes were induced by NP exposure. Necrotic changes, likewise, could not be solely associated with the NP treatment.

Overall, results from this thesis provided evidences that liver toxicity is an important part of the hazard evaluation of pulmonary-deposited NPs. In the present study assessment of hepatotoxicity elicited after exposure to NPs was performed using one exposure dose only and there is a need to include more doses as well as include more liver endpoints to fully understand the mechanism of NPs-induced systemic toxicity.

Detailed mechanism involved in extrapulmonary translocation to the systemic circulation and further deposition in the secondary organs is not yet fully elucidated and therefore it would be very interesting to investigate how exactly NPs are hauled in the blood, what governs deposition of NPs in the secondary organs and what is the exact mechanism of NP uptake by different cell

types. In addition, potential adverse effects following extrapulmonary translocation to other secondary organs (e.g. spleen, heart and brain) deserve further attention.

Conducted epidemiological studies reported association between exposure to particulate matter air pollution and increased risk of hepatic cancer. Therefore, due to the genotoxic effects expressed as increased DNA SB levels observed in the liver of mice exposed to CB NPs it would in the future studies be of interest to assess mutagenicity of CB NPs and conduct additional long-term animal studies investigating tumorigenic and carcinogenic outcomes in the liver following prolonged presence of CB NPs in that organ.

In addition, in order to assess the risk posed by NPs more studies are needed to evaluate which of the observed toxic effects are due to the direct interaction between particles and target cell/tissue and which are mediated by the chemical messengers (like cytokines, chemokines etc.).

Contradictory results from different studies of the same nanomaterials and exposure routes indicate that detailed and standardized characterization of various physicochemical properties of the tested NPs is required to make the comparison of endpoints assessed in different studies feasible. Moreover, further studies are needed to extend the current knowledge concerning physical and chemical properties that influence toxicity of NPs.

My PhD study was one of many other studies investigating mechanisms of particle-driven toxicity. More studies using realistic exposure levels are needed to fully understand noxious effects following exposure to NPs present in the real-life and not in the laboratory environment. Moreover, more human studies on occupational and accidental exposure to NPs with the assessment of several liver endpoints would contribute substantially to the evaluation of NPs-pose health threat.

REFERENCES

1. Nel A, Xia T, Madler L, Li N. Toxic Potential of Materials at the Nanolevel. Science (80-.). 2006;311:622–7.

2. Hoet PH, Bruske-Hohlfeld I, Salata O V. Nanoparticles - known and unknown health risks. J. Nanobiotechnology. England; 2004;2.

3. The Royal Society. Nanoscience, and Nanotechnology: Opportunities and Uncertainties. 2004.

4. Oberdörster G, Oberdörster E, Oberdörster J. Nanotoxicology: An emerging discipline evolving from studies of ultrafine particles. Environ. Health Perspect. 2005;113:823–39.

5. Gwinn MR, Vallyathan V. Nanoparticles: Health effects - Pros and cons. Environ. Health Perspect. 2006;114:1818–25.

6. Riedl M, Diaz-Sanchez D. Biology of diesel exhaust effects on respiratory function. J. Allergy Clin. Immunol. 2005;115:221–8.

7. Cohen AJ, Pope CA, 3rd. Lung cancer and air pollution. Environ. Health Perspect. 1995;103:219–24.

8. Kim JW, Park S, Lim CW, Lee K, Kim B. The role of air pollutants in initiating liver disease. Toxicol. Res. 2014;30:65–70.

9. Yang W, Peters JI, Williams RO. Inhaled nanoparticles-A current review. Int. J. Pharm. 2008;356:239–47.

10. Geiser M, Kreyling WG. Deposition and biokinetics of inhaled nanoparticles. Part. Fibre Toxicol. 2010;7.

11. Heyder J, Gebhart J, Rudolf G, Schiller CF, Stahlhofen W. Deposition of particles in the human respiratory tract in the size range 0.005-15 μm. J. Aerosol Sci. 1986;17:811–25.

12. Patton JS. Mechanisms of macromolecule absorption by the lungs. Adv. Drug Deliv. Rev. 1996;19:3–36.

13. Kreyling WG, Semmler M, Erbe F, Mayer P, Takenaka S, Schulz H, et al. Translocation of Ultrafine Insoluble Iridium Particles From Lung Epithelium To Extrapulmonary Organs Is Size Dependent But Very Low. J. Toxicol. Environ. Heal. PartA. 2002;65:1513–30.

14. Oberdorster G, Ferin J, Morrow PE. Volumetric loading of alveolar macrophages (AM): a possible basis for diminished AM-mediated particle clearance. Exp. Lung Res. England; 1992;18:87–104.

15. Oberdörster Gunter. Toxicology of Ultrafine Particles: In vivo Studies. Philos. Trans. R. Soc. London Ser. a-Mathematical Phys. Eng. Sci. 2000;358:2719–40.

16. Semmler M, Seitz J, Erbe F, Mayer P, Heyder J, Oberdörster G, et al. Long-term clearance kinetics of inhaled ultrafine insoluble iridium particles from the rat lung, including transient translocation into secondary organs. Inhal. Toxicol. 2004;16:453–9.

17. Semmler-Behnke M, Takenaka S, Fertsch S, Wenk A, Seitz J, Mayer P, et al. Efficient elimination of inhaled nanoparticles from the alveolar region: Evidence for interstitial uptake and subsequent reentrainment onto airways epithelium. Environ. Health Perspect. 2007;115:728–33.

18. Oberdörster G, Sharp Z, Atudorei V, Elder A, Gelein R, Lunts A, et al. Extrapulmonary Translocation of Ultrafine Carbon Particles Following Whole-Body Inhalation Exposure of Rats. J. Toxicol. Environ. Heal. Part A. 2002;65:1531–43.

19. Husain M, Wu D, Saber AT, Decan N, Jacobsen NR, Williams A, et al. Intratracheally instilled titanium dioxide nanoparticles translocate to heart and liver and activate complement cascade in the heart of C57BL/6 mice. Nanotoxicology. 2015;9:1013–22.

20. Takenaka S, Karg E, Kreyling WG, Lentner B, Möller W, Behnke-Semmler M, et al. Distribution pattern of inhaled ultrafine gold particles in the rat lung. Inhal. Toxicol. 2006;18:733–40.

21. Oberdorster G, Ferin J, Gelein R, Soderholm SC, Finkelstein J. Role of the alveolar macrophage in lung injury: Studies with ultrafine particles. Environ. Health Perspect. 1992;97:193–9.

22. Oberdörster G, Sharp Z, Atudorei V, Elder A, Gelein R, Kreyling W, et al. Translocation of Inhaled Ultrafine Particles to the Brain. Inhal. Toxicol. 2004;16:437–45.

23. Elder A, Gelein R, Silva V, Feikert T, Opanashuk L, Carter J, et al. Translocation of inhaled ultrafine manganese oxide particles to the central nervous system. Environ. Health Perspect. 2006;114:1172–8.

24. Wang Y, Chen Z, Ba T, Pu J, Chen T, Song Y, et al. Susceptibility of young and adult rats to the oral toxicity of titanium dioxide nanoparticles. Small. 2013;9:1742–52.

25. Wang J, Zhou G, Chen C, Yu H, Wang T, Ma Y, et al. Acute toxicity and biodistribution of different sized titanium dioxide particles in mice after oral administration. Toxicol. Lett. 2007;168:176–85.

26. Park E-J, Park Y-K, Park K. Acute toxicity and tissue distribution of cerium oxide nanoparticles by a single oral administration in rats. Toxicol. Res. 2009;25:79–84.

27. Geraets L, Oomen AG, Krystek P, Jacobsen NR, Wallin H, Laurentie M, et al. Tissue distribution and elimination after oral and intravenous administration of different titanium dioxide nanoparticles in rats. Part. Fibre Toxicol. 2014;11.

28. MacNicoll A, Kelly M, Aksoy H, Kramer E, Bouwmeester H, Chaudhry Q. A study of the uptake and biodistribution of nano-titanium dioxide using in vitro and in vivo models of oral intake. J. Nanoparticle Res. 2015;17.

29. Kreyling WG, Holzwarth U, Haberl N, Kozempel J, Wenk A, Hirn S, et al. Quantitative biokinetics of titanium dioxide nanoparticles after oral application in rats: Part 2. Nanotoxicology. Taylor 8 Francis; 2017;0:1–11.

30. Florence AT, Hussain N. Transcytosis of nanoparticle and dendrimer delivery systems: Evolving vistas. Adv. Drug Deliv. Rev. 2001;50:S69–89.

31. Hussain N, Jaitley V, Florence AT. Recent advances in the understanding of uptake of microparticulates across the gastrointestinal lymphatics. Adv. Drug Deliv. Rev. 2001;50:107–42.

32. Aprahamian M, Michel C, Humbert W, Devissaguet JP, Damge C. Transmucosal passage of polyalkylcyanoacrylate nanocapsules as a new drug carrier in the small intestine. Biol. cell. England; 1987;61:69–76.

33. Murthy SK. Nanoparticles in modern medicine: state of the art and future challenges. Int. J. Nanomedicine. 2007;2:129–41.

34. Almeida JPM, Chen AL, Foster A, Drezek R. In vivo biodistribution of nanoparticles. Nanomedicine (Lond). 2011;6:815–35.

35. Aggarwal P, Hall JB, Mcleland CB, Dobrovolskaia MA, Mcneil SE. Nanoparticle interaction with plasma proteins as it relates to particle biodistribution, biocompatibility and therapeutic efficacy. Adv. Drug Deliv. Rev. 2009;61:428–37.

36. Owens DE, Peppas NA. Opsonization, biodistribution, and pharmacokinetics of polymeric nanoparticles. Int. J. Pharm. 2006;307:93–102.

37. Sadauskas E, Wallin H, Stoltenberg M, Vogel U, Doering P, Larsen A, et al. Kupffer cells are central in the removal of nanoparticles from the organism. Part. Fibre Toxicol. 2007;4.

38. Longmire M, Choyke PL, Kobayashi H. Clearance properties of nano-sized particles and molecules as imaging agents: considertaions and caveats. Nanomedicine. 2008;3:703–17.

39. Stone V, Barlow PG, Hutchison GR, Brown D. Proinflammatory effects of particles on macrophages and epithelial cells. Part. Toxicol. 2007. p. 285–98.

40. Gordon SB, Read RC. Macrophage defences against respiratory tract infections. Br. Med. Bull. England; 2002;61:45–61.

41. Driscoll KE. TNF and MIP-2: Role in particle-induced inflammation and regulation by oxidative stress. Toxicol. Lett. 2000;112–113:177–84.

42. Nicod LP. Pulmonary defence mechanisms. Respiration. 1999;66:2–11.

43. Saber AT, Jacobsen NR, Jackson P, Poulsen SS, Kyjovska ZO, Halappanavar S, et al. Particle-induced pulmonary acute phase response may be the causal link between particle inhalation and cardiovascular disease. Wiley Interdiscip. Rev. Nanomedicine Nanobiotechnology. 2014;6:517–31.

44. Bourdon JA, Halappanavar S, Saber AT, Jacobsen NR, Williams A, Wallin H, et al. Hepatic and

pulmonary toxicogenomic profiles in mice intratracheally instilled with carbon black nanoparticles reveal pulmonary inflammation, acute phase response, and alterations in lipid homeostasis. Toxicol. Sci. 2012;127:474–84.

45. Halappanavar S, Jackson P, Williams A, Jensen KA, Hougaard KS, Vogel UB, et al. Pulmonary Response to Surface-CoatedNanotitanium Dioxide Particles Includes Induction of Acute Phase Response Genes, Inflammatory Cascades, and Changes inMicroRNAs: AToxicogenomic Study. Environ. Mol. 2011;52:425–39.

46. Saber AT, Lamson JS, Jacobsen NR, Ravn-Haren G, Hougaard KS, Nyendi AN, et al. Particle-Induced Pulmonary Acute Phase Response Correlates with Neutrophil Influx Linking Inhaled Particles and Cardiovascular Risk. PLoS One. 2013;8:1–10.

47. Cray C, Zaias J, Altman NH. Acute phase response in animals: A review. Comp. Med. 2009;59:517–26.

48. Gabay C, Kushner I. Acute-phase proteins and other systemic responses to inflammation. N. Engl. J. Med. 1999;340:448–54.

49. Jensen LE, Whitehead a S. Regulation of serum amyloid A protein expression during the acute-phase response. Biochem. J. 1998;334 (Pt 3:489–503.

50. Elsabahy M, Wooley KL. Cytokines as biomarkers of nanoparticle immunotoxicity. Chem Soc Rev. 2013;42:5552–76.

51. Moshage H. Review Article Cytokines and the Hepatic Acute Phase. J. Pathol. 1996;181:257–66.

52. Uhlar CM, Whitehead AS. Serum amyloid A, the major vertebrate acute-phase reactant. Eur. J. Biochem. 1999;265:501–23.

53. Bourdon JA, Saber AT, Halappanavar S, Jackson PA, Wu D, Hougaard KS, et al. Carbon black nanoparticle intratracheal installation results in large and sustained changes in the expression of miR-135b in mouse lung. Environ. Mol. Mutagen. United States; 2012;53:462–8.

54. Bourdon JA, Saber AT, Jacobsen NR, Jensen KA, Madsen AM, Lamson JS, et al. Carbon black

nanoparticle instillation induces sustained inflammation and genotoxicity in mouse lung and liver. Part. Fibre Toxicol. BioMed Central Ltd; 2012;9:5.

55. Bourdon JA, Saber AT, Halappanavar S, Jackson PA, Wu D, Hougaard KS, et al. Carbon Black Nanoparticle Intratracheal Installation Results in Large and Sustained Changes in the Expression of miR-135b in Mouse Lung. Environ. Mol. 2012;53:462–8.

56. Husain M, Saber AT, Guo C, Jacobsen NR, Jensen KA, Yauk CL, et al. Pulmonary instillation of low doses of titanium dioxide nanoparticles in mice leads to particle retention and gene expression changes in the absence of inflammation. Toxicol. Appl. Pharmacol. Elsevier B.V.; 2013;269:250–62.

57. Jackson P, Hougaard KS, Boisen AMZ, Jacobsen NR, Jensen KA, Møller P, et al. Pulmonary exposure to carbon black by inhalation or instillation in pregnant mice: Effects on liver DNA strand breaks in dams and offspring. Nanotoxicology. 2012;6:486–500.

58. Poulsen SS, Knudsen KB, Jackson P, Weydahl IEK, Saber AT, Wallin H, et al. Multi-walled carbon nanotube-physicochemical properties predict the systemic acute phase response following pulmonary exposure in mice. PLoS One. 2017;12:e0174167.

59. Cabana VG, Reardon CA, Wei B, Lukens JR, Getz GS. SAA-only HDL formed during the acute phase response in apoA-I+/+ and apoA-I-/- mice. J. Lipid Res. 1999;40:1090–103.

60. Cabana VG, Lukens JR, Rice KS, Hawkins TJ, Getz GS. HDL content and composition in acute phase response in three species: triglyceride enrichment of HDL a factor in its decrease. J. Lipid Res. 1996;37:2662–74.

61. Steinmetz A, Hocke G, Saïle R, Puchois P, Fruchart JC. Influence of serum amyloid A on cholesterol esterification in human plasma. Biochim. Biophys. Acta (BBA)/Lipids Lipid Metab. 1989;1006:173–8.

62. Knaapen AM, Borm PJA, Albrecht C, Schins RPF. Inhaled particles and lung cancer. Part A: Mechanisms. Int. J. Cancer. 2004;109:799–809.

63. Pope CA, Burnett RT, Thun MJ, Calle EE, Krewski D, Ito K, et al. Lung cancer, cardiopulmonary

mortality, and long-term exposure to fine particulate air pollution. JAMA. 2002;287:1132–41.

64. Wong CM, Tsang H, Lai HK, Thomas GN, Lam KB, Chan KP, et al. Cancer Mortality Risks from Long-term Exposure to Ambient Fine Particle. Cancer Epidemiol. Biomarkers Prev. 2016;25:839–45.

65. Nyberg F, Gustavsson P, Jarup L, Bellander T, Berglind N, Jakobsson R, et al. Urban air pollution and lung cancer in Stockholm. Epidemiology. 2000;11:487–95.

66. Raaschou-Nielsen O, Bak H, Sørensen M, Jensen SS, Ketzel M, Hvidberg M, et al. Air pollution from traffic and risk for lung cancer in three Danish cohorts. Cancer Epidemiol. Biomarkers Prev. 2010;19:1284–91.

67. Tao F, Gonzalez-Flecha B, Kobzik L. Reactive oxygen species in pulmonary inflammation by ambient particulates. Free Radic. Biol. Med. 2003;35:327–40.

68. Donaldson K, Poland C a, Schins RPF. Possible genotoxic mechanisms of nanoparticles: criteria for improved test strategies. Nanotoxicology. 2010;4:414–20.

69. Schins R. Genotoxicity of Nanoparticles. Nanomaterials. 2013. p. 60–4.

70. Schins RPF. Mechanisms of Genotoxicity of Particles and Fibers. Inhal. Toxicol. 2002;14:57–78.

71. Borm PJA, Driscoll K. Particles, inflammation and respiratory tract carcinogenesis. Toxicol. Lett. 1996;88:109–13.

72. Marnett LJ. Oxyradicals and DNA damage. Carcinogenesis. 2000;21:361–70.

73. Azad N, Rojanasakul Y, Vallyathan V. Inflammation and lung cancer: roles of reactive oxygen/nitrogen species. J. Toxicol. Environ. Health. B. Crit. Rev. 2008;11:1–15.

74. Sarhan OMM, Hussein RM. Effects of intraperitoneally injected silver nanoparticles on histological structures and blood parameters in the albino rat. Int. J. Nanomedicine. 2014;9:1505–17.

75. Cui Y, Liu H, Ze Y, Zengli Z, Hu Y, Cheng Z, et al. Gene expression in liver injury caused by long-

term exposure to titanium dioxide nanoparticles in mice. Toxicol Sci. 2012;128:171–85.

76. Nalabotu SK, Kolli MB, Triest WE, Ma JY, Manne NDPK, Katta A, et al. Intratracheal instillation of cerium oxide nanoparticles induces hepatic toxicity in male Sprague-Dawley rats. Int. J. Nanomedicine. 2011;6:2327–35.

77. Chang XH, Zhu A, Liu FF, Zou LY, Su L, Liu SK, et al. Nickel oxide nanoparticles induced pulmonary fibrosis via TGF-beta1 activation in rats. Hum. Exp. Toxicol. England; 2016;

78. Srinivas A, Rao PJ, Selvam G, Murthy PB, Reddy PN. Acute inhalation toxicity of cerium oxide nanoparticles in rats. Toxicol. Lett. Elsevier Ireland Ltd; 2011;205:105–15.

79. Sung JH, Ji JH, Yoon JU, Kim DS, Song MY, Jeong J, et al. Lung function changes in Sprague-Dawley rats after prolonged inhalation exposure to silver nanoparticles. Inhal. Toxicol. 2008;20:567–74.

80. Chen H-W, Su S-F, Chien C-T, Lin W-H, Yu S-L, Chou C-C, et al. Titanium dioxide nanoparticles induce emphysema-like lung injury in mice. FASEB J. Off. Publ. Fed. Am. Soc. Exp. Biol. United States; 2006;20:2393–5.

81. Kmiec Z. Cooperation of liver cells in health and disease. Adv. Anat. Embryol. Cell Biol. 2001;161.

82. Https://bio.mox.polimi.it/nanomedicine/perfusion-characteristics-liver-tissue/. Simulation of the Perfusion Characteristic of the Liver Tissue.

83. Bilzer M, Roggel F, Gerbes AL. Role of Kupffer cells in host defense and liver disease. Liver Int. 2006;26:1175–86.

84. Dixon L, Barnes M, Tang H, Pritchard M, Nagy L. Kupffer Cells in the Liver. Compr Physiol. 2013;3:785–97.

85. Kermanizadeh A, Chauché C, Balharry D, Brown DM, Kanase N, Boczkowski J, et al. The role of Kupffer cells in the hepatic response to silver nanoparticles. Nanotoxicology. 2014;8 Suppl 1:149–54.

86. Tseng MT, Fu Q, Lor K, Fernandez-Botran GR, Deng Z-B, Graham U, et al. Persistent Hepatic Structural Alterations Following Nanoceria Vascular Infusion in the Rat. Toxicol. Pathol. 2014;42:984–96.

87. Chen Q, Xue Y, Sun J. Kupffer cell-mediated hepatic injury induced by silica nanoparticles in vitro and in vivo. Int J Nanomedicine. 2013;8:1129–40.

88. Ma L, Zhao J, Wang J, Liu J, Duan Y, Liu H, et al. The Acute Liver Injury in Mice Caused by Nano-Anatase TiO2. Nanoscale Res. Lett. 2009;4:1275–85.

89. Liu H, Ma L, Liu J, Zhao J, Yan J, Hong F. Toxicity of nano-anatase TiO 2 to mice: Liver injury, oxidative stress. Toxicol. Environ. Chem. 2010;92:175–86.

90. Liu H, Ma L, Zhao J, Liu J, Yan J, Ruan J, et al. Biochemical toxicity of nano-anatase TiO2 particles in mice. Biol. Trace Elem. Res. 2009;129:170–80.

91. Cui Y, Liu H, Zhou M, Duan Y, Li N, Gong X, et al. Signaling pathway of inflammatory responses in the mouse liver caused by TiO2 nanoparticles. J. Biomed. Mater. Res. - Part A. 2010;221–9.

92. Vesterdal LK, Danielsen PH, Folkmann JK, Jespersen LF, Aguilar-Pelaez K, Roursgaard M, et al. Accumulation of lipids and oxidatively damaged DNA in hepatocytes exposed to particles. Toxicol. Appl. Pharmacol. Elsevier B.V.; 2014;274:350–60.

93. Raaschou-Nielsen O, Andersen ZJ, Hvidberg M, Jensen SS, Ketzel M, Sorensen M, et al. Air pollution from traffic and cancer incidence: a Danish cohort study. Env. Heal. 2011;10:67.

94. Soll-Johanning H, Bach E, Olsen JH, Tüchsen F. Cancer incidence in urban bus drivers and tramway employees: a retrospective cohort study. Occup. Environ. Med. 1998;55:594–8.

95. Pan WC, Wu C Da, Chen MJ, Huang YT, Chen CJ, Su HJ, et al. Fine Particle Pollution, Alanine Transaminase, and Liver Cancer: A Taiwanese Prospective Cohort Study (REVEAL-HBV). J. Natl. Cancer Inst. 2016;108:1–7.

96. Pedersen M, Andersen ZJ, Stafoggia M, Weinmayr G, Galassi C, Sørensen M, et al. Ambient air pollution and primary liver cancer incidence in four European cohorts within the ESCAPE project. Environ. Res. 2017;154:226–33.

97. Levin M, Rojas E, Vanhala E, Vippola M, Liguori B, Kling K, et al. Influence of relative humidity and physical load during storage on dustiness of inorganic nanomaterials: implications for testing and risk assessment. J. Nanoparticle Res. Springer Netherlands; 2015;17.

98. Halappanavar S, Saber AT, Decan N, Jensen KA, Wu D, Jacobsen NR, et al. Transcriptional profiling identifies physicochemical properties of nanomaterials that are determinants of the in vivo pulmonary response. Environ. Mol. Mutagen. 2015;56:245–64.

99. Jacobsen NR, Pojana G, White P, Moller P, Cohn CA, Korsholm KS, et al. Genotoxicity, Cytotoxicity, and Reactive Oxygen Species Induced by Single-Walled Carbon Nanotubes and C60 Fullerenes in the FE1-MutaTM Mouse Lung Epithelial Cells. Environ. Mol. 2008;49:476–87.

100. Saber AT, Jensen KA, Jacobsen NR, Birkedal R, Mikkelsen L, Møller P, et al. Inflammatory and genotoxic effects of nanoparticles designed for inclusion in paints and lacquers. Nanotoxicology. 2012;6:453–71.

101. Saber AT, Bornholdt J, Dybdahl M, Sharma AK, Loft S, Vogel U, et al. Tumor necrosis factor is not required for particle-induced genotoxicity and pulmonary inflammation. Arch. Toxicol. 2005;79:177–82.

102. Lide DR. CRC Handbook of Chemistry and Physics 84th Edition. 2004.

103. Shi H, Magaye R, Castranova V, Zhao J. Titanium dioxide nanoparticles: a review of current toxicological data. Part Fibre Toxicol. 2013;10:15.

104. Efsa. Opinion of the Scientific Panel on Food Additives , Flavourings , Processing Aids and Materials in Contact with Food on a request from the Commission related to Use of formaldehyde as a preservative during the manufacture and preparation of food additives. EFSA J. 2004;415:1–10.

105. IARC Working Group on the Evaluation of Carcinogenic Risks to Humans. Carbon black, titanium dioxide, and talc. IARC Monogr. Eval. Carcinog. Risks Hum. 2010;93:1–413.

106. Kermanizadeh A, Gaiser BK, Hutchison GR, Stone V. An in vitro liver model--assessing oxidative stress and genotoxicity following exposure of hepatocytes to a panel of engineered

nanomaterials. Part. Fibre Toxicol. Particle and Fibre Toxicology; 2012;9:28.

107. Ghosh M, Chakraborty A, Mukherjee A. Cytotoxic, genotoxic and the hemolytic effect of titanium dioxide (TiO2) nanoparticles on human erythrocyte and lymphocyte cells in vitro. J. Appl. Toxicol. 2013;33:1097–110.

108. Trouiller B, Reliene R, Westbrook A, Solaimani P, Schiestl RH. Titanium dioxide nanoparticles induce DNA damage and genetic instability in vivo in mice. Cancer Res. 2009;69:8784–9.

109. Sycheva LP, Zhurkov VS, Iurchenko V V., Daugel-Dauge NO, Kovalenko MA, Krivtsova EK, et al. Investigation of genotoxic and cytotoxic effects of micro- and nanosized titanium dioxide in six organs of mice in vivo. Mutat. Res. - Genet. Toxicol. Environ. Mutagen. Elsevier B.V.; 2011;726:8–14.

110. Gurr JR, Wang ASS, Chen CH, Jan KY. Ultrafine titanium dioxide particles in the absence of photoactivation can induce oxidative damage to human bronchial epithelial cells. Toxicology. 2005;213:66–73.

111. Shukla RK, Kumar A, Vallabani NVS, Pandey AK, Dhawan A. Titanium dioxide nanoparticle-induced oxidative stress triggers DNA damage and hepatic injury in mice. Nanomedicine (Lond). England; 2014;9:1423–34.

112. Meena R, Paulraj R. Oxidative stress mediated cytotoxicity of TiO 2 nano anatase in liver and kidney of Wistar rat. Toxicol. Environ. Chem. 2012;94:146–63.

113. Li Y, Yan J, Ding W, Chen Y, Pack LM, Chen T. Genotoxicity and gene expression analyses of liver and lung tissues of mice treated with titanium dioxide nanoparticles. Mutagenesis. 2017;32:33–46.

114. Renwick LC, Brown D, Clouter A, Donaldson K. Increased inflammation and altered macrophage chemotactic responses caused by two ultrafine particle types. Occup Env. Med. 2004;61:442–7.

115. Warheit DB, Webb TR, Reed KL, Frerichs S, Sayes CM. Pulmonary toxicity study in rats with

three forms of ultrafine-TiO2 particles: Differential responses related to surface properties. Toxicology. 2007;230:90–104.

116. Johnston HJ, Hutchison GR, Christensen FM, Peters S, Hankin S, Stone V. Identification of the mechanisms that drive the toxicity of TiO(2)particulates: the contribution of physicochemical characteristics. Part. Fibre Toxicol. 2009;6:33.

117. Cassee FR, van Balen EC, Singh C, Green D, Muijser H, Weinstein J, et al. Exposure, health and ecological effects review of engineered nanoscale cerium and cerium oxide associated with its use as a fuel additive. Crit. Rev. Toxicol. 2011;41:213–29.

118. Jasinski P, Suzuki T, Anderson HU. Nanocrystalline undoped ceria oxygen sensor. Sensors Actuators, B Chem. 2003;95:73–7.

119. Zhu WZ, Deevi SC. A review on the status of anode materials for solid oxide fuel cells. Mater. Sci. Eng. A. 2003;362:228–39.

120. OECD. GUIDANCE MANUAL FOR THE TESTING OF MANUFACTURED NANOMATERIALS: OECD's SPONSORSHIP PROGRAMME; FIRST REVISION. Development. 2010;1–92.

121. Demokritou P, Gass S, Pyrgiotakis G, Cohen JM, Mckinney W, Frazer D, et al. An in vivo and in vitro toxicological characterization of realistic nanoscale CeO2 inhalation exposures. 2015;7:1338–50.

122. Ma, Zhao, Mercer, Barger, Rao, Meighan, et al. Cerium oxide nanoparticle-induced pulmonary inflammation and alveolar macrophage functional change in rats. Nanotoxicology. 2011;5:312–25.

123. Snow SJ, McGee J, Miller DB, Bass V, Schladweiler MC, Thomas RF, et al. Inhaled diesel emissions generated with cerium oxide nanoparticle fuel additive induce adverse pulmonary and systemic effects. Toxicol. Sci. 2014;142:403–17.

124. Morimoto Y, Izumi H, Yoshiura Y, Tomonaga T, Oyabu T, Myojo T, et al. Pulmonary toxicity of well-dispersed cerium oxide nanoparticles following intratracheal instillation and inhalation. J. Nanoparticle Res. Springer Netherlands; 2015;17:1–16.

125. Ma JKJY, Mercer RR, Barger M, Schwegler-Berry D, Scabilloni J, Ma JKJY, et al. Induction of pulmonary fibrosis by cerium oxide nanoparticles. Toxicol. Appl. Pharmacol. Elsevier B.V.; 2012;262:255–64.

126. Kumari M, Kumari SI, Kamal SSK, Grover P. Genotoxicity assessment of cerium oxide nanoparticles in female Wistar rats after acute oral exposure. Mutat. Res. - Genet. Toxicol. Environ. Mutagen. Elsevier B.V.; 2014;775–776:7–19.

127. Auffan M, Rose J, Orsiere T, De Meo M, Thill A, Zeyons O, et al. CeO2 nanoparticles induce DNA damage towards human dermal fibroblasts in vitro. Nanotoxicology. 2009;3:161–71.

128. Tseng MT, Lu X, Duan X, Hardas SS, Sultana R, Wu P, et al. Alteration of hepatic structure and oxidative stress induced by intravenous nanoceria. Toxicol. Appl. Pharmacol. 2012;260:173–82.

129. Niu J, Azfer A, Rogers LM, Wang X, Kolattukudy PE. Cardioprotective effects of cerium oxide nanoparticles in a transgenic murine model of cardiomyopathy. Cardiovasc. Res. 2007;73:549–59.

130. Schubert D, Dargusch R, Raitano J, Chan SW. Cerium and yttrium oxide nanoparticles are neuroprotective. Biochem. Biophys. Res. Commun. 2006;342:86–91.

131. Chen J, Patil S, Seal S, McGinnis JF. Rare earth nanoparticles prevent retinal degeneration induced by intracellular peroxides. Nat. Nanotechnol. 2006;1:142–50.

132. IARC. IARC monographs on the evaluation of carcinogenic risks to humans. A review of human carcinogens: chemical agents and related occupations. 2012;Vol. 100F:225–48.

133. Baan R, Straif K, Grosse Y, Secretan B, El Ghissassi F, Cogliano V, et al. Carcinogenicity of carbon black, titanium dioxide, and talc. Lancet Oncol. 2006;7:295–6.

134. Kyjovska ZO, Jacobsen NR, Saber AT, Bengtson S, Jackson P, Wallin H, et al. DNA strand breaks, acute phase response and inflammation following pulmonary exposure by instillation to the diesel exhaust particle NIST1650b in mice. Mutagenesis. 2015;30:499–507.

135. Saber AT, Halappanavar S, Folkmann JK, Bornholdt J, Boisen AMZ, Møller P, et al. Lack of acute phase response in the livers of mice exposed to diesel exhaust particles or carbon black by

inhalation. Part. Fibre Toxicol. 2009;6:12.

136. Husain M, Kyjovska ZO, Bourdon-Lacombe J, Saber AT, Jensen KA, Jacobsen NR, et al. Carbon black nanoparticles induce biphasic gene expression changes associated with inflammatory responses in the lungs of C57BL/6 mice following a single intratracheal instillation. Toxicol. Appl. Pharmacol. Elsevier B.V.; 2015;289:573–88.

137. Bourdon JA, Saber AT, Jacobsen NR, Williams A, Vogel U, Wallin H, et al. Carbon black nanoparticle intratracheal instillation does not alter cardiac gene expression. Cardiovasc. Toxicol. 2013;13:406–12.

138. Malvern Instruments. Dynamic Light Scattering: An Introduction in 30 Minutes. Http://Www.Malvern.Com/En/Products/Technology/Dynamic-Light-Scattering/. 2000;1–8.

139. Goldburg WII. Dynamic light scattering. Am. J. Phys. 1999;67:1152–60.

140. Guttenberg M, Bezerra L, Neu-Baker NM, del Pilar Sosa Pena M, Elder A, Oberdörster G, et al. Biodistribution of inhaled metal oxide nanoparticles mimicking occupational exposure: a preliminary investigation using enhanced darkfield microscopy. J Biophotonics. 2016;9:987–93.

141. Roth GA, Tahiliani S, Neu-Baker NM, Brenner SA. Hyperspectral microscopy as an analytical tool for nanomaterials. Wiley Interdiscip. Rev. Nanomedicine Nanobiotechnology. 2015;7:565–79.

142. Cheatham B. CytoViva Enhanced Darkfield Hyperspectral Microscope. https://www.youtube.com/watch?v=h_dN4HdMnAo. 2015.

143. PerkinElmer. The 30-Minute Guide to ICP-MS Technical note.

144. Harris D c. Quantitative Chemical Analysis. New York. 2007.

145. Husted S, Hansen TH, de Bang TC, Persson D. Quantitative multi-elemental ICP-MS analysis of plant tissue.

146. Laborda F, Bolea E, Jiménez-Lamana J. Single particle inductively coupled plasma mass spectrometry: Aapowerful tool for nanoanalysis. Anal. Chem. 2014;86:2270–8.

147. Stephan C, Hineman A. Analysis of NIST Gold Nanoparticles Reference Materials Using the NexION 300 ICP-MS in Single Particle Mode. Perkin Elmer Appl. note. 2012;5 pages.

148. Pace HE, Rogers NJ, Jarolimek C, Coleman VA, Higgins P, Ranville JF. Determining transport efficiency for the purpose of counting and sizing nanoparticles via single particle inductively coupled plasma-mass spectrometry. Anal. Chem. 2012;83:9361–9.

149. Stephan C, Neubauer K. Single Particle Inductively Coupled Plasma Mass Spectrometry : Understanding How and Why. Perkin Elmer, White note. 2014;1–5.

150. Wallin H, Kyjovska ZO, Poulsen SS, Jacobsen NR, Saber AT, Bengtson S, et al. Surface modification does not influence the genotoxic and inflammatory effects of TiO2 nanoparticles after pulmonary exposure by instillation in mice. Mutagenesis. 2017;gew046-.

151. Jacobsen NR, Møller P, Jensen KA, Vogel U, Ladefoged O, Loft S, et al. Lung inflammation and genotoxicity following pulmonary exposure to nanoparticles in ApoE-/- mice. Part. Fibre Toxicol. 2009;6.

152. Khanna KK, Jackson SP. DNA double-strand breaks: signaling, repair and the cancer connection. Nat. Genet. 2001;27:247–54.

153. Hoeijmakers JHJ. Genome Maintenance Mechanisms for Preventing Cancer. Nature. 2001;411:366–74.

154. Collins AR. The comet assay for DNA damage and repair: principles, applications, and limitations. Mol. Biotechnol. 2004;26:249–61.

155. Tice RR, Agurell E, Anderson D, Burlinson B, Hartmann A, Kobayashi H, et al. Single cell gel/comet assay: Guidelines for in vitro and in vivo genetic toxicology testing. Environ. Mol. Mutagen. 2000;35:206–21.

156. Olive PL, Banáth JP. The comet assay: a method to measure DNA damage in individual cells. Nat. Protoc. 2006;1:23–9.

157. Fang SC, Cassidy A, Christiani DC. A systematic review of occupational exposure to particulate matter and cardiovascular disease. Int. J. Environ. Res. Public Health. 2010;7:1773–

806.

158. Kuchipudi S V, Tellabati M, Nelli RK, White GA, Perez B, Sebastian S, et al. 18S rRNA is a reliable normalisation gene for real time PCR based on influenza virus infected cells. Virol. J. Virology Journal; 2012;9.

159. Heid C, Stevens J, Livak KJ, Williams PM. Real time quantitative PCR. Genome Res. 1996;6:986–94.

160. Huggett J, Dheda K, Bustin S, Zumla A. Real-time RT-PCR normalisation; strategies and considerations. Genes Immun. 2005;6:279–84.

161. Bustin, Stephen A., Mueller R. Real-time reverse transcription PCR (qRT-PCR) and its potential use in clinical diagnosis. Clin. Sci. (Lond). 2005;109:365–79.

162. Livak KJ, Schmittgen TD. Analysis of relative gene expression data using real-time quantitative PCR and the 2(-Delta Delta C(T)) Method. Methods. United States; 2001;25:402–8.

163. Poulsen SS, Saber AT, Williams A, Andersen O, Købler C, Atluri R, et al. MWCNTs of different physicochemical properties cause similar inflammatory responses, but differences in transcriptional and histological markers of fibrosis in mouse lungs. Toxicol. Appl. Pharmacol. Elsevier B.V.; 2015;284:16–32.

164. Manke A, Wang L, Rojanasakul Y. Mechanisms of nanoparticle-induced oxidative stress and toxicity. Biomed Res. Int. 2013;

165. LeBel CP, Ischiropoulos H, Bondys SC. Evaluation of the Probe 2',7'-Dichiorofluorescin as an Indicator of Reactive Oxygen Species Formation and Oxidative Stress. Chem. Res. Toxicol. 1992;5:227–31.

166. Espinosa-Cristobal LF, Martinez-Castañon GA, Loyola-Rodriguez JP, Patiño-Marin N, Reyes-Macías JF, Vargas-Morales JM, et al. Toxicity, distribution, and accumulation of silver nanoparticles in Wistar rats. J. Nanoparticle Res. 2013;15.

167. Zhang XD, Wu HY, Wu D, Wang YY, Chang JH, Zhai Z Bin, et al. Toxicologic effects of gold nanoparticles in vivo by different administration routes. Int. J. Nanomedicine. 2010;5:771–81.

168. Zhang XD, Wu D, Shen X, Liu PX, Yang N, Zhao B, et al. Size-dependent in vivo toxicity of PEG-coated gold nanoparticles. Int. J. Nanomedicine. 2011;6:2071–81.

169. Morsy GM, Abou El-Ala KS, Ali A a. Studies on fate and toxicity of nanoalumina in male albino rats: lethality, bioaccumulation and genotoxicity. Toxicol. Ind. Health. 2016;32:634–55.

170. Chen J, Dong X, Zhao J, Tang G. In vivo acute toxicity of titanium dioxide nanoparticles to mice after intraperitioneal injection. J. Appl. Toxicol. 2009;29:330–7.

171. Madl AK, Pinkerton KE. Health effects of inhaled engineered and incidental nanoparticles. Crit. Rev. Toxicol. 2009;39:629–58.

172. Poulsen SS, Jackson P, Kling K, Knudsen KB, Skaug V, Kyjovska ZO, et al. Multi-walled carbon nanotube physicochemical properties predict pulmonary inflammation and genotoxicity. Nanotoxicology. 2016;10:1263–75.

173. Mikkelsen L, Sheykhzade M, Jensen KA, Saber AT, Jacobsen NR, Vogel U, et al. Modest effect on plaque progression and vasodilatory function in atherosclerosis-prone mice exposed to nanosized TiO2. Part. Fibre Toxicol. 2011;8:32.

174. Osier M, Oberdorster G. Intratracheal Inhalation vs Intratracheal Instillation: Differences in Particle Effects. Fundam. Appl. Toxicol. 1997;40:220–7.

175. Weir A, Westerhoff P, Fabricius L, Hristovski K, von Goetz N. Titanium dioxide nanoparticles in food and personal care products. Environ. Sci. Technol. American Chemical Society; 2012;46:2242–50.

176. Tiede K, Boxall ABA, Tear SP, Lewis J, David H, Hassellov M. Detection and characterization of engineered nanoparticles in food and the environment. Food Addit. Contam. 2008;25:795–821.

177. Win KY, Feng SS. Effects of particle size and surface coating on cellular uptake of polymeric nanoparticles for oral delivery of anticancer drugs. Biomaterials. 2005;26:2713–22.

178. Yu LE, Yung LL, Ong C, Tan Y, Balasubramaniam KS, Hartono D, et al. Translocation and effects of gold nanoparticles after inhalation exposure in rats. Nanotoxicology. 2007;1:235–42.

179. Berry JP, Arnoux B, Stanislas G, Galle P, Chretien J. A microanalytic study of particles transport across the alveoli: role of blood platelets. Biomedicine. France; 1977;27:354–7.

180. Wu L, Chen L, Liu F, Qi X, Ge Y, Shen S. Remotely controlled drug release based on iron oxide nanoparticles for specific therapy of cancer. Colloids Surfaces B Biointerfaces. Elsevier B.V.; 2017;152:440–8.

181. Xin Y, Liu T, Yang CL. Development of PLGA-lipid nanoparticles with covalently conjugated indocyanine green as a versatile nanoplatform for tumor-targeted imaging and drug delivery. Int. J. Nanomedicine. 2016;11:5807–21.

182. Nemmar A, Hoet PHM, Vanquickenborne B, Dinsdale D, Thomeer M, Hoylaerts MF, et al. Passage of inhaled particles into the blood circulation in humans. Circulation. 2002;105:411–4.

183. Levy L, Chaudhuri IS, Krueger N, McCunney RJ. Does carbon black disaggregate in lung fluid? A critical assessment. Chem. Res. Toxicol. 2012;25:2001–6.

184. McCunney R. Particle Overload In The Rat Lung And Lung Cancer: Implications For Human Risk Assessment. 1996.

185. Dybing E, Sanner T, Roelfzema H, Kroese D, Tennant RW. T25: a simplified carcinogenic potency index: description of the system and study of correlations between carcinogenic potency and species/site specificity and mutagenicity. Pharmacol. Toxicol. 1997;80:272–9.

186. Marquis BJ, Love SA, Braun KL, Haynes CL. Analytical methods to assess nanoparticle toxicity. Analyst. 2009;134:425–39.

187. Gunsolus IL, Haynes CL. Analytical Aspects of Nanotoxicology. Anal. Chem. 2016;88:451–79.

188. Scheffer A, Engelhard C, Sperling M, Buscher W. ICP-MS as a new tool for the determination of gold nanoparticles in bioanalytical applications. Anal. Bioanal. Chem. 2008;390:249–52.

189. Loeschner K, Hadrup N, Hansen M, Pereira SA, Gammelgaard B, Møller LH, et al. Absorption, distribution, metabolism and excretion of selenium following oral administration of elemental selenium nanoparticles or selenite in rats. Metallomics. 2014;6:330–7.

190. Hougaard KS, Jackson P, Jensen K a, Sloth JJ, Löschner K, Larsen EH, et al. Effects of prenatal exposure to surface-coated nanosized titanium dioxide (UV-Titan). A study in mice. Part. Fibre Toxicol. 2010;7.

191. Badireddy AR, Wiesner MR, Liu J. Detection, characterization, and abundance of engineered nanoparticles in complex waters by hyperspectral imagery with enhanced darkfield microscopy. Environ. Sci. Technol. 2012;46:10081–8.

192. Park E-J, Cho W-S, Jeong J, Yi J, Choi K, Kim Y, et al. Induction of Inflammatory Responses in Mice Treated with Cerium Oxide Nanoparticles by Intratracheal Instillation. J. Heal. Sci. 2010;56:387–96.

193. Chen S, Yin R, Mutze K, Yu Y, Takenaka S, Königshoff M, et al. No involvement of alveolar macrophages in the initiation of carbon nanoparticle induced acute lung inflammation in mice. Part. Fibre Toxicol. Particle and Fibre Toxicology; 2015;13:33.

194. Wang J, Liu Y, Jiao F, Lao F, Li W, Gu Y, et al. Time-dependent translocation and potential impairment on central nervous system by intranasally instilled TiO2 nanoparticles. Toxicology. 2008;254:82–90.

195. Ayyagari VN, Januszkiewicz A, Nath J. Pro-inflammatory responses of human bronchial epithelial cells to acute nitrogen dioxide exposure. Toxicology. 2004;197:149–64.

196. Poulsen SS, Saber AT, Mortensen A, Szarek J, Wu D, Williams A, et al. Changes in cholesterol homeostasis and acute phase response link pulmonary exposure to multi-walled carbon nanotubes to risk of cardiovascular disease. Toxicol. Appl. Pharmacol. Elsevier B.V.; 2015;283:210–22.

197. Donaldson K, Tran CL. Inflammation Caused By Particles and Fibers. Inhal. Toxicol. 2002;14:5–27.

198. Renwick LC, Donaldson K, Clouter A. Impairment of Alveolar Macrophage Phagocytosis by Ultrafine Particles. Toxicol. Appl. Pharmacol. 2001;172:119–27.

199. Khandoga A, Stampfl A, Takenaka S, Schulz H, Radykewicz R, Kreyling W, et al. Ultrafine

Particles Exert Prothrombotic but Not Inflammatory Effects on the Hepatic Microcirculation in Healthy Mice In Vivo. Circulation. 2004;109:1320–5.

200. Pepys MHG. C-reactive protein: a critical update. J. Clin. Invest. 2003;111:1805–12.

201. Whitehead AS, Zahedi K, Rits M, Mortensen RF, Lelias JM. Mouse C-reactive protein. Generation of cDNA clones, structural analysis, and induction of mRNA during inflammation. Biochem. J. 1990;266:283–90.

202. Jackson P, Halappanavar S, Hougaard KS, Williams A, Madsen AM, Lamson JS, et al. Maternal inhalation of surface-coated nanosized titanium dioxide (UV-Titan) in C57BL/6 mice: effects in prenatally exposed offspring on hepatic DNA damage and gene expression. Nanotoxicology. 2013;7:85–96.

203. Schins RPF, Knaapen AM. Genotoxicity of poorly soluble particles. Inhal. Toxicol. 2007;19 Suppl 1:189–98.

204. Clancy L, Goodman P, Sinclair H, Dockery DW. Effect of air-pollution control on death rates in Dublin, Ireland: An intervention study. Lancet. 2002;360:1210–4.

205. Simak J. Nanotoxicity in Blood: Effects of Engineered Nanomaterials on Platelets. Nanotoxicity From Vivo Vitr. Model. to Heal. Risks. 2009.

206. Saber AT, Mortensen A, Szarek J, Koponen IK, Levin M, Jacobsen NR, et al. Epoxy composite dusts with and without carbon nanotubes cause similar pulmonary responses, but differences in liver histology in mice following pulmonary deposition. Part. Fibre Toxicol. Particle and Fibre Toxicology; 2016;13.

207. Loomis D, Grosse Y, Lauby-Secretan B, Ghissassi F El, Bouvard V, Benbrahim-Tallaa L, et al. The carcinogenicity of outdoor air pollution. Lancet Oncol. 2013;14:1262–3.

208. P Michelozzi, D Fusco, F Forastiere, C Ancona, V Dell'Orco CP, P Michelozzi F Forastiere, C Ancona, V Dell'Orco, CA Perucci DF. Small area study of mortality among people living near multiple sources of air pollution. Occup. Environ. Med. 1998;55:611–5.

209. Lee YCA, Cohet C, Yang YC, Stayner L, Hashibe M, Straif K. Meta-analysis of epidemiologic

studies on cigarette smoking and liver cancer. Int. J. Epidemiol. 2009;38:1497–511.

210. Sadauskas E, Danscher G, Stoltenberg M, Vogel U, Larsen A, Wallin H. Protracted elimination of gold nanoparticles from mouse liver. Nanomedicine Nanotechnology, Biol. Med. Elsevier Inc.; 2009;5:162–9.

211. Nemmar A, Yuvaraju P, Beegam S, Fahim MA, Ali BH. Cerium Oxide Nanoparticles in Lung Acutely Induce Oxidative Stress , Inflammation , and DNA Damage in Various Organs of Mice. 2017;2017.

212. Nelson B, Johnson M, Walker M, Riley K, Sims C. Antioxidant Cerium Oxide Nanoparticles in Biology and Medicine. Antioxidants. 2016;5:15.

213. DeCoteau W, Heckman KL, Estevez AY, Reed KJ, Costanzo W, Sandford D, et al. Cerium oxide nanoparticles with antioxidant properties ameliorate strength and prolong life in mouse model of amyotrophic lateral sclerosis. Nanomedicine Nanotechnology, Biol. Med. Elsevier Inc.; 2016;12:2311–20.

214. Kumari M, Kumari SI, Grover P. Genotoxicity analysis of cerium oxide micro and nanoparticles in Wistar rats after 28 days of repeated oral administration. Mutagenesis. 2014;29:467–79.

215. Yokel RA, Au TC, MacPhail R, Hardas SS, Butterfield DA, Sultana R, et al. Distribution, elimination, and biopersistence to 90 days of a systemically introduced 30 nm ceria-engineered nanomaterial in rats. Toxicol. Sci. 2012;127:256–68.

216. Hirst SM, Karakoti A, Singh S, Self W, Tyler R, Seal S, et al. Bio-distribution and in vivo antioxidant effects of cerium oxide nanoparticles in mice. Environ. Toxicol. 2013;28:107–18.

217. Liu H-L, Yang H-L, Lin B-C, Zhang W, Tian L, Zhang H-S, et al. Toxic effect comparison of three typical sterilization nanoparticles on oxidative stress and immune inflammation response in rats. Toxicol. Res. Royal Society of Chemistry; 2015;4:486–93.

218. Liang G, Pu Y, Yin L, Liu R, Ye B, Su Y, et al. Influence of different sizes of titanium dioxide nanoparticles on hepatic and renal functions in rats with correlation to oxidative stress. J.

Toxicol. Environ. Health. A. 2009;72:740–5.

219. Yin J, Kang C, Li Y, Li Q, Zhang X, Li W. Aerosol inhalation exposure study of respiratory toxicity induced by 20 nm anatase titanium dioxide nanoparticles. Toxicol. Res. (Camb). Royal Society of Chemistry; 2014;3:367–74.

220. Geraets L, Oomen AG, Krystek P, Jacobsen NR, Wallin H, Laurentie M, et al. Tissue distribution and elimination after oral and intravenous administration of different titanium dioxide nanoparticles in rats. Part. Fibre Toxicol. 2014;11:30.

221. Cui Y, Gong X, Duan Y, Li N, Hu R, Liu H, et al. Hepatocyte apoptosis and its molecular mechanisms in mice caused by titanium dioxide nanoparticles. J. Hazard. Mater. 2010;183:874–80.

222. Shrivastava R, Raza S, Yadav A, Kushwaha P, Flora SJS. Effects of sub-acute exposure to TiO2, ZnO and Al2O3 nanoparticles on oxidative stress and histological changes in mouse liver and brain. Drug Chem. Toxicol. 2014;37:336–47.

223. Oberdörster G, Ferin J, Lehnert BE. Correlation betwen Particle Size, In Vivo Particle Persistence, and Lung injury. Environ. Health Perspect. 1994;102:173–9.

224. Suzuki T, Miura N, Hojo R, Yanagiba Y, Suda M, Hasegawa T, et al. Genotoxicity assessment of intravenously injected titanium dioxide nanoparticles in gpt delta transgenic mice. Mutat. Res. - Genet. Toxicol. Environ. Mutagen. Elsevier B.V.; 2016;802:30–7.

225. Umbreit TH, Francke-Carroll S, Weaver JL, Miller TJ, Goering PL, Sadrieh N, et al. Tissue distribution and histopathological effects of titanium dioxide nanoparticles after intravenous or subcutaneous injection in mice. J. Appl. Toxicol. 2012;32:350–7.

226. Elgrabli D, Beaudouin R, Jbilou N, Floriani M, Pery A, Rogerieux F, et al. Biodistribution and clearance of TiO2 nanoparticles in rats after intravenous injection. PLoS One. 2015;10:1–13.

227. Xu J, Shi H, Ruth M, Yu H, Lazar L, Zou B, et al. Acute Toxicity of Intravenously Administered Titanium Dioxide Nanoparticles in Mice. PLoS One. 2013;8:1–6.

228. Alarifi S, Ali D, Al-Doaiss AA, Ali BA, Ahmed M, Al-Khedhairy AA. Histologic and apoptotic

changes induced by titanium dioxide nanoparticles in the livers of rats. Int. J. Nanomedicine. 2013;8:3937–43.

229. Jeon Y-M, Park S-K, Lee M-Y. Proteomic analysis of hepatotoxicity induced by titanium nanoparticles in mouse liver. J. Korean Soc. Appl. Biol. Chem. 2011;54:852–9.

230. Rizk MZ, Ali SA, Hamed MA, El-Rigal NS, Aly HF, Salah HH. Toxicity of titanium dioxide nanoparticles: Effect of dose and time on biochemical disturbance, oxidative stress and gentoxicity in mice. Biomed. Pharmacother. Elsevier Masson SAS; 2017;90:466–72.

231. Bruno ME, Tasat DR, Ramos E, Paparella ML, Evelson P, Rebagliati RJ, et al. Impact through time of different sized titanium dioxide particles on biochemical and histopathological parameters. J. Biomed. Mater. Res. - Part A. 2014;102:1439–48.

232. Jackson P, Hougaard KS, Vogel U, Wu D, Casavant L, Williams A, et al. Exposure of pregnant mice to carbon black by intratracheal instillation: Toxicogenomic effects in dams and offspring. Mutat. Res. - Genet. Toxicol. Environ. Mutagen. Elsevier B.V.; 2012;745:73–83.

233. Kroll A, Dierker C, Rommel C, Hahn D, Wohlleben W, Schulze-Isfort C, et al. Cytotoxicity screening of 23 engineered nanomaterials using a test matrix of ten cell lines and three different assays. Part. Fibre Toxicol. BioMed Central Ltd; 2011;8:9.

234. Manke A, Wang L, Rojanasakul Y. Mechanisms of nanoparticle-induced oxidative stress and toxicity. Biomed Res. Int. 2013;2013:1–14.

235. Risom L, Moller P, Vogel U, Kristjansen PE, Loft S. X-ray induced oxidative stress: dna damage and gene expression of HO-1, ERCC1 and OGG1 in mouse lung. Free Radic. Res. 2003;37.

236. Kreyling WG, Semmler-Behnke M, Seitz J, Scymczak W, Wenk A, Mayer P, et al. Size dependence of the translocation of inhaled iridium and carbon nanoparticle aggregates from the lung of rats to the blood and secondary target organs. Inhal. Toxicol. 2009;21 Suppl 1:55–60.

237. Lindhorst E, Young D, Bagshaw W, Hyland M, Kisilevsky R. Acute inflammation, acute phase serum amyloid A and cholesterol metabolism in the mouse. Biochim. Biophys. Acta. 1997;1339:143–54.

MANUSCRIPT 1

In vivo-induced size transformation of CeO_2 NPs in both lung and liver does not affect long-term accumulation of Ce in liver following pulmonary exposure

Justyna Modrzyńska, Trine Berthing, Gitte Ravn-Haren, Kirsten Kling, Alicja Mortensen, Rie R. Rasmussen, Erik H. Larsen, Anne T. Saber, Ulla Vogel, Katrin Loeschner

Submitted to a *BioMed* journal

In vivo-induced size transformation of CeO_2 NPs in both lung and liver does not affect long-term accumulation of Ce in liver following pulmonary exposure

Justyna Modrzynska[1,2], Trine Berthing[2], Gitte Ravn-Haren[1], Kirsten Kling[2], Alicja Mortensen[2], Rie R. Rasmussen[1], Erik H. Larsen[1], Anne T. Saber[2], Ulla Vogel[2,3], Katrin Loeschner[1]*

[1] National Food Institute, Technical University of Denmark, Kongens Lyngby, Denmark

[2] The National Research Centre for the Working Environment, Copenhagen, Denmark

[3] Department of Micro- and Nanotechnology, Technical University of Denmark, Kongens Lyngby, Denmark

* Corresponding author: Katrin Loeschner, Research Group for Nano-Bio Science, National Food Institute, Technical University of Denmark, Kemitorvet Building 201, room 130, 2800 Kgs. Lyngby, Denmark. Tel: +45 35 88 70 29. Fax: +45 35 88 74 48. E-mail: kals@food.dtu.dk

ABSTRACT

Background:
Recent findings indicate that cerium oxide (CeO_2) nanoparticles (NPs) may undergo *in vivo*-induced size transformation with the formation of smaller particles that could result in a higher translocation following pulmonary exposure compared to virtually insoluble particles, like titanium dioxide (TiO_2). Therefore, we compared liver deposition of CeO_2 and TiO_2 NPs of similar primary sizes 1, 28 or 180 days after intratracheal instillation of 162 µg of NPs in female C57BL/6 mice. Mice exposed to 162 µg CeO_2 or TiO_2 NPs by intravenous injection and oral gavage were included as reference groups to assess the amount of NPs that reach the liver bypassing the lungs and the translocation of NPs from the gastrointestinal tract to the liver, respectively. Mice exposed to vehicle by all exposure routes were included as controls.

Results:
Pulmonary deposited CeO_2 NPs were detected in the liver tissue 28 and 180 days post-exposure and TiO_2 NPs were detected in the liver tissue 180 days post-exposure as determined by darkfield imaging and by the quantification of Ce and Ti mass concentration by inductively coupled plasma mass spectrometry (ICP-MS). Both Ce and Ti concentrations increased over time and 180 days post-exposure the calculated translocation was 2.87 ± 3.37 % and 1.24 ± 1.98 %, respectively, of the initial pulmonary dose. Size distributions of CeO_2 NPs determined by single particle ICP-MS showed that the size of CeO_2 NPs in both lung and liver tissue decreased over time. No NPs were detected in the liver following oral gavage.

Conclusion:
Our results suggest that pulmonary deposited CeO_2 and TiO_2 NPs translocate to the liver with similar calculated translocation rates despite their different chemical composition and shape. The observed particle size distributions of CeO_2 NPs indicate that CeO_2 NPs undergo *in vivo* processing over time both in lung and liver. The fact that no particles were detected in the liver following oral exposure indicates direct translocation of NPs from lung to the systemic circulation being the most important route of translocation for pulmonary-deposited particles. Overall, our data indicates that liver toxicity may be an important part of the hazard evaluation of inhaled NPs.

Keywords – *Cerium oxide, Titanium dioxide, Nanoparticles, Liver, Translocation, Size transformation, Intratracheal instillation, Intravenous injection, Oral gavage*

BACKGROUND

Unique properties exhibited by nanoparticles (NPs) such as small size, large surface area and high reactivity as compared to fine particles or bulk material has led to the development of a wide range applications of NPs in science, technology and medicine. NPs can be used in various day-to-day consumer products including cosmetics, electronics, sporting goods, paints, lacquers and tires. They could also serve as food additives, pharmaceuticals and be utilized in medical applications (e.g. targeted drug delivery and bioimaging). Therefore, several portals of entry and different target tissues exist [1–4]. Understanding the deposition fate of NPs after administration to the body is a crucial part of hazard evaluation of nanomaterials.

Both CeO_2 and TiO_2 NPs have versatile applications and are widely use in everyday life products. Cerium oxide (CeO_2) can be used as an abrasive agent for chemical-mechanical planarization of advanced integrated circuits [5], polishing agent for glass mirrors, television tubes and ophthalmic lenses [6], oxygen sensor [7], diesel fuel catalyst to improve combustion and reduce consumption of the fuels [6] and in solid oxide fuel cells [8]. Titanium dioxide (TiO_2) is widely used as white pigment due to its brightness and high refractive index [9] and therefore utilize in paints, coatings, cosmetics (sunscreen, toothpaste) and in pharmaceuticals [10]. Moreover, it has been approved as a food additive in Europe (also known as E171) used in candy and chewing gum [11].

Inhalation is the most relevant exposure route for occupational exposure to NPs. It has been previously observed that particles deposited in the lungs after inhalation or intratracheal instillation are cleared from the respiratory tract by various clearance mechanisms and various routes. Inhaled particles, deposited preferentially in the alveolar region, are cleared mainly by macrophage-mediated phagocytosis. Internalized particles gradually moved toward the mucociliary escalator in the upper airways [12]. Once the particles reach the bronchi, they are transported up into the pharynx and when swallowed, cause gastrointestinal tract (GIT) exposure [2,13–15]. Nonetheless, the uptake of NPs by the GIT has been shown to be very low [9,15–17]. Inhaled NPs may also migrate across the alveolar epithelium, through interstitium, access systemic circulation directly or via lymphatic vessels and accumulate in the liver and spleen [18–23]. Inconsistent results regarding the fraction of ultrafine particles (UFP) that undergo extrapulmonary translocation and further deposition in the secondary organs have been reported [14,23–25]. The degree of translocation is influenced by various physicochemical properties like size, chemical composition, shape, electrical charge [14,26].

The liver, among other reticuloendothelial organs, seems to be the major organ for particles deposition after accessing systemic circulation [27–31]. When translocated particles reach the liver, they accumulate in the Kupffer cells, specialized macrophages located in the liver [27,32,33]. The Kupffer cells constitute the first line of the defense against xenobiotics. The clearance rate of NPs from Kupffer cells is very slow. Thus, 90% of injected gold nanoparticle (40 nm) dose was still detected in the liver tissue 6 months after exposure [34]. Previous studies indicate that pulmonary exposure to reactive NPs is associated with genotoxic effect observed in the liver tissue [13,35,36].

Graham and colleagues [37] recently showed that hydro-thermally derived CeO_2 NPs undergo *in vivo* processing in the liver tissue over time. The originally cube-shaped CeO_2 NPs became highly fragmented and rounded along their edges ninety days after exposure. No NP transformation was observed thirty days after exposure. Additionally, the accumulation of 1–3 nm crystallites in close proximity to the parental CeO_2 NPs was observed. Dissolution of high-energy edge sites was suggested as the underlying mechanism.

The aim of the present study was to evaluate extrapulmonary translocation of lung-deposited CeO_2 and TiO_2 and to assess whether the partial solubility of CeO_2 affect hepatic accumulation. We also wanted to determine size distribution changes of long-term deposited particles in the lung and liver tissue.

METHODS

Preparation of NP suspensions and characterization of exposure media

Powdered cerium oxide (CeO_2) was provided by Degussa-Quimidroga and powdered titanium dioxide (TiO_2) was provided by NanoAmor (Nanostructured & Amorphous Materials). NP suspensions of 3.24 mg/ml were prepared in 2% mouse serum as described in [38,39]. In short, stock suspensions of 3.24 mg/ml alongside control vehicle were sonicated for 15 min on ice, to prevent sample overheating, using a probe sonicator operating at 100 W/22.5 kHz (Microson ultrasonic cell disruptor, XL-2000 Microson™, Qsonica, LLC., equipped with disruptor horn with a diameter of 3.2 mm and maximum peak-to-peak amplitude of 180 μm). The size distribution of each produced NP suspension was determined by dynamic light scattering (Zetasizer Nano-ZS, Malvern Instruments, UK) as described in [36,40]. The refractive index and light absorption for the test materials were: 2.2 and 0.1, respectively, for CeO_2, 2.903 and 0.1, respectively, for TiO_2. Optical data for water were used for the control vehicle.

Preparation and analysis of electron microscopy samples

Samples were dispersed on TEM (Transmission Electron Microscope) grids covered with holy carbon foil according to a standard protocol for diameter and morphological analyses of nanomaterial in SEM

Table 1. Instrumental settings for ICP-MS analysis

Parameter (unit)	Ce analysis	Ce single particle analysis	Ti analysis
RF power (W)	1550	1550	1550
Plasma gas flow rate (l/min)	14	14	15
Nebulizer gas flow rate (ml/min)	~1.1	~1.1	~1.1
Auxiliary gas flow rate (ml/min)	~0.8	~0.8	~0.1
Cell gas flow rate (ml/min)	n/a	n/a	2 ml/min NH_3/He (10/90) + 1 ml/min He
Monitored isotopes (*m/z*)	^{140}Ce	^{140}Ce, ^{197}Au	Q1 → Q2 masses: 48→ 150 (Ti); 45 → 130 (Sc)
Dwell time (ms)	10	3	100
Nebulizer type	Low-flow concentric nebulizer	Low-flow concentric nebulizer	Agilent MicroFlow (model no. G3139A-100)
Spray chamber type	Cyclonic, Peltier-cooled (quartz)	Cyclonic, Peltier-cooled (quartz)	Scott double-pass, Peltier-cooled (quartz)

(Scanning Electron Microscope) and TEM. 0.2 mg of CeO_2 and 0.5 mg of TiO_2 were dispersed in 8 ml of N-methyl 2-pyrrolidone and incubated for 10 min in an ultrasound bath. The dispersion was sonicated using a probe sonicator with a 13 mm probe tip for 10 min at 10 % amplitude on ice. After sonication, 10 µL of sample was dispersed onto a TEM-grid. The samples were dried in a vacuum chamber for 5 min. Afterwards samples were further dried under red light (warming lamp) for 24 h.

Images were recorded at the ZEISS facility in Oberkochen, Germany by curtesy of Dr. Xiong Liu, using a GeminiSEM 300 equipped with a STEM detector (ZEISS, Oberkochen, Germany). Plasma cleaning was applied to the samples inside the microscope chamber, to derive a better image quality.

Animal study

216 young adult C57BL/6 (B6JBOM-F) female mice were purchased from Taconic (Ry, Denmark) at 6 weeks of age and body weight of 17.5 ± 0.9 g (mean ± SD). Mice were acclimated for 2 weeks before the beginning of the experiment. Upon delivery mice were randomly divided into experimental groups and control groups (n=9) and housed in polypropylene cages (Type III with Tapvei bedding and enrichment – nesting material and den), 5 or 4 mice in each, under the following conditions: 12 h light/12 h dark cycle, room temperature of 22°C ± 1° and the relative humidity of 55% ± 5. Throughout the whole experiment mice were given a standard pellet diet (Altromin No. 1324) and acidified water (pH 4) *ad libitum*. All mice were weighted weekly and food intake was noted. For 6 months exposure groups, body weight was recorded once in 2 weeks intervals after day 28. Mice were observed daily for any sign of abnormalities in their clinical appearance.

Mice were dosed a single dose of 162 µg of CeO_2 or TiO_2 NPs in 50 µl of 2% serum in nanopure water by intratracheal instillation (IT), oral gavage (PO) or intravenous injection (IV). Control mice received 50 µl of 2 % serum. The dose corresponds to the pulmonary deposition during 13 8-h working days at the Danish occupational exposure limit of 10 mg/m^3 for TiO_2 assuming 9% alveolar deposition [41,42]. Prior to the administration of NP suspension by either intravenous injection or intratracheal instillation animals were anaesthetized by subcutaneously injection in the neck with 0.5 ml/100g of Hypnorm® (Fentanyl citrate 0.315 mg/ml and Fluanisone 10 mg/ml, Nomeco) and Dormicum® (Midazolam 5 mg/ml, Roche) diluted 1:1 in a sterile water and mixed together. Orally administered mice were not anaesthetized during dosing. Intratracheal instillation was performed as previously described [42] In brief, mice were placed on a 40° slope (upside down, with the head towards the floor) and a diode lamp was located on the larynx for a better visualization. A small spatula was used to press the tongue towards the lower jaw and the 22 GA BD Insyte catheter (Becton Dickinson, Utah, USA) with a shortened needle was used to intubate the trachea. A volume of 50 µl followed by 200 µl air in a 250 µl SGE glass syringe (250F-LT-GT, MicroLab, Aarhus, Denmark) was instilled.

In order not to block the airways and to assure that the NP suspension maintains in the lung, mice were placed back into a vertical position with the head up as soon as the catheter was removed. For oral gavage, mice were gently restrained in a vertical position to immobilize the head and the gavage needle (0.9 x 38 mm, NOVA-SCB, Sweden) was inserted into the esophagus and further toward the stomach. For intravenous injection anaesthetized mice were restrained in a Plexiglas restraining tube. A tail-vein injection was performed with a 0.4 × 20 mm needle (Terumo Europe, n.v. 3001, Leuven, Belgium). After intratracheal instillation, gavage and intravenous injection animals were transferred back to their cages, heated with a heating lamp and/or warming blanket and monitored until they fully recovered from anesthesia. The animals did not show any adverse effects caused by the administration procedure. The study was conducted in the agreement with the Danish law regulating experiment on animals (Permission 2012-15-2934-00089 C6) and the Technical University of Denmark´s animal welfare protocol.

Necropsy and organ collection

After the exposure period – 1 day, 28 days or 180 days, animals were weighted and prepared for necropsy. Mice were terminated by the overdose of Hypnorm – Dormicum mixture (0.5 – 0.7 ml/100 g). The mice abdomen and thorax were opened and all macroscopic abnormalities were noted in the autopsy report. Pieces of liver and lung tissue for further ICP-MS analysis were collected and snapped frozen in cryotubes (NUNC) in liquid nitrogen and stored at -80 °C until used. A piece of liver tissue was fixated in 4% neutral buffered formalin for 24 hours and embedded in paraffin blocks on the next day. Lungs were removed intact, filled with formalin and submerged in 4% neutral buffered formalin. Liver and lungs tissue sections of 3 µm thickness were cut and stained with hematoxylin and eosin for further light and darkfield microscopy.

Enhanced darkfield microscopy

Cytoviva enhanced darkfield hyperspectral system (Auburn, AL, USA) was used to detect particles in liver and lung, by scanning histological sections at 40x magnification in enhanced darkfield mode. Images were acquired at 40x and 100x on an Olympus BX 43 microscope with a Qimaging Retiga4000R camera. Uneven illumination in brightfield images was corrected using ImageJ [43] and the Calculator Plus plugin via the formula: Corrected_image = (image / background) * 255. The background image was a maximum projection of 3 background brightfield images without tissue.

Determination of mass concentration of Ce and Ti in mouse organs by ICP-MS

The total mass concentration of cerium (Ce) and titanium (Ti) in animal tissues (liver and lung) was determined by inductively coupled plasma-mass spectrometry (ICP-MS). Ultrapure water (18.2 mΩ/cm) was obtained from a Millipore Element apparatus (Millipore, Milford, MA, USA) and used throughout the work.

Sample preparation

For analysis of Ce by ICP-MS, approximately 100 mg of the liver tissue was thawed, exactly weighed, mixed with 1.5 ml of ultrapure water and homogenized using an Ultra Turrax homogenizer (DI 25 Basic, Ika-Werke, Staufen, Germany) for 3 min at 8000 rpm. For Ti analysis Ceramic Bead Tubes (⌀ 1.4 mm, made of zirconium oxide, MoBio, Denmark) were used for liver tissue homogenization to avoid potential release of Ti-containing particles from the Ultra Turrax homogenizer. Approximately 100 mg of the liver tissue was thawed, exactly weighed, mixed with 1.5 ml of ultrapure water and ceramic beads and subsequently homogenized for 3 min using a Tissue Lyser (Qiagen, manufactured by Retsch). A volume of tissue homogenate corresponding to 40 mg of tissue was transferred to disposable standard glass vials (Wheaton® 15x46 mm, cap 13-425) and subsequently digested in a mixture of 0.250 ml concentrated nitric acid (68% HNO_3, PlasmaPure, SCP Science, Quebec, Canada) and 0.125 ml hydrogen peroxide (Suprapur, Merck, Darmstadt, Germany) in a microwave oven (Multiwave 3000, Anton Paar GmbH, Graz, Austria) equipped with a 64MG5 rotor at elevated temperature and pressure (~ 140°C; max. 20 bar). After digestion, ultrapure water was added to a final sample weight of 3 g. Samples were further diluted 10- to 1000-fold with ultrapure water prior to analysis. The rest of the Ce and Ti homogenate was stored at -20 °C for single particle ICP-MS analysis. Approximately 40 mg of the lung tissue was prepared as described above excluding the homogenization procedure.

Analytical technique

The Ce mass concentration in the tissues was determined by using an iCAP Q ICP-MS instrument (Thermo Fisher Scientific GmbH, Bremen, Germany) equipped with an ASX-520 autosampler (Cetac Technologies, Omaha, USA). Typical instrumental settings for the analysis are given in Table 1. The concentration of Ce was quantified against an external calibration curve prepared in 2% nitric acid from a Ce stock solution of 1000 µg/ml (SCP Science, Quebec, Canada). To reduce carry-over, careful rinsing with 2% nitric acid between samples was performed.

The Ti mass concentration in the tissues was determined by using an Agilent 8800 Triple Quadrupole ICP-MS instrument (Agilent Technologies, California, USA) equipped with an ASX-520 autosampler (Cetac Technologies, Omaha, USA). Typical instrumental settings for the analysis are given in Table 1. The concentration of Ti was quantified against an external calibration curve prepared in 2% nitric acid from Ti stock solution of 1.000 µg/ml (SCP Science, Quebec, Canada) and with scandium (Sc) as an internal standard (stock solution of 1.000 µg/ml, SCP Science, Quebec, Canada).

To reduce carry-over, careful rinsing with 2% nitric acid between samples was performed.

Blank samples, laboratory duplicates and spiked samples were included in all analyses for quality control. No suitable certified reference materials for CeO_2 or TiO_2 were available. The limit of detection (LOD) in the liver tissue was estimated to be 63 ± 21 ng/g for Ce and 676 ± 123 ng/g for Ti. LOD in the lung tissue was estimated to be 1400 ng/g for Ce and 1467 ± 1025 ng/g for Ti. The LOD in tissues varied for the different sample types due to different sample intake in the digestion step and the sample dilution prior to analysis.

Determination of size distribution of CeO_2 NPs in mouse organs by spICP-MS

Sample preparation

A previously developed enzymatic digestion procedure was modified and applied [44]. Briefly, a volume of liver homogenate which contained 25 mg of liver tissue or ~ 25 mg of unhomogenized lung tissue was mixed with 3 ml of 3 mg/ml Proteinase K solution in 50 mM ammonium bicarbonate buffer at pH 7.4, containing 5 mg/ml SDS and 0.2 mg/ml NaN_3 as antimicrobial agent and 1 ml of ultrapure water. The mixture was incubated over night at 40 °C in a water bath under continuous stirring. As a blank sample, unexposed liver or lung tissue was included. Prior to the spICP-MS measurement, samples were further diluted between 100- and 50.000-fold with ultrapure water, depending on the Ce mass concentration measured by conventional ICP-MS.

Analytical technique

The iCAP Q ICP-MS instrument was used for spICP-MS analysis. Instrument settings are given in Table 1. The peristaltic pump was set to 40 rpm for all experiments, which corresponded to a sample flow rate of approximately 0.4 ml/min, which was accurately determined daily by weighing the amount of water that was delivered by the peristaltic pump for 1 min.

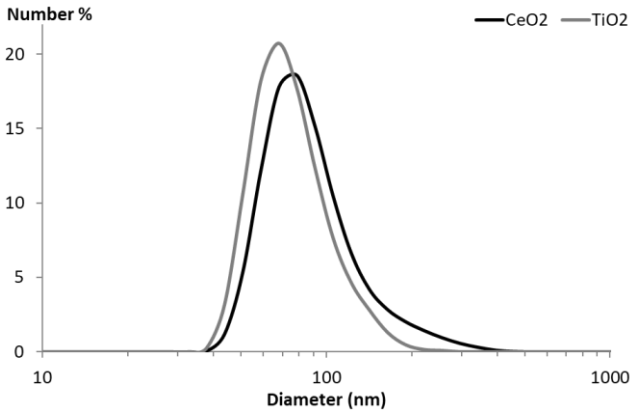

Figure 1. Size distribution of CeO_2 and TiO_2 particle suspensions obtained by DLS. CeO_2 and TiO_2 particle were suspended in 2% serum in nanopure water and sonicated as described.

Instrument calibration was achieved by analysis of a blank and five Ce standards ranging from 0.2 to 5.0 ng/l diluted from a certified solution in 100x diluted enzymatically digested liver tissue. The ^{140}Ce intensity for each solution was then averaged from the entire length of the analysis (180 s). To evaluate for possible instrumental drift over time the standards were analyzed at the beginning and the end of the analysis sequence. The transport efficiency of the liquid samples through the sample introduction system was determined according to the "particle frequency" method as described by [45] by the measurement of reference gold nanoparticle (AuNP) suspension (RM 8013, National Institute of Standards and Technology, Gaithersburg (NIST), MD, USA) with a known average particle diameter of 56 nm (based on the measurements by transmission electron microscopy provided by NIST) and a gold mass concentration of 51.86 ± 0.64 µg/g (information value provided by NIST), diluted 10^6-times with ultrapure water. The transport efficiency was calculated as the percentage of all Au NPs detected by spICP-MS versus the theoretical (calculated) particle number in the introduced sample volume, derived from the TEM-based average size, the measured uptake rate and time of introduction of the sample suspension into the ICP-MS instrument.

For each sample the ^{140}Ce signal intensity was continuously monitored for 60 s or 180 s which corresponded to 20.000 or 60.000 data points, respectively, when using 3 ms dwell time. Following the analysis of each sample, ultrapure water was analyzed to illustrate if carry-over from the previous measurement could be excluded. Intensity data were recorded by the ICP-MS software and exported to Microsoft Excel 2010 for Windows (Microsoft Inc., USA) for further processing. Raw signal intensity data were plotted (in counts per second) versus number of events to create a signal distribution histogram. Very low signal intensities were considered to be instrument background or for slightly higher intensity values dissolved cerium or cerium clusters. An iterative algorithm was applied where particle events were distinguished as outliers from the background/dissolved ion signal if the measured intensity was more than five times the standard deviation of the whole data set as described by [46].

Statistical analysis

All presented values are expressed as mean ± standard deviation of the mean (SD) unless stated differently. One-way or two-way analysis of variance (ANOVA) was used to analyze the data sets. In order to fulfil the normality and variance homogeneity criteria some variables were logarithmically transformed. Non-normally distributed data were ranked before applying nonparametric one-way or two-way ANOVA analysis. If the statistical significance was reached in the ANOVA analysis, Tukey *post-hoc* multiple comparison test was used to test the differences between the test groups. P-

value of 0.05 was considered significant. All statistical analyses were calculated using SAS 9.4 statistical software (SAS Institute Inc., Cary, NC, USA).

RESULTS

Mortality

After administration of NPs mice were monitored daily for any signs of sickness or injury, abnormalities in their general appearance as well as changes in their behavior. Among 216 mice used in the experiment, 3 unexpected deaths were reported during the up to 6 months long post exposure period. These were one mouse from the PO 6 months CeO_2 group, one mouse from IV 28 days control group, one mouse was from IV 6 months TiO_2 group. The causes of death were not established and the mice were excluded from the experiment.

Physicochemical characterization of nanomaterials

The key physicochemical parameters of the studied nanomaterials have been previously published and are summarized in Table 2. Agglomerate size of particle suspensions was determined using dynamic light scattering (DLS). The hydrodynamic number-based size distribution showed a single peak with the average diameter below 100 nm for both CeO_2 and TiO_2 NP suspensions (Fig. 1). Median particle diameters measured for CeO_2 and TiO_2 were 79 nm and 68 nm, respectively. Z-average and polydispersity index were 159.7 and 0.216, respectively, for CeO_2 and 125.9 and 0.122, respectively, for TiO_2.

TEM images

CeO_2 NPs appear as aggregates of primary crystals (Fig. 2A). Images taken at high magnification in STEM mode (results not shown) showed that the size of primary particles varies from few nm up to several tens of nanometer. The aggregate size cannot be determined from the images obtained. Particles regardless of size appear cubic (fluorite structure, space group Fm3m) however, the crystalline structure and phase of particles was not investigated in the scope of this study.

TiO_2 NPs appear as aggregates of primary crystals (Fig. 2B). Images taken at high magnification in STEM mode (results not shown) showed that the primary particles are needle-like crystals with a length of 50 to 60 nm and a diameter of 10 to 15 nm.

Brightfield and enhanced darkfield microscopy of lung and liver tissues

Figures 3 and 4 show lung and liver sections, respectively, from mice intratracheally instilled with a control vehicle (2 % serum) or 162 µg/animal of CeO_2 or TiO_2 180 days post exposure. Lung sections from mice

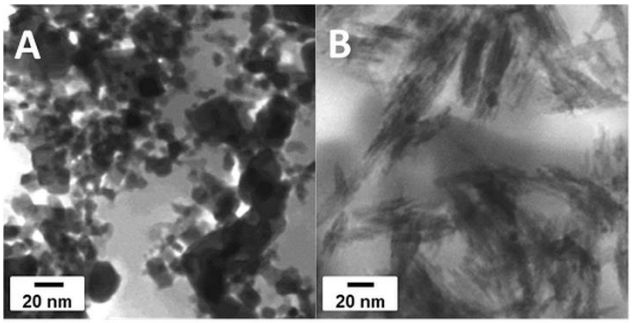

Figure 2. STEM images of CeO_2 NPs (A) and TiO_2 NPs (B).

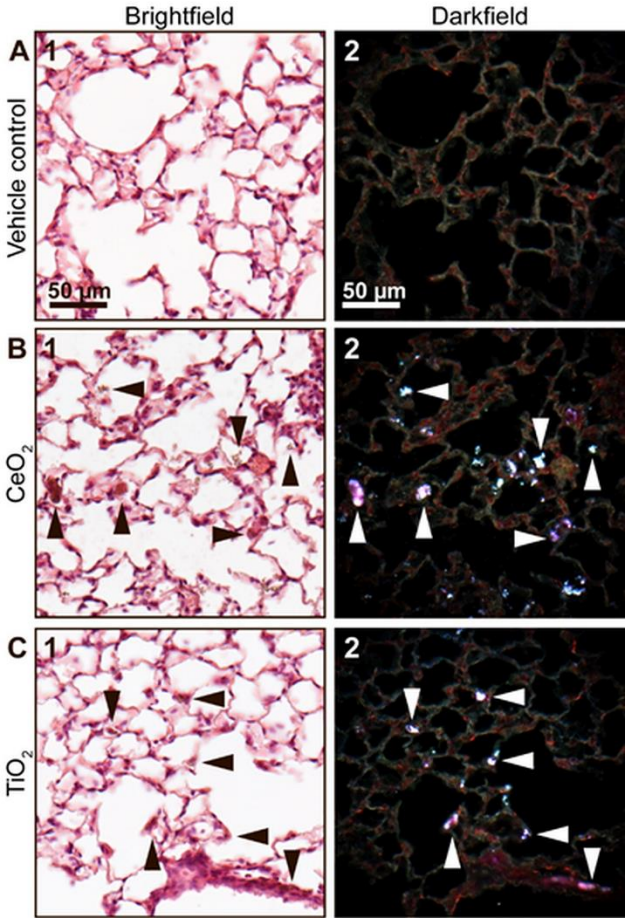

Figure 3. Brightfield (1) and enhanced darkfield (2) microscopy images of H&E stained lung tissue from intratracheally instilled mice that received a control vehicle (A) or 162 µg/animal of CeO_2 (B) or TiO_2 (C) NPs at 180 days post exposure. In the lung sections from mice exposed to CeO_2 and TiO_2 light scattering aggregates of foreign material were observed using enhanced darkfield microscopy (B2 and C2, respectively, white arrowheads). The aggregates exhibited a brownish appearance in brightfield (B1 and C1, black arrowheads).

exposed to CeO_2 and TiO_2 revealed presence of foreign material aggregates in the pulmonary region, thus documenting successful pulmonary dosing. The aggregates showed intense light scattering in enhanced darkfield (Fig. 3 B2 and C2, white arrowheads) and had a brownish appearance in brightfield (Fig. 3 B1 and C1,

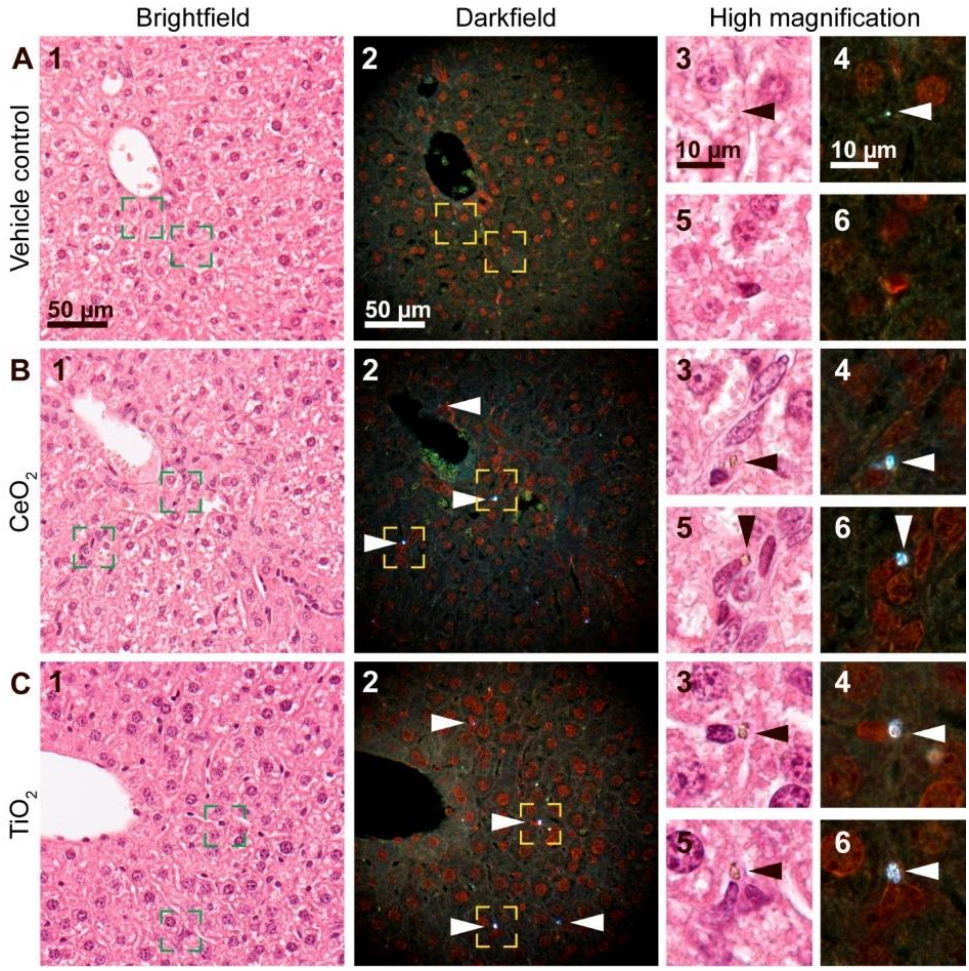

Figure 4. Brightfield (1) and enhanced darkfield (2) microscopy images of H&E stained liver tissue from intratracheally instilled mice that received a control vehicle (A) or 162 µg/animal of CeO_2 (B) or TiO_2 (C) NPs at 180 days post-exposure. In the liver sections from mice exposed to CeO_2 and TiO_2 foreign material aggregates were observed using enhanced darkfield microscopy, mainly in sinusoids and often close to small nuclei (B and C, respectively, 2, 4 and 6, white arrowheads). The aggregates were not detectable in brightfield at 40x magnification (B1, C1) but exhibited a brownish appearance at 100x magnification (B and C, 3 and 5, black arrowheads). Appearance of a typical artefact is shown (A, 3-4, arrowheads). Panels 3-6 correspond to the rectangular zones in panel 1-2 captured at higher magnification.

Table 2. Key physicochemical parameters of the tested nanomaterials

	CeO_2	**TiO_2 (rutile)**
Source	Degussa/Quimidroga[a]	NanoAmor[b]
Product form	Powder	Powder
Primary particle size	13.0 ± 12.1 nm[a]	10.5 nm[b]
Specific surface area	56.7 m^2/g[a]	139.1 m^2/g[b]
Particle density	7.29 g/cm^3[3a]	4.23 g/cm^3[3c]

[a] [47]; [b] [48]; [c][49]

Table 3. Mass recovery of CeO_2 as particles by spICP-MS compared to ICP-MS (%) and median particle diameters in the lungs 1 and 180 days post-exposure. Values are given as mean ± standard deviation.

Lungs	Mass recovery of CeO_2 as particles compared to ICP-MS (%)	Median particle diameter (nm)
IT 1 day (N=6)	40 ± 28	35 ± 3
IT 180 days (N=4)	6 ± 8	25 ± 1

Table 4. Mass recovery of CeO_2 as particles by spICP-MS compared to ICP-MS (%) and median particle diameters in the liver 1, 28 and 180 days post-exposure. Values are given as mean ± standard deviation.

Liver	Mass recovery of CeO_2 as particles compared to ICP-MS (%)	Median particle diameter (nm)
IV 1day (N=3)	66 ± 1	33 ± 1
IV 28 days (N=2)	39 ± 4	33 ± 1
IV 180 days (N=3)	13 ± 5	28 ± 1
IT 180 days (N=5)	13 ± 7	25 ± 1

black arrowheads). In the two exposure groups the foreign material was predominantly found in the

Sections of liver tissue were scanned for presence of foreign material. Liver sections from mice exposed to CeO_2 and TiO_2 by intratracheal instillation revealed the presence of light scattering aggregates of foreign material that were also visible in brightfield at high magnification. The foreign material was predominantly found in sinusoids and often in close proximity to small nuclei, probably phagocytized by Kupffer cells (Fig. 4 B-C, white and black arrowheads). In all groups, including vehicle controls, highly scattering material with a different appearance (intensity, size or color) was occasionally found (example in Fig. 4A, arrowheads). The localization indicated artefacts from tissue preparation.

Following oral gavage, neither CeO_2 nor TiO_2 NPs could be detected in liver tissue (Additional file 1).

Biodistribution of NPs in the liver and lung tissue

TiO_2 and CeO_2 content in the liver and lung tissues was assessed by quantifying Ce and Ti mass concentrations by inductively coupled plasma mass spectrometry (ICP-MS). Ce concentrations in the liver were statistically significantly increased 28 and 180 days after intratracheal exposure to CeO_2 NPs when compared to the vehicle control ($P \leq 0.001$ and $P \leq 0.0001$, respectively) and when compared to the PO exposed groups ($P \leq 0.0001$ and $P \leq 0.0001$, respectively) (Fig. 5 A). Ti concentrations in the liver were statistically significantly increased 180 days after intratracheal exposure to TiO_2 NPs ($P \leq 0.05$) when compared to the vehicle control, but no statistically significant differences between IT and PO groups were found at any of the analyzed time points (Fig. 5 B). The proportion of particles that had accumulated in the liver 180 days post exposure for CeO_2 and TiO_2 was 2.87 ± 3.37 % and 1.24 ± 1.98 % (mean ± SD), respectively, of the total lung-delivered dose (162 000 ng/lung). The observed difference in the translocation was not statistically significant. No elevated Ti or Ce concentrations were detected in the livers from orally gavaged mice (Fig. 5A and 5B). The Ce and Ti concentrations in liver of vehicle exposed mice were below detection limit at all assessed time points.

alveolar region, retained in macrophages, in the interstitium, and in the alveolar lumen (Fig. 3, B-C).

After intratracheal instillation of CeO_2 NPs, Ce concentrations in lung were statistically significantly increased at all assessed time points ($P \leq 0.001$ after day 1, $P \leq 0.0001$ after day 28 and $P \leq 0.0001$ after day 180) compared to vehicle control (Additional file 2). Ti concentrations in lung after intratracheal instillation of TiO_2 NPs were also statistically significantly increased at all assessed time points ($P \leq 0.05$ after day 1, $P \leq 0.001$ after day 28, $P \leq 0.001$ after day 180) compared to vehicle control (Additional file 2). At day 1 and day 28 CeO_2 contents in the lungs were statistically significantly different compared to TiO_2 contents ($P \leq 0.05$ and $P \leq 0.05$, respectively) (Additional file 2). The Ce and Ti concentrations in lung of vehicle-exposed mice were below detection limit at all assessed time points.

Assessment of Ce NPs size distribution by single particle ICP-MS

The size distributions of CeO_2 NPs in the liver and lung tissue were assessed by single particle ICP- MS (spICP-MS). The spICP-MS was used to analyze CeO_2 NPs in the size range between 18 and 150 nm. Larger NPs were detected in all tissue samples but excluded from the quantification. Smaller NPs were below the detection limit. The size distribution of CeO_2 NPs in lung tissue (Fig. 7) 1 day after pulmonary exposure was similar to the size distribution of the administered particles when subjected to the same enzymatic treatment as the tissue samples. The mode of the size distribution was at around 20 nm and in the same range as the size LOD of the method. The median particle diameter was 35 nm. 180 days post exposure, the size distribution of pulmonary particles shifted towards smaller sizes with the median particle diameter decreasing from 35 nm (1 day) to 25 nm (180 days). The mass recovery of CeO_2 NPs compared to ICP-MS decreased from 40% ± 28 (1 day, N=6) to 6% ± 8% (180 days, N=4) presumably due to the shift of the size distribution to values below the size LOD of the method (Table 3). CeO_2 NPs frequency in the lung tissue 1 day and 180 days following intratracheal instillation and normalized to the % of recovery is presented in Additional file 3.

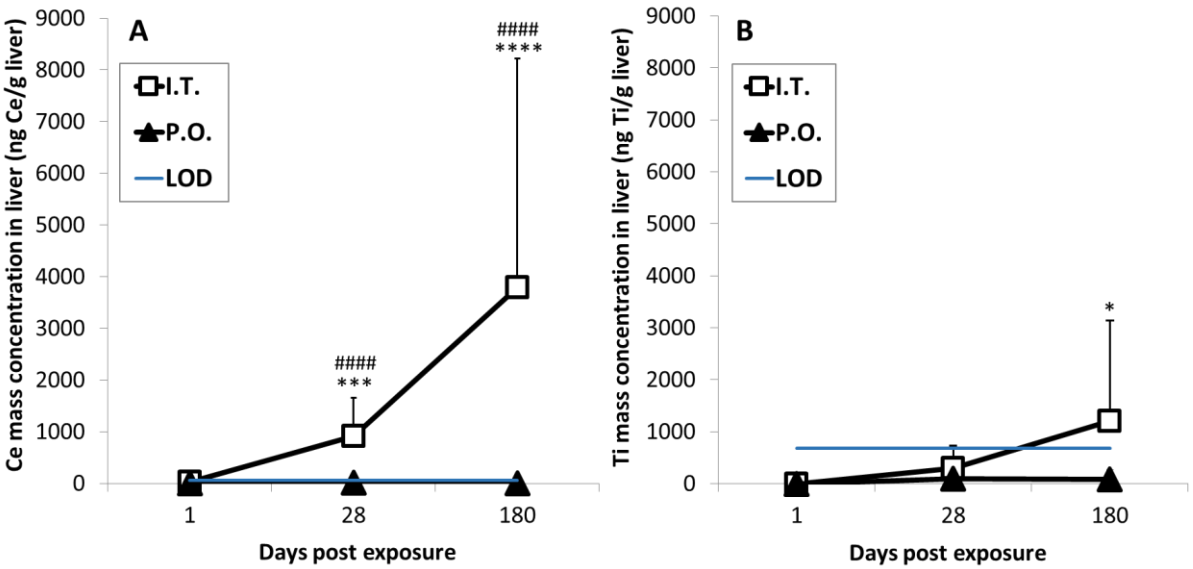

Figure 5. Mass concentration of Ce (A) and Ti (B) in liver tissue measured by ICP-MS following intratracheal instillation and oral gavage of CeO_2 and TiO_2 NPs, respectively. Data are presented as mean + SD. An asterisk (*) denotes $P \leq 0.05$, (***) $P \leq 0.001$, (****) $P < 0.0001$ of Ce or Ti mass concentration in exposed groups compared to vehicle controls. Hashtags (###) denote $P < 0.001$ and (####) $P < 0.0001$ of Ce mass concentration in intratracheally exposed group (IT) compared to orally exposed groups (PO). LOD – Limit of detection.

One day post exposure, the IV dosed particles residing in the liver had the same size distribution as the dosed NP dispersion (Fig. 8). The particle size distributions were similar 1 and 28 days post exposure (median diameter 33 nm). Smaller CeO_2 NPs were detected 180 days post exposure (median diameter 28 nm). Similarly to the lung tissues, the mass recovery of CeO_2 NPs in comparison to ICP-MS decreased from 66% ± 1 (1 day, N=3) to 13% ± 5 (180 days, N=3) (Table 4). CeO_2 NPs frequency in the liver tissue 1 day, 28 days and 180 days following intravenous injection and 180 days following intratracheal instillation and normalized to % of recovery is presented in Additional file 4.

The size distribution of the NPs that had translocated from lung to liver had a size distribution that was comparable to the size distribution of the IV dosed particles 180 days post-exposure (Fig. 8). Thus, the spICP-MS analysis suggested that the CeO_2 NP size decreased over time both in lung and liver tissue.

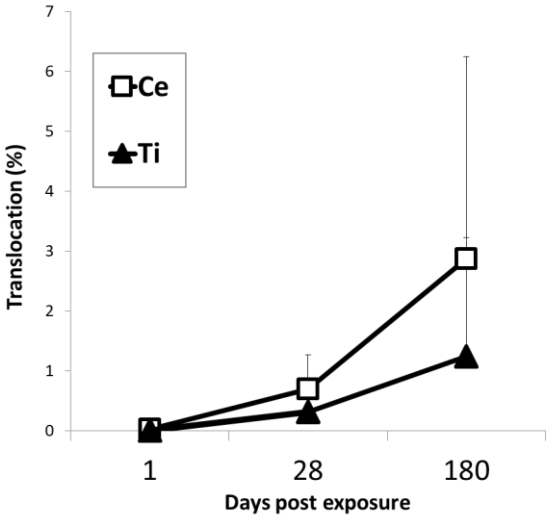

Figure 6. Liver content of Ce and Ti NPs detected in the liver 1 day, 28 days and 180 days following intratracheal instillation measured by ICP-MS expressed as percentage (%) of the total pulmonary dose of CeO_2 and TiO_2 found in the liver. Data are presented as mean + SD.

DISCUSSION

Study concept

We studied liver deposition of CeO_2 and TiO_2 NPs over time following pulmonary exposure in mice. NPs deposited in the lungs undergo extrapulmonary translocation and liver is one of the major secondary organs for particles sequestration [19,50]. NPs may be cleared from the lungs via mucociliary escalator resulting in subsequent oral exposure or may migrate across the alveolar epithelium, through interstitium and gain access to the systemic circulation. We show that pulmonary deposited CeO_2 NPs were detected in the liver tissue 28 and 180 days post exposure and TiO_2 NPs were detected in the liver tissue 180 days post exposure as determined by darkfield imaging and by the quantification of Ce and Ti mass concentration by ICP-MS. Darkfield imaging showed that the foreign material was predominantly found in sinusoids and often in close proximity to small nuclei, probably phagocytized by

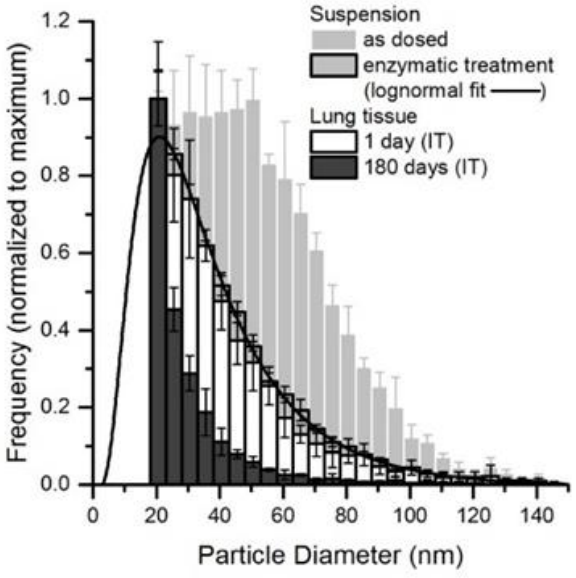

Figure 7. Particle size distribution of CeO_2 NPs in lung tissue 1 day (N=6) and 180 days (N=4) after intratracheal instillation measured by spICP-MS and normalized to the maximum of the distribution. The particle size distribution of CeO_2 NP in the dosed suspension with and without enzymatic treatment is shown for comparative reasons.

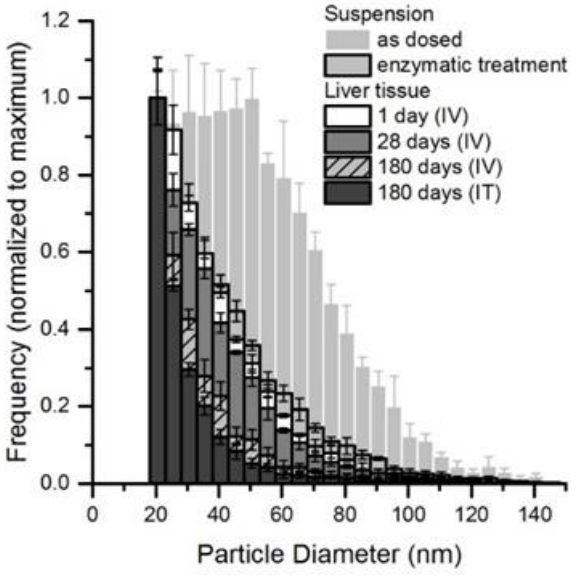

Figure 8. Particle size distribution of CeO_2 NPs in liver tissue 1 day (N=3), 28 days (N=2), 180 days (n=3) after intravenous injection and 180 days (N=5) after intratracheal instillation measured by spICP-MS and normalized to the maximum of the distribution. The particle size distribution of CeO_2 NPs in the dosed suspension with and without enzymatic treatment is shown for comparative reasons.

Kupffer cells. Similarly, previous study reported that IV dosed gold NPs accumulated in Kupffer cells in the liver [27]. The lack of detection of NPs in the liver following oral gavage by either method indicates that the presence of NPs in the liver after intratracheal instillation cannot be explained by the swallowing of fraction of the instilled dose that was transported from the respiratory tract via mucociliary escalator movements as a clearance mechanism of deposited particles. It also suggests that the direct translocation of NPs from lung to the systemic circulation is the most important route of translocation for pulmonary-deposited particles. In agreement with this, TiO_2 NPs have previously been detected in blood smears taken 24 hours after pulmonary exposure [20].

Inhalation is a physiological route for exposure to NPs present in the ambient air, but we decided to use intratracheal instillation since it allowed precise control of the delivered dose. In the present study, we exposed animals via three different routes therefore it was important to deliver the same dose regardless the administration method in order to compare results from different groups. The dose used in the present study is relevant for the occupational exposure and corresponds to the pulmonary deposition during thirteen 8-h working days at the Danish occupational exposure limit of 10 mg/m^3 for TiO_2 assuming the particle size distribution previously shown for aerosolisation of similarly sized TiO_2 NPs [41].

Extrapulmonary translocation of NPs

In the present study 180 days following pulmonary exposure 2.87 ± 3.37 % of the total lung-delivered dose was found in the liver of mice intratracheally instilled with CeO_2 NPs while 1.24 ± 1.98 % of the total TiO_2 dose translocated to the liver. The observed difference in the amount of NPs found in the liver was not statistically significant despite the difference in solubility as described in [51] and the different shapes of the particles (cubic in the case of CeO_2 and needle-like in the case of TiO_2 NPs).

Inconsistent results regarding the fraction of NPs that undergo extrapulmonary translocation and further accumulation in the secondary organs have been previously reported. Some studies [21,23,24,52] reported negligible or low rates (below 1 %) of translocation of particles primarily deposited in the lung to the secondary tissue. Kreyling [23] demonstrated "minute" (<1 %) extrapulmonary translocation of ultrafine radio-labelled ^{192}Ir particles (15 and 80 nm count median diameter) to liver, spleen, kidneys, heart and brain of WKY male rats following 1h inhalation and measured up to 7 days post-exposure. Size dependent translocation was observed with an order of magnitude lower ^{192}Ir fraction found in the secondary organs following inhalation of 80 nm Ir NPs. Similarly, negligible translocation was reported by Sadauskas and co-workers [24] who found 1.4‰ (measured by ICP-MS) to 1.9‰ (measured by neuron activation analysis, NAA) of the dose in the liver of C57BL mice intratracheally instilled with 5 repeated doses of 50 µl 2 nm Au NPs (15 x 10^{13} particles/ml) and terminated 24h following the last exposure. No gold was detected in the liver of mice instilled with 40 nm Au NPs (9 x 10^{10} particles/ml) and

100 nm (6 x 10^9 particles/ml). A study of the distribution pattern in male Wistar-Kyoto rats exposed by inhalation to ultrafine Au NPs (5 – 8 nm and concentration of 88µg/m^3) demonstrated low, but significant increase of gold in blood on day 0 (0.05% of the lung burden) and on day 7 (0.04% of the lung burden) (Takenaka et al. 2006). A human study of ultrafine inhaled technetium 99m (^{99m}Tc)-labelled carbonaceous particles (100 nm, mean + SD deposited activity was 26 + 11 MBq) showed negligible pulmonary clearance with no detected liver radioactivity during the 48-h observation period [52].

In contrast to the mentioned studies, Yu and colleagues [25] demonstrated higher translocation (above 1%) of inhaled Au NPs (median size between 76 and 79 nm and concentration of 2 x 10^6 #NSPs/cm^3) in various distant organs of male Wistar rats including kidney, spleen, heart, blood, liver, testis and several others with 4.9% of the lung concentration detected in blood 15 days after exposure. Increased hepatic content of Ce NPs following intratracheal instillation was also found in male Sprague-Dawley rats. Animals exposed to high concentration (7.0 mg/kg b.w.) of CeO_2 NPs (~10 nm) exhibited significantly elevated Ce concentration ~7% of the initial dose (500 ng/g) 28 days post-exposure [30].

The conflicting results regarding the extent of extrapulmonary translocation in the mentioned studies are likely due to the differences in the particle composition, size, surface properties as well as in the experimental set-ups (inhalation vs. instillation or method used to determined concentration of NPs in the secondary tissues). What is more, most of the studies measure extrapulmonary translocation over a short period of time and therefore higher translocation over longer post-exposure period cannot be excluded. For example, Mercer and colleagues [53] detected 7.3 % of the initial inhaled dose of MWCNT (5 mg/m^3, 5h per day for 12 days, 4 times per week) in the liver of C57BL6/J mice one year following exposure. In contrast, they reported “only” 1.1 % translocation to the liver found on day 1.

Rapid and significant translocation of inhaled ultrafine ^{13}C particles (count median diameter of 20-29 nm) into systemic circulation following subsequent deposition in liver was observed [19]. Fisher 344 rats were exposed by 6 h whole-body inhalation to 80 or 180 µg/m^3 of ^{13}C NPs and liver burden was monitored up to 24 h following exposure. A significant amount of ^{13}C NPs was detected in the liver as early as 0.5 h post-inhalation at the higher exposure concentration. However, in our study we found no translocation of particles to the liver 24 h following the exposure, but this may be caused by a high limit of detection in our method. Lack or low level of detected particles in the secondary organs could be related to the analytical method sensitivity as only a small fraction of the administered dose is initially translocated.

Absorption of NPs from the GIT

In the present study, we found no digestive tract absorption of either CeO_2 or TiO_2 following oral gavage. Our findings are consistent with other studies which have shown that NPs pass through the GIT with no or negligible absorption and are eliminated rapidly via feces [12].

Wang [9] found no liver deposition of TiO_2 NPs in either young or adult Sprague-Dawley rats following repeated oral exposure to 200 mg/kg bw of TiO_2 NPs (75 ± 15 nm) for 30 consecutive days. The measured Ti content in blood, liver, kidney and spleen was not statistically different from the control group indicating very low absorption of Ti NPs from the gastrointestinal tract. Another study on biodistribution of orally administered TiO_2 NPs demonstrated minute absorption from the GIT, but to a very limited extent. Male and female Wistar rats were once or repeatedly gavaged with 1 ml (exposure suspension concentration of 2.56 mg/ml) of 5 different TiO_2 NPs (mean particles size from 38 – 267 nm) and investigated up to 90 days. Increased Ti-levels were detected in liver and spleen of only a few rats. Low Ti levels in mesenteric lymph nodes were detected. Overall, this results indicate minor absorption of TiO_2 in the GIT [17].

Moreover, a single gavage study conducted by other investigators reported no uptake of ultrafine (15 – 80 nm) ^{192}Ir particles (5 kBq, 0.2 ml) from the GIT of male WKY rats demonstrated as lack of detectable ^{192}Ir in any of the analyzed tissues and revealed immense fecal excretion of particles within 2 - 3 d post-exposure [23]. Similarly, a study conducted by Semmler and colleagues [15] investigated lung retention and clearance of inhaled ^{192}Ir-radiolabelled ultrafine iridium particles (15 – 20 nm) in male Wistar-Kyoto rats (terminated either 3 weeks, 2 or 6 months post-exposure) revealed that particles were cleared from the peripheral lung via mucociliary escalator action into the gastrointestinal tract and were found in feces suggesting predominance of this clearance pathway.

Significantly increased contents of Ti in liver and kidney of female CD-1 (ICR) mice exposed by single oral gavage to 80 nm TiO_2 NPs and in kidney of mice exposed to 25 nm TiO_2 NPs were reported 14 days post exposure [54]. It is worth to emphasize that extremely high dose of NPs (5 g/kg bw) was used in this study compared to the dose administered in our study (~ 0.009 g/kg bw) which could explain the different results. Park and colleagues [55] found elevated (however, not statistically significantly compared to the control group) content of orally administered CeO_2 NPs (30 nm) in all examined tissues (liver, kidney, spleen, lung, testis and brain) of male SD rats. Significantly increased level of Ce in lung tissue was found in animals exposed to high dose (5 g/kg bw) at all assessed time points (1, 7 and 14 days) while it was seen only in lungs of animals exposed to the low dose (100 mg/kg bw) after day 1. The presence of CeO_2 NPs in the lungs could be explained as a side-effect of inaccurate dosing method.

In vivo-induced size transformation of CeO_2 NPs

We have observed that the median particle diameter decreased for CeO_2 NPs deposited both in the liver and lung tissue over the 180 days post exposure period. A shift towards smaller particle size of IV-administered CeO_2 NPs and increased reactive surface area has been previously demonstrated [37]. They claimed that *in vivo* induced size transformation took place in the liver 90 days after exposure resulting in the onset of very small, 1 – 3 nm, ultrafine crystallites (called second-generation ceria particles). In the present study, we report shifts in size distributions of CeO_2 NPs and show in addition, that the change occurs both in liver and lung. As a possible mechanism for the *in vivo* processing Graham suggested partial dissolution of ceria in the liver with the acidic environments of lysosomes promoting the process. Since NPs are primarily found in macrophages in both liver and lung tissues [27,56], it is very likely that the dissolution occurs intracellularly in the lysosomal structures.

The CeO_2 NPs studied by Graham et al. were hydrothermally derived CeO_2 and the question was raised if the *in vivo* transformation of industrially used CeO_2 NPs would be different than for hydrothermal CeO_2. Our study could confirm that a change of size distribution *in vivo* occurs also for CeO_2 NPs that are used in commercial applications.

The observed size distributions of CeO_2 NPs were similar for NPs dosed directly to the liver by IV and the NPs that had translocated from the lung. Particle translocation from lung has been shown to be strongly size dependent [23,26]. However, given the similar size distribution of NPs in the liver following IV and IT exposure, we were unable to determine whether dissolution took place in the lungs resulted in the translocation of the smaller particles or whether the translocated primary particles underwent partial dissolution in the liver.

In the present study, both CeO_2 NPs that underwent *in vivo* hepatic- and pulmonary-induced size distribution transformation and virtually insoluble TiO_2 NPs accumulated in liver over time following pulmonary exposure. Graham and co-workers have previously shown that the dissolved Ce recrystallizes as 1-3 nm NPs, which is in the size range that allows urinary excretion [27]. However, we have no indication that the rate of accumulation of CeO_2 NPs was lower than the accumulation of TiO_2 NPs. Thus, the shift in a size distribution towards smaller particles that took place both in lung and liver did not lead to reduced liver accumulation by increased clearance of Ce NPs from the liver.

Conclusions

The present results indicate that pulmonary deposited CeO_2 and TiO_2 NPs translocate to the liver. Despite different chemical composition and shape of particles used in the study the calculated translocation rates for Ce and Ti are not significantly different. The observed particle size distributions of CeO_2 NPs indicate that CeO_2 NPs undergo *in vivo* processing over time both in lung and liver. There is no indication that the partial dissolution in lungs and liver results in increased clearance of CeO_2 NPs from the organism. The results underscore liver toxicity as an important endpoint when assessing toxicity of NPs. It is important to establish whether the 2.87 % of CeO_2 and 1.24 % of TiO_2 cleared from the lungs and translocated to the liver are sufficient to elicit toxic effects in extrapulmonary tissue.

List of abbreviations

NPs – nanoparticles
CeO_2 – cerium oxide
TiO_2 – titanium dioxide
EDFM – enhanced darkfield microscopy
BFM – brightfield microscopy
ICP-MS – inductively coupled plasma mass spectrometry
spICP-MS – single particle inductively coupled plasma mass spectrometry
LOD – limit of detection
DLS – dynamic light scattering
TEM – transmission electron microscopy
STEM – scanning transmission electron microscopy

DECLARATIONS

Ethics approval and consent to participate

The mice study was conducted in the agreement with the Danish Animal Experimental Inspectorate under the Ministry of Justice (Permission 2012-15-2934-00089 C6) and the Technical University of Denmark´s animal welfare protocol.

Consent for publication

Not applicable.

Availability of data and materials

All data generated or analyzed during this study are included in this published article (and its supplementary information files).

Competing interests

All authors declare that they have no competing interests.

Funding

The project was supported by the Danish Centre for Nanosafety (grant no. 20110092173-3) from the Danish Working Environment Research Foundation.

Authors' contributions

JM, GRH, AM, ATS, UV, KL contributed to the project idea and design. JM carried out exposures and animal study, ICP-MS and spICP-MS analysis and statistical analysis of all data. TB provided BFM and EDFM images. KK provided EM images. RRR contributed to the ICP-MS analysis. KL contributed to the ICP-MS and spICP-MS analysis. All authors contributed to the writing of the manuscript, read and approved the final manuscript.

Acknowledgements

We gratefully acknowledge Erik H. Larsen for his invaluable contribution in the study designing. The authors would also like to thank Annette Landin, Maja Danielsen, Sarah G. Simonsen, Marianne Hansen, Birgitte K. Herbst, Michael Guldbrandsen, Nicklas R. Jacobsen for excellent technical assistance.

References

1. Nel A, Xia T, Madler L, Li N. Toxic Potential of Materials at the Nanolevel. Science (80-.). 2006;311:622–7.
2. Hoet PH, Bruske-Hohlfeld I, Salata O V. Nanoparticles - known and unknown health risks. J. Nanobiotechnology. England; 2004;2.
3. Madl AK, Pinkerton KE. Health effects of inhaled engineered and incidental nanoparticles. Crit. Rev. Toxicol. 2009;39:629–58.
4. Halappanavar S, Vogel U, Wallin H, Yauk CL. Promise and peril in nanomedicine: the challenges and needs for integrated systems biology approaches to define health risk. Wiley Interdiscip. Rev. Nanomedicine Nanobiotechnology. 2017;
5. Feng X, Sayle DC, Wang ZL, Paras MS, Santora B, Sutorik AC, et al. Converting Ceria Polyhedral Nanoparticles into Single-Crystal Nanospheres. Science (80-.). 2006;312:1504–8.
6. Cassee FR, van Balen EC, Singh C, Green D, Muijser H, Weinstein J, et al. Exposure, health and ecological effects review of engineered nanoscale cerium and cerium oxide associated with its use as a fuel additive. Crit. Rev. Toxicol. 2011;41:213–29.
7. Jasinski P, Suzuki T, Anderson HU. Nanocrystalline undoped ceria oxygen sensor. Sensors Actuators, B Chem. 2003;95:73–7.
8. Zhu WZ, Deevi SC. A review on the status of anode materials for solid oxide fuel cells. Mater. Sci. Eng. A. 2003;362:228–39.
9. Wang Y, Chen Z, Ba T, Pu J, Chen T, Song Y, et al. Susceptibility of young and adult rats to the oral toxicity of titanium dioxide nanoparticles. Small. 2013;9:1742–52.
10. Shi H, Magaye R, Castranova V, Zhao J. Titanium dioxide nanoparticles: a review of current toxicological data. Part Fibre Toxicol. 2013;10:15.
11. EFSA. Opinion of the Scientific Panel on Food Additives , Flavourings , Processing Aids and Materials in Contact with Food on a request from the Commission related to Use of formaldehyde as a preservative during the manufacture and preparation of food additives. EFSA J. 2004;415:1–10.
12. Oberdörster G, Oberdörster E, Oberdörster J. Nanotoxicology: An emerging discipline evolving from studies of ultrafine particles. Environ. Health Perspect. 2005;113:823–39.
13. Jackson P, Hougaard KS, Boisen AMZ, Jacobsen NR, Jensen KA, Møller P, et al. Pulmonary exposure to carbon black by inhalation or instillation in pregnant mice: Effects on liver DNA strand breaks in dams and offspring. Nanotoxicology. 2012;6:486–500.
14. Semmler-Behnke M, Kreyling WG, Lipka J, Fertsch S, Wenk A, Takenaka S, et al. Biodistribution of 1.4- and 18-nm gold particles in rats. Small. 2008;4:2108–11.
15. Semmler M, Seitz J, Erbe F, Mayer P, Heyder J, Oberdörster G, et al. Long-term clearance kinetics of inhaled ultrafine insoluble iridium particles from the rat lung, including transient translocation into secondary organs. Inhal. Toxicol. 2004;16:453–9.
16. Park E-J, Yoon J, Choi K, Yi J, Park K. Induction of chronic inflammation in mice treated with titanium dioxide nanoparticles by intratracheal instillation. Toxicology. 2009;260:37–46.
17. Geraets L, Oomen AG, Krystek P, Jacobsen NR, Wallin H, Laurentie M, et al. Tissue distribution and elimination after oral and intravenous administration of different titanium dioxide nanoparticles in rats. Part. Fibre Toxicol. 2014;11.
18. Semmler-Behnke M, Takenaka S, Fertsch S, Wenk A, Seitz J, Mayer P, et al. Efficient elimination of inhaled nanoparticles from the alveolar region: Evidence for interstitial uptake and subsequent reentrainment onto airways epithelium. Environ. Health Perspect. 2007;115:728–33.
19. Oberdörster G, Sharp Z, Atudorei V, Elder A, Gelein R, Lunts A, et al. Extrapulmonary Translocation of Ultrafine Carbon Particles Following Whole-Body Inhalation Exposure of Rats. J. Toxicol. Environ. Heal. Part A. 2002;65:1531–43.
20. Husain M, Wu D, Saber AT, Decan N, Jacobsen NR, Williams A, et al. Intratracheally instilled titanium dioxide nanoparticles translocate to heart and liver and activate complement cascade in the heart of C57BL/6 mice. Nanotoxicology. 2015;9:1013–22.
21. Takenaka S, Karg E, Kreyling WG, Lentner B, Möller W, Behnke-Semmler M, et al. Distribution pattern of inhaled ultrafine gold particles in the rat lung. Inhal. Toxicol. 2006;18:733–40.
22. Oberdorster G, Ferin J, Gelein R, Soderholm SC, Finkelstein J. Role of the alveolar macrophage in lung injury: Studies with ultrafine particles. Environ. Health Perspect. 1992;97:193–9.
23. Kreyling WG, Semmler M, Erbe F, Mayer P, Takenaka

S, Schulz H, et al. Translocation of Ultrafine Insoluble Iridium Particles From Lung Epithelium To Extrapulmonary Organs Is Size Dependent But Very Low. J. Toxicol. Environ. Heal. PartA. 2002;65:1513–30.

24. Sadauskas E, Jacobsen NR, Danscher G, Stoltenberg M, Vogel U, Larsen A, et al. Biodistribution of gold nanoparticles in mouse lung following intratracheal instillation. Chem. Cent. J. 2009;3.

25. Yu LE, Yung LL, Ong C, Tan Y, Balasubramaniam KS, Hartono D, et al. Translocation and effects of gold nanoparticles after inhalation exposure in rats. Nanotoxicology. 2007;1:235–42.

26. Kreyling WG, Semmler-Behnke M, Seitz J, Scymczak W, Wenk A, Mayer P, et al. Size dependence of the translocation of inhaled iridium and carbon nanoparticle aggregates from the lung of rats to the blood and secondary target organs. Inhal. Toxicol. 2009;21 Suppl 1:55–60.

27. Sadauskas E, Wallin H, Stoltenberg M, Vogel U, Doering P, Larsen A, et al. Kupffer cells are central in the removal of nanoparticles from the organism. Part. Fibre Toxicol. 2007;4.

28. Geiser M, Kreyling WG. Deposition and biokinetics of inhaled nanoparticles. Part. Fibre Toxicol. 2010;7.

29. Lipka J, Semmler-Behnke M, Sperling RA, Wenk A, Takenaka S, Schleh C, et al. Biodistribution of PEG-modified gold nanoparticles following intratracheal instillation and intravenous injection. Biomaterials. Elsevier Ltd; 2010;31:6574–81.

30. Nalabotu SK, Kolli MB, Triest WE, Ma JY, Manne NDPK, Katta A, et al. Intratracheal instillation of cerium oxide nanoparticles induces hepatic toxicity in male Sprague-Dawley rats. Int. J. Nanomedicine. 2011;6:2327–35.

31. Xie G, Wang C, Sun J, Zhong G. Tissue distribution and excretion of intravenously administered titanium dioxide nanoparticles. Toxicol. Lett. Elsevier Ireland Ltd; 2011;205:55–61.

32. Kermanizadeh A, Chauché C, Balharry D, Brown DM, Kanase N, Boczkowski J, et al. The role of Kupffer cells in the hepatic response to silver nanoparticles. Nanotoxicology. 2014;8 Suppl 1:149–54.

33. Park JK, Utsumi T, Seo YE, Deng Y, Satoh A, Saltzman WM, et al. Cellular distribution of injected PLGA-nanoparticles in the liver. Nanomedicine Nanotechnology, Biol. Med. Elsevier Inc.; 2016;12:1365–74.

34. Sadauskas E, Danscher G, Stoltenberg M, Vogel U, Larsen A, Wallin H. Protracted elimination of gold nanoparticles from mouse liver. Nanomedicine Nanotechnology, Biol. Med. Elsevier Inc.; 2009;5:162–9.

35. Bourdon JA, Saber AT, Jacobsen NR, Jensen KA, Madsen AM, Lamson JS, et al. Carbon black nanoparticle instillation induces sustained inflammation and genotoxicity in mouse lung and liver. Part. Fibre Toxicol. BioMed Central Ltd; 2012;9:5.

36. Wallin H, Kyjovska ZO, Poulsen SS, Jacobsen NR, Saber AT, Bengtson S, et al. Surface modification does not influence the genotoxic and inflammatory effects of TiO2 nanoparticles after pulmonary exposure by instillation in mice. Mutagenesis. 2017;gew046-.

37. Graham UM, Tseng MT, Jasinski JB, Yokel RA, Unrine JM, Davis BH, et al. In vivo processing of ceria nanoparticles inside liver: Impact on free-radical scavenging activity and oxidative stress. Chempluschem. 2014;79:1083–8.

38. Poulsen SS, Jackson P, Kling K, Knudsen KB, Skaug V, Kyjovska ZO, et al. Multi-walled carbon nanotube physicochemical properties predict pulmonary inflammation and genotoxicity. Nanotoxicology. 2016;10:1263–75.

39. Poulsen SS, Saber AT, Williams A, Andersen O, Køpler C, Atluri R, et al. MWCNTs of different physicochemical properties cause similar inflammatory responses, but differences in transcriptional and histological markers of fibrosis in mouse lungs. Toxicol. Appl. Pharmacol. Elsevier B.V.; 2015;284:16–32.

40. Kyjovska ZO, Jacobsen NR, Saber AT, Bengston S, Jackson P, Wallin H, et al. DNA damage following pulmonary exposure by instillation to low doses of carbon black (Printex 90) nanoparticles in mice. Environ. Mol. Mutagen. 2015;56:41–9.

41. Hougaard KS, Jackson P, Jensen K a, Sloth JJ, Löschner K, Larsen EH, et al. Effects of prenatal exposure to surface-coated nanosized titanium dioxide (UV-Titan). A study in mice. Part. Fibre Toxicol. 2010;7.

42. Jacobsen NR, Møller P, Jensen KA, Vogel U, Ladefoged O, Loft S, et al. Lung inflammation and genotoxicity following pulmonary exposure to nanoparticles in ApoE-/- mice. Part. Fibre Toxicol. 2009;6.

43. Schneider C a, Rasband WS, Eliceiri KW. NIH Image to ImageJ: 25 years of image analysis. Nat. Methods. Nature Publishing Group; 2012;9:671–5.

44. Loeschner K, Navratilova J, Købler C, Mølhave K, Wagner S, Von Der Kammer F, et al. Detection and characterization of silver nanoparticles in chicken meat by asymmetric flow field flow fractionation with detection by conventional or single particle ICP-MS. Anal. Bioanal. Chem. 2013;405:8185–95.

45. Pace HE, Rogers NJ, Jarolimek C, Coleman VA, Higgins P, Ranville JF. Determining transport efficiency for the purpose of counting and sizing nanoparticles via single particle inductively coupled plasma-mass spectrometry. Anal. Chem. 2012;83:9361–9.

46. Tuoriniemi J, Cornelis G, Hassellöv M. Size discrimination and detection capabilities of single-particle ICPMS for environmental analysis of silver nanoparticles. Anal. Chem. 2012;84:3965–72.

47. Levin M, Rojas E, Vanhala E, Vippola M, Liguori B, Kling K, et al. Influence of relative humidity and physical load during storage on dustiness of inorganic nanomaterials: implications for testing and risk

assessment. J. Nanoparticle Res. Springer Netherlands; 2015;17.

48. Halappanavar S, Saber AT, Decan N, Jensen KA, Wu D, Jacobsen NR, et al. Transcriptional profiling identifies physicochemical properties of nanomaterials that are determinants of the in vivo pulmonary response. Environ. Mol. Mutagen. 2015;56:245–64.

49. Lide DR. CRC Handbook of Chemistry and Physics 84th Edition. 2004.

50. Han SG, Lee JS, Ahn K, Kim YS, Kim JK, Lee JH, et al. Size-dependent clearance of gold nanoparticles from lungs of Sprague-Dawley rats after short-term inhalation exposure. Arch. Toxicol. 2015;89:1083–94.

51. Kermanizadeh A, Balharry D, Wallin H, Loft S, Møller P. Nanomaterial translocation-the biokinetics, tissue accumulation, toxicity and fate of materials in secondary organs-a review. Crit. Rev. Toxicol. 2015;45:837–72.

52. Wiebert P, Sanchez-Crespo A, Seitz J, Falk R, Phillipson K, Kreyling WG, et al. Negligible clearance of ultrafine particles retained in healthy and affected human lungs. Eur. Respir. J. 2006;28:286–90.

53. Mercer RR, Scabilloni JF, Hubbs AF, Wang L, Battelli LA, McKinney W, et al. Extrapulmonary transport of MWCNT following inhalation exposure. Part. Fibre Toxicol. 2013;10.

54. Wang J, Zhou G, Chen C, Yu H, Wang T, Ma Y, et al. Acute toxicity and biodistribution of different sized titanium dioxide particles in mice after oral administration. Toxicol. Lett. 2007;168:176–85.

55. Park E-J, Park Y-K, Park K. Acute toxicity and tissue distribution of cerium oxide nanoparticles by a single oral administration in rats. Toxicol. Res. 2009;25:79–84.

56. Lehnert BE. Pulmonary and thoracic macrophage subpopulations and clearance of particles from the lung. Environ. Health Perspect. 1992;97:17–46.

Supporting Information – Manuscript 1

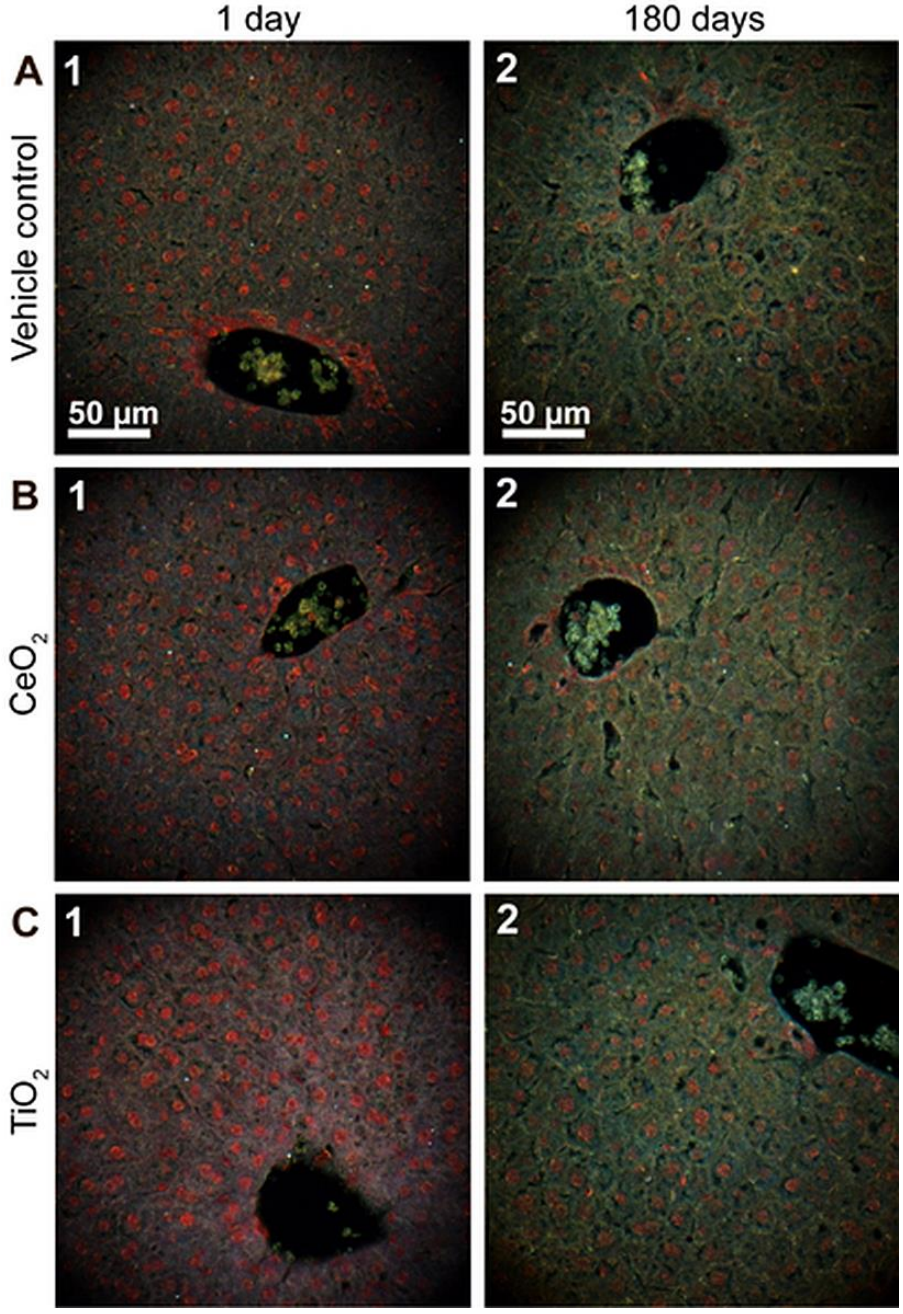

Additional file 1.

Enhanced darkfield microscopy images of H&E stained liver tissue from orally administered mice that received a control vehicle (A) or 162 µg/animal of CeO_2 (B) or TiO_2 (C) nanoparticles 1 day (1) or 180 days (2) post exposure. No apparent foreign material was detected.

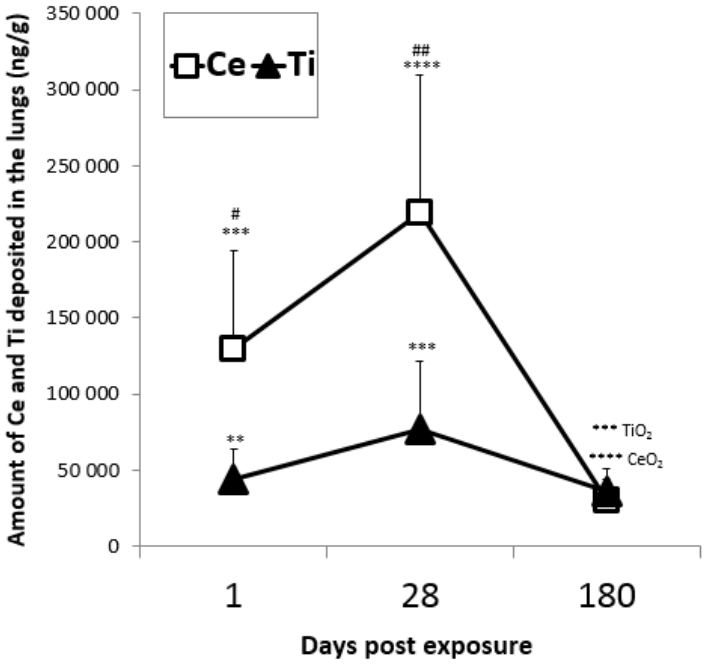

Additional file 2.

Lung content of Ce and Ti NPs measured by ICP-MS following intratracheal instillation. Data are presented as mean ± SD. Asterisks (**) denote P ≤ 0.01, (***) P ≤ 0.001, (****) P ≤ 0.0001 in exposed groups compared to vehicle controls. Hashtag (#) denotes P ≤ 0.05 and (##) P < 0.01 between Ce and Ti exposed groups.

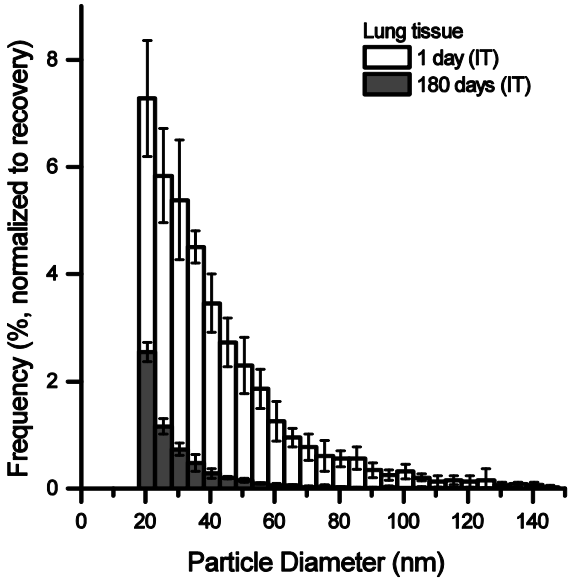

Additional file 3.

CeO_2 nanoparticles frequency in lung tissue 1 day (N=6) and 180 days (N=4) after intratracheal instillation measured by spICP-MS and normalized to the % of recovery.

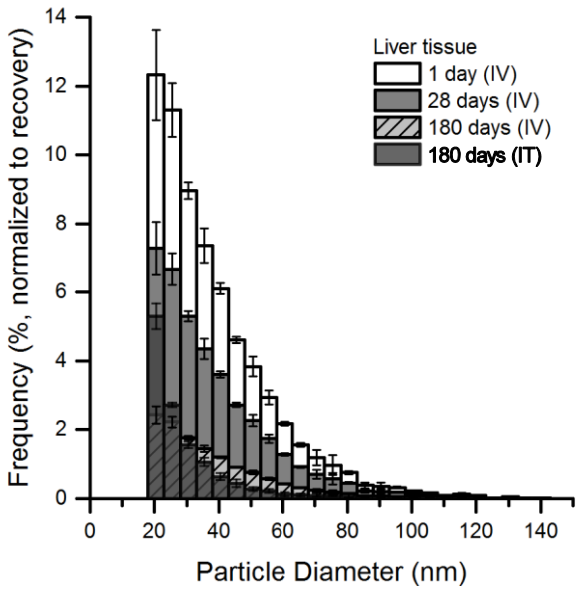

Additional file 4.

CeO_2 nanoparticles frequency in liver tissue 1 day (N=3), 28 days (N=2), 180 days (n=3) after intravenous injection and 180 days (N=5) after intratracheal instillation measured by spICP-MS and normalized to % of recovery.

MANUSCRIPT 2

Primary genotoxicity in the liver following pulmonary exposure to carbon black nanoparticles in mice

Justyna Modrzyńska, Trine Berthing, Gitte Ravn-Haren, Nicklas R. Jacobsen, Ingrid E.K. Weydahl, Katrin Loeschner, Alicja Mortensen, Anne T. Saber, Ulla Vogel,

Submitted to *Particle and Fibre Toxicology*

Primary genotoxicity in the liver following pulmonary exposure to carbon black nanoparticles in mice

Justyna Modrzynska[1,2], Trine Berthing[2], Gitte Ravn-Haren[1], Nicklas R. Jacobsen[2], Ingrid E.K. Weydahl[2], Katrin Loeschner[1], Alicja Mortensen[2], Anne T. Saber[2], Ulla Vogel[2,3]*

[1] National Food Institute, Technical University of Denmark, Kongens Lyngby, Denmark

[2] The National Research Centre for the Working Environment, Copenhagen, Denmark

[3] Department of Micro- and Nanotechnology, Technical University of Denmark, Kongens Lyngby, Denmark

* Correspondence: Ulla Vogel, National Research Centre for the Working Environment, Lersø Parkalle´ 105, DK-2100 Copenhagen Ø, Denmark. Tel: +45 39165200. Fax: +45 39165201. E-mail: ubv@nrcwe.dk

ABSTRACT

Background:

Little is known about the mechanism underlying the genotoxicity observed in the liver following pulmonary exposure to carbon black (CB) nanoparticles (NPs). The genotoxicity could be caused by the presence of translocated particles or by circulating inflammatory mediators released during pulmonary inflammation and acute-phase response. To address this, we evaluated induction of pulmonary inflammation, pulmonary and hepatic acute-phase response and genotoxicity following exposure to titanium dioxide (TiO_2), cerium oxide (CeO_2) or CB NPs. Female C57BL/6 mice were exposed by intratracheal instillation, intravenous injection or oral gavage to a single dose of 162 µg NPs/mouse and terminated 1, 28 or 180 days post-exposure alongside vehicle control.

Results:

Liver DNA damage assessed by the Comet Assay was observed after intravenous injection and intratracheal instillation of CB NPs but not after exposure to TiO_2 or CeO_2. Intratracheal exposure to NPs resulted in pulmonary inflammation in terms of increased neutrophils influx for all NPs 1 and 28 days post-exposure. Persistent pulmonary acute phase response was detected for all NPs at all three time points while only a transient induction of hepatic acute phase response was observed. All 3 materials were detected in the liver by enhanced darkfield microscopy up to 180 days post-exposure. In contrast to TiO_2 and CeO_2 NPs, CB NPs generated ROS in an acellular assay.

Conclusion:

Our results suggest that the observed hepatic DNA damage following intravenous and intratracheal dosing with CB NPs was caused by the presence of translocated, ROS-generating, particles detected in the liver rather than by the secondary effects of pulmonary inflammation or hepatic acute phase response.

Keywords – *Carbon black, Cerium oxide, Titanium dioxide, Nanoparticles, Liver, Intratracheal instillation, Intravenous injection, Oral gavage, Genotoxicity, DNA strand breaks*

BACKGROUND

The wide range of nanoparticles (NPs) applications leads to increased risk of unintended human exposure for consumers as well as for workers in the occupational environment. Inhaled NPs constitute a potential health risk [1] and therefore, understanding the fate and toxicity following pulmonary exposure to NPs has become an important issue.

Inhalation of particles leads to size dependent pulmonary deposition [2,3]. A large fraction of the pulmonary deposited particles is removed from the upper airways by the mucociliary escalator and subsequently swallowed resulting in secondary exposure through the oral route [4–6]. In addition, a small fraction of the pulmonary deposited particles undergo translocation and primarily accumulate in the liver but also in other secondary organs [7–11].

Inhalation and intratracheal instillation of NPs induce pulmonary inflammation which is accompanied by a pulmonary acute phase response [12–14]. We have previously shown that instillation and inhalation of CB Printex 90 NPs induced hepatic genotoxicity in terms of increased DNA strand break levels and increased levels of oxidative DNA damage [13,15,16]. However, the underlying mechanism is not clear. Exposure to particles can cause primary or secondary genotoxicity. Primary genotoxicity refers to DNA damage caused by direct physical interaction between particles and the genomic DNA and by ROS-mediated DNA damage in the absence of inflammation. Secondary genotoxicity refers to DNA damage as a result of action of reactive oxygen species (ROS) and reactive nitrogen species (RNS) as well as other secondary mediators (cytokines, chemokines) that are generated during particle-induced inflammation and acute phase response in the lungs that could initiate DNA damaging processes in the liver including induction of a hepatic acute phase response [17,18].

The NPs used in this work, i.e. titanium dioxide (TiO_2), cerium oxide (CeO_2) and carbon black (CB) are all worldwide-used high-volume nanomaterials. Moreover, CB is a well-known ROS generator [19] and has been shown to be mutagenic [20]. TiO_2-induced oxidative stress [21] and genotoxicity [22,23] were also previously reported. In addition, CeO_2-mediated DNA damages were confirmed in both *in vivo* [24] and *in vitro* [25] studies. CB NPs were included in the study as the DNA damaging test material in liver whereas TiO_2 and CeO_2 NPs were included as inflammogenic NPs with relatively low ROS generating abilities.

The objective of the present study was to assess the etiology of particle-induced genotoxicity in the liver. We therefore dosed mice with 3 different nanomaterials: TiO_2, CeO_2 and CB by pulmonary, oral and intravenous dosing to determine whether the observed hepatic DNA strand breaks are caused by secondary genotoxicity from pulmonary or hepatic inflammatory and acute phase responses or by direct genotoxicity from translocated NPs. Oral exposure was included to assess the contribution from the secondary oral exposure that accompanies particle clearance by the mucociliary escalator. Intravenous (IV) exposure was included to assess the effect of particle translocation and hepatic accumulation.

METHODS

Animal study

324 young adult C57BL/6 (B6JBOM-F) female mice were purchased from Taconic (Ry, Denmark) at 6 weeks of age and allowed to acclimate for 2 weeks before exposure. All animals were provided with the standard pellet diet (Altromin No. 1324) and acidified water *ad libitum* and housed in polypropylene cages with bedding and enrichment at controlled temperature 22 ± 1 °C and humidity of 55 % ± 5 and with the reverse 12 h light/12 h dark cycle. The study was conducted in the agreement with the Danish Animal Experimental Inspectorate under the Ministry of Justice (Permission 2012-15-2934-00089 C6) and the Technical University of Denmark's animal welfare protocol.

Preparation of exposure stock

TiO_2 was provided by NanoAmor, CeO_2 was provided by Degussa-Quimidroga and CB was provided by Evonik Degussa. Physicochemical characteristics of particles are presented in Table 1. All three materials were suspended in 2% v/v mouse serum from C57BL/6 mice to a final concentration of 3.24 mg/ml and dispersed by sonication for 15 min using Microson ultrasonic cell disruptor (XL-2000, Microson™, Qsonica, LLC.) equipped with disruptor horn with a diameter of 3.2 mm and maximum peak-to-peak amplitude of 180 µm. Suspensions were cooled on ice during the sonication procedure to prevent sample overheating. Control vehicle, 2 % serum, was also sonicated prior to exposure as described above.

Dynamic light scattering (Malvern Zetasizer Nano ZS, Malvern Instruments, UK) was used to determine the hydrodynamic size distribution in the sonicated suspensions before administration. The suspensions were prepared as described above and measured in transparent 1 ml disposable cuvettes at the temperature of 25 °C. Six consecutively repeated measurements were performed. Duration of each measurement as well as attenuator index and measurement position within the cuvette were determined automatically by the instrument. For the calculation of the number-based particle size distribution, refractive index and extinction coefficient (absorption) for the tested materials were as followed: 2.9 and 0.1, respectively, for TiO_2, 2.2 and 0.1, respectively, for CeO_2, 2.02 and 2.0, respectively, for CB NPs.

Exposure of mice

The mice (n=9 per group) were given a single dose of 162 µg of TiO_2, CeO_2, or CB NPs suspension in a volume of 50 µl by intratracheal instillation, intravenous injection and oral gavage. Control mice received 50 µl of 2% serum that served as a vehicle for the preparation of NPs suspension. The dose used in the experiment was equal to the pulmonary deposition after nine 8 h working days at the Danish occupational exposure limit of 3.5 mg/m^3 for CB [13]. Mice subjected to intratracheal instillation and intravenous injection were anaesthetized with 0.5 ml/100 g body weight of Hypnorm® (Fentanyl citrate 0.315 mg/ml and Fluanisone 10 mg/ml, Nomeco) and Dormicum® (Midazolam 5 mg/ml, Roche) by subcutaneous injection in the neck prior the NP administration. Orally gavaged mice were not anaesthetized before the administration. Pulmonary exposed mice were dosed by intratracheal instillation as described previously [28]. In short, the sedated mice devoted for intratracheal instillation were placed on a

Table 1. Selected physicochemical parameters of the tested nanomaterials

	TiO_2	CeO_2	CB
Source	NanoAmor[b]	Degussa/Quimidroga[a]	Evonik-Degussa
Product form	Powder	Powder	Powder
Primary particle size	10.5 nm[b]	13.0 ± 12.1 nm[a]	14 nm[c]
Specific surface area	139.1 m^2/g[b]	56.7 m^2/g[a]	295 m^2/g[d]
Particle density	4.23 g/cm^3 [e]	7.29 g/cm^3 [a]	2.1 g/cm^3 [d]

[a] [26]; [b] [27];[c] [28]; [d] [29]; [e] [30]

40° slope (upside down, with the head towards the floor) and a diode lamp was placed on the larynx to assure better visualization of the airways. The tongue was pressed down towards the lower jaw using a small spatula. 22 GA BD Insyte catheter (Becton Dickinson, Utah, USA) with a shortened needle used to intubate the trachea. The proper position of each catheter was confirmed by a highly sensitive pressure transducer. In a 250 µl SGE glass syringe (250F-LT-GT, MicroLab, Aarhus, Denmark) a volume of 50 µl of NP suspension followed by 200 µl air was instilled. Control groups received 50 µl of a control vehicle prepared as described above. After the removal of the catheter mice were placed back into vertical position with the head up to assure that the NP suspension remains in the lung and that the airways are unobstructed. We have previously shown the overall and even pulmonary distribution of particles using this exposure technique [31,32]. Mice devoted for intravenous injection were restrained in plexiglas restraining tubes with the tail hanging out of the tube. Injection was performed using 0.4 × 20 mm needle (Terumo Europe, n.v. 3001, Leuven, Belgium). After the exposure, sedated mice were placed back to their cages, heated with a heating lamp and/or warming blanket and monitored until they fully recovered from anesthesia. Mice devoted for oral gavage were immobilized in a vertical position and the gavage needle was inserted into the esophagus and further toward the stomach to release the suspension of particles. After the exposure, mice returned to the cages and were closely monitored.

Necropsy and cells & tissues collection

1, 28 and 180 days following administration of NPs mice were sedated by Hypnorm/Dormicum mixture (0.5 – 0.7 ml/100g body weight) followed by the exsanguination by withdrawing the heart blood. Abdomen and thorax of mice were opened and macroscopic examination of all organs was performed. All observed abnormalities were noted. After withdrawal of the heart blood in the intratracheally instilled mice bronchoalveolar lavage (BAL) was performed (N=6 mice/group). Lungs were flushed twice through the trachea with 0.8 ml of 0.9% sterile saline (NaCl) as described [33]. Each flush consisted of 3 up and down movements and was performed slowly (5-10 seconds each). The BAL was stored on ice until the centrifugation at 400 g for 10 minutes at 4 °C (Ole Dich centrifuge) was performed. The supernatant, BAL fluid (BALF), was collected in 1.5 ml tubes, snap-frozen in liquid nitrogen and stored at -80 °C until used. The BAL cells were re-suspended in 100 µl HAMS-F12 medium (HAMS-F12, GIBCO #21765, with 1% penicillin/streptomycin and 10% fetal bovine serum). BAL cells devoted for comet assay were prepared by the following procedure as described [33]: 40 µl of the cell suspension was mixed with 60 µl of cell culture freezing medium (HAMS-F12 with 1% penicillin/streptomycin, 10% fetal bovine serum and 10% of DMSO), divided into two 50 µl aliquots and stored at -80 °C until used. The total number of cells presented in the BAL fluid was determined using the Nucleo-Counter NC-100 with NucleoCassette™ (Chemometec, Allerød, Denmark). 20 µl of the cell suspension was mixed with 180 µl HAMS F12 medium, suspension was divided into 2 aliquots and live/dead cells were counted according to the manufacturer's instructions. For the estimation of cellular composition in BAL fluid rest of the cell suspension (approximately 40 µl) was deposited on the microscope slide by centrifugation at room temperature for 4 min. at 55 000 g in a Cytofuge® 2 (StatSpin, TRIOLAB, Brønby, Denmark). The slides were fixed in 96% ethanol for 5 minutes and stained with May-Grünwald-Giemsa dye using standard staining protocol. The cellular composition was quantified on 200 cells under light microscope (100 x magnifications). The liver (N=9/group) and lungs (N=6/group) were divided into specific pieces, snap frozen in liquid nitrogen in cryotubes (NUNC) and stored at – 80 °C for later use. For all mice throughout the whole experiment samples were taken from the same parts of organs. Specimens from livers (N=9/group) and lungs (N=3/group) were fixed in 4% neutral buffered formaldehyde, paraffin-embedded and 4 µm thick sections were stained with hematoxylin and eosin for microscopical examination.

Brightfield and darkfield microscopy

Cytoviva enhanced darkfield hyperspectral system (Auburn, AL, USA) was used to detect particles in the liver tissue, by scanning histological sections at 40 x in enhanced darkfield mode. Darkfield images were acquired at 40 x and brightfield images were acquired at

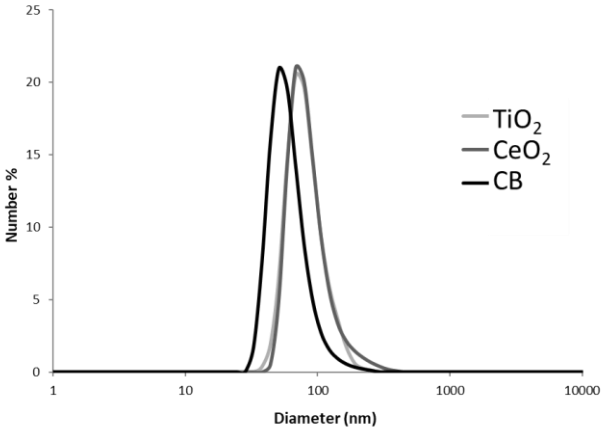

Figure 1. Dynamic light scattering number-based size distribution graph of TiO2, CeO2 and CB particles suspension (3.24 mg/ml in 2% serum) with a unimodal peak of the average diameter below 100 nm.

40x and 100 x on an Olympus BX 43 microscope with a Qimaging Retiga4000R camera. Uneven illumination in brightfield images was corrected using ImageJ [34] and the Calculator Plus plugin via the formula: Corrected_image = (image / background) * 255. The background image was a maximum projection of 3 background brightfield images without tissue.

Preparation of mRNA and cDNA from the liver and lung tissue

Total RNA was isolated from the frozen liver and lung tissue (16 – 20 mg) on Maxwell ® 16 (Promega, USA) using Maxwell® 16 LEV simply RNA Tissue Kit (AS1280, Promega, USA) following the manufacturer's protocol. Tissue lysis was performed by vigorously shaking the samples using a Tissuelyser (Qiagen, Denmark) with a 5 mm stainless steel beads for 60 s. DEPC-treated nuclease-free water was used to elute the mRNA. Complementary DNA (cDNA) was prepared using TaqMan® reverse transcription reagents (Applied Biosystem, USA) as stated in manufacturer's protocol. Concentration of total mRNA was determined by NanoDrop 2000c (ThermoFisher, USA).

Real-time RT-PCR

Gene expression levels of *Saa1* in the liver tissue and *Saa3* in the lung tissue were assessed using quantitative PCR as described previously [23,35]. 18S RNA served as a reference gene. Each of the analyzed samples was run in triplicates using ViiA7 Real-Time PCR detector (Applied Biosystem, USA). TaqMan® predeveloped reagents were used throughout the analysis. Target and reference gene expression was quantified in triplicates in separate wells. Target gene expression was determined by the comparative method $2^{-\Delta Ct}$.

Comet assay

DNA strand break levels were quantified by the comet assay in the liver and lung tissue and BAL cells as described in [36]. In brief, single-cell suspension of the liver and lung tissue was obtained by the homogenization of the deep frozen liver and lung piece in an ice-cold Merchant's buffer through a stainless steel mesh (diameter 0.5 cm, mesh size 0.4 mm) mounted on a syringe, to yield individual cells. The BAL fluid cells were thawed in a 37 °C water bath before diluting with the Mechant's buffer without the filtration step. The cell suspension was embedded in a low melting point agarose (0.7 %) and deposited on microscope Travigen 20-Well CometSlides™. The slides were immersed in a lysing solution and stored overnight at 4 °C. Subsequently, samples were treated with an alkaline buffer and alkaline electrophoresis with circulating ice-cold electrophoresis buffer was performed (25 min, 38 V/cm, 0.700 A). Thereafter, slides were neutralized in neutralization buffer (0.4 M Tris, pH 7.5), fixed with 96 % ethanol and stained with a fluorescent DNA intercalating dye SYBRGreen®. DNA strand breaks determined as the % of DNA in the comet tail (%TDNA) and as the comet tail length (TL) were scored by the fully automated PatchFinder™ system (IMSTAR, France). In order to control the day-to-day variation and to ensure equal electrophoresis efficiency both negative (A549 human lung epithelial cell line treated with PBS for 30 min at 4° C) and positive (A549 human lung epithelial cell line treated with 60 µM H_2O_2 for 30 min at 4° C,) controls were included. The high throughput comet assay analysis allowed analysis of all related sample on the same day decreasing potential variation due to the different electrophoresis or the duration of the incubation procedure.

Determination of ROS-generating ability of NPs

Assessment of NPs ability to generate ROS was performed *in vitro* in a cell-free environment as described previously [19,37]. Briefly, 500 µl of 1 mM 2',7'-dichlorodihydrofluorescein diacetate ($DCFH_2$-DA) (Invitrogen) was chemically hydrolyzed with 2 ml of 0.01 M NaOH for 30 min to 2',7'-dichlorodihydrofluorescein ($DCFH_2$). $DCFH_2$-DA probe is light sensitive therefore the experiment was conducted in a dark environment. The formed $DCFH_2$ was further diluted with 10 ml of 25 mM phosphate buffer (pH 7.4) to 0.04 mM. The NPs' ability to generate ROS production was determined in Hank's balanced saline solution (HBSS, without phenol) using a final $DCFH_2$ concentration of 0.01 mM. Prior to the assay, NPs were sonicated (Branson S-450D) for 16 min without a pause and further diluted in HBSS. Generated ROS caused formation of 2',7'-dichlorofluorescein (DCF) from $DCFH_2$ that was spectrofluorimetrically measured following 3 h of incubation in the dark (37°C and 5% CO_2). Excitation and emission wavelengths were λ_{ex} = 490 nm and λ_{em} = 520 nm, respectively (Victor Wallac-2 1420; PerkinElmer, Skovlunde, Denmark).

Statistical analysis

All presented values are expressed as mean ± standard deviation (SD) unless stated differently. One-way or two-way analysis of variance (ANOVA) was used to analyze the data sets. In order to fulfil the normality and variance homogeneity criteria some variables were logarithmically transformed. Non-normally distributed data were ranked before applying nonparametric one-way or two-way ANOVA analysis. If the statistical significance was reached in the ANOVA analysis, Tukey *post-hoc* multiple comparison test was used to test the differences between the test groups. P-value ≤ 0.05 was considered significant. All statistical analyses were calculated using SAS 9.4 statistical software (SAS Institute Inc., Cary, NC, USA).

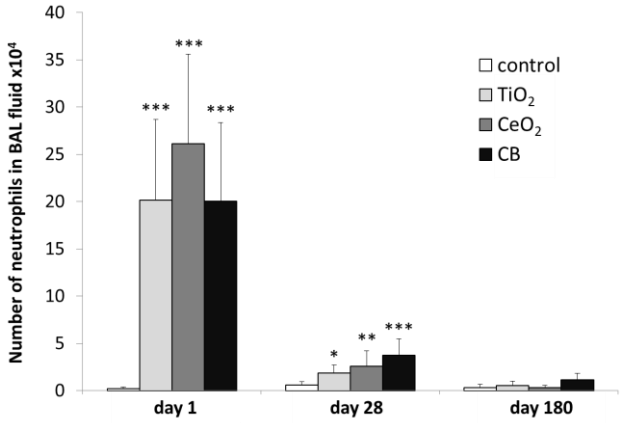

Figure 2. Number of neutrophils detected in BAL fluid following intratracheal instillation of 162 μg of TiO_2, CeO_2 or CB NPs measured 1, 28 and 180 days after exposure. Particle exposed groups n=6, vehicle control n=6. All values are presented as mean + SD. An asterisk (*) denotes P ≤ 0.05, (**) P ≤ 0.01, (***) P ≤ 0.001 of neutrophil levels in exposed groups versus vehicle control.

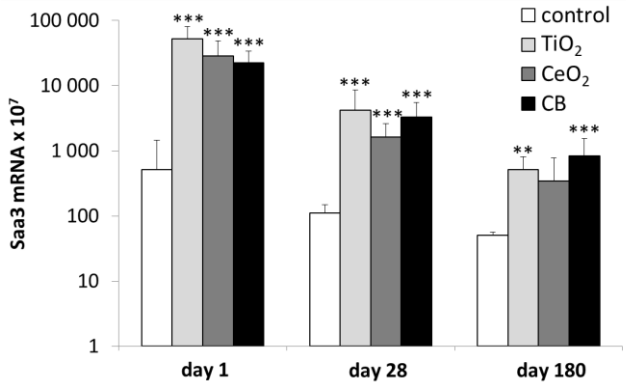

Figure 3. Pulmonary Saa3 mRNA expression levels in mice following intratracheal instillation of 162 μg of TiO_2, CeO_2 or CB NPs measured 1, 28 and 180 days after the exposure. Saa3 mRNA levels were normalized to 18S rRNA. Particle exposed groups n=6, vehicle control n=6. All values are presented as mean + SD. Asterisks (**) denote P ≤ 0.01, (***) P ≤ 0.001 of Saa3 mRNA level in exposed groups versus vehicle control.

RESULTS

DLS

Dynamic light scattering (DLS) was used to determine particle agglomerate size of TiO_2, CeO_2 and CB NPs suspensions. The hydrodynamic number-based size distribution revealed a narrow, unimodal peak with the average diameter below 100 nm for all particle suspensions (Fig. 1). The median particle diameter measured for TiO_2, CeO_2 and CB NPs was 68 nm, 68 nm, and 51 nm, respectively. Z-average and polydispersity index were 131.4 and 0.120, respectively, for TiO_2, 148.8 and 0.174, respectively, for CeO_2, 104.3 and 0.157, respectively, for CB NPs.

BAL fluid cellular composition

Analysis of BAL fluid cellular composition following pulmonary exposure to the NPs revealed that intratracheal instillation of all three particles resulted in increased numbers of total cell counts after day 1 as well as increased neutrophil influx in lungs 1 and 28 days post-exposure (Fig. 2 and Table 2). Elevation in number of total cell counts after day 1 as well as increased number of neutrophils at day 1 and day 28 is consistent with previous studies [28,38,39]. The distributions of total cells, neutrophils, macrophages, lymphocytes, eosinophils are shown in Table 2.

Saa3 mRNA expression in the lung tissue

Pulmonary acute phase response was assessed as *Saa3* mRNA expression levels. Analysis of *Saa3* gene expression revealed acute phase response in the lungs following intratracheal instillation of TiO_2, CeO_2 and CB NPs at all three time points. After day 1 and day 28 pulmonary *Saa3* mRNA levels were statistically significantly increased compare to the vehicle control for all three particles (P ≤ 0.001) with no differences between particles. After day 180, pulmonary *Saa3* mRNA levels were statistically significantly increased for TiO_2 (P ≤ 0.01) and CB (P ≤ 0.001) groups with no observed differences between particles (Fig. 3 and Additional file 1).

Overall, our results indicate that pulmonary exposure to all three NPs induces pulmonary inflammation and pulmonary acute phase response.

Hepatic presence of NPs

Hepatic detection of NPs 180 days after intravenous injection and intratracheal instillation by enhanced darkfield microscopy and brightfield microscopy is presented in Figure 4. Aggregates of foreign material, visible as white spots were present in the liver tissue from mice exposed to TiO_2 and CeO_2 NPs (Figure 4B and 4C, selected NPs marked with white arrowheads). In the livers from mice exposed to CB NPs black aggregates of foreign material were present (Figure 4D, selected NPs marked with black

Table 2. BAL fluid cellular composition following intratracheal instillation of 162 µg of TiO_2, CeO_2 or CB NPs 1, 28 and 180 days post-exposure

BAL fluid cellular composition after day 1

	Control	TiO_2	CeO_2	CB
Total cells (x 10^5)	0.9 ± 0.6	2.5 ± 0.9**	3.4 ± 1.1***	2.4 ± 1.0**
Neutrophils (x 10^4)	0.2 ± 0.2	20.2 ± 8.5***	26.1 ± 9.5***	20.1 ± 8.3***
Macrophages (x 10^4)	9.0 ± 5.7	4.5 ± 1.9	6.1 ± 1.5	2.9 ± 1.5**
Lymphocytes (x 10^2)	1.9 ± 2.9	0.0 ± 0.0	7.1 ± 7.9	0.0 ± 0.0
Eosinophils (x10^3)	0.0 ± 0.1	3.0 ± 2.5**	13.3 ± 9.2***	7.6 ± 6.8**

BAL fluid cellular composition after day 28

	Control	TiO_2	CeO_2	CB
Total cells (x 10^5)	1.4 ± 0.5	1.1 ± 0.2	1.6 ± 0.7	1.6 ± 0.8
Neutrophils (x10^4)	0.6 ± 0.3	1.9 ± 0.9*	2.6 ± 1.6**	3.8 ± 1.7***
Macrophages (x10^4)	7.9 ± 2.0	9.3 ± 2.3	12.9 ± 5.5	11.9 ± 5.5
Lymphocytes (x10^2)	8.5 ± 13.7	35.5 ± 44.3	28.3 ± 55.4	53.7 ± 78.1
Eosinophils (x10^3)	51.2 ± 39.3	0.1 ± 0.2**	0.2 ± 0.3*	0.0 ± 0.0***

BAL fluid cellular composition after day 180

	Control	TiO_2	CeO_2	CB
Total cells (x 10^5)	0.7 ± 0.3	1.0 ± 0.2	0.9 ± 0.3	1.3 ± 0.6
Neutrophils (x10^4)	0.3 ± 0.4	0.6 ± 0.4	0.3 ± 0.3	1.1 ± 0.7
Macrophages (x10^4)	7.0 ± 2.9	9.4 ± 2.1	8.4 ± 2.9	11.9 ± 4.9
Lymphocytes (x10^2)	0.0 ± 0.0	0.0 ± 0.0	0.5 ± 1.1	0.0 ± 0.0
Eosinophils (x10^3)	0.3 ± 0.4	0.4 ± 0.5	4.9 ± 6.8	4.9 ± 4.4

Particle exposed groups n=6, vehicle control n=6. All values are presented as mean ± SD. An asterisk (*) denotes $P \leq 0.05$, (**) $P \leq 0.01$, (***) $P \leq 0.001$ of different cells level in exposed groups versus vehicle control.

Table 3. DNA strand break levels (% tail DNA) in liver tissue following intratracheal instillation, intravenous injection and oral gavage of 162 µg of TiO_2, CeO_2 or CB NPs 1, 28 and 180 days after the exposure determined by the Comet assay

DNA SB in the liver following intratracheal instillation				
	Control	TiO_2	CeO_2	CB
day 1	4.1 ± 4.6	4.3 ± 1.5	3.7 ± 1.4	5.6 ± 3.7
day 28	3.0 ± 1.4	2.9 ± 0.8	5.2 ± 5.9	9.4 ± 7.2**##
day 180	3.5 ± 0.8	3.4 ± 1.0	5.5 ± 2.4	12.2 ± 8.7***###†
DNA SB in the liver following intravenous injection				
	Control	TiO_2	CeO_2	CB
day 1	3.1 ± 0.9	3.0 ± 1.0	3.7 ± 1.1	17.9 ± 7.9***###†††
day 28	5.2 ± 4.0	3.6 ± 1.1	9.7 ± 4.9	16.1 ± 10.2***###
day 180	3.3 ± 0.7	5.8 ± 7.2	3.7 ± 2.0	22.8 ± 11.1***###†††
DNA SB in the liver following oral gavage				
	Control	TiO_2	CeO_2	CB
day 1	5.5 ± 3.8	4.6 ± 3.5	7.9 ± 8.6	13.9 ± 10.4
day 28	3.0 ± 0.6	2.8 ± 0.6	3.3 ± 0.7	2.4 ± 0.6
day 180	2.8 ± 0.8	3.5 ± 0.9	3.8 ± 3.5	7.2 ± 6.5

Particle exposed groups n=9, vehicle control n=9. All values are presented as mean ± SD. Asterisks (**) denote $P \leq 0.01$, (***) $P \leq 0.001$ of DNA SB levels in exposed groups versus vehicle control. Hashtags (##) denote $P \leq 0.01$ and (###) $P \leq 0.001$ of DNA SB levels in the CB groups compared to TiO_2 groups. Cross (†) denotes $P \leq 0.05$, (†††) $P \leq 0.001$ of DNA SB levels in the CB groups compared to CeO_2 groups.

Table 4. DNA strand break levels (% tail DNA) in lung tissue 1, 28 and 180 days following intratracheal instillation and from the BAL cells 1 and 28 days following intratracheal instillation of 162 µg of TiO_2, CeO_2 or CB determined by the Comet assay

DNA SB in the lungs following intratracheal instillation				
	Control	TiO_2	CeO_2	CB
day 1	3.3 ± 0.8	3.2 ± 0.9	3.8 ± 0.6	4.6 ± 1.0
day 28	6.1 ± 1.3	5.9 ± 0.9	5.5 ± 1.1	5.3 ± 1.2
day 180	3.6 ± 1.0	5.2 ± 0.9*	4.2 ± 1.1	5.1 ± 1.4
DNA SB in the BAL cells following intratracheal instillation				
	Control	TiO_2	CeO_2	CB
day 1	4.5 ± 0.7	4.4 ± 0.9	5.6 ± 1.3	5.8 ± 1.2
day 28	5.9 ± 1.1	4.0 ± 1.0	4.3 ± 1.0	4.0 ± 1.4

Particle exposed groups n=6, vehicle control n=6. All values are presented as mean ± SD. An asterisk (*) denotes $P \leq 0.05$ of DNA SB levels in exposed groups versus vehicle control.

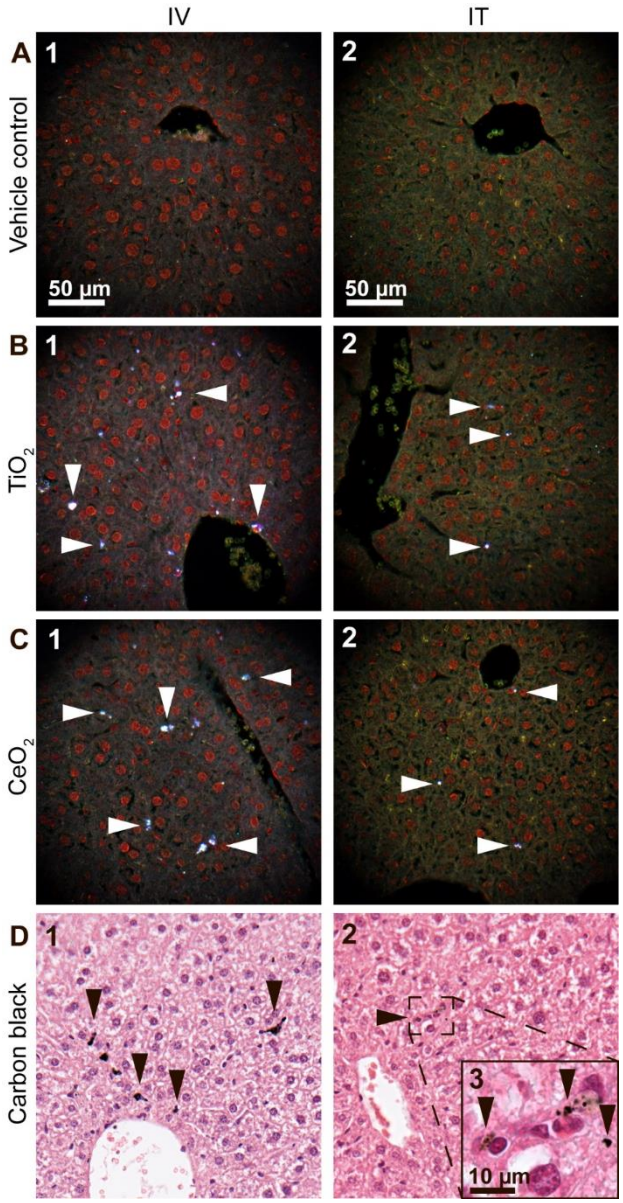

Figure 4. Enhanced darkfield (A-C) and brightfield (D) results of H&E stained liver tissue from intravenously (IV) and intratracheally (IT) exposed mice that received control vehicle (A) or 162 µg/animal of TiO_2 (B), CeO_2 (C) or CB (D) NPs 180 days post-exposure. In the liver sections of mice exposed to TiO_2 and CeO_2 light scattering aggregates were observed using enhanced darkfield microscopy (B and C, selected NPs marked with white arrowheads). In the liver sections of mice exposed to CB NPs black aggregates were observed using brightfield microscopy (D, selected NPs marked with black arrowheads).

arrowheads). Following IT exposure (Figure 4B-D, panel 2) foreign material aggregates were smaller and much less frequent than aggregates detected in the liver tissue after IV exposure (Figure B-D, panel 1). In all exposure groups aggregates were primarily detected in sinusoids and partly perivascular and often appeared to be phagocytized by Kupffer cells. Black or white spots were occasionally also seen in vehicle controls, but the appearance and location indicated artefacts from tissue preparation.

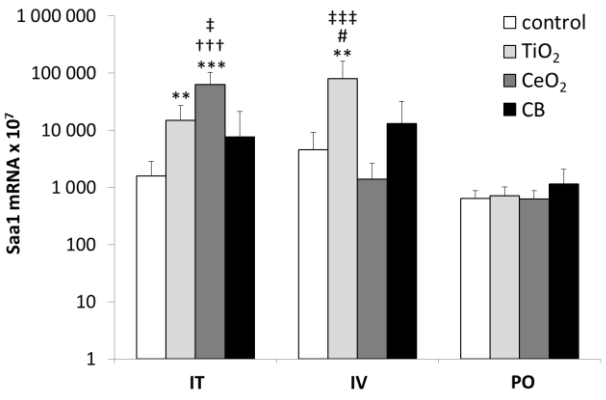

Figure 5. Hepatic Saa1 mRNA expression levels in mice following intratracheal instillation (I.T.), intravenous injection (I.V.) and oral gavage (P.O.) of 162 µg of TiO_2, CeO_2 or CB measured 1 day after exposure. Particle exposed groups n=9, vehicle control n=9. All values are presented as mean + SD. Asterisks (**) denote $P \leq 0.01$ and (***) $P \leq 0.001$ of Saa1 mRNA level in exposed groups versus vehicle control. Hashtag (#) denotes $P \leq 0.05$ of Saa1 mRNA level in TiO_2 vs CB groups. Crosses (†††) denote $P \leq 0.001$ of Saa1 mRNA level in CeO_2 vs CB groups. Double cross (‡) denotes $P \leq 0.05$ and (‡‡‡) denote $P \leq 0.001$ of Saa1 mRNA level in TiO_2 vs CeO_2 groups.

Saa1 mRNA expression in liver tissue

Hepatic acute phase response was assessed by the measurement of *Saa1* mRNA expression levels. Analysis of *Saa1* gene expression revealed hepatic acute phase response on day 1 following intratracheal instillation and intravenous injection (Fig. 5 and Additional file 2). No other time or particle-related changes in hepatic *Saa1* expression level were observed.

One day following intratracheal instillation hepatic *Saa1* mRNA levels were statistically significantly increased compared to the vehicle control for TiO_2 ($P \leq 0.01$) and CeO_2 ($P \leq 0.001$) exposed groups. CeO_2 NPs exposure induced statistically significant higher hepatic acute phase response than TiO_2 ($P \leq 0.05$) and CB ($P \leq 0.001$) exposed groups.

One day following intravenous injection hepatic *Saa1* mRNA level was statistically significantly increased only for TiO_2 compared to the vehicle control ($P \leq 0.01$). There were statistically significant differences between TiO_2 and CeO_2 ($P \leq 0.001$) and between TiO_2 and CB ($P \leq 0.05$) exposed groups.

DNA strand breaks in liver and lung

DNA strand break levels were determined in the liver and lung tissue as well as in the BAL cells using comet assay (Table 3 and 4).

In the pulmonary exposed groups DNA strand break levels in the liver tissue expressed as % tail DNA (%TDNA) were statistically significantly increased compared to the vehicle control in the CB group (3.2 fold increase, $P \leq 0.01$) 28 days following exposure. CB

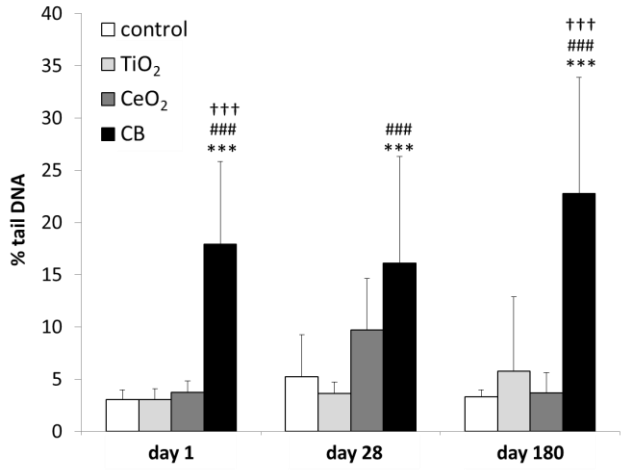

Figure 6. DNA strand break levels in the liver tissue (% tail DNA) detected by comet assay following intravenous injection of 162 µg of TiO_2, CeO_2 or CB NPs measured 1, 28 and 180 days after exposure. Particle exposed groups n=9, vehicle control n=9. All values are presented as mean + SD. Asterisks (***) denote P ≤ 0.001 of DNA SB level in exposed groups versus vehicle control. Hashtags (###) denote P ≤ 0.001 of DNA SB level in TiO_2 vs CB groups. Crosses (†††) denote P ≤ 0.001 of DNA SB level in CeO_2 vs CB groups.

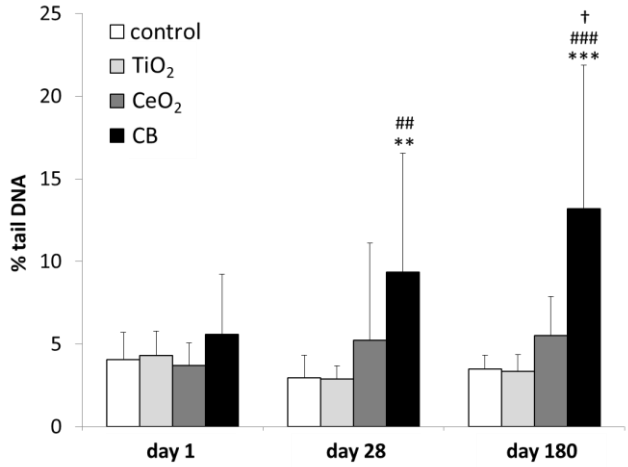

Figure 7. DNA strand break levels in the liver tissue (% tail DNA) detected by comet assay following intratracheal instillation of 162 µg of TiO2, CeO2, CB measured 1, 28 and 180 days after exposure. Particle exposed groups n=9, vehicle control n=9. All values are presented as mean + SD. Asterisks (**) denote P ≤ 0.01, (***) denote P ≤ 0.001 of DNA SB level in exposed groups versus vehicle control. Hashtags (##) denote P ≤ 0.01, (###) denote P ≤ 0.001 of DNA SB level in TiO2 vs CB groups. Cross (†) denotes P ≤ 0.05 of DNA SB level in CeO2 vs CB groups.

exposure also induced statistically significantly higher DNA strand break levels than TiO_2 exposure (3.2 fold, P ≤ 0.01). 180 days after intratracheal instillation %TDNA was statistically significantly increased for CB exposed group compared to vehicle control (3.8 fold, P ≤ 0.001), TiO_2 (3.9 fold, P ≤ 0.0001) and CeO_2 (2.4 fold, P ≤ 0.05) (Table 3).

Analysis of the %TDNA in intravenously exposed groups revealed statistically significantly differences between CB and vehicle control and between CB and TiO_2 and CeO_2 exposed groups (5.8, 5.9 and 4.8 fold increase, respectively, P ≤ 0.0001 for all groups) 1 day following intravenous injection. 28 days post-exposure, DNA strand break levels in the CB group were statistically significantly increased compared to vehicle control (3.1 fold, P ≤ 0.001) and TiO_2 exposed group (4.4 fold, P ≤ 0.0001). 180 days following exposure, DNA strand break levels in the CB group were statistically significantly increased compared to vehicle control and TiO_2 and CeO_2 exposed groups (6.9, 4.0 and 6.2 fold, respectively, P ≤ 0.0001 for all groups) (Table 3).

In the orally exposed groups %TDNA levels the liver tissue were unaffected by exposure at all assessed time points (Table 3).

In the lung tissue after intratracheal instillation %TDNA was unaffected by the exposure after day 1 and day 28 whereas significant increase in %TDNA was measured in TiO_2 group compared to vehicle control (1.5 fold increase, P ≤ 0.05) 180 days post instillation (Table 4). In the BAL cells %TDNA was unaffected by the exposure after day 1 and day 28 (Table 4). DNA strand breaks in the BAL cells 180 days following exposure were not analyzed as the samples were lost.

ROS-generation assay

Among analyzed NPs, CB exhibited the greatest ability to generate ROS (Fig. 8). CeO_2 NPs also generated ROS but the level was negligible and only marginally elevated above background. There was no signal detected for TiO_2 at any of the analyzed concentrations.

DISCUSSION

We have previously observed that pulmonary exposure to reactive NPs induced genotoxicity in the liver tissue [13,16,23,40]. Therefore, in the present work, we wanted to determine whether the observed hepatic DNA strand breaks following pulmonary exposure to CB NPs were caused by primary genotoxicity due to the direct effects of translocated particles and their ability to induce reactive oxygen species formation [19] or by secondary genotoxicity caused by pulmonary inflammation and acute phase response triggering molecular signaling cascade (release of cytokines, chemokines and ROS/RNS) that, in turn, initiate downstream toxic effects in the liver [40,41].

Hepatic genotoxicity and possible mechanism for the adverse hepatic effects

We have recently reported extrapulmonary translocation of CeO_2 and TiO_2 NPs following intratracheal exposure (Modrzynska et al., unpublished manuscript). Inductively coupled plasma mass spectrometry (ICP-MS) analysis revealed increased concentrations of Ce and Ti in the liver following

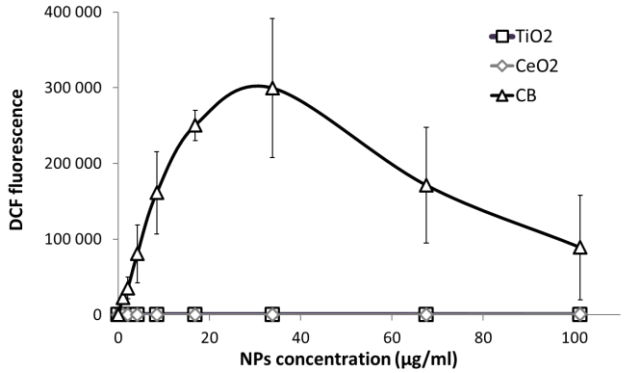

Figure 8. NPs-induced generation of reactive oxygen species (ROS) measured in a cell-free assay. All values are presented as mean +/- SD from 3 independent measurements.

intratracheal instillation. Moreover, enhanced darkfield microscopy showed that CB NPs, which due to the high abundance of carbon in the ambient air are not detectable by ICP-MS, were also present in the liver tissue following pulmonary exposure.

In the present study, intravenous injection of CB NPs resulted in increased DNA strand break (SB) levels 1, 28 and 180 days post-exposure, whereas intratracheal instillation of CB induced DNA SBs 28 and 180 days post-exposure. We recently reported that intratracheally instilled TiO_2 and CeO_2 NPs were detected in the liver 28 and 180 days post-exposure (in case of CeO_2 NPs) or 180 days (in case of TiO_2 NPs) but no NPs were detected 1 day following the exposure (Modrzynska et al., unpublished manuscript). Therefore, of the fact that hepatic genotoxicity was only observed at the later time points following pulmonary exposure might reflect the time needed for particles to translocate in sufficient amounts from lungs to the liver.

It has been previously suggested by Jackson [40] that the observed liver DNA SBs could be a result of gastrointestinal tract exposure due to the whole-body inhalation and further fur grooming. However, our results showed lack of translocated CeO_2 and TiO_2 NPs in the liver after oral exposure (Modrzynska et al., unpublished manuscript). Overall, no hepatotoxic effects were observed following oral gavage since the dosing did not elicit neither acute phase response nor genotoxicity in the liver. This indicates that the secondary oral exposure caused by swallowing a portion of lung-deposited particles did not contribute to the observed adverse effects. In general, larger dose or repeated oral exposure were needed to evoke the toxic effect observed in the other studies [24,42,43]

CB is a well characterized carbonaceous nanomaterial and very potent ROS generators [20,44,45]. Exposure to CB NPs has been shown to induce oxidative DNA damage, increased levels of DNA strand breaks [19,46] as well as mutagenicity *in vivo* and *in vitro* [20,47]. The mutation spectrum observed *in vitro* is consistent with being caused by oxidative DNA damage [44]. The aforementioned studies are in a good agreement with the present results, showing that CB is much more potent in terms of generating ROS than TiO_2 and CeO_2 NPs. Moreover, CB NPs contain very low levels of organic impurities [20,48,49] that excludes the hypothesis that CB-induced genotoxicity is caused by polycyclic aromatic hydrocarbons (PAH) that are absorbed on particles' surface.

Pulmonary acute phase response but no hepatic acute phase response

In our previous studies [12,14,50–52] we demonstrated that *Saa3* was the most upregulated acute phase gene during pulmonary acute phase response and, frequently, the most differentially expressed gene. *Saa1* was the most differentially expressed acute phase response gene in the liver [53]. Therefore, *Saa3* mRNA expression levels were used as a biomarker for pulmonary acute phase response whereas *Saa1* gene as a biomarker for hepatic acute phase response [54,55].

Pulmonary exposure to all three NPs induced similar pulmonary inflammation in terms of neutrophil influx that persisted up to day 28 and long-lasting pulmonary acute phase response that sustained for 180 days. The highest induction of acute phase was observed after day 1 and declined in a time-dependent manner remaining elevated for TiO_2 and CB NPs 180 days following exposure. Pulmonary acute phase response was similar for all three particles when compared to the control and no differences between particles were observed. Thus, if the hepatic genotoxicity was caused by systemic circulation of pulmonary inflammatory messengers, then all the assessed NPs would induce hepatic genotoxicity. Instead, hepatic genotoxicity was only observed in CB exposed groups. Therefore, it is unlikely that circulating cytokines released by pulmonary-mediated inflammation and acute phase response caused the DNA lesions. Moreover, a recent meta-analysis of global transcriptional pattern following pulmonary exposure to CB and TiO_2 NPs indicated that exposure to CB and TiO_2 induced similar changes in pulmonary transcription [56]. Both materials evoked comparable neutrophilic-dominated lung inflammation and similarly altered expression level of many pro-inflammatory genes. In addition, our previous studies indicated that CB [15] and TiO_2 [51] NPs induced similar alterations in the expression profile of selected cytokines genes in the lung tissue. Demonstrated resemblances in the elicited pulmonary response following exposure to CB and TiO_2 should lead to the similar induction level of different secondary mediators that would cause similar level of hepatic DNA SBs in both exposure groups. Instead, we have only observed hepatic genotoxicity in the CB NPs exposed mice, which is an additional evidence of primary genotoxicity caused by the deposited CB NPs rather than by the effects of circulating secondary mediators.

In the present study, we found induction of hepatic acute phase response following lung instillation of TiO_2 NPs and CeO_2 NPs and following intravenous injection of TiO_2 NPs that was present at day 1 but has already subsided by the day 28. Induction of hepatic acute phase response was much weaker and shorter than the pulmonary acute-phase response. Pulmonary exposure to TiO_2 increased pulmonary *Saa3* expression level 100-fold whereas 17.3 fold induction and 9.4 fold induction of hepatic *Saa1* was measured after intravenous injection and intratracheal instillation, respectively. No acute phase response was detected in the liver of orally gavaged animals. In addition CB NPs exposure by IV or IT, in contrast to TiO_2 and CeO_2 did not induce hepatic acute phase response, therefore hepatic acute phase response is also not a likely cause of the observed genotoxicity.

We have previously reported negligible or no hepatic acute phase response following pulmonary exposure measured by analysis of the transcriptional changes in liver mRNA of mice exposed to diesel exhaust particles (DEP), CB, multi walled carbon nanotubes [12,54]. Transient acute phase response in the liver tissue was also reported after pulmonary exposure to 162 µg/mouse of TiO_2 as reported by [23]. Hepatic acute phase response induced by intravenous injection of gold particles has been reported by Zhang and co-workers [57]. They used *Saa* reporter mouse model to detect transcriptional activation of hepatic *Saa* using bioluminescence imaging. Their results demonstrated that among all of the assessed particles 50 nm Au nanospheres exhibited the highest capacity to induce activation of hepatic *Saa*. The highest activation was detected 4 h following intravenous injection. The signal was transient and gradually declined. In the present study lack of detection of hepatic acute phase response after intravenous injection of CeO_2 and CB at all three time points as well as temporary induction of acute phase response in the TiO_2 group on day 1 could be explained by the brief and transient nature of acute phase response induction in the liver that causes difficulties in the measurement.

Overall, our results suggest that the observed hepatic DNA damage following IV and IT exposure to CB was caused by the presence of translocated NPs in the liver and their ability to induce oxidative stress rather than by secondary effects of pulmonary inflammation and acute phase response. Particles deposited in the liver are primary accumulated in the Kupffer cells [58]. Thus, only a small fraction of the liver cells are directly exposed to the particle-generated ROS [40]. Apparently, this was sufficient to induce hepatic genotoxicity.

Our results may also imply that inhaled carbon nanoparticles could induce hepatic genotoxicity leading to liver carcinogenesis. It is supported by epidemiological studies showing that exposure to traffic related air pollution is associated with risk of liver cancer [59,60]. The International Agency for Research on Cancer (IARC) has classified CB NPs as possibly carcinogenic to humans [61]. It can be speculated that the presence of CB NPs in the liver may, in a long-time perspective, contribute to the onset of cancer.

Conclusions

Pulmonary exposure to three different NPs, TiO_2, CeO_2 and CB induced long lasting pulmonary inflammation and acute phase response. Indications of translocation to the liver were found for all NPs. However, only CB dosed by IT and IV induced hepatic genotoxicity. Therefore, our findings indicate that hepatic DNA strand breaks following pulmonary exposure to CB are likely caused by direct effects of CB NPs that translocate from lung to liver rather than being caused by inflammatory or acute phase responses. Furthermore, the lack of particle translocation, inflammation and acute phase response following oral exposure to NPs suggest that the secondary oral exposure following pulmonary clearance of inhaled particles does not contribute to the observed hepatic genotoxicity.

List of abbreviations

NPs – nanoparticles
CeO_2 – cerium oxide
TiO_2 – titanium dioxide
CB – carbon clack
EDFM – enhanced darkfield microscopy
BFM – brightfield microscopy
ICP-MS – inductively coupled plasma mass spectrometry
DLS – dynamic light scattering
RT-PCR - reverse transcription polymerase chain reaction
SAA – serum amyloid A
BAL – bronchoalveolar lavage
DNA SBs – DNA strand breaks
TL – tail length
%TDNA - % of the DNA in the comet tail
ROS – reactive oxygen species
RNS – reactive nitrogen species
IL-6 – interleukin 6
IL-1 – interleukin 1
TNFα – tumor necrosis factor α
IV – intravenous
IT – intratracheal
PO – per oral

DECLARATIONS

Ethics approval and consent to participate

The mice study was conducted in the agreement with the Danish Animal Experimental Inspectorate under the Ministry of Justice (Permission 2012-15-2934-00089

C6) and the Technical University of Denmark´s animal welfare protocol.

Consent for publication

Not applicable.

Availability of data and materials

All data generated or analyzed during this study are included in this published article (and its supplementary information files).

Competing interests

All authors declare that they have no competing interests.

Funding

The project was supported by the Danish Centre for Nanosafety (grant no. 20110092173-3) from the Danish Working Environment Research Foundation.

Authors' contributions

JM, GRH, KL, AM, ATS, UV contributed to the project idea and design. JM carried out exposures and animal study, real-time RT-PCR, comet assay and statistical analysis of all data. TB provided BFM and EDFM images. NRJ contributed to the animal exposure. NRJ and IEKW carried out ROS assay. JM, TB, GRH, NRJ, IEKW, KL, AM, ATS, UV contributed to the writing of the manuscript, read and approved the final manuscript.

Acknowledgements

We gratefully acknowledge Erik H. Larsen for his invaluable contribution in the study designing. The authors would also like to thank Annette Landin, Maja Danielsen, Sarah G. Simonsen, Michael Guldbrandsen, Lourdes M. Pedersen, Elzbieta Christiansen, Anne-Karin Asp, Anne Abildtrup for excellent technical assistance.

References

1. Stone V, Miller MR, Clift MJD, Elder A, Mills NL, Moller P, et al. Nanomaterials vs Ambient Ultrafine Particles: an Opportunity to Exchange Toxicology Knowledge. Environ. Health Perspect. United States; 2016;
2. Oberdörster G, Oberdörster E, Oberdörster J. Nanotoxicology: An emerging discipline evolving from studies of ultrafine particles. Environ. Health Perspect. 2005;113:823–39.
3. Geiser M, Kreyling WG. Deposition and biokinetics of inhaled nanoparticles. Part. Fibre Toxicol. 2010;7.
4. Kreyling WG, Semmler-Behnke M, Takenaka S, Möller W. Differences in the biokinetics of inhaled nano- versus micrometer-sized particles. Acc. Chem. Res. 2013;46:714–22.
5. Fröhlich E, Salar-Behzadi S. Toxicological assessment of inhaled nanoparticles: Role of in vivo, ex vivo, in vitro, and in Silico Studies. Int. J. Mol. Sci. 2014;15:4795–822.
6. Paranjpe M, Muller-Goymann CC. Nanoparticle-mediated pulmonary drug delivery: A review. Int. J. Mol. Sci. 2014;15:5852–73.
7. Sadauskas E, Jacobsen NR, Danscher G, Stoltenberg M, Vogel U, Larsen A, et al. Biodistribution of gold nanoparticles in mouse lung following intratracheal instillation. Chem. Cent. J. 2009;3.
8. Takenaka S, Karg E, Kreyling WG, Lentner B, Möller W, Behnke-Semmler M, et al. Distribution pattern of inhaled ultrafine gold particles in the rat lung. Inhal. Toxicol. 2006;18:733–40.
9. Semmler M, Seitz J, Erbe F, Mayer P, Heyder J, Oberdörster G, et al. Long-term clearance kinetics of inhaled ultrafine insoluble iridium particles from the rat lung, including transient translocation into secondary organs. Inhal. Toxicol. 2004;16:453–9.
10. Kreyling WG, Semmler M, Erbe F, Mayer P, Takenaka S, Schulz H, et al. Translocation of Ultrafine Insoluble Iridium Particles From Lung Epithelium To Extrapulmonary Organs Is Size Dependent But Very Low. J. Toxicol. Environ. Heal. PartA. 2002;65:1513–30.
11. Oberdörster G, Sharp Z, Atudorei V, Elder A, Gelein R, Lunts A, et al. Extrapulmonary Translocation of Ultrafine Carbon Particles Following Whole-Body Inhalation Exposure of Rats. J. Toxicol. Environ. Heal. Part A. 2002;65:1531–43.
12. Saber AT, Lamson JS, Jacobsen NR, Ravn-Haren G, Hougaard KS, Nyendi AN, et al. Particle-Induced Pulmonary Acute Phase Response Correlates with Neutrophil Influx Linking Inhaled Particles and Cardiovascular Risk. PLoS One. 2013;8:1–10.
13. Bourdon JA, Saber AT, Jacobsen NR, Jensen KA, Madsen AM, Lamson JS, et al. Carbon black nanoparticle instillation induces sustained inflammation and genotoxicity in mouse lung and liver. Part. Fibre Toxicol. BioMed Central Ltd; 2012;9:5.
14. Halappanavar S, Jackson P, Williams A, Jensen KA, Hougaard KS, Vogel UB, et al. Pulmonary Response to Surface-CoatedNanotitanium Dioxide Particles Includes Induction of Acute Phase Response Genes, Inflammatory Cascades, and Changes inMicroRNAs: AToxicogenomic Study. Environ. Mol. 2011;52:425–39.
15. Jackson P, Hougaard KS, Vogel U, Wu D, Casavant L, Williams A, et al. Exposure of pregnant mice to carbon black by intratracheal instillation: Toxicogenomic effects in dams and offspring. Mutat. Res. - Genet. Toxicol. Environ. Mutagen. Elsevier B.V.; 2012;745:73–83.
16. Husain M, Kyjovska ZO, Bourdon-Lacombe J, Saber AT, Jensen KA, Jacobsen NR, et al. Carbon black nanoparticles induce biphasic gene expression changes associated with inflammatory responses in the lungs of C57BL/6 mice following a single intratracheal instillation. Toxicol. Appl. Pharmacol. Elsevier B.V.; 2015;289:573–88.
17. Schins RPF, Knaapen AM. Genotoxicity of poorly soluble particles. Inhal. Toxicol. 2007;19 Suppl 1:189–

98.

18. Saber AT, Mortensen A, Szarek J, Koponen IK, Levin M, Jacobsen NR, et al. Epoxy composite dusts with and without carbon nanotubes cause similar pulmonary responses, but differences in liver histology in mice following pulmonary deposition. Part. Fibre Toxicol. Particle and Fibre Toxicology; 2016;13.
19. Jacobsen NR, Pojana G, White P, Moller P, Cohn CA, Korsholm KS, et al. Genotoxicity, Cytotoxicity, and Reactive Oxygen Species Induced by Single-Walled Carbon Nanotubes and C60 Fullerenes in the FE1-MutaTM Mouse Lung Epithelial Cells. Environ. Mol. 2008;49:476–87.
20. Jacobsen NR, Saber AT, White P, Moller P, POjana G, Vogel U, et al. Increased mutant frequency by carbon black, but not quartz, in the lacZ and cII transgenes of muta mouse lung epithelial cells. Environ. Mol. Mutagen. 2007;48:451–61.
21. Shukla RK, Kumar A, Vallabani NVS, Pandey AK, Dhawan A. Titanium dioxide nanoparticle-induced oxidative stress triggers DNA damage and hepatic injury in mice. Nanomedicine (Lond). England; 2014;9:1423–34.
22. Kermanizadeh A, Gaiser BK, Hutchison GR, Stone V. An in vitro liver model--assessing oxidative stress and genotoxicity following exposure of hepatocytes to a panel of engineered nanomaterials. Part. Fibre Toxicol. Particle and Fibre Toxicology; 2012;9:28.
23. Wallin H, Kyjovska ZO, Poulsen SS, Jacobsen NR, Saber AT, Bengtson S, et al. Surface modification does not influence the genotoxic and inflammatory effects of TiO2 nanoparticles after pulmonary exposure by instillation in mice. Mutagenesis. 2017;gew046-.
24. Kumari M, Kumari SI, Kamal SSK, Grover P. Genotoxicity assessment of cerium oxide nanoparticles in female Wistar rats after acute oral exposure. Mutat. Res. - Genet. Toxicol. Environ. Mutagen. Elsevier B.V.; 2014;775–776:7–19.
25. Auffan M, Rose J, Orsiere T, De Meo M, Thill A, Zeyons O, et al. CeO2 nanoparticles induce DNA damage towards human dermal fibroblasts in vitro. Nanotoxicology. 2009;3:161–71.
26. Levin M, Rojas E, Vanhala E, Vippola M, Liguori B, Kling K, et al. Influence of relative humidity and physical load during storage on dustiness of inorganic nanomaterials: implications for testing and risk assessment. J. Nanoparticle Res. Springer Netherlands; 2015;17.
27. Halappanavar S, Saber AT, Decan N, Jensen KA, Wu D, Jacobsen NR, et al. Transcriptional profiling identifies physicochemical properties of nanomaterials that are determinants of the in vivo pulmonary response. Environ. Mol. Mutagen. 2015;56:245–64.
28. Saber AT, Jensen KA, Jacobsen NR, Birkedal R, Mikkelsen L, Møller P, et al. Inflammatory and genotoxic effects of nanoparticles designed for inclusion in paints and lacquers. Nanotoxicology. 2012;6:453–71.
29. Saber AT, Bornholdt J, Dybdahl M, Sharma AK, Loft S, Vogel U, et al. Tumor necrosis factor is not required for particle-induced genotoxicity and pulmonary inflammation. Arch. Toxicol. 2005;79:177–82.
30. Lide DR. CRC Handbook of Chemistry and Physics 84th Edition. 2004.
31. Mikkelsen L, Sheykhzade M, Jensen KA, Saber AT, Jacobsen NR, Vogel U, et al. Modest effect on plaque progression and vasodilatory function in atherosclerosis-prone mice exposed to nanosized TiO2. Part. Fibre Toxicol. 2011;8:32.
32. Poulsen SS, Jackson P, Kling K, Knudsen KB, Skaug V, Kyjovska ZO, et al. Multi-walled carbon nanotube physicochemical properties predict pulmonary inflammation and genotoxicity. Nanotoxicology. 2016;10:1263–75.
33. Kyjovska ZO, Jacobsen NR, Saber AT, Bengston S, Jackson P, Wallin H, et al. DNA damage following pulmonary exposure by instillation to low doses of carbon black (Printex 90) nanoparticles in mice. Environ. Mol. Mutagen. 2015;56:41–9.
34. Schneider C a, Rasband WS, Eliceiri KW. NIH Image to ImageJ: 25 years of image analysis. Nat. Methods. Nature Publishing Group; 2012;9:671–5.
35. Saber AT, Halappanavar S, Folkmann JK, Bornholdt J, Boisen AMZ, Møller P, et al. Lack of acute phase response in the livers of mice exposed to diesel exhaust particles or carbon black by inhalation. Part. Fibre Toxicol. 2009;6:12.
36. Jackson P, Pedersen LM, Kyjovska ZO, Jacobsen NR, Saber AT, Hougaard KS, et al. Validation of freezing tissues and cells for analysis of DNA strand break levels by comet assay. Mutagenesis. 2013;28:699–707.
37. Høgsberg T, Jacobsen NR, Clausen PA, Serup J. Black tattoo inks induce reactive oxygen species production correlating with aggregation of pigment nanoparticles and product brand but not with the polycyclic aromatic hydrocarbon content. Exp. Dermatol. 2013;22:464–9.
38. Bourdon JA, Saber AT, Halappanavar S, Jackson PA, Wu D, Hougaard KS, et al. Carbon black nanoparticle intratracheal installation results in large and sustained changes in the expression of miR-135b in mouse lung. Environ. Mol. Mutagen. United States; 2012;53:462–8.
39. Saber AT, Jacobsen NR, Mortensen A, Szarek J, Jackson P, Madsen AM, et al. Nanotitanium dioxide toxicity in mouse lung is reduced in sanding dust from paint. Part. Fibre Toxicol. BioMed Central Ltd; 2012;9:4.
40. Jackson P, Hougaard KS, Boisen AMZ, Jacobsen NR, Jensen KA, Møller P, et al. Pulmonary exposure to carbon black by inhalation or instillation in pregnant mice: Effects on liver DNA strand breaks in dams and offspring. Nanotoxicology. 2012;6:486–500.
41. Knaapen AM, Borm PJA, Albrecht C, Schins RPF. Inhaled particles and lung cancer. Part A: Mechanisms. Int. J. Cancer. 2004;109:799–809.
42. Sycheva LP, Zhurkov VS, Iurchenko V V., Daugel-

Dauge NO, Kovalenko MA, Krivtsova EK, et al. Investigation of genotoxic and cytotoxic effects of micro- and nanosized titanium dioxide in six organs of mice in vivo. Mutat. Res. - Genet. Toxicol. Environ. Mutagen. Elsevier B.V.; 2011;726:8–14.

43. Trouiller B, Reliene R, Westbrook A, Solaimani P, Schiestl RH. Titanium dioxide nanoparticles induce DNA damage and genetic instability in vivo in mice. Cancer Res. 2009;69:8784–9.

44. Jacobsen NR, White PA, Gingerich J, Moller P, Saber AT, Douglas GR, et al. Mutation spectrum in FE1-MUTA(TM) Mouse lung epithelial cells exposed to nanoparticulate carbon black. Environ. Mol. Mutagen. United States; 2011;52:331–7.

45. Hussain S, Boland S, Baeza-Squiban A, Hamel R, Thomassen LCJ, Martens JA, et al. Oxidative stress and proinflammatory effects of carbon black and titanium dioxide nanoparticles: Role of particle surface area and internalized amount. Toxicology. 2009;260:142–9.

46. Jacobsen NR, Møller P, Jensen KA, Vogel U, Ladefoged O, Loft S, et al. Lung inflammation and genotoxicity following pulmonary exposure to nanoparticles in ApoE-/- mice. Part. Fibre Toxicol. 2009;6.

47. Driscoll KE, Carter JM, Howard BW, Hassenbein DG, Pepelko W, Baggs RB, et al. Pulmonary Inflammatory, Chemokine, and Mutagenic Responses in Rats after Subchronic Inhalation of Carbon Black. Toxicol. Appl. Pharmacol. 1996;136:372–80.

48. Jackson P, Vogel U, Wallin H, Hougaard KS. Prenatal exposure to carbon black (printex 90): effects on sexual development and neurofunction. Basic Clin. Pharmacol. Toxicol. 2011;109:434–7.

49. Borm PJA, Robbins D, Haubold S, Kuhlbusch T, Fissan H, Donaldson K, et al. The potential risks of nanomaterials: a review carried out for ECETOC. Part. Fibre Toxicol. 2006.

50. Saber AT, Jacobsen NR, Jackson P, Poulsen SS, Kyjovska ZO, Halappanavar S, et al. Particle-induced pulmonary acute phase response may be the causal link between particle inhalation and cardiovascular disease. Wiley Interdiscip. Rev. Nanomedicine Nanobiotechnology. 2014;6:517–31.

51. Husain M, Saber AT, Guo C, Jacobsen NR, Jensen KA, Yauk CL, et al. Pulmonary instillation of low doses of titanium dioxide nanoparticles in mice leads to particle retention and gene expression changes in the absence of inflammation. Toxicol. Appl. Pharmacol. Elsevier B.V.; 2013;269:250–62.

52. Jackson P, Halappanavar S, Hougaard KS, Williams A, Madsen AM, Lamson JS, et al. Maternal inhalation of surface-coated nanosized titanium dioxide (UV-Titan) in C57BL/6 mice: effects in prenatally exposed offspring on hepatic DNA damage and gene expression. Nanotoxicology. 2013;7:85–96.

53. Poulsen SS, Knudsen KB, Jackson P, Weydahl IEK, Saber AT, Wallin H, et al. Multi-walled carbon nanotube-physicochemical properties predict the systemic acute phase response following pulmonary exposure in mice. PLoS One. 2017;12:e0174167.

54. Saber AT, Halappanavar S, Folkmann JK, Bornholdt J, Boisen AMZ, Møller P, et al. Lack of acute phase response in the livers of mice exposed to diesel exhaust particles or carbon black by inhalation. Part. Fibre Toxicol. 2009;6:12.

55. Poulsen SS, Saber AT, Mortensen A, Szarek J, Wu D, Williams A, et al. Changes in cholesterol homeostasis and acute phase response link pulmonary exposure to multi-walled carbon nanotubes to risk of cardiovascular disease. Toxicol. Appl. Pharmacol. Elsevier B.V.; 2015;283:210–22.

56. Nikota J, Williams A, Yauk CL, Wallin H, Vogel U, Halappanavar S. Meta-analysis of transcriptomic responses as a means to identify pulmonary disease outcomes for engineered nanomaterials. Part. Fibre Toxicol. Particle and Fibre Toxicology; 2015;13.

57. Zhang Y, Zhou Q, Yan S, Zhang N, Zhao M, Ma C, et al. Non-Invasive Imaging Serum Amyloid A Activation through the NF-KB Signal Pathway upon Gold Nanostructure Exposure. Small. 2016;3270–82.

58. Sadauskas E, Wallin H, Stoltenberg M, Vogel U, Doering P, Larsen A, et al. Kupffer cells are central in the removal of nanoparticles from the organism. Part. Fibre Toxicol. 2007;4.

59. Soll-Johanning H, Bach E, Olsen JH, Tüchsen F. Cancer incidence in urban bus drivers and tramway employees: a retrospective cohort study. Occup. Environ. Med. 1998;55:594–8.

60. Raaschou-Nielsen O, Andersen ZJ, Hvidberg M, Jensen SS, Ketzel M, Sorensen M, et al. Air pollution from traffic and cancer incidence: a Danish cohort study. Env. Heal. 2011;10:67.

61. Baan R, Straif K, Grosse Y, Secretan B, El Ghissassi F, Cogliano V, et al. Carcinogenicity of carbon black, titanium dioxide, and talc. Lancet Oncol. 2006;7:295–6.

Supporting Information – Manuscript 2

Additional file 1. Pulmonary *Saa3* mRNA expression level following intratracheal instillation of 162 µg of TiO_2, CeO_2 or CB NPs 1, 28 and 180 days post-exposure

Pulmonary *Saa3* mRNA expression following intratracheal instillation				
	Control	TiO_2	CeO_2	CB
day 1	511 ± 938	51977 ± 28702***	28509 ± 20645***	22295 ± 11663***
day 28	112 ± 36	4227 ± 4388***	1623 ± 1003***	3297 ± 2204***
day 180	51 ± 6	515 ± 288**	344 ± 433	838 ± 715***

Particle exposed groups n=6, vehicle control n=6. All values are presented as mean ± SD. Asterisks (**) denote P ≤ 0.01, (***) P ≤ 0.001 of *Saa3* mRNA level in exposed groups versus vehicle control.

Additional file 2. Hepatic *Saa1* mRNA expression level following intratracheal instillation, intravenous injection and oral gavage of 162 µg of TiO_2, CeO_2 or CB NPs 1, 28 and 180 days post-exposure

Hepatic *Saa1* mRNA expression following intratracheal instillation

	Control	TiO_2	CeO_2	CB
		**	***†††‡	
day 1	1608 ± 1250	15044 ± 12053	62975 ± 40137	7649 ± 13853
day 28	1388 ± 634	1321 ± 512	852 ± 724	943 ± 590
day 180	671 ± 242	1311 ± 1122	852 ± 556	682 ± 147

Hepatic *Saa1* mRNA expression following intravenous injection

	Control	TiO_2	CeO_2	CB
		**#‡‡‡		
day 1	4601 ± 4707	79551 ± 80452	1410 ± 1213	13115 ± 19003
day 28	961 ± 524	753 ± 419	542 ± 255	543 ± 306
day 180	592 ± 387	732 ± 739	910 ± 445	848 ± 351

Hepatic *Saa1* mRNA expression following oral gavage

	Control	TiO_2	CeO_2	CB
day 1	649 ± 228	715 ± 306	625 ± 260	1158 ± 923
day 28	875 ± 485	650 ± 315	654 ± 249	332 ± 125
day 180	945 ± 1322	751 ± 553	984 ± 1324	677 ± 576

Particle exposed groups n=9, vehicle control n=9. Messenger RNA expression levels were normalized to 18S rRNA. All values are presented as mean ± SD. Asterisks (**) denote $P \leq 0.01$ and (***) $P \leq 0.001$ of *Saa1* mRNA level in exposed groups versus vehicle control. Hashtag (#) denotes $P \leq 0.05$ of *Saa1* mRNA level in TiO_2 vs CB groups. Crosses (†††) denote $P \leq 0.001$ and below of *Saa1* mRNA level in CeO_2 vs CB groups. Double cross (‡) denotes $P \leq 0.05$ and (‡‡‡) denote $P \leq 0.001$ of *Saa1* mRNA level in TiO_2 vs CeO_2 groups.

MANUSCRIPT 3

Histopathological changes in the liver following pulmonary, oral and intravenous exposure to three different nanoparticles in mice

Justyna Modrzyńska, Trine Berthing, Gitte Ravn-Haren, Józef Szarek, Anne T. Saber, Ulla Vogel, Alicja Mortensen

Draft

Histopathological changes in the liver following pulmonary, oral and intravenous exposure to three different nanoparticles in mice

Justyna Modrzynska[1,2], Trine Berthing[2], Gitte Ravn-Haren[1], Jozef Szarek[4], Anne T. Saber[2], Ulla Vogel[2,3], Alicja Mortensen[2]*

Justyna Modrzynska: modrzynska.j@gmail.com, Trine Berthing: trb@nrcwe.dk, Gitte Ravn-Haren: girh@food.dtu.dk, Jozef Szarek szarek@uwm.edu.pl, Anne T. Saber: ats@nrcwe.dk, Ulla Vogel: ubv@nrcwe.dk, Alicja Mortensen: aam@nrcwe.dk

Affiliations

1. Technical University of Denmark, National Food Institute, Kongens Lyngby, Denmark

2. The National Research Centre for the Working Environment, Copenhagen, Denmark

3. Department of Micro- and Nanotechnology, Technical University of Denmark, Kongens Lyngby, Denmark

4. Faculty of Veterinary Medicine, University of Warmia and Mazury, Olsztyn, Poland

* Correspondence: Alicja Mortensen, National Research Centre for the Working Environment, Lersø Parkalle´ 105, DK-2100 Copenhagen Ø, Denmark. Tel: +45 3916 5295. E-mail: aam@nrcwe.dk

BACKGROUND

Widespread use of nanoparticles (NPs) in various consumer products as well as in medicine or industry led to increased human exposure through different portal routes. It has been previously shown that particles upon inhalation [1,2], intratracheal instillation (IT) [3,4], intravenous injection (IV) [5,6] and oral exposure (PO) [7,8] reach the systemic circulation and primarily accumulate in the Kupffer cells in the liver [5,9–12]. Intrasinusoidal localization of Kupffer cells, make them efficient scavengers of different invading pathogens from the blood circulation [13]. Clearance of particles from the liver appears to be very slow [14] and this raises the question of the possible toxicological effects of prolonged hepatic accumulation of NPs.

Liver, as a major metabolic center of the body, plays an important role in detoxification of most drugs and other foreign substances. High flow of blood through the liver causes substantial exposure to several xenobiotics, including NPs [15]. Our former studies demonstrated that intratracheal and intravenous exposure to titanium dioxide (TiO_2), cerium oxide (CeO_2) and carbon black (CB) NPs resulted in liver deposition of all three NPs as assessed by inductively coupled plasma mass spectrometry (ICP-MS) and enhanced darkfield microscopy (EDFM) (Modrzynska et al., unpublished manuscript 1). Moreover, presence of deposited CB NPs induced primary hepatic genotoxicity expressed as increased DNA strand break levels evoked by augmented production of reactive oxygen species (ROS) (Modrzynska et al., unpublished manuscript 2). NP-induced genotoxicity in the liver following exposure to CB and TiO_2 NPs was also formerly reported [16–19].

Previous studies have shown that sequestration of NPs in the liver is correlated with cellular dysfunction and liver injury. IT of CeO_2 NPs caused dose-dependent hydropic

degeneration, hepatocyte enlargement, sinusoidal dilatation and accumulation of granular materials. Concomitant findings demonstrated significant reduction in liver weight as well as elevations in serum alanine transaminase level (ALT) [20]. Long-term exposure of intragastrically administered TiO_2 NPs in mice led to focal inflammatory cell infiltration, nucleus vacancy, vein congestion and oedema in the liver tissue. Significant elevation in serum biochemical parameters including alkaline phosphatase (ALP), aspartate aminotransferase (AST), ALT and lactate dehydrogenase (LDH) was observed [21]. In mice intravenously injected with citrate (CT) or polyvinylpyrrolidone (PVP) coated silver NPs (10 nm, 40 nm, 100 nm) administration of the smallest particles caused severe midzonal hepatocellular necrosis and hemorrhage and occasional portal vein endothelial damage, regardless of coating. Moreover, mice injected with 10 nm Ag NPs exhibited significant difference in percentage of body weight loss and relative spleen weight compared to control group and 40 and 100 nm exposed mice [22].

Therefore, to address the possible toxicological effects of hepatic accumulation of NPs we dosed mice with three high volume NPs, i.e. TiO_2, CeO_2 and CB NPs by three different routes intratracheal instillation (IT), intravenous injection (IV) and oral gavage (PO) and assessed liver function and liver morphology 1, 28 and 180 days post-exposure.

MATERIALS & METHODS

Animal study

324 young adult C57BL/6 (B6JBOM-F) female mice were purchased from Taconic (Ry, Denmark) at 6 weeks of age and body weight of 17.5 ± 0.9 g (mean ± SD). Mice were acclimated for 2 weeks before the beginning of the experiment. Upon delivery mice were randomly divided into experimental groups and control groups (n=9) and housed in polypropylene cages (Type III with Tapvei bedding and enrichment – nesting material and den), 5 or 4 mice in each, under the following conditions: 12 h light/12 h dark cycle, room temperature of 22 °C ± 1 °C and the relative humidity of 55 % ± 5. Throughout the whole study mice were given a standard pellet diet (Altromin No. 1324) and acidified water *ad libitum*. All mice were weighted weekly and feed intake was recorded. For 6 months exposure groups, body weight was recorded once in 2 weeks intervals after day 28. Mice were observed daily for any sign of abnormalities in their clinical appearance. The study was conducted in the agreement with the Danish Animal Experimental Inspectorate under the Ministry of Justice (Permission 2012-15-2934-00089 C6) and the Technical University of Denmark's animal welfare protocol.

Preparation of NP suspensions and characterization of exposure media

TiO_2 was provided by NanoAmor, CeO_2 was provided by Degussa-Quimidroga and CB was provided by Evonik Degussa. NP suspensions of 3.24 mg/ml were prepared in 2% mouse serum as previously described [23,24]. In short, stock suspensions of 3.24 mg/ml alongside control vehicle were sonicated for 15 min on ice, using a probe sonicator operating at 100 W/22.5 kHz (Microson ultrasonic cell disruptor, XL-2000 Microson™, Qsonica, LLC., equipped with disruptor horn with a diameter of 3.2 mm and maximum

peak-to-peak amplitude of 180 μm). The size distribution of each produced NP suspension was determined by dynamic light scattering (DLS, Zetasizer Nano-ZS, Malvern Instruments, UK) as described in [18,25]. The refractive index and light absorption for the test materials were: 2.9 and 0.1, respectively, for TiO_2, 2.2 and 0.1, respectively, for CeO_2, 2.0 and 2.0, respectively, for CB NPs. Optical data for water were used for the control vehicle. Selected physicochemical parameters of the tested nanomaterials are presented in Table 1.

Table 1. Selected physicochemical parameters of the tested nanomaterials

	TiO_2	**CeO_2**	**CB**
Source	NanoAmor[b]	Degussa/Quimidroga[a]	Evonik-Degussa
Product form	Powder	Powder	Powder
Primary particle size	10.5 nm[b]	13.0 ± 12.1 nm[a]	14 nm[c]
Specific surface area	139.1 m^2/g[b]	56.7 m^2/g[a]	295 m^2/g[d]
Particle density	4.23 g/cm^3 [e]	7.29 g/cm^3 [a]	2.1 g/cm^3 [d]

a [26]; b [27];c [28]; d [29]; e [30];

Exposure of mice

The mice (n=9 per group) were given a single dose of 162 μg of TiO_2, CeO_2, or CB NPs suspension in 50 μl 2% sibling serum by IT, IV or PO. Control mice received 50 μl of 2% serum. The dose used in the experiment was equal to the pulmonary deposition after nine 8 h working days at the Danish occupational exposure limit of 3.5 mg/m^3 for CB. Mice subjected to IT and IV were anaesthetized with 0.5 ml/100 g body weight of Hypnorm® (Fentanyl citrate 0.315 mg/ml and Fluanisone 10 mg/ml, Nomeco) and Dormicum® (Midazolam 5 mg/ml, Roche) by subcutaneous injection in the neck prior the NPs administration. Orally gavaged mice were not anaesthetized before the

administration. Pulmonary exposed mice were dosed by IT as described previously [28]. In short, the sedated mice devoted for IT were placed on a 40° slope (upside down, with the head towards the floor) and a diode lamp was placed on the larynx to assure better visualization of the airways. The tongue was pressed down towards the lower jaw using a small spatula. 22 GA BD Insyte catheter (Becton Dickinson, Utah, USA) with a shortened needle used to intubate the trachea. The proper position of each catheter was confirmed by a highly sensitive pressure transducer. In a 250 µl SGE glass syringe (250F-LT-GT, MicroLab, Aarhus, Denmark) a volume of 50 µl of NP suspension followed by 200 µl air was instilled. Control groups received 50 µl of a control vehicle prepared as described above. After the removal of the catheter mice were placed back into vertical position with the head up to assure that the NP suspension remains in the lung and that the airways are unobstructed. We have previously shown the overall and even pulmonary distribution of particles using this exposure technique [31]. Mice devoted for IV were restrained in plexiglas restraining tubes with the tail hanging out of the tube. Injection was performed using 0.4 × 20 mm needle (Terumo Europe, n.v. 3001, Leuven, Belgium). After the exposure, sedated mice were placed back to their cages, heated with a heating lamp and/or warming blanket and monitored until they fully recovered from anesthesia. Mice devoted for oral gavage were immobilized in a vertical position and the gavage needle was inserted into the esophagus and further toward the stomach to release the suspension of particles. After the exposure, mice returned to the cages and were closely monitored.

Necropsy, blood sampling and tissues collection

One, 28 and 180 days following administration of NPs mice were sedated by the Hypnorm/Dormicum mixture (0.5 – 0.7 ml/100g body weight) followed by the

exsanguination by withdrawing the heart blood. Prior the sedation, approximately 100 µl of blood was taken from the facial vein by a quick incision, without anesthesia, and collected in EDTA covered tubes for further hematology analysis. Fresh blood samples were rotated for approximately 20 min using a rotating device prior to the measurement on the abc™ Animal Blood Counter instrument (Horiba Abx Scil Abc Vet Animal Blood Counter) to equally distribute EDTA powder. Hematological parameters measured in this study included: white blood cells (WBC), red blood cells (RBC), hemoglobin (HGB), hematocrit (HCT), mean corpuscular volume (MCV), mean cell hemoglobin (MCH), mean corpuscular hemoglobin concentration (MCHC) and platelets (PLT). The rest of the heart blood was collected in heparin covered tubes and centrifuged for 10 min, at 4 °C, at 2500g. Plasma was transferred into a new tube and stored at -80 °C until used. Abdomen and thorax of mice were opened and macroscopic examination of all organs was performed. All observed abnormalities were noted in the necropsy report. Liver weights were registered. The lungs from three mice from each group (except for the vehicle control group - 1 day and 28 days after oral exposure where lungs from four animals were taken) were fixed *in situ*, by cannulating the trachea and delivering 4% neutral buffered formaldehyde solution via the cannula at a constant fluid pressure of 25 cm before the thorax was opened. Thereafter, the lungs were excised and immersed in 4% neutral buffered formaldehyde solution until further processing. Livers from all animals from all groups were excised and specimens were fixed in 4% neutral buffered formaldehyde solution. The tissue samples were then embedded in paraffin, sectioned in 4–6 µm slices and stained with hematoxylin and eosin (H&E staining) for histological examination.

Liver enzyme activities

ALT, ALP and AST enzyme activities in plasma collected from IT, IV or PO administered mice were determined on Pentra 400 (Horiba ABX, Montpellier, France) using commercially available kits (Horiba ABX Medical, Montpellier, France; catalogue no. A11A01627, A11A01626 and A11A01629, respectively). Samples from each exposure group were run in the same batch in a random order to decrease variation and a control sample was included for every 15^{th} sample.

Enhanced darkfield microscopy

Cytoviva enhanced darkfield hyperspectral system (Auburn, AL, USA) was used to detect particles in the liver tissue, by scanning histological sections at 40 x in enhanced darkfield mode. Darkfield images were acquired at 40x and brightfield images were acquired at 40x and 100x on an Olympus BX 43 microscope with a Qimaging Retiga4000R camera. Uneven illumination in brightfield images was corrected using ImageJ [32] and the Calculator Plus plugin via the formula: Corrected_image = (image / background) * 255. The background image was a maximum projection of 3 background brightfield images without tissue.

Statistical analysis

All presented values are expressed as mean ± standard deviation (SD) unless stated differently. One-way or two-way analysis of variance (ANOVA) was used to analyze the data sets. In order to fulfil the normality and variance homogeneity criteria some variables were logarithmically transformed whereas some were ranked before applying nonparametric one-way or two-way ANOVA analysis. If the statistical significance was reached in the ANOVA analysis, Tukey *post-hoc* multiple comparison test was used to

test the differences between the test groups. P-value < 0.05 was considered significant. All statistical analyses were calculated using SAS 9.4 statistical software (SAS Institute Inc., Cary, NC, USA). The data on the incidence of histological changes in the liver were analyzed by Fisher's exact test (the software package Graph Pad Prism 7.02, Graph Pad Software Inc., La Jolla, CA, USA).

RESULTS

DLS

Dynamic light scattering (DLS) was used to evaluate size distribution profile of TiO_2, CeO_2 and CB NPs suspensions used for animal exposure. The measurement revealed a narrow, unimodal peak of hydrodynamic number-based size distribution with the average diameter below 100 nm for all the analyzed suspensions (Fig. 1). Median particle diameters measured for TiO_2, CeO_2 and CB NPs were 68 nm, 68 nm and 51 nm, respectively. Z-average and polydispersity index determined for TiO_2, CeO_2 and CB NPs were 127.3 and 0.162, 146.6 and 0.173, 188.2 and 0.261, respectively.

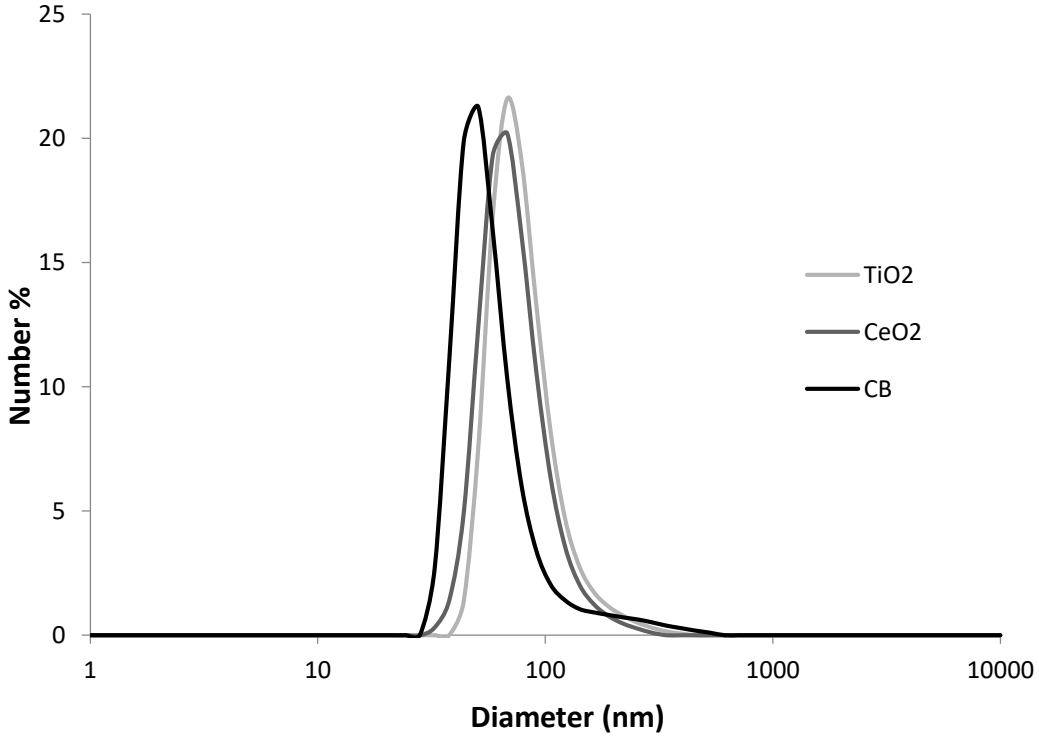

Figure 1. Dynamic light scattering number-based size distribution of TiO_2, CeO_2 and CB NP suspensions.

General appearance and mortality of mice used in the study

Throughout the experiment mice were closely monitored to ensure well-being of the animals. None of the mice showed any signs of pain, injury or abnormalities in their clinical appearance during the up to 6 months post-exposure period. However, among 324 mice used in the experiment, 4 unexpected deaths were reported. These were one mouse from the PO 6 months CeO_2 group, one mouse from IV 28 days control group, one mouse was from IV 6 months TiO_2 group, one mouse from IT 6 months CB group. The causes of death were not established at the necropsy and the mice were excluded from the experiment.

Body and liver weight

In order to assess toxicity induced by exposure to NPs body weights and liver weights were recorded on the termination days. There were no alterations of body weight at any of the analyzed time points compared to the vehicle control groups (data not shown). IT, IV and PO administration of CeO_2 and CB NPs had no significant effects on mice liver weight compared to the vehicle control. PO treatment induced statistically significant decrease in liver weight 28 days following exposure to TiO_2 NPs when compared to the vehicle control group ($P < 0.05$), to the CeO_2 group ($P < 0.05$) and to the CB group ($P < 0.01$). Relative liver weight (g/100g body weight) was statistically significantly decreased 180 days following PO exposure to TiO_2 when compared to the vehicle control group ($P < 0.05$) and to the CeO_2 group ($P < 0.05$). IT and IV exposure did not alter liver weight following exposure to TiO_2 NPs at any time point (data not shown).

Hematology

The following hematological markers were analyzed: white blood cells (WBC), red blood cells (RBC), hemoglobin (HGB), hematocrit (HCT), mean corpuscular volume (MCV), mean corpuscular hemoglobin (MCH), mean corpuscular hemoglobin concentration (MCHC) and platelets (PLT) (Table 2). One day post-exposure IT administration of CB NPs significantly decreased MCHC level compared to the vehicle control group ($P < 0.05$). PLT level was statistically significantly decreased 1 day after IV administration of TiO_2 NPs compared to the vehicle control group ($P < 0.001$) and in TiO_2 vs CeO_2 group ($P < 0.01$). 28 days post-exposure in IT exposed mice alterations in MCV, MCH, MCHC and HGB levels were measured. MCV level was significantly increased in TiO_2 group compared to the vehicle control ($P < 0.05$). MCH level was decreased in TiO_2 group compared to the vehicle control ($P < 0.05$) as well as in CeO_2 group compared to the vehicle control ($P < 0.001$) and in CeO_2 vs CB group ($P < 0.05$). Exposure to CeO_2 significantly decreased MCHC level when compared to the vehicle control group ($P < 0.01$). HGB was significantly decreased in CeO_2 and CB groups compared to the vehicle control ($P < 0.05$). 180 days after intratracheal exposure MCV, MCH and MCHC levels were altered. MCV was significantly decreased in CB group compared to the vehicle control group ($P < 0.05$). MCH level was significantly decreased in TiO_2 group and CB compared to the vehicle control group ($P < 0.05$ and $P < 0.01$, respectively). Similar alterations were measured for MCHC level where significant decrease was detected in TiO_2 and CB group compared to the vehicle control group ($P < 0.05$ and $P < 0.01$, respectively). Intravenous exposure to TiO_2 NPs caused significant decrease in MCHC level when compared to the vehicle control group ($P < 0.05$). In orally gavaged animals 180 days post-exposure significant changes were detected in MCH and MCHC. Level of MCH was significantly decreased in TiO_2, CeO_2 and CB groups compared to the vehicle

control ($P < 0.01$, $P < 0.01$ and $P < 0.001$, respectively). MCHC was significantly decreased in CeO_2 and CB exposed groups compared to the vehicle control ($P < 0.001$ and $P < 0.0001$, respectively) as well as in CB vs TiO_2 group ($P < 0.01$) (Table 2).

Table 2. Hematology results from mice exposed by intratracheal instillation, intravenous injection and oral gavage to 162 μg of TiO_2, CeO_2 or CB NPs

	IT 1 day				IT 28 days				IT 6 months			
	Control	**TiO_2**	**CeO_2**	**CB**	**Control**	**TiO_2**	**CeO_2**	**CB**	**control**	**TiO_2**	**CeO_2**	**CB**
	mean ± SD	mean ± SD	mean ± SD	mean ± SD	mean ± SD	mean ± SD	mean ± SD	mean ± SD	mean ± SD	mean ± SD	mean ± SD	mean ± SD
WBC	37 ± 1.2	3.8 ± 1.3	4.7 ± 1.3	3.6 ± 0.8	5.7 ± 1.0	5.4 ± 1.4	5.4 ± 1.9	5.5 ± 1.5	5.4 ± 2.5	4.4 ± 1.1	5.1 ± 1.9	6.4 ± 2.2
RBC	10.7 ± 0.5	10.3 ± 1.5	9.9 ± 1.9	10.9 ± 0.2	10.5 ± 0.4	10.3 ± 0.3	9.5 ± 2.5	10.6 ± 0.4	10.2 ± 0.4	10.5 ± 0.5	10.2 ± 0.4	10.3 ± 0.3
HGB	16.3 ± 0.6	15.6 ± 2.1	14.9 ± 2.8	16.2 ± 0.3	15.6 ± 0.6	15.3 ± 0.4	14.0 ± 3.5*	15.5 ± 0.4*	15.5 ± 0.7	15.4 ± 0.6	14.9 ± 0.4	15.0 ± 0.3
HCT	51.9 ± 2.0	49.4 ± 7.2	47.5 ± 9.2	52.0 ± 1.1	49.7 ± 1.7	48.9 ± 1.1	45.2 ± 12.2	50.2 ± 1.5	47.5 ± 2.2	47.9 ± 2.4	46.8 ± 1.6	47.4 ± 1.4
MCV	48.4 ± 0.5	48.0 ± 0.5	48.1 ± 0.6	47.9 ± 0.6	47.6 ± 0.5	47.7 ± 0.9*	47.2 ± 0.7	47.3 ± 0.7	46.7 ± 0.9	45.8 ± 0.4	46.2 ± 1.0	46.1 ± 0.4*
MCH	15.2 ± 0.2	15.2 ± 0.3	15.0 ± 0.2	14.9 ± 0.3	15.0 ± 0.2	14.9 ± 0.3*	14.8 ± 0.6***†	14.6 ± 0.2	15.2 ± 0.4	14.7 ± 0.3*	14.7 ± 0.3	14.6 ± 0.2**
MCHC	31.3 ± 0.3	31.6 ± 0.4	31.4 ± 0.3	31.1 ± 0.5*	31.5 ± 0.5	31.2 ± 0.4	31.3 ± 1.4**	31.9 ± 3.5	32.6 ± 0.2	32.2. ± 0.5*	31.9 ± 0.3	31.6 ± 0.3*
PLT	713.8 ± 163.4	655.8 ± 177.1	686.6 ± 133.3	750.1 ± 62.6	742.8 ± 82.2	717.8 ± 80.1	687.6 ± 114.3	685.3 ± 92.7	755.7 ± 92.9	771.0 ± 197.5	814.6 ± 133.4	856.0 ± 212.6
	IV 1 day				**IV 28 days**				**IV 6 months**			
	Control	**TiO_2**	**CeO_2**	**CB**	**Control**	**TiO_2**	**CeO_2**	**CB**	**control**	**TiO_2**	**CeO_2**	**CB**
	mean ± SD	mean ± SD	mean ± SD	mean ± SD	mean ± SD	mean ± SD	mean ± SD	mean ± SD	mean ± SD	mean ± SD	mean ± SD	mean ± SD
WBC	4.2 ± 1.4	4.5 ± 1.4	4.2 ± 1.1	3.6 ± 1.2	5.8 ± 1.6	5.2 ± 1.8	4.6 ± 1.5	4.8 ± 0.9	6.6 ± 3.0	4.5 ± 1.8	4.6 ± 1.7	4.3 ± 1.5
RBC	10.1 ± 1.5	10.5 ± 0.4	10.3 ± 0.7	10.4 ± 0.7	10.3 ± 0.5	9.9 ± 1.3	10.4 ± 0.3	10.2 ± 0.4	10.5 ± 0.6	10.9 ± 0.4	10.1 ± 0.5	10.2 ± 0.4
HGB	15.6 ± 2.2	16.0 ± 0.6	15.8 ± 0.8	15.9 ± 1.0	15.6 ± 0.8	14.8 ± 1.7	15.5 ± 0.3	15.3 ± 0.6	15.6 ± 0.5	15.6 ± 0.5	14.9 ± 0.7	15.1 ± 0.5
HCT	48.5 ± 7.4	50.6 ± 2.1	49.5 ± 3.6	49.9 ± 3.2	49.0 ± 2.4	47.5 ± 6.2	49.5 ± 1.1	48.4 ± 2.1	48.6 ± 2.0	49.7 ± 1.5	46.8 ± 2.4	47.5 ± 1.4
MCV	48.0 ± 0.9	48.0 ± 0.5	48.0 ± 0.0	48.1 ± 0.6	47.9 ± 0.4	47.8 ± 0.7	47.8 ± 0.4	47.7 ± 0.7	46.3 ± 0.7	45.8 ± 0.7	46.2 ± 0.7	46.3 ± 1.1
MCH	15.5 ± 0.2	15.2 ± 0.1	15.3 ± 0.5	15.4 ± 0.2	15.2 ± 0.2	14.9 ± 0.5	15.0 ± 0.3	15.0 ± 0.3	14.8 ± 0.4	14.4 ± 0.4	14.7 ± 0.4	14.8 ± 0.5
MCHC	32.3 ± 0.6	31.6 ± 0.4	32.1 ± 1.2	31.9 ± 0.2	31.8 ± 0.4	31.3 ± 0.9	31.3 ± 0.4	31.5 ± 0.4	32.0 ± 0.4	31.4 ± 0.4*	31.8 ± 0.6	31.9 ± 0.2
PLT	827.8 ± 50.4	482.8 ± 222.8***‡‡	795.9 ± 46.2	686.0 ± 217.9	676.4 ± 80.7	673.2 ± 197.2	714.1 ± 48.1	765.1 ± 42.3	794.7 ± 143.9	742.9 ± 240.1	892.3 ± 156.0	807.6 ± 120.4
	PO 1 day				**PO 28 days**				**PO 6 months**			
	Control	**TiO_2**	**CeO_2**	**CB**	**Control**	**TiO_2**	**CeO_2**	**CB**	**control**	**TiO_2**	**CeO_2**	**CB**
	mean ± SD	mean ± SD	mean ± SD	mean ± SD	mean ± SD	mean ± SD	mean ± SD	mean ± SD	mean ± SD	mean ± SD	mean ± SD	mean ± SD
WBC	4.5 ± 1.5	4.5 ± 0.8	4.3 ± 1.2	4.1 ± 0.9	4.3 ± 1.2	5.3 ± 2.1	3.2 ± 1.6	5.8 ± 1.3	4.5 ± 1.3	5.4 ± 2.1	4.3 ± 0.7	5.0 ± 0.9
RBC	10.4 ± 0.3	10.4 ± 0.9	10.7 ± 0.5	10.7 ± 0.4	10.4 ± 0.3	10.2 ± 1.6	10.1 ± 1.3	10.1 ± 0.6	10.4 ± 0.4	10.9 ± 0.4	10.7 ± 0.3	10.5 ± 0.5
HGB	15.8 ± 0.6	15.5 ± 1.3	15.9 ± 0.5	15.9 ± 0.6	15.6 ± 0.3	14.8 ± 2.2	14.4 ± 1.8	14.9 ± 0.7	14.9 ± 0.6	15.1 ± 0.7	15.0 ± 0.5	14.5 ± 0.7
HCT	50.3 ± 1.6	50.0 ± 4.5	51.2 ± 1.9	51.4 ± 1.9	49.3 ± 1.3	48.2 ± 7.7	47.8 ± 6.2	48.1 ± 2.7	47.8 ± 1.8	49.5 ± 2.1	48.8 ± 1.4	47.6 ± 2.4
MCV	48.2 ± 0.7	48.2 ± 0.4	48.0 ± 0.5	48.1 ± 0.6	47.6 ± 0.5	47.0 ± 0.0	47.3 ± 0.5	47.8 ± 0.4	46.0 ± 0.5	45.4 ± 0.5	45.5 ± 0.5	45.3 ± 0.5
MCH	15.2 ± 0.3	15.0 ± 0.2	14.9 ± 0.4	14.9 ± 0.1	15.0 ± 0.3	14.5 ± 0.3	14.3 ± 0.5	14.8 ± 0.2	14.3 ± 0.3	13.9 ± 0.3**	14.0 ± 0.2**	13.8 ± 0.3***
MCHC	31.5 ± 0.3	31.1 ± 0.4	31.1. ± 0.5	31.0 ± 0.3	31.6 ± 0.5	30.9 ± 0.6	30.2 ± 1.1	31.0 ± 0.5	31.2 ± 0.3	30.6 ± 0.5	30.7 ± 0.3***	30.5 ± 0.4****##
PLT	746.2 ± 129.7	723.0 ± 157.7	750.6 ± 96.8	771.0 ± 36.6	701.0 ± 138.0	705.7 ± 140.6	649.0 ± 179.6	624.8 ± 142.3	839.0 ± 195.5	963.0 ± 140.3	719.6 ± 248.0	832.8 ± 64.4

WBC - white blood cells ($x10^3$/μl), RBC – red blood cells ($x10^6$/ μl), HGB – hemoglobin (g/dl), HCT – hematocrit (%), MCV – mean corpuscular volume (fL), MCH – mean corpuscular hemoglobin (pG), MCHC – mean corpuscular hemoglobin concentration (%), PLT – platelets ($x10^3$/μl), IT – intratracheal instillation, IV – intravenous injection, PO – oral gavage;

Particle exposed groups n=9, vehicle control n=9. All values are presented as mean ± SD. Asterisk (*) denotes $P \leq 0.05$, (**) denote $P \leq 0.01$, (***) $P \leq 0.001$, (****) $P \leq 0.0001$ of blood marker level in exposed group versus vehicle control. Hashtags (##) denote $P \leq 0.01$ of blood marker level in CB group compared to TiO_2 group. Cross (†) denotes $P \leq 0.05$ of blood marker level in CeO_2 group compared to CB group. Double crosses (‡‡) denote $P \leq 0.01$ of blood marker level in TiO_2 group compared to CeO_2 group.

Plasma liver enzyme activities

Alkaline phosphatase (ALP), aspartate aminotransferase (AST) and alanine transaminase (ALT) activities were measured in plasma 28 days post-exposure in order to assess NP-induced hepatotoxic effects on liver function. There were no significant changes in any of the analyzed liver enzyme activities (Table 3).

Table 3. Alkaline phosphatase (ALP), aspartate aminotransferase (AST) and alanine transaminase (ALT) enzyme activities in plasma following intratracheal instillation, intravenous injection and oral gavage to 162 μg of TiO_2, CeO_2 or CB NPs measured 28 days post-exposure

Liver enzymes activity 28 days following IT exposure			
	ALP	AST	ALT
	mean ± SD	mean ± SD	mean ± SD
Control	119 ± 17	185 ± 141	35 ± 8
TiO_2	138 ± 16	132 ± 78	38 ± 3
CeO_2	113 ± 13	293 ± 179	41 ± 9
CB	133 ± 19	329 ± 366	47 ± 13
Liver enzymes activity 28 days following IV exposure			
	ALP	AST	ALT
	mean ± SD	mean ± SD	mean ± SD
Control	125 ± 17	151 ± 85	39 ± 5
TiO_2	121 ± 13	91 ± 20	34 ± 7
CeO_2	119 ± 13	136 ± 25	39 ± 8
CB	128 ± 14	120 ± 56	38 ± 8
Liver enzymes activity 28 days following PO exposure			
	ALP	AST	ALT
	mean ± SD	mean ± SD	mean ± SD
Control	136 ± 17	109 ± 48	42 ± 8
TiO_2	145 ± 22	94 ± 26	43 ± 7
CeO_2	133 ± 17	180 ± 131	51 ± 20
CB	123 ± 12	156 ± 205	40 ± 18

Alkaline phosphatase (ALP), aspartate aminotransferase (AST) and alanine transaminase (ALT), intratracheal instillation (IT), intravenous injection (IV), oral gavage (PO)

Particle detection in lung and liver by enhanced darkfield microscopy

Particle presence was assessed at day 1 and day 180 in lung after IT exposure (Fig. 2) and in liver after IT and IV exposure (Fig. 3), using enhanced darkfield microscopy.

In lungs 24 hours after IT of TiO_2 and CeO_2, aggregates of foreign material were observed mainly in the alveolar region, either phagocytized by macrophages or free in alveolar lumen or at alveolar walls (Fig. 2C and E). 180 days after IT, the foreign material was additionally found accumulated in laden macrophages (Fig. 2D and F) and occasionally near blood vessels.

Aggregates in the liver 24h after IV were dispersed across whole tissue sections (Fig. 3D and H), mainly in sinusoids and often close to Kupffer cells (inserts in Fig. 3D and H). 180 days after IT, particles were partly accumulated in fewer and larger aggregates in parenchyma (Fig. 3E and I) and occasionally near blood vessels.

Foreign material was also present in some but not all infiltrations of inflammatory cells in lung after IT exposure (Fig. 2D and F) and in liver after IV exposure at day 1 and 180.

Foreign material aggregates were seen in liver 180 days after IT exposure (Fig. 3F and J). These aggregates were smaller and much less frequent than aggregates detected in the liver 180 days after IV exposure. The aggregates were predominantly found in sinusoids and often appeared to be phagocytized by Kupffer cells.

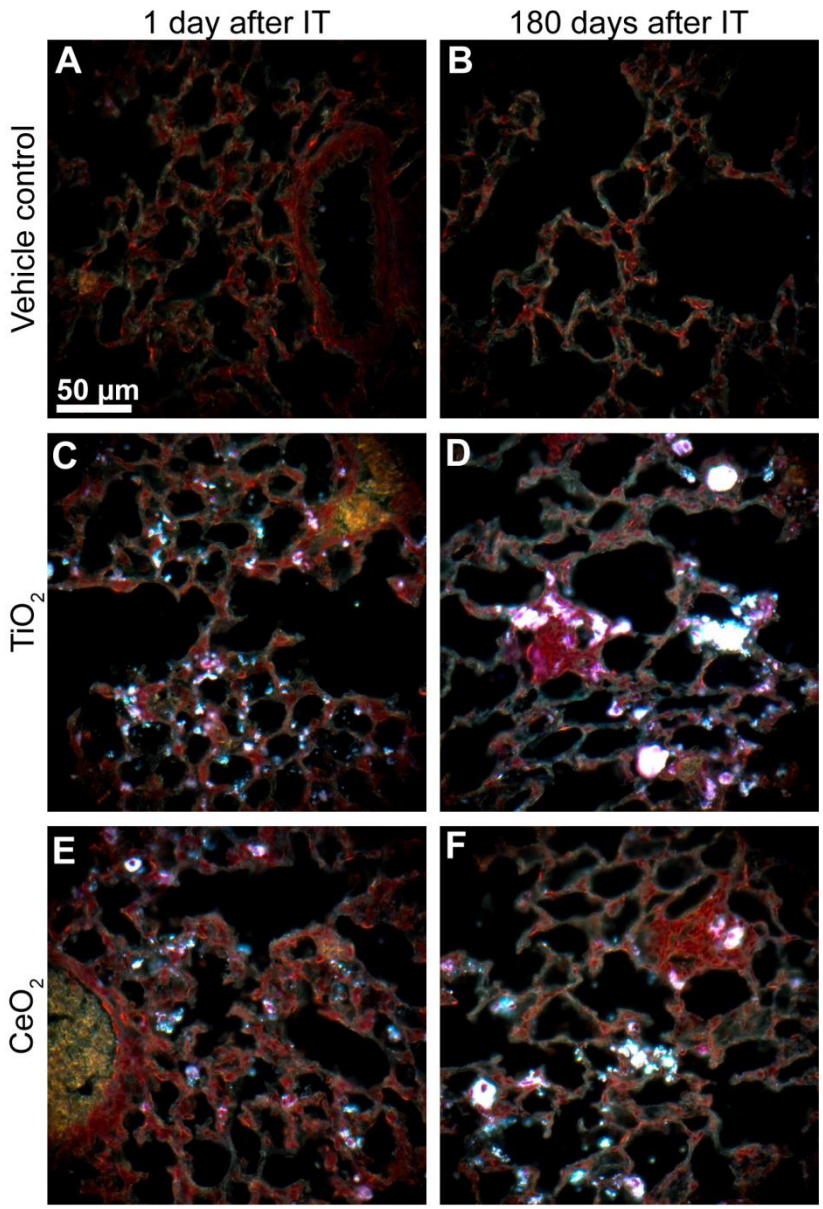

Figure 2. Lung tissue 1 and 180 days after IT exposure to vehicle control (A-B), TiO_2 (C-D) and CeO_2 (E-F) NPs. C and E: Using enhanced darkfield microscopy, light scattering aggregates of foreign material (white) were observed in the alveolar region 1 day after exposure. D and F: 180 days after exposure, aggregates were additionally accumulated in laden macrophages and occasionally at blood vessels and in inflammatory cell infiltrates. Scale bar in A applies to all images.

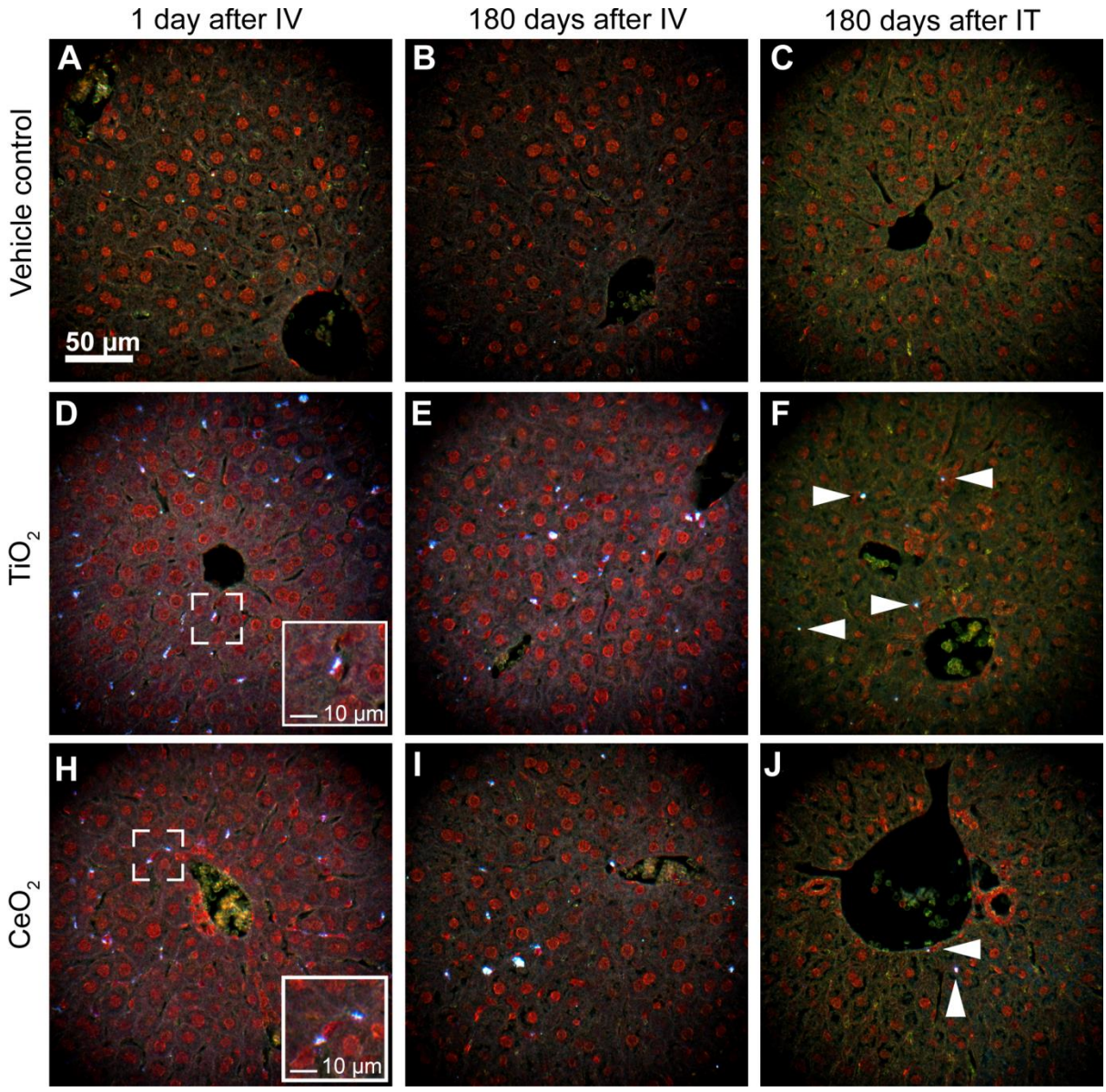

Figure 3. Liver tissue 1 and 180 days after IV and IT exposure to vehicle control (A-C), TiO_2 (D-F) and CeO_2 (H-J) NPs. D and H: Aggregates of foreign material (white) were dispersed across liver sections 1 day after IV exposure and often appeared phagocytized by Kupffer cells (inserts in D and H). E and I: 180 days after IV exposure, material was partly accumulated in larger aggregates in liver parenchyma. F and J: Aggregates seen 180 days after IT were small and much less frequent (arrowheads). Scale bar in A applies to all images.

Liver and lungs histopathology

The histopathological evaluations of lungs and livers from mice exposed by IT, IV and PO to a single dose of 162 μg of TiO_2, CeO_2 or CB NPs are summarized in Tables 4 and 5.

The microscopic changes observed in the lungs after IT and IV exposures indicated inflammation. One day after IT exposure, extravasation, oedema of connective tissue, inflammatory cell infiltration peribronchial and/or perivascular were recorded in all NPs treated groups and single macrophages or single laden macrophages in the surface of alveoli were recorded in the TiO_2 and in CeO_2 groups (Table 4). These changes were also observed 28 and 180 days after exposure. Aggregates of inflammatory cells 180 days after exposure were both small and big in TiO_2 group (Fig. 4C), big in CeO_2 group (Fig. 4F), and relatively small in CB group (Fig. 4I) as compared to the two other treated groups. Small aggregates of macrophages were observed on day 28 in all NP exposed groups. Aggregates of macrophages appeared biggest in size after exposure to TiO_2 (Fig. 4B) on day 28 and were also observed 180 days after exposure.

One day after IV exposure, extravasation was only recorded in the CB group (Table 4). Oedema of connective tissue between bronchioles and blood vessels was present in the vehicle control and NPs treated groups (Fig. 5A and B) and it was the most expressed in the CeO_2 group as indicated by its presence in all examined animals (Table 4). Inflammatory cell infiltrations were recorded in the vehicle control and TiO_2 groups. Single macrophages were seen in all groups but the laden with test material (as indicated by the larger and dark appearance) were only recorded in the CB group. In this group the agglomerated test material was present in the lumen of blood vessels (Fig. 5E) and in the alveolar lumen, which could indicate its migration to the alveolar space. 28

days after IV exposure oedema of connective tissue was still present in all groups. The oedema was also visible in the TiO_2 and CB groups 180 days after IV exposure. Single macrophages were recorded in the control group on day 180, and in the TiO_2 and CB groups on days 28 and 180.

Other microscopic changes in lung recorded in groups exposed either by IT or IV were: (a) desquamation of bronchiole epithelium following IT exposure on day 28 in the vehicle control (1/3), following IV exposure on days 1 and 28 in the vehicle control (1/3 at both time points) and in the TiO_2 group (2/3 and 1/3 respectively); (b) hyperplasia of connective tissue (visible as single fibroblasts of supportive tissue surrounding bronchioles) after IV exposure on 1 day in the CeO_2 (1/3) and CB (1/3) groups and on day 28 in the TiO_2 group (1/3), and (c) emphysema after IV exposure in CB group (1/3).

The observed microscopic changes after PO exposure included: (a) small infiltration of inflammatory cells on day 1 in the CeO_2 group and on day 180 in all NPs groups, (b) oedema of connective tissue on day 1 in the CeO_2 group and on day 180 in the TiO_2 and CB groups, and (c) single macrophages in the CeO_2 group on day 180.

Furthermore, congestion was seen in all groups regardless of exposure route and time and therefore it was not considered treatment related but as a consequence of insufficient exsanguination of the carcass.

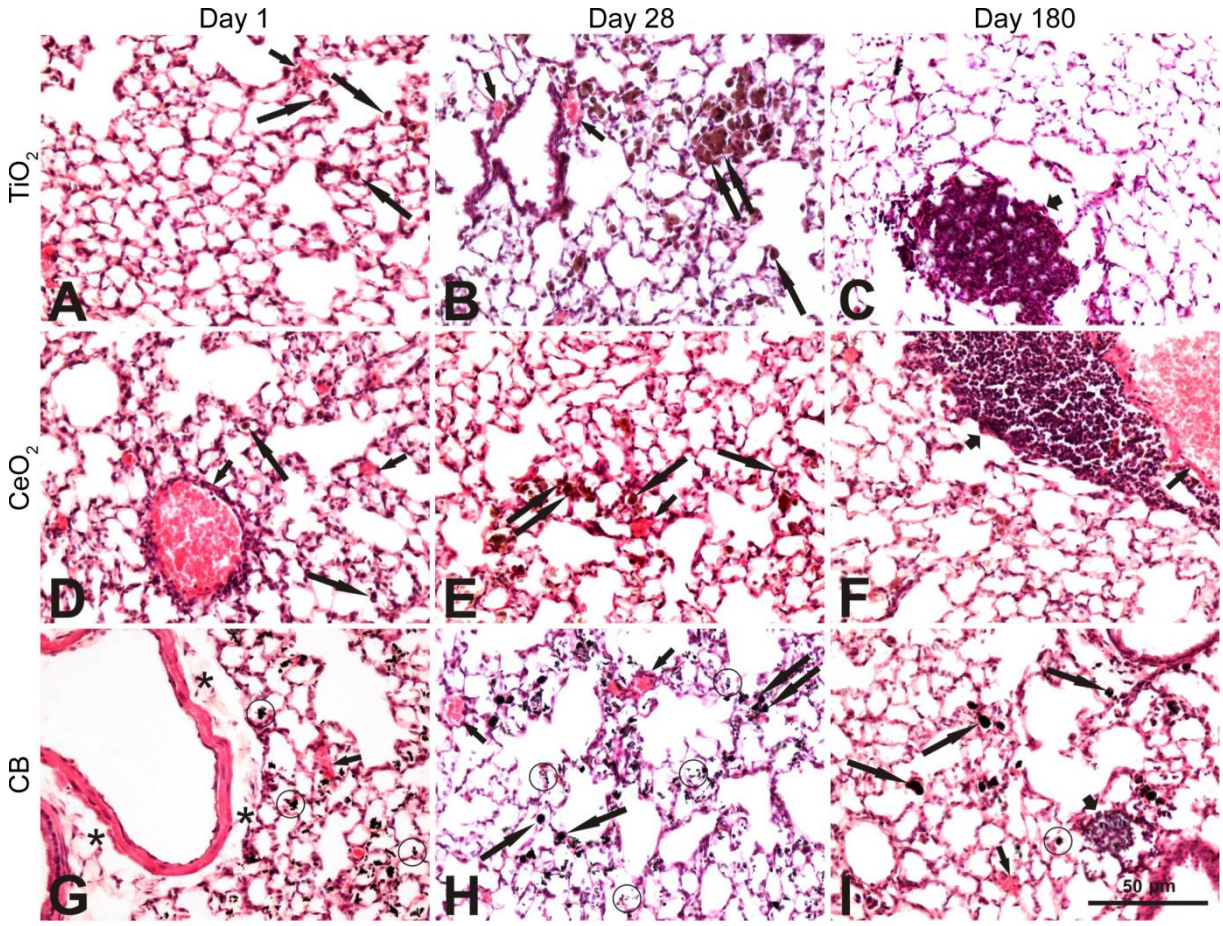

Figure 4. Microscopic changes in the lungs of mice after intratracheal instillation (IT) with TiO_2 (A-C), CeO_2 (D-F) and CB (G-I) NPs 1, 28, or 180 days respectively. A-C: congestion (short arrows), single macrophages (arrows), big aggregates of macrophages (double arrows), inflammatory cell aggregate (short wide arrow); D-F: congestion (short arrows), single (arrows) and small aggregates (double arrows) of macrophages, perivascular inflammatory cell aggregate (short wide arrow); G-I: congestion (short arrows), oedema (asterisks), single macrophages (arrows), aggregate of inflammatory cells (short wide arrow), test material (circle).

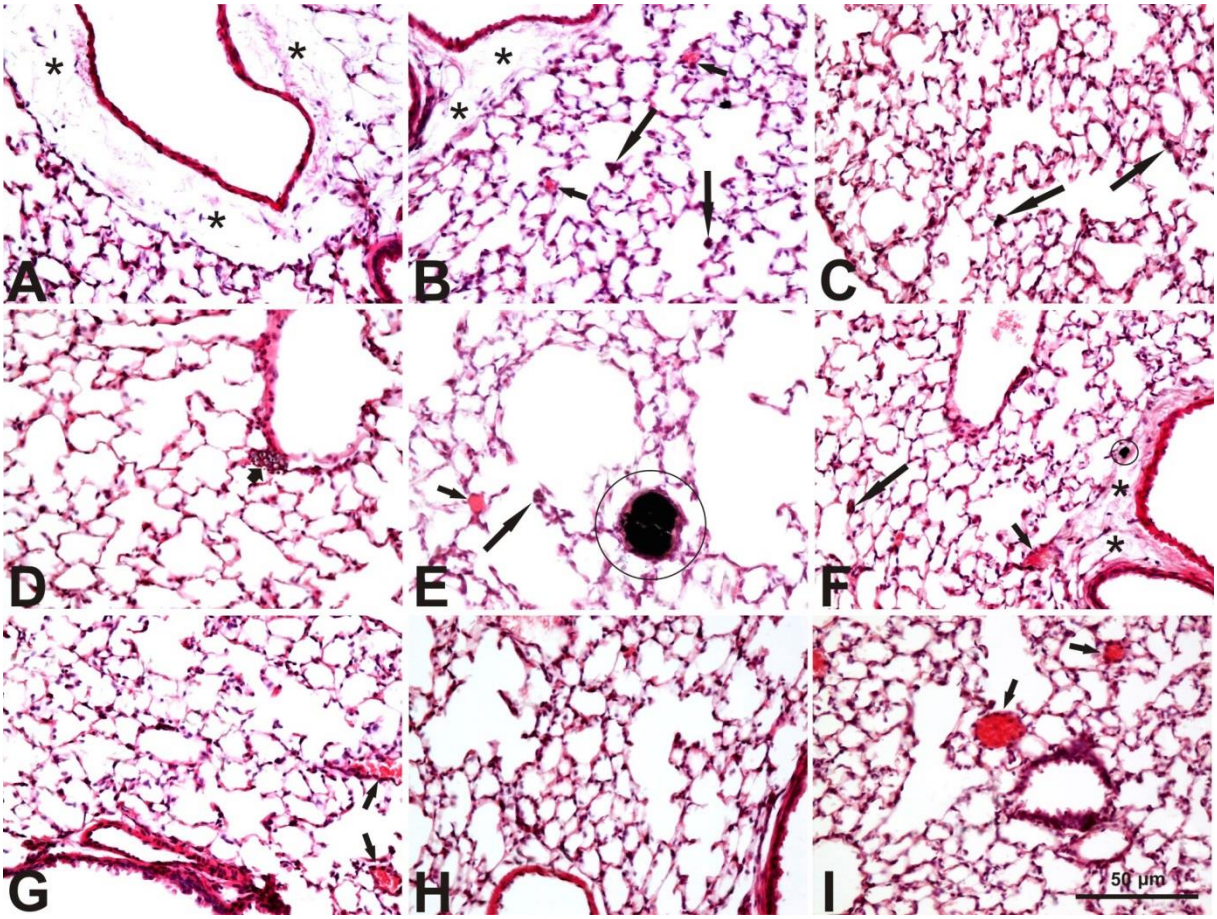

Figure 5. Microscopic changes in the lungs of mice scarified at different times after intravenous (IV) or per oral (PO) exposures to the test nanomaterials or a vehicle. A-C: TiO_2 1, 28 or 180 days after IV exposure respectively: congestion (short arrows), single macrophages (arrows), perivascular oedema (asterisks); D: CeO_2 IV 180 days after exposure: perivascular small infiltration of inflammatory cells; E-F: CB 1 or 28 days after IV exposure: small congestion (short arrows), oedema (asterisks), single macrophages (arrows), test material (circle); G – TiO_2 180 days after PO exposure, H - vehicle control 1 day after PO and I – vehicle control 28 days after IV exposure: normal structure of the lungs with congestion (short arrows).

Table 4. Type and incidence of typical microscopic changes in the lungs of mice 1, 28 or 180 days after a single exposure to 162 μg of TiO_2, CeO_2 or CB NPs administered by intratracheal instillation, intravenous injection or oral gavage

Change	Intratracheal instillation				Intravenous injection				Oral gavage			
	Control	TiO_2	CeO_2	CB	Control	TiO_2	CeO_2	CB	Control	TiO_2	CeO_2	CB
Inflammatory cell infiltration peribronchial and/or perivascular												
day 1	0/3	1/3	1/3	1/3	1/3	1/3	0/3	0/3	0/4	0/3	1/3	0/3
day 28	1/3	1/3	1/3	1/3	0/3	0/3	0/3	1/3	0/4	0/3	0/3	0/3
day 180	0/3	3/3	2/3	2/3	1/3	0/3	2/3	0/3	0/3	1/3	1/3	1/3
Macrophages single												
day 1	0/3	3/3	1/3	0/3	1/3	1/3	1/3	0/3	0/4	0/3	0/3	0/3
day 28	1/3	2/3	1/3	0/3	0/3	0/3	0/3	1/3	0/4	0/3	0/3	0/3
day 180	0/3	2/3	2/3	0/3	1/3	1/3	0/3	0/3	1/3	0/3	1/3	0/3
Macrophages single laden (with the test material)												
day 1	0/3	3/3	0/3	0/3	0/3	0/3	0/3	1/3	0/4	0/3	0/3	0/3
day 28	0/3	3/3	3/3	3/3	0/3	1/3	0/3	0/3	0/4	0/3	0/3	0/3
day 180	0/3	1/3	1/3	3/3	0/3	1/3	0/3	1/3	0/3	0/3	0/3	0/3
Macrophages (laden), aggregates small[a])												
day 1	0/3	0/3	0/3	0/3	0/3	0/3	0/3	0/3	0/4	0/3	0/3	0/3
day 28	0/3	3/3	1/3	1/3	0/3	0/3	0/3	0/3	0/4	0/3	0/3	0/3
day 180	0/3	0/3	0/3	1/3	0/3	0/3	0/3	0/3	0/3	0/3	0/3	0/3
Macrophages (laden) aggregates big[b])												
day 1	0/3	1/3	0/3	0/3	0/3	0/3	0/3	0/3	0/4	0/3	0/3	0/3
day 28	0/3	1/3	0/3	0/3	0/3	0/3	0/3	0/3	0/4	0/3	0/3	0/3
day 180	0/3	1/3	0/3	0/3	0/3	0/3	0/3	0/3	0/3	0/3	0/3	0/3

Oedema of connective tissue peribronchial and/or perivascular												
day 1	0/3	2/3	3/3	1/3	1/3	2/3	3/3	2/3	0/4	0/3	1/3	0/3
day 28	3/3	2/3	3/3	1/3	1/3	3/3	2/3	1/3	0/4	0/3	0/3	0/3
day 180	0/3	3/3	1/3	2/3	0/3	1/3	0/3	1/3	0/3	1/3	0/3	1/3
Congestion												
day 1	2/3	3/3	3/3	2/3	2/3	1/3	2/3	1/3	4/4	3/3	3/3	3/3
day 28	3/3	3/3	3/3	3/3	3/3	3/3	3/3	3/3	4/4	3/3	3/3	3/3
day 180	2/3	1/3	3/3	2/3	3/3	3/3	0/3	0/3	2/3	3/3	3/3	2/3
Extravasation												
day 1	2/3	3/3	1/3	1/3	0/3	0/3	0/3	1/3	0/4	0/3	0/3	0/3
day 28	0/3	1/3	0/3	0/3	0/3	0/3	0/3	0/3	0/4	0/3	0/3	0/3
day 180	2/3	1/3	1/3	0/3	0/3	0/3	0/3	0/3	0/3	0/3	0/3	0/3

a): 1-4 macrophages at one site close to each other; b): more than 5 macrophages at one site close to each other;

The microscopic changes in the liver were of inflammatory, regressive, degenerative and circulatory types (Table 5 and Fig. 6 liver after IV). The recorded inflammatory changes were defined as foci small of inflammatory cells (FsIC: focal small infiltrates or aggregates consisting of mononuclear, polymorphonuclear and/or hystiocytic cells), which occasionally accompanied hepatocellular necrosis or as polymorphonuclear cell foci (PNCF: bigger in size focal infiltrates or aggregates of mono- and polymorphonuclear and/or hystiocytic cells surrounded by eosinophilic necrotic hepatocytes, with apopototic bodies/debris often present). In general, the incidence of inflammatory changes regardless of the route of exposure and the type of NPs used was high and comparable to the vehicle controls. Regressive changes comprised different types from slight, like presence of single hepatocytes with pyknotic nuclei, to advanced, like areas of necrosis.

After IT exposure a statistically significantly increased incidence of regressive changes was recorded in the CeO_2 group on day 28 for the presence of hepatocytes with pyknotic nuclei, on day 180 for the areas of hepatocytes with pyknotic nuclei and for microfoci of necrosis. Also areas of necrosis were seen on day 180 in all livers in the CeO_2 group but the incidence was not statistically significantly increased compared to the vehicle controls. In the TiO_2 group the only regressive change with a statistically significantly increased incidence was the presence of areas of hepatocytes with pyknotic nuclei. Other statistically significantly increased incidences after IT exposure when compared to the vehicle control group were recorded for increased number of binucleate hepatocytes on day 1 in the TiO_2 group, and for vacuolar degeneration on day 28 in the CeO_2 group.

Following IV exposure a statistically significantly increased incidence was recorded on day 1 for hypertrophy of Kupffer cells and of binucleate hepatocytes in the TiO_2 and CB groups, and on day 28 for the presence of areas of hepatocytes with pyknotic nuclei in the CeO_2 group.

No noteworthy changes were observed following PO exposure. The only statistically increased incidence was recorded for areas of hepatocytes with pyknotic nuclei on day 180 in the CB group.

Table 5. Type and incidence of microscopic changes in the livers of mice 1, 28 or 180 days after a single exposure to 162 μg of TiO_2, CeO_2 and CB NPs administered by intratracheal instillation, intravenous injection or oral gavage

Change	Intratracheal instillation				Intravenous injection				Oral gavage			
	Control	TiO_2	CeO_2	CB	Control	TiO_2	CeO_2	CB	Control	TiO_2	CeO_2	CB
Foci small of inflammatory cells												
day 1	5/8	3/9	8/9	9/9	8/9	9/9	9/9	9/9	6/9	7/9	5/9	5/9
day 28	8/9	8/9	6/9	9/9	6/8	9/9	8/9	6/9	9/9	9/9	7/9	7/9
day 180	7/9	8/9	679	5/8	5/9	6/8	4/9	3/9	7/9	6/9	8/9	8/8
Polymorphonuclear cell foci												
day 1	3/8	5/9	3/9	2/9	9/9	6/9	8/9	4/9	3/9	2/9	5/9	3/9
day 28	8/9	7/9	7/9	8/9	7/8	6/9	8/9	8/9	6/9	8/9	7/9	5/9
day 180	8/9	5/9	8/9	4/8	6/9	1/8	4/9	2/9	6/9	6/9	9/9	5/8
Hepatocytes with pyknotic nuclei (single)												
day 1	0/8	0/9	0/9	1/9	1/9	0/9	1/9	0/9	0/9	0/9	0/9	0/9
day 28	0/9	1/9	5/9*	2/9	3/8	1/9	0/9	2/9	5/9	2/9	2/9	0/9
day 180	1/9	0/9	0/9	1/8	1/9	3/8	5/9	2/9	2/9	1/9	1/9	0/8
Hepatocytes with pyknotic nuclei (area of)												
day 1	0/8	0/9	1/9	0/9	3/9	7/9	1/9	4/9	0/9	0/9	0/9	0/9
day 28	1/9	1/9	2/9	0/9	0/8	2/9	7/9**	2/9	0/9	0/9	0/9	0/9
day 180	3/9	8/9*	8/9*	3/8	0/9	2/8	1/9	5/9	0/9	4/9	4/9	7/8***
Eosinophilic necrosis of hepatocytes												
day 1	3/8	4/9	5/9	4/9	8/9	9/9	8/9	8/9	3/9	2/9	3/9	3/9
day 28	5/9	6/9	7/9	6/9	5/8	7/9	7/9	9/9	4/9	8/9	7/9	6/9
day 180	4/9	5/9	6/9	3/8	2/9	1/8	3/9	4/9	3/9	5/9	7/9	5/8
Microfoci of necrosis in centrilobular (area of)												
day 1	1/8	3/9	1/9	2/9	7/9	4/9	5/9	7/9	0/9	0/9	0/9	3/9
day 28	3/9	7/9	7/9	4/9	4/8	2/9	5/9	8/9	3/9	4/9	3/9	7/9
day 180	1/9	5/9	7/9*	4/8	2/9	2/8	7/9	7/9	3/9	7/9	5/9	1/8
Necrosis (area of)												
day 1	0/8	0/9	0/9	2/9	8/9	9/9	3/9	4/9	2/9	0/9	0/9	0/9
day 28	3/9	4/9	6/9	2/9	1/8	1/9	6/9	4/9	0/9	0/9	0/9	0/9
day 180	5/9	8/9	9/9	6/8	2/9	1/9	5/9	6/9	6/9	5/9	7/9	8/8

Hypertrophy of Kupffer cells												
day 1	0/8	0/9	0/9	0/9	3/9	9/9**	3/9	9/9**	0/9	1/9	1/9	0/9
day 28	2/9	0/9	0/9	2/9	5/8	4/9	4/9	7/9	0/9	0/9	1/9	0/9
day 180	1/9	0/9	1/9	1/8	0/9	1/8	0/9	2/9	0/9	0/9	2/9	0/8
Hyperplasia (increased number) of Kupffer cells												
day 1	0/8	1/9	1/9	0/9	0/9	1/9	0/9	4/9	0/9	2/9	4/9	3/9
day 28	1/9	1/9	1/9	2/9	2/8	0/9	6/9	1/9	0/9	0/9	0/9	0/9
day 180	0/9	0/9	1/9	0/8	0/9	0/8	0/9	0/9	0/9	1/9	2/9	0/8
Hyperplasia of bile duct epithelial cells												
day 1	0/8	0/9	0/9	0/9	9/9	7/9	0/9	6/9	0/9	0/9	0/9	0/9
day 28	1/9	2/9	1/9	3/9	2/8	2/9	4/9	6/9	0/9	0/9	0/9	0/9
day 180	3/9	1/9	3/9	0/8	0/9	1/8	0/9	0/9	1/9	1/9	0/9	1/8
Hyperplasia of connective tissue near bile ductules or venules (fibrosis)												
day 1	0/8	0/9	0/9	0/9	2/9	7/9	1/9	0/9	0/9	0/9	0/9	2/9
day 28	0/9	2/9	0/9	0/9	0/8	0/9	1/9	3/9	0/9	0/9	0/9	2/9
day 180	0/9	0/9	2/9	1/8	1/9	1/8	1/9	0/9	1/9	3/9	2/9	0/8
Increased number of binucleate hepatocytes												
day 1	0/8	6/9**	1/9	1/9	0/9	5/9*	3/9	5/9*	0/9	0/9	0/9	4/9
day 28	0/9	4/9	2/9	4/9	1/8	2/9	0/9	0/9	0/9	0/9	0/9	1/9
day 180	0/9	2/9	0/9	0/8	0/9	0/8	0/9	2/9	0/9	0/9	1/9	0/8
Vacuolar (hydropic) degeneration of hepatocytes												
day 1	0/8	0/9	0/9	0/9	0/9	0/9	2/9	0/9	2/9	7/9	0/9	1/9
day 28	2/9	4/9	8/9*	0/9	6/8	4/9	6/9	5/9	0/9	1/9	1/9	5/9
day 180	2/9	7/9	3/9	6/8	5/9	0/8	4/9	6/9	5/9	3/9	4/9	7/8
Sinusoid dilatation												
day 1	0/8	0/9	0/9	0/9	3/9	8/9	3/9	2/9	0/9	0/9	0/9	0/9
day 28	1/9	0/9	2/9	0/9	0/8	0/9	0/9	0/9	0/9	2/9	1/9	0/9
day 180	0/9	2/9	0/9	0/8	0/9	0/8	0/9	0/9	0/9	4/9	3/9	0/9
Congestion												
day 1	0/8	0/9	0/9	0/9	1/9	5/9	1/9	4/9	0/9	0/9	1/9	0/9
day 28	6/9	0/9	0/9	0/9	3/8	0/9	6/9	0/9	0/9	0/9	0/9	0/9
day 180	0/9	1/9	1/9	0/8	0/9	2/8	0/9	1/9	5/9	7/9	6/9	2/8

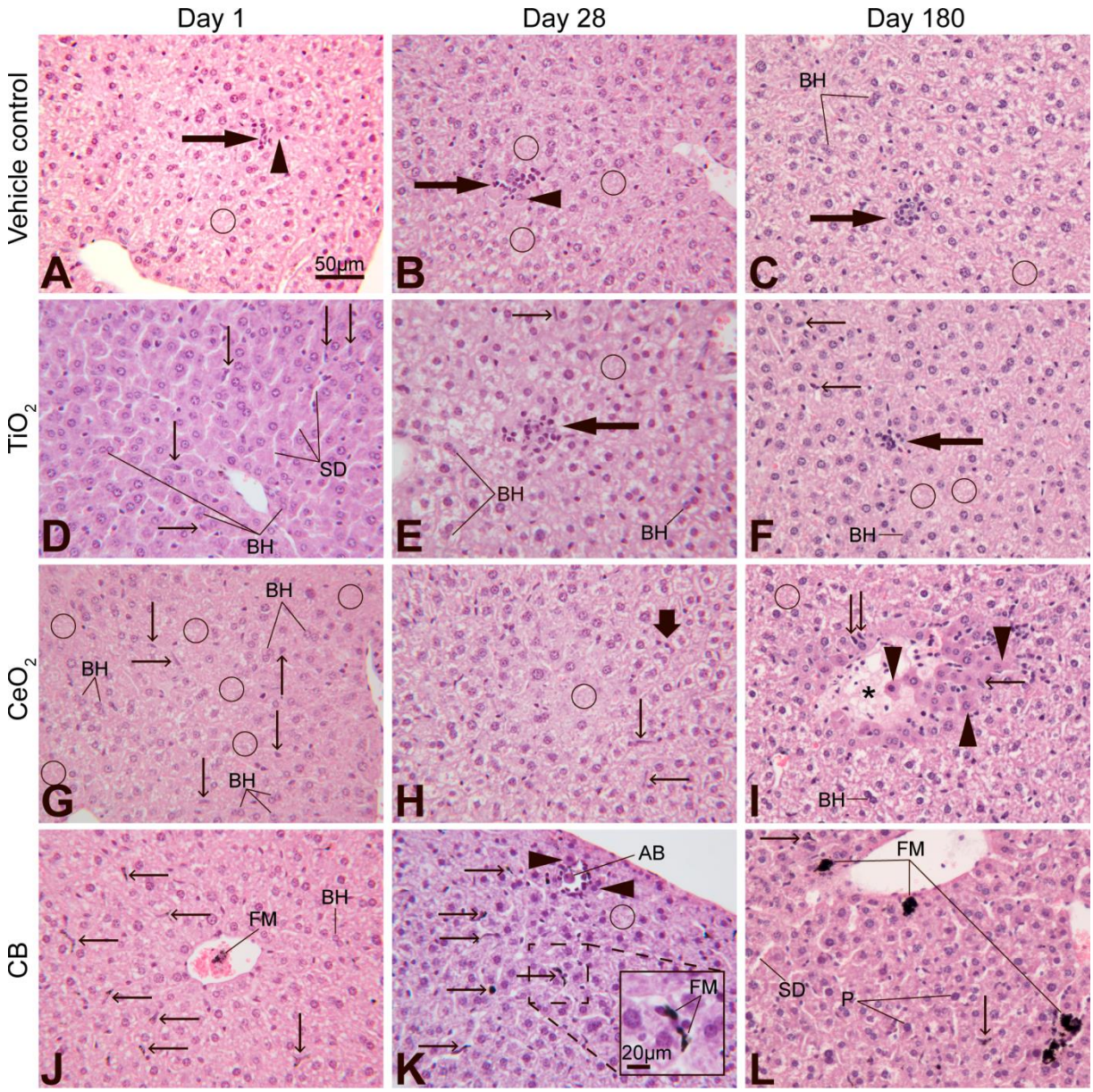

Figure 6. Microscopic changes in the liver of mice 1, 28, or 180 days after single intravenous injection (IV) of a vehicle (A-C), TiO_2 (D-F), CeO_2 (G-I) or CB (J-L) NPs. A-C: FsIC (long arrows), eosinophilic necrosis (arrowheads), microfoci of necrosis (circles), binucleate hepatocytes (BH), vacuolar degeneration (white spaces in hepatocytes). D-F: FsIC (long arrows), microfoci of necrosis (circles), hypertrophy of Kupffer cells (tiny arrows), binucleate hepatocytes (BH), sinusoidal dilatations (SD), vacuolar degeneration (white spaces in hepatocytes). G-I: microfoci of necrosis (circles), eosinophilic necrosis (arrowheads), area of necrosis (asterisk), hypertrophy of Kupffer cells (tiny arrows), binucleate hepatocytes (BH), vacuolar degeneration (white spaces in hepatocytes), hyperplasia of Kupffer cells (thick arrow). J-L: eosinophilic necrosis (arrowheads), apoptotic body (AB), microfocus of necrosis (circle), hypertrophy of Kupffer cells

(tiny arrows), some of them with black foreign material, sinusoidal dilatation (white long spaces, SD), pyknosis of nuclei (P), black foreign material (FM). HE stain, scale bar in A applies to all images.

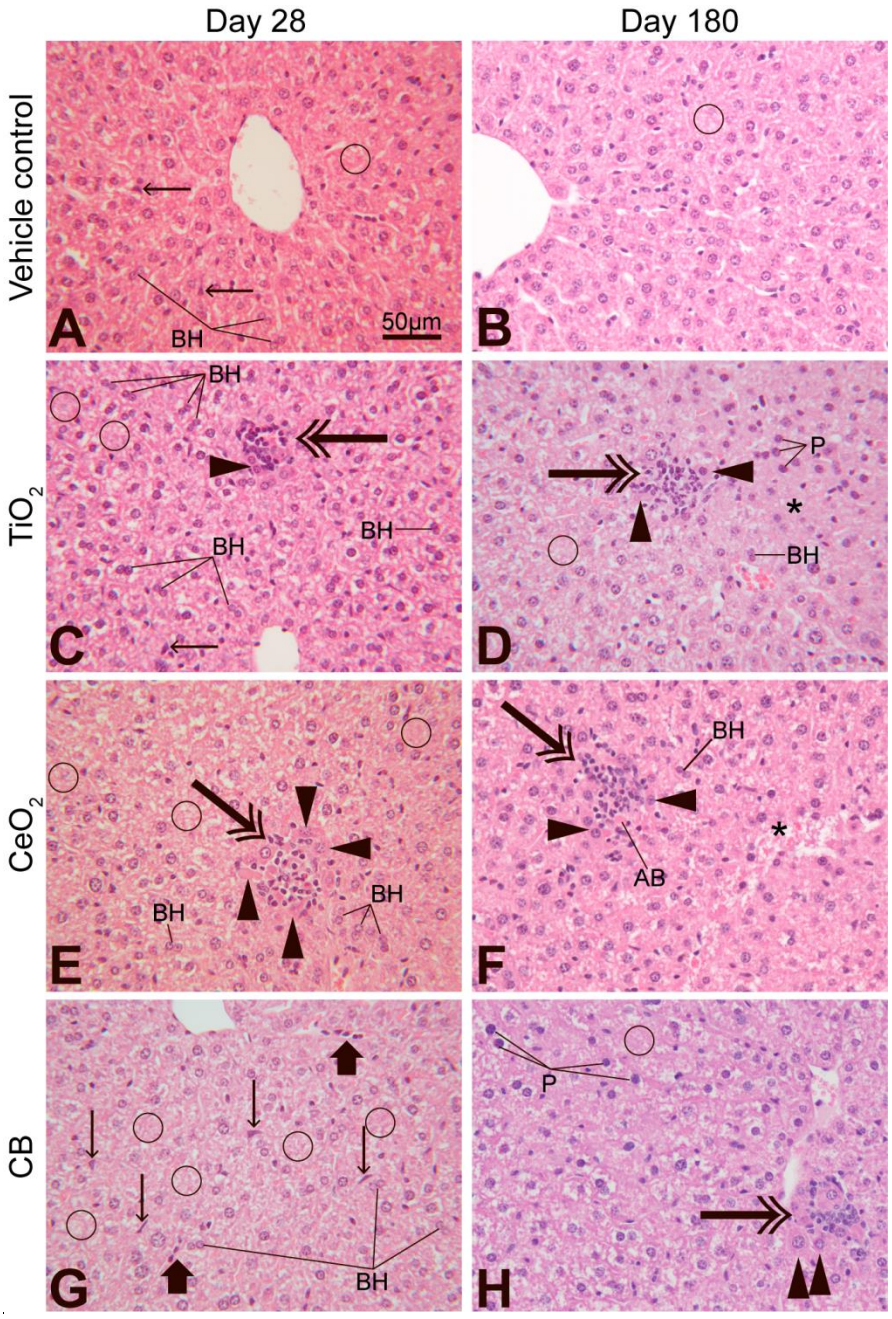

Figure 7. Microscopic changes in the liver of mice 28 or 180 days after single intratracheal instillation (IT) of a vehicle (A-B), TiO_2 (C-D), CeO_2 (E-F) or CB (G-H) NPs. A-B: microfoci of necrosis (circles), hypertrophy of Kupffer cells (tiny arrows), binucleate hepatocytes (BH). C-D: PNCF (double arrows), eosinophilic necrosis (arrowheads), microfoci of necrosis (circles), pyknosis of nuclei (P), hyperplasia of Kupffer cells (thick arrow), binucleate hepatocytes (BH), vacuolar degeneration (white spaces in hepatocytes). E-F: PNCF (double arrows), eosinophilic necrosis (arrowheads), microfoci of necrosis (circles), area of necrosis

(asterisk), binucleate hepatocytes (BH), apoptotic body (AB). G-H: PNCF (double arrow), eosinophilic necrosis (arrowheads), microfoci of necrosis (circles), hypertrophy of Kupffer cells (tiny arrows), hyperplasia of Kupffer cells (thick arrows), pyknosis of nuclei (P), vacuolar degeneration (white spaces in hepatocytes). HE stain, scale bar in A applies to all images.

DISCUSSION

In our recent study ICP-MS analysis demonstrated that lung-deposited TiO_2 and CeO_2 underwent extrapulmonary translocation that resulted in increased hepatic Ti and Ce concentration. Moreover, CB NPs, that due to the high abundance of carbon in the ambient air as well as in the tissues are not feasible to be measured by the applied analytical technique, were also detected in the liver following intratracheal exposure as assessed by EDFM (Modrzynska et al. unpublished manuscript 1). In addition, we have shown that IT of all three NPs resulted in a long lasting pulmonary inflammation and acute phase response and that IV and IT administration of CB NPs induced primary genotoxicity in the liver 28 and 180 days post-exposure in terms of increased DNA strand break levels (Modrzynska et al., unpublished manuscript 2). Therefore, in the present work we wanted to determine possible systemic toxic effects of hepatic accumulation of NPs following IT, IV and PO exposure to TiO_2, CeO_2 and CB NPs. Thus, we investigated if administration of NPs is associated with alterations in morphological structure of the liver and if the exposure induced systemic toxicity expressed as changes in body and liver weight and in hematological and biochemical parameters.

The three NPs studied in this work are produced in large quantities and are extensively used in high-volumes in many everyday-life areas. Thus, they are high-priority nanomaterials for the toxicological assessment. It has been demonstrated that inhalation and IT of CB NPs is associated with pulmonary inflammation [33] and induction of acute phase response [16]. Moreover, recent studies demonstrated genotoxic effects of CB NPs in the liver after pulmonary exposure [16,34]. TiO_2 also exhibited ability to induce pulmonary toxicity [35], inflammation [36] and oxidative stress [37]. Pulmonary damage [38], oxidative stress [39] and genotoxicity [8] were also reported for CeO_2 NPs.

The dose used in the present study is considered relevant for the occupational exposure and is equal to the pulmonary deposition after nine 8 h working days at the Danish occupational exposure limit of 3.5 mg/m^3 for CB.

Body and liver weight

In the present study no alterations of body weight were measured after IT, IV and PO administration of TiO_2, CeO_2 and CB NPs when compared with the vehicle control groups. In addition, exposure to CeO_2 and CB NPs had no impact on the absolute and relative liver weight. The decreases in the absolute and relative liver weights following oral exposure to TiO_2 NPs in our study could be considered as spurious findings since the oral dose was low, absorption of TiO_2 NPs from the gastrointestinal tract was shown to be low (49) and that previously conducted ICP-MS analysis demonstrated only background levels of Ti in the livers from orally treated mice compared to those exposed intravenously (Modrzynska et al. unpublished manuscript 1).

Reduced body weight gain following vascular infusion of CeO_2 NPs [40] has been previously reported however, relatively high dose, i.e. 85 mg/kg bw, was used in the study compared to 9 mg/kg bw administered in my study which could be responsible for the observed differences. Significant reduction of the liver weight was also demonstrated after intratracheal instillation of CeO_2 NPs [20] and after intravenous injection of TiO_2 NPs [41]. In the study conducted by Xu and colleagues [41] decrease in the relative liver weight could be explained by the extremely high doses, i.e. 300 and 645 mg/kg bw, administered in the mentioned study. In the study conducted by Nalabotu and co-workers [20] differences in physicochemical properties between CeO_2 NPs used in their and my study might be a reason for the divergent results.

Hematology

The knowledge of the changes in basic blood parameters is essential to evaluate welfare of animals exposed to NPs and might be an indication of the toxicity induced by the test material. Therefore, in the present study several important hematology parameters i.e. WBC, RBC, HGB, HCT, MCV, MCH, MCHC and PLT were measured for the further assessment of NP-induced toxicity. Occasional differences in hematological parameters, i.e. HCT, MCV, MCH, MCHC following exposure to TiO_2, CeO_2 or CB NPs administered by all three routes of exposure were observed. Minor differences were also measured for PLT and HGB levels however, since no consistent pattern in the induced changes were found, we believe that these could be regarded as chance findings. Similarly, negligible alterations in the basic blood parameters were found after oral exposure to Ag NPs [42]. Furthermore, Yang and co-workers [43] also demonstrated that there were no distinct changes in any of the assessed hematological parameters following intravenous administration of Ag and Au NPs in mice.

Liver enzyme activities

Biochemical analysis of plasma revealed no significant changes in any of the analyzed liver enzymes activities. Lack of changes in the clinical biochemistry was also reported after oral exposure to Ag NPs [42]. On the contrary, a study conducted by Nalabotu and co-workers [20] showed that intratracheal administration of CeO_2 NPs (7 mg/kg) was associated with hepatic toxicity in terms of decreased liver weight, elevated serum alanine transaminase levels and histopathological alterations in the liver tissue. Similar results were reported by Chen and colleagues [44] who demonstrated elevation in ALT and AST levels following intraperitoneal injection of different TiO_2 NPs doses (i.e. 324, 648, 972, 1296, 1944 or 2592 mg/kg). They also reported hepatocellular necrosis,

apoptosis and hepatic fibrosis in the high-dose groups. Therefore, these incoherence could be explained by the higher dose used in the mentioned studies or by differences in physicochemical properties exhibited by the TiO_2 and CeO_2 NPs used in our and their studies.

Lung and liver histology

The observed inflammatory changes in the lung tissue were in accordance with previous reports that the air borne exposure to particulate material causes pneumonia [45] and indicates that the blood circulatory supply of nanomaterials could also cause transitory inflammation in pulmonary tissue [46]. We have also previously reported similar inflammatory changes in the lungs [24,47,48].

Hyperplasia of connective tissue recorded one day after IV exposure in 1 animal from the CeO_2 and CB groups and on day 28 in TiO_2 group was considered as an incidental finding, not related to the treatment. The inflammatory cell infiltrations, oedema of connective tissue as well as single macrophages recorded after PO exposure were considered as not treatment related considering that the absorption of Ti after oral exposure to TiO_2 was reported to be very low [7,49]. Furthermore, pulmonary macrophages in the surface of alveoli or in the interstitium and small numbers of migratory cells including monocytes and lymphocytes can physiologically be present in the lung tissue [50].

In the present study the incidences of inflammatory changes in the liver were high in all vehicle and the NPs exposed groups regardless of the route of administration. Solitary or multiple inflammatory changes in the liver may result from toxicant insult, infections with viruses and bacteria but they also belong to common incidental findings in the liver

of aging mice and sometimes accompany hepatocellular necrosis [50,51]. The high background of inflammatory liver changes (of unclear etiology) in the vehicle controls in the present study made it impossible to determine whether these changes in the NPs exposed mice could be treatment-related. However, inflammatory changes in the liver were previously reported after IT exposure to Nano-TiO_2 and Printex 90 (carbon black) [52]. Furthermore, the ICP-MS analysis demonstrated the presence of Ti and Ce in the liver tissues in the exposed mice (Modrzynska et al., unpublished manuscript 1). Additionally, aggregates of foreign material originating from exposure to TiO_2 and CeO_2 were detected by the enhanced darkfield microscopy and black foreign material was seen in the liver tissue in the brightfield set-ups.

Similarly, it was not possible to determine whether necrosis in the NPs exposed mice could be treatment related. Hepatocellular necrosis is another non-specific entity commonly encountered as a focal incidental finding in the liver of aging mice, the typical morphological feature of which is coagulation necrosis of hepatocytes with distinct eosinophilic cytoplasm and pyknotic or absent nuclei. The etiology of spontaneous necrosis is usually unknown, but it may be caused by ischemia, toxicants and infection with viruses or bacteria [50]. The incidence of necrosis in the present study increased with age in all IT exposed groups but it was not statistically significantly higher in the TiO_2, CeO_2 and CB groups compared to the vehicle control group (89%, 100%, 75% vs 56%, respectively). No clear relation to age was seen for the incidences of necrosis in IV vehicle control and NPs exposed groups, and incidences though appeared higher than in the respective age controls were not statistically significantly increased after IV exposure. Thus necrosis could not be uniquely associated with the treatment in the present study although necrotic changes were previously reported in mice after IT exposure [24,47]. On the other hand the increase with age in the incidence of necrosis in

all PO treated groups suggested lack of treatment dependency. The latter seems to be in accordance with the lack of detection of Ti and Ce in the liver after oral exposure by ICP-MS quantification and darkfield microscopy (Modrzynska et al., unpublished manuscript 1) and in accordance with negligible absorption of nanoparticulate TiO_2 [7,49].

Binucleate hepatocytes are common finding in the mouse liver and are often noted in aging mice [50]. In the present study binucleate hepatocytes were often seen in all vehicle controls and all NPs exposed groups. However, a significant increase relative to the background level in vehicle controls on day 1 after IT exposure in TiO_2 group and after IV exposure in TiO_2 and CB groups could indicate hepatocytic regeneration typically seen after a toxic insult [53]. Similar increase in binucleate hepatocytes have previously been reported following NPs exposure [24,47,52].

The significantly increased incidence of hypertrophy of Kupffer cells observed after IV exposure in the present study could be related to the phagocytosis of material originating from the exposure to NPs, as shown by microscopy, as well as their function in the liver as secretion of inflammatory mediators [50].

Conclusions

NPs can enter the human body by several exposure routes and are further distributed to the other parts of the body by systemic circulation. Among other secondary organs liver seems to be the primary site for NPs accumulation. Therefore, concerns regarding potential adverse hepatotoxic effects have arisen.

Data from the present study suggest that a single dose of TiO_2, CeO_2 or CB NPs administered either by intratracheal instillation, intravenous injection or by oral gavage did not induced systemic toxicity in the mice since no consistent alterations in body or liver weight, biochemical or hematological parameters were observed. However, due to the high incidences of inflammatory and necrotic changes in the liver of mice from the vehicle control groups it was not possible to unambiguously determined whether the observed changes in the liver morphology were induced by NPs exposure.

REFERENCES

1. Kreyling WG, Semmler-Behnke M, Seitz J, Scymczak W, Wenk A, Mayer P, et al. Size dependence of the translocation of inhaled iridium and carbon nanoparticle aggregates from the lung of rats to the blood and secondary target organs. Inhal. Toxicol. 2009;21 Suppl 1:55–60.

2. Han SG, Lee JS, Ahn K, Kim YS, Kim JK, Lee JH, et al. Size-dependent clearance of gold nanoparticles from lungs of Sprague-Dawley rats after short-term inhalation exposure. Arch. Toxicol. 2015;89:1083–94.

3. Semmler-Behnke M, Kreyling WG, Lipka J, Fertsch S, Wenk A, Takenaka S, et al. Biodistribution of 1.4- and 18-nm gold particles in rats. Small. 2008;4:2108–11.

4. Kreyling WG, Hirn S, Moller W, Schleh C, Wenk A, Celik G, et al. Air-blood barrier translocation of tracheally instilled gold nanoparticles inversely depends on particle size. ACS Nano. 2014;8:222–33.

5. Sadauskas E, Wallin H, Stoltenberg M, Vogel U, Doering P, Larsen A, et al. Kupffer cells are central in the removal of nanoparticles from the organism. Part. Fibre Toxicol. 2007;4.

6. Hirn S, Semmler-behnke M, Schleh C, Wenk A, Schäffler M, Takenaka S, et al. Partilce size-dependent and surface charge-dependent biodistribution of gold nanoparticles after intravenous injection. Eur J Pharm Biopharm. 2011;77:407–16.

7. Wang J, Zhou G, Chen C, Yu H, Wang T, Ma Y, et al. Acute toxicity and biodistribution of different sized titanium dioxide particles in mice after oral administration. Toxicol. Lett. 2007;168:176–85.

8. Kumari M, Kumari SI, Kamal SSK, Grover P. Genotoxicity assessment of cerium oxide nanoparticles in female Wistar rats after acute oral exposure. Mutat. Res. - Genet. Toxicol. Environ. Mutagen. Elsevier B.V.; 2014;775–776:7–19.

9. Oberdörster G, Sharp Z, Atudorei V, Elder A, Gelein R, Lunts A, et al. Extrapulmonary Translocation of Ultrafine Carbon Particles Following Whole-Body Inhalation Exposure of Rats. J. Toxicol. Environ. Heal. Part A. 2002;65:1531–43.

10. Husain M, Wu D, Saber AT, Decan N, Jacobsen NR, Williams A, et al. Intratracheally instilled titanium dioxide nanoparticles translocate to heart and liver and activate complement cascade in the heart of C57BL/6 mice. Nanotoxicology. 2015;9:1013–22.

11. Kermanizadeh A, Chauché C, Balharry D, Brown DM, Kanase N, Boczkowski J, et al. The role of Kupffer cells in the hepatic response to silver nanoparticles. Nanotoxicology. 2014;8 Suppl 1:149–54.

12. Park JK, Utsumi T, Seo YE, Deng Y, Satoh A, Saltzman WM, et al. Cellular distribution

of injected PLGA-nanoparticles in the liver. Nanomedicine Nanotechnology, Biol. Med. Elsevier Inc.; 2016;12:1365–74.

13. Dixon L, Barnes M, Tang H, Pritchard M, Nagy L. Kupffer Cells in the Liver. Compr Physiol. 2013;3:785–97.

14. Sadauskas E, Danscher G, Stoltenberg M, Vogel U, Larsen A, Wallin H. Protracted elimination of gold nanoparticles from mouse liver. Nanomedicine Nanotechnology, Biol. Med. Elsevier Inc.; 2009;5:162–9.

15. Sahu SC. Hepatotoxic Potential of Nanomaterials. Nanotoxicity From Vivo Vitr. Model. to Heal. Risks. 2009. p. 183–9.

16. Bourdon JA, Saber AT, Jacobsen NR, Jensen KA, Madsen AM, Lamson JS, et al. Carbon black nanoparticle instillation induces sustained inflammation and genotoxicity in mouse lung and liver. Part. Fibre Toxicol. BioMed Central Ltd; 2012;9:5.

17. Jackson P, Hougaard KS, Vogel U, Wu D, Casavant L, Williams A, et al. Exposure of pregnant mice to carbon black by intratracheal instillation: Toxicogenomic effects in dams and offspring. Mutat. Res. - Genet. Toxicol. Environ. Mutagen. Elsevier B.V.; 2012;745:73–83.

18. Wallin H, Kyjovska ZO, Poulsen SS, Jacobsen NR, Saber AT, Bengtson S, et al. Surface modification does not influence the genotoxic and inflammatory effects of TiO2 nanoparticles after pulmonary exposure by instillation in mice. Mutagenesis. 2017;gew046-.

19. Husain M, Kyjovska ZO, Bourdon-Lacombe J, Saber AT, Jensen KA, Jacobsen NR, et al. Carbon black nanoparticles induce biphasic gene expression changes associated with inflammatory responses in the lungs of C57BL/6 mice following a single intratracheal instillation. Toxicol. Appl. Pharmacol. Elsevier B.V.; 2015;289:573–88.

20. Nalabotu SK, Kolli MB, Triest WE, Ma JY, Manne NDPK, Katta A, et al. Intratracheal instillation of cerium oxide nanoparticles induces hepatic toxicity in male Sprague-Dawley rats. Int. J. Nanomedicine. 2011;6:2327–35.

21. Cui Y, Liu H, Ze Y, Zengli Z, Hu Y, Cheng Z, et al. Gene expression in liver injury caused by long-term exposure to titanium dioxide nanoparticles in mice. Toxicol Sci. 2012;128:171–85.

22. Recordati C, De Maglie M, Bianchessi S, Argentiere S, Cella C, Mattiello S, et al. Tissue distribution and acute toxicity of silver after single intravenous administration in mice: nano-specific and size-dependent effects. Part. Fibre Toxicol. 2016;13.

23. Poulsen SS, Jackson P, Kling K, Knudsen KB, Skaug V, Kyjovska ZO, et al. Multi-walled carbon nanotube physicochemical properties predict pulmonary inflammation and genotoxicity. Nanotoxicology. 2016;10:1263–75.

24. Poulsen SS, Saber AT, Williams A, Andersen O, Købler C, Atluri R, et al. MWCNTs of different physicochemical properties cause similar inflammatory responses, but differences in transcriptional and histological markers of fibrosis in mouse lungs. Toxicol. Appl. Pharmacol. Elsevier B.V.; 2015;284:16–32.

25. Kyjovska ZO, Jacobsen NR, Saber AT, Bengston S, Jackson P, Wallin H, et al. DNA damage following pulmonary exposure by instillation to low doses of carbon black (Printex 90) nanoparticles in mice. Environ. Mol. Mutagen. 2015;56:41–9.

26. Levin M, Rojas E, Vanhala E, Vippola M, Liguori B, Kling K, et al. Influence of relative humidity and physical load during storage on dustiness of inorganic nanomaterials: implications for testing and risk assessment. J. Nanoparticle Res. Springer Netherlands; 2015;17.

27. Halappanavar S, Saber AT, Decan N, Jensen KA, Wu D, Jacobsen NR, et al. Transcriptional profiling identifies physicochemical properties of nanomaterials that are determinants of the in vivo pulmonary response. Environ. Mol. Mutagen. 2015;56:245–64.

28. Saber AT, Jensen KA, Jacobsen NR, Birkedal R, Mikkelsen L, Møller P, et al. Inflammatory and genotoxic effects of nanoparticles designed for inclusion in paints and lacquers. Nanotoxicology. 2012;6:453–71.

29. Saber AT, Bornholdt J, Dybdahl M, Sharma AK, Loft S, Vogel U, et al. Tumor necrosis factor is not required for particle-induced genotoxicity and pulmonary inflammation. Arch. Toxicol. 2005;79:177–82.

30. Lide DR. CRC Handbook of Chemistry and Physics 84th Edition. 2004.

31. Mikkelsen L, Sheykhzade M, Jensen KA, Saber AT, Jacobsen NR, Vogel U, et al. Modest effect on plaque progression and vasodilatory function in atherosclerosis-prone mice exposed to nanosized TiO2. Part. Fibre Toxicol. 2011;8:32.

32. Schneider C a, Rasband WS, Eliceiri KW. NIH Image to ImageJ: 25 years of image analysis. Nat. Methods. Nature Publishing Group; 2012;9:671–5.

33. Saber AT, Halappanavar S, Folkmann JK, Bornholdt J, Boisen AMZ, Møller P, et al. Lack of acute phase response in the livers of mice exposed to diesel exhaust particles or carbon black by inhalation. Part. Fibre Toxicol. 2009;6:12.

34. Jackson P, Hougaard KS, Boisen AMZ, Jacobsen NR, Jensen KA, Møller P, et al. Pulmonary exposure to carbon black by inhalation or instillation in pregnant mice: Effects on liver DNA strand breaks in dams and offspring. Nanotoxicology. 2012;6:486–500.

35. Renwick LC, Brown D, Clouter A, Donaldson K. Increased inflammation and altered macrophage chemotactic responses caused by two ultrafine particle types. Occup Env.

Med. 2004;61:442–7.

36. Warheit DB, Webb TR, Reed KL, Frerichs S, Sayes CM. Pulmonary toxicity study in rats with three forms of ultrafine-TiO2 particles: Differential responses related to surface properties. Toxicology. 2007;230:90–104.

37. Gurr JR, Wang ASS, Chen CH, Jan KY. Ultrafine titanium dioxide particles in the absence of photoactivation can induce oxidative damage to human bronchial epithelial cells. Toxicology. 2005;213:66–73.

38. Ma, Zhao, Mercer, Barger, Rao, Meighan, et al. Cerium oxide nanoparticle-induced pulmonary inflammation and alveolar macrophage functional change in rats. Nanotoxicology. 2011;5:312–25.

39. Morimoto Y, Izumi H, Yoshiura Y, Tomonaga T, Oyabu T, Myojo T, et al. Pulmonary toxicity of well-dispersed cerium oxide nanoparticles following intratracheal instillation and inhalation. J. Nanoparticle Res. Springer Netherlands; 2015;17:1–16.

40. Tseng MT, Fu Q, Lor K, Fernandez-Botran GR, Deng Z-B, Graham U, et al. Persistent Hepatic Structural Alterations Following Nanoceria Vascular Infusion in the Rat. Toxicol. Pathol. 2014;42:984–96.

41. Xu J, Shi H, Ruth M, Yu H, Lazar L, Zou B, et al. Acute Toxicity of Intravenously Administered Titanium Dioxide Nanoparticles in Mice. PLoS One. 2013;8:1–6.

42. Hadrup N, Gao X, Lam HR, Loeschner K, Vogel U, Bergström A, et al. Subacute oral toxicity investigation of nanoparticulate and ionic silver in rats. Arch. Toxicol. 2012;86:543–51.

43. Yang L, Kuang H, Zhang W, Aguilar ZP, Wei H, Xu H. Comparisons of the biodistribution and toxicological examinations after repeated intravenous administration of silver and gold nanoparticles in mice. Sci. Rep. Springer US; 2017;1–12.

44. Chen J, Dong X, Zhao J, Tang G. In vivo acute toxicity of titanium dioxide nanoparticles to mice after intraperitioneal injection. J. Appl. Toxicol. 2009;29:330–7.

45. Anderson JO, Thundiyil JG, Stolbach A. Clearing the Air: A Review of the Effects of Particulate Matter Air Pollution on Human Health. J. Med. Toxicol. 2012;8:166–75.

46. Ma JYC, Young SH, Mercer RR, Barger M, Schwegler-Berry D, Ma JK, et al. Interactive effects of cerium oxide and diesel exhaust nanoparticles on inducing pulmonary fibrosis. Toxicol. Appl. Pharmacol. 2014;278:135–47.

47. Hougaard KS, Jackson P, Kyjovska ZO, Birkedal RK, De Temmerman PJ, Brunelli A, et al. Effects of lung exposure to carbon nanotubes on female fertility and pregnancy. A study in mice. Reprod. Toxicol. Elsevier Inc.; 2013;41:86–97.

48. Jacobsen NR, Stoeger T, van den Brule S, Saber AT, Beyerle A, Vietti G, et al. Acute and subacute pulmonary toxicity and mortality in mice after intratracheal instillation of ZnO nanoparticles in three laboratories. Food Chem. Toxicol. Elsevier Ltd; 2015;85:84–95.

49. Panel EE. Re-evaluation of titanium dioxide (E 171) as a food additive. EFSA J. 2016;14:4545.

50. Harrada T, Enomoto A, Boorman GA, Moronpot RR. Liver and gallbladder. Pathol. mouse. 1999. p. 119–71.

51. Haschek W, Rousseaux CG, Wallig MA. Respiratory System. Fundamentals of Toxicologic Pathology. 2010. p. 93–133.

52. Saber AT, Jacobsen NR, Mortensen A, Szarek J, Jackson P, Madsen AM, et al. Nanotitanium dioxide toxicity in mouse lung is reduced in sanding dust from paint. Part. Fibre Toxicol. BioMed Central Ltd; 2012;9:4.

53. Kostka G, Palut D, Kopeć-Szlezak J, Ludwicki JK. Early hepatic changes in rats induced by permethrin in comparison with DDT. Toxicology. 1999;142:135–43.

National Food Institute
Technical University of Denmark
Kemitorvet
DK-2800 Kgs. Lyngby

www.food.dtu.dk

ISBN: 978-87-93565-05-0